

DOCTORAL THESIS

Transcription Factors FOXO3 and TCF4 in Huntington's Disease

Kaja Nurm

TALLINN UNIVERSITY OF TECHNOLOGY
DOCTORAL THESIS
55/2021

Transcription Factors FOXO3 and TCF4 in Huntington's Disease

KAJA NURM



TALLINN UNIVERSITY OF TECHNOLOGY
School of Science
Department of Chemistry and Biotechnology

This dissertation was accepted for the defence of the degree 27/10/2021

Supervisor: Professor Tõnis Timmusk, PhD
Department of Chemistry and Biotechnology
Tallinn University of Technology
Tallinn, Estonia

Co-supervisor: Research scientist Mari Sepp, PhD
Department of Chemistry and Biotechnology
Tallinn, Estonia
Present address: Heidelberg University
Center of Molecular Biology (ZMBH)
Heidelberg, Germany

Opponents: Luis M. Valor, PhD
Principal Investigator Miguel Servet II
Instituto de Investigación Sanitaria y Biomédica de
Alicante (ISABIAL)
Alicante, Spain

Prof. Pärt Peterson, PhD
Institute of Biomedicine and Translational Medicine
University of Tartu
Tartu, Estonia

Defence of the thesis: 10/12/2021, Tallinn

Declaration:

Hereby I declare that this doctoral thesis, my original investigation and achievement, submitted for the doctoral degree at Tallinn University of Technology has not been submitted for doctoral or equivalent academic degree.

Kaja Nurm

signature



European Union
European Regional
Development Fund



Investing
in your future

Copyright: Kaja Nurm, 2021

ISSN 2585-6898 (publication)

ISBN 978-9949-83-753-3 (publication)

ISSN 2585-6901 (PDF)

ISBN 978-9949-83-754-0 (PDF)

TALLINNA TEHNIKAÜLIKOOL
DOKTORITÖÖ
55/2021

Transkriptisoonifaktorid FOXO3 ja TCF4 Huntingtoni tõves

KAJA NURM



Contents

List of Publications	7
Author's Contribution to the Publications	8
Introduction	9
Abbreviations	11
1 Huntington's disease.....	13
1.1 Huntingtin gene and protein.....	13
1.2 Huntington's disease models	14
1.2.1 Chemical models of HD	14
1.2.2 Genetically modified mouse models of HD.....	14
1.3 Molecular mechanisms of Huntington's disease	17
1.3.1 Transcriptional dysregulation	17
1.3.2 Mechanisms of transcription dysregulation	20
2 Transcription Factor TCF4	23
2.1 TCF4 gene and protein structure and expression	25
2.2 Functions of TCF4 in the nervous system.....	27
2.3 Target genes of TCF4 in the nervous system	29
2.4 Dimerization partners of TCF4	31
3 Transcription Factor FOXO3 – a member of FOXO family.....	32
3.1 Post-translational regulation of FOXOs.....	32
3.2 Roles of FOXOs in Huntington's disease	37
4 Aims of the study	42
5 Material and methods.....	43
6 Results	44
7 Discussion.....	49
7.1 Identification of transcription factors with altered subcellular localization and/or expression in Huntington's disease.....	49
7.2 FOXO3 in Huntington's disease.....	49
7.3 TCF4 in health	52
7.4 TCF4 in Huntington's disease	55
8 Conclusions	58
References	59
Acknowledgements.....	82
Abstract.....	83
Lühikokkuvõte.....	85
Appendix 1	89

Appendix 2	105
Appendix 3	121
Appendix 4	135
Curriculum vitae	155
Elulookirjeldus.....	157

List of Publications

The list of author's publications, based on which the thesis has been prepared:

- I Mari Sepp, **Kaja Kannike**, Ave Eesmaa, Mari Urb and Tõnis Timmusk (2011). Functional Diversity of Human Basic Helix-Loop-Helix Transcription Factor TCF4 Isoforms Generated by Alternative 5' Exon Usage and Splicing. *PLoS ONE* 6(7): e22138. doi: 10.1371/journal.pone.0022138.
- II **Kaja Kannike**, Mari Sepp, Chiara Zuccato, Elena Cattaneo, and Tõnis Timmusk (2014). Forkhead Transcription Factor FOXO3a Levels Are Increased in Huntington Disease Because of Overactivated Positive Autofeedback Loop. *J. Biol. Chem.* 289: 32845–32857. doi: 10.1074/jbc.M114.612424.
- III Mari Sepp, Hanna Vihma*, **Kaja Nurm***, Mari Urb*, Stephanie Cerceo Page, Kaisa Roots, Anu Hark, Brady J. Maher, Priit Pruunsild and Tõnis Timmusk (2017). The Intellectual Disability and Schizophrenia Associated Transcription Factor TCF4 Is Regulated by Neuronal Activity and Protein Kinase A. *J. Neurosci.* 37: 10516–10527. doi: 10.1523/JNEUROSCI.1151-17.2017.
- IV **Kaja Nurm**, Mari Sepp, Carla Castany-Pladevall, Jordi Creus Munchunill, Jürgen Tuvikene, Alex Sirp, Hanna Vihma, Derek J. Blake, Esther Perez Navarro, Tõnis Timmusk (2021). Isoform-Specific Reduction of the Basic Helix-Loop-Helix Transcription Factor TCF4 Levels in Huntington's Disease. *eNeuro* 8(5): ENEURO.0197-21.2021. doi: 10.1523/ENEURO.0197-21.2021.

* Equal contribution

Author's Contribution to the Publications

- I The author performed and analysed quantitative reverse transcription PCR analysis of *TCF4* expression in human tissues and cloned several expression vectors.
- II The author designed, performed, and analysed majority of the experiments and wrote the article.
- III The author performed and analysed the data of luciferase assay for identification of signalling pathways involved in the induction of TCF4-dependent transcription by neuronal activity
- IV The author performed, and analysed majority of the experiments (except Western blot experiments on brain lysates from R6/1 mice and human Huntington's disease patients and reporter assays) and wrote the article.

Introduction

Neurodegenerative disorder Huntington's disease (HD) has been recognized as a disease with distinctive chorea already for centuries, and was medically first described in detail by physician George Huntington more than 100 years ago as an autosomal dominant hereditary progressive disease. HD is quite common in western populations, affecting 3-5 persons in 100,000 according to conservative estimation, although its prevalence varies hugely between different geographical regions (Rawlins et al., 2016). The underlying gene huntingtin (*Htt*) was identified in 1993, which boosted the generation of genetic models of HD and search to discover the roles of this protein. For a long time, HD was neuropathologically characterized mainly with a progressive degeneration of striatum and cortex, although advancements in imaging and biotechnology have enabled detection of alterations also in other brain regions (McColgan and Tabrizi, 2018). Clinical onset of HD is confirmed by motor disturbances, albeit the cognitive and psychiatric functions have recently become more acknowledged and seem to be impaired already in the prodromal phase of the disease. Another aspect of HD that has gained attention lately is that although HD is a neurodegenerative disease and considerable neuronal death is reported, more recent studies have also revealed aberrant features of neurodevelopment and neurogenesis. At the molecular level the general dysregulation of gene expression in HD has been known already for decades.

In this study, we focused on two transcription factors, FOXO3 and TCF4 that we found to be altered in HD model cells in a screen using antibodies raised against a panel of transcription factors. First, we studied the transcription factor FOXO3 that acts as cellular sensor and integrator of stress and survival signals. We found that the levels of FOXO3 mRNA and protein are increased in HD model cells and in HD patients' cortex and caudate nucleus tissue. Furthermore, we described autoregulation of FOXO3 and post-translational modifications of effector kinases and their changes, potentially playing a role in balancing cell survival and apoptosis in the HD neurons. Second, we demonstrated that the basic helix-loop-helix (bHLH) transcription factor TCF4, a regulator of neurogenesis and neuronal differentiation, is downregulated in cellular models of HD. Given the limited systematic knowledge about the expression of TCF4 and its function in the regulation of gene expression, we described the complete structure of human and mouse *TCF4* genes and characterized the alternative protein isoforms. We showed wide expression of *TCF4* mRNA in human tissues, with the highest expression in the brain. Next, we reported neuronal activity-dependence of TCF4-mediated gene transcription and regulation of TCF4 transcriptional activity by protein kinase A (PKA). Then, we conducted extensive analysis of *Tcf4* alternative transcripts' expression in different brain regions of transgenic HD model mouse R6/1, with the most significant changes occurring in hippocampus and cerebral cortex. The findings of TCF4 downregulation in HD models were corroborated in the CA1 hippocampal region and cerebral cortex of HD patients. Interestingly, changes of specific TCF4-isoform encoding mRNAs were brain region-specific. Finally, we showed differences in transactivation of different TCF4 isoforms on dimerization with ASCL1 by reporter gene assay in rat primary cortical and hippocampal neurons. Furthermore, TCF4 isoforms differ also in activating gene transcription at basal and depolarization conditions and additional differences exist between cortical and hippocampal neurons.

In conclusion, here we demonstrated altered FOXO3 and TCF4 levels in several *in vitro* and *in vivo* HD models and substantiated these findings in HD patients. Furthermore, we discovered that FOXO3 is regulated by a positive auto-feedback loop, imbalance of which

could underlie the upregulation of FOXO3 levels in HD. Our study is the first linking TCF4 with HD and we suggest that dysregulated TCF4 may play a role in impaired neurocognitive functions in HD. Moreover, we described molecular mechanisms of TCF4 activation and shed light on the functional differences between TCF4 isoforms. The results of this study add pieces to the puzzle of HD pathogenesis, lending support to both neurodegenerative and neurodevelopmental theories of HD.

Abbreviations

14-3-3	Protein encoded from different genes of <i>YWHA</i> family
3-NP	3-nitropropionic acid
AAV	Adeno-associated virus
AD1/AD2	Activation domain 1/activation domain 2
AKT	Alternative name of protein kinase B (PKB)
AMPK	AMP-activated protein kinase
ASCL1	Achaete-scute homolog 1 protein encoded by the <i>ASCL1</i> gene
BDNF	Brain-derived neurotrophic factor
bHLH	Basic helix-loop-helix
CA1	Cornu ammonis subfield 1 (a region of hippocampus)
cAMP	cyclic adenosine 3',5' monophosphate
CBP	CREB binding protein
CDK	Cyclin-dependent kinase
CHDI	a United States-based non-profit biomedical foundation of HD
ChIP	Chromatin immunoprecipitation
CK1	Casein kinase 1
CMV	Cytomegalovirus
CREB	cAMP response element-binding protein
Da	Daughterless, the ortholog of E proteins in <i>D. melanogaster</i>
Daf-16	Ortholog of FOXO proteins in <i>C. elegans</i>
DBD	DNA-binding domain
DEG	Differentially expressed gene
dFOXO	Ortholog of FOXO proteins in <i>D. melanogaster</i>
DG	Dentate gyrus
EF1 α	Elongation factor 1 alpha
ER	Endoplasmic reticulum
ERK	Extracellular signal-regulated kinase
FHRE	Forkhead responsive element
FOXO3	Forkhead box O3 protein encoded by the <i>FOXO3</i> gene
GABA	Gamma-aminobutyric acid
GADD45G	Growth arrest and DNA-damage-inducible protein gamma encoded by the <i>GADD45G</i> gene
GSK	Glycogen synthase kinase
HAP1	Huntingtin interactin protein 1
HD	Huntington's disease
Hdh	Former name of the murine <i>Htt</i> gene
HTT	Huntingtin protein encoded by the <i>HTT</i> gene (previously known as <i>IT15</i> gene)
ID	bHLH protein Inhibitor of DNA-binding

JNK	c-Jun N-terminal kinase
MAPK	Mitogen-activated protein kinase
mPFC	Medial prefrontal cortex
MSN	Medium spiny neurons
MST1	Mammalian sterile twenty-like kinase encoded by the <i>STK4</i> gene
NES	Nuclear export signal
NLS	Nuclear localization signal
NMDA	N-methyl-D-aspartate receptor
NPC	Neural progenitor cell
NRSE	Neuron-restrictive silencer element (also known as RE1)
NSC	Neural stem cell
p300	Histone acetyltransferase and co-transcriptional factor, also known as E1A-associated protein or EP300 (encoded by gene <i>EP300</i>)
PGK	3-phospho-glycerate kinase encoded by the <i>PGK-1</i> gene
PI3K	Phosphoinositide 3-kinase
PKA	cAMP-dependent protein kinase A
PKB	Protein kinase B (also known as AKT)
polyQ	Polyglutamine (CAG trinucleotide) repeat
PTM	Posttranslational modification
RE-1	Response-element 1 (also known as NSRE), REST/NRSF binding site
REST/NRSF	RE-1 silencing transcription factor/neuron-restrictive silencer factor
RISC	RNA-induced silencing complex
RT-PCR	Reverse transcription polymerase chain reaction
RT-qPCR	Reverse transcription quantitative polymerase chain reaction
sAC	Soluble adenylyl cyclase
SCZ	Schizophrenia
SGK	Serine/threonine-protein kinase also known as serum and glucocorticoid-regulated kinase
shRNA	Short hairpin RNA
siRNA	Small interfering RNA
SR α	Synthetic promoter combined from <i>simian virus 40</i> promoter and <i>R-U5</i> segment of human T-cell leukemia virus type 1 long terminal repeat
TCF4	Transcription factor 4 encoded by the <i>TCF4</i> gene; the most common aliases are E2-2, ITF2, SEF2
TF	Transcription factor
UTR	Untranslated region
VGCC	Voltage-gated calcium channel

1 Huntington's disease

Huntington's disease (HD) is devastating hereditary autosomal dominant neurodegenerative disease that is caused by increase of CAG trinucleotide repeats in exon 1 of huntingtin (*HTT*) gene (The Huntington's Disease Collaborative Research Group, 1993). It is a rare genetic disorder affecting 5-10 individuals per 100,000 in Caucasian populations (Rawlins et al., 2016). In the non-HD population polymorphic polyglutamine stretch varies between 9-35 repeats, and repeats over 35 result in HD. Furthermore, CAG expansion of about 75 or more triplets is associated with juvenile onset (Kremer et al., 1994; Lee et al., 2012). Symptoms of HD differ between patients, although progressive motor, cognitive, and psychiatric symptoms are common (reviewed in Bates et al., 2015). Classically, in the mid-adulthood clear motor symptoms appear and all symptoms worsen gradually until the death of the patient (10-15 years from onset). The neuropathology of HD is characterized by neuronal death specifically in striatum and cerebral cortex, and definite subsets of neurons are more affected (GABAergic medium spiny neurons in the striatum) or spared (other interneurons). Both of these brain regions are highly degenerated at terminal stages of the disease.

1.1 Huntingtin gene and protein

Human huntingtin (*HTT*) gene is localized in chromosome 4 p-arm. The *HTT* locus is large, spanning 180 kb and consisting of 67 exons. *HTT* gene encodes a 348 kDa protein that is conserved from flies to mammals. *HTT* mRNA is widely expressed across tissues and development, from embryonic stages to adulthood (Landwehrmeyer et al., 1995; Li et al., 1993; Strong et al., 1993; Thomson and Leavitt, 2018). Functions of wild type HTT have been extensively studied in parallel with mutant HTT. Loss of HTT in early embryos is lethal and many functions of HTT have been described for developing as well as mature organism (Nasir et al., 1995; Saudou and Humbert, 2016; Zeitlin et al., 1995).

At the molecular level HTT operates in vesicle trafficking, coordinates cell division, regulates ciliogenesis, mediates endocytosis, vesicle recycling and endosomal trafficking, autophagy, and transcription, to name a few of its known functions (reviewed in (Saudou and Humbert, 2016). Besides being essential for embryonic development in general, *HTT* haploinsufficiency has been shown to result in defects in neuron precursors, imbalance between differentiation and proliferation, and impaired migration of newborn neurons and motile cilium biogenesis (Godin et al., 2010; Keryer et al., 2011; Reiner et al., 2001; White et al., 1997). Additionally, neurodevelopmental changes have been described in mouse and rat HD models, supporting the hypothesis of neurodevelopmental basis of HD (Siebzehnrübl et al., 2018). Together, these studies provide evidence for the importance of HTT in the formation of whole nervous system.

Compared to the loss-of-function effects of wild type HTT, more of the HD research has been concentrated on deciphering the cellular consequences of the expression of mutant HTT. Mainly gain-of-functions have been described for mutant HTT. The current knowledge on mechanisms of pathogenesis has been thoroughly reviewed by Jimenez-Sanchez and colleagues (Jimenez-Sanchez et al., 2017). In HD, mutant HTT is proteolytically cleaved, N-terminal fragments translocate into the nucleus and interfere with transcription leading to cell death, whereas C-terminal fragments dysregulate dynamin 1, a component of trafficking machinery (El-Daher et al., 2015; Saudou et al., 1998; Sugars and Rubinsztein, 2003). Additionally, aggregation and inclusion formation

of mutant HTT has been reported widely, however, contradictory conclusions have been drawn in whether the formed aggregates are toxic or a protective form of mutant HTT (reviewed in (Bates et al., 2015).

1.2 Huntington's disease models

Huntington's disease, characterized by choreiform movements, has been known for centuries. The characteristic of neurodegeneration in HD affecting certain brain regions was described thoroughly 50 years ago (Vonsattel et al., 1985). Based on these observations the first HD models were chemically induced to mimic those symptoms known to occur in HD patients at that time. The discovery of the disease-causing mutation in *HTT* gene enhanced possibilities to study HD in more relevant genetical settings and since then many model cell lines and animal models have been created.

1.2.1 Chemical models of HD

The energy metabolism deficits in HD patients are characterized by mitochondrial defects, and decrease of succinate oxidation and ATP synthesis (Beal, 1992; Oliveira, 2010). This led to search and usage of chemical compounds to model HD.

Malonate and 3-nitropropionic acid (3-NP) have been used to alter mitochondrial metabolism in non-genetic models of HD. Mitochondrial toxin 3-NP is an irreversible inhibitor of succinate dehydrogenase that was first reported to be responsible for motor alteration and neuronal death in caudate and putamen nuclei in poisoned cattle and children (Ludolph et al., 1991). Further studies have additionally described excitotoxic properties of 3-NP that lead to increased sensitivity to basal glutamate levels (Borlongan, 1997). Years of studies have revealed that 3-NP treated animals exhibit neurodegeneration, abnormal motor behaviour, excitotoxicity and energy deficit, therefore mimicking many of HD symptoms (Beal et al., 1993; Brouillet et al., 2005, 1995; Palfi et al., 1996; Túnez et al., 2010). Extensive comparisons of impairments reproduced by chemical 3-NP and genetic HD models have revealed differences in 3-NP effects between species, strains, sexes, and administration protocols (Brouillet et al., 2005; Ramaswamy et al., 2007). 3-NP has been successfully utilized in neural cell cultures as well (Liot et al., 2009), although it has been suggested that in 3-NP models mechanisms of cell death are more accurately reproduced in cell heterologous ("contextual") than cell autonomous ("intracellular") context (Brouillet et al., 2005). Nevertheless, an integral pathological feature of HD, HTT inclusion formation, cannot be replicated in the chemical models of HD. Furthermore, cell death in toxin-treated model animals is immediate, compared to progressive neurodegeneration characteristic of HD, which depends also on the CAG repeat size (Andrew et al., 1993; Beal et al., 1993).

1.2.2 Genetically modified mouse models of HD

An exceptionally good and extensive guide of mouse models of HD has been compiled by The Jackson Laboratories in collaboration with privately-funded biomedical research organization of HD - CHDI Foundation (Menalled et al., 2014). Mouse models of HD can be divided into N-terminal and full-length transgenic, and *knock-in* model mice.

The first transgenic mouse models of HD were R6 lines, where the N-terminal human *mHTT* fragments (repeat formula (CAG)_nCAACAG) are expressed in addition to endogenous mouse huntingtin (*Htt*) (Mangiarini et al., 1996). Originally, R6/1 had 115 and R6/2 150 polyQ repeats, respectively, although today many sub-lines exist with diverse repeat numbers and frequent testing of the repeat length is advised. The repeat

size of R6/2 mice was found to vary from 43 to 600, and is probably a confounding factor for greatly diverged phenotypes of R6/2 mice (Cummings et al., 2012; Menalled et al., 2014). It has been shown that R6/2 transgene functions as a single copy integrant, whereas studies on R6/1 transgene copy number have remained inconclusive (Chiang et al., 2012; Mangiarini et al., 1996). Moreover, high throughput sequencing revealed 5.4 kb deletion near the integration site of *mHTT* fragment in R6/2 mice, therefore demonstrating that transgenic insertions can be disruptive to mouse original chromosomal DNA sequence (Chiang et al., 2012). Although R6/2 line is widely used, it has very severe symptoms and therefore is thought to better mimic juvenile HD (Ramaswamy et al., 2007). R6/1 mice exhibit later onset of symptoms and slower disease progression, and are therefore more suitable for investigating development of a disease and could be used for observing long-term effects of different treatments. Later on many more N-terminal human *HTT* expressing mouse models have been created, including N171-82Q (Schilling, 1999) and HD190QG (Kotliarova et al., 2005).

Mouse models carrying full-length human *HTT* utilize a yeast or a bacterial artificial chromosome (YAC and BAC, respectively), that is integrated into a single locus of the mouse genome with low copy numbers, therefore HD phenotype develops progressively over time and mice display relatively normal survival (reviewed in Menalled et al., 2014). Advantage of these full-length models is that *HTT* is expressed within the context of its endogenous genomic regulatory elements, therefore being suitable for testing therapies precisely targeting human *HTT* gene and protein (Pouladi et al., 2013). On the other hand, unusual weight gain has been observed in these mice; therefore, these mice are unsuitable for studies of metabolic changes, and increased body weight can also confound evaluation of motor functions. Furthermore, the natural polyglutamine-encoding sequence of the human *HTT* gene is (CAG)_nCAACAG, whereas in the BACHD and YAC128 mice the CAG repeat is interspersed with CAA triplets that may modify *HTT* RNA structure and its potential pathogenicity in cells. For instance, formation of small CAG-repeated RNAs with neurotoxic activity have been shown to cause somatic instability and reduce neuronal viability in HD and the severity of the toxic effect correlates with CAG expansion length (Bañez-Coronel et al., 2012). Recently it was demonstrated that other classes of small RNAs produced in the putamen of HD patients induce HD pathology *in vivo* in mice suggesting that multiple small RNA species contribute to striatal dysfunction in HD (Creus-Muncunill et al., 2021).

The most accurate mouse models of HD from genetic standpoint are knock-in mice, where CAG repeat tracks are introduced into the endogenous context of one functional mouse *Htt* allele. This modification creates heterozygous animals where wild-type *HTT* levels are altered as well, accurately mimicking the *HTT* genetic status in most HD patients (Lee et al., 2012). Several allelic series of knock-in mice with various CAG repeat size in exon 1 in congenic C57BL/6J inbred backgrounds are available, therefore enabling to investigate the influence of CAG repeat length on HD (reviewed in Menalled et al., 2014). There are series of knock-in mice expressing mutant form of mouse *Htt*, although some other contain humanized exon 1 sequence resulting in chimeric mouse-human *HTT*. Nevertheless, none of them express full-length human *HTT* gene or protein that might be required for pre-clinical experiments (Menalled, 2005). Wheeler and MacDonald created and described the first series of such knock-in mice with 18, 48, 78, 90 and 109 CAG repeats in human exon 1 sequence engineered into mouse *Htt* gene (Wheeler, 1999). From this series the HdhQ¹¹¹ mouse with 111 glutamines encoded by a (CAG)₁₀₉CAACAG sequence is one of the most studied and the best described knock-in

mouse of HD (Wheeler et al., 2000). The second group of HD knock-in mice were established by Lin and Detloff (Lin et al., 2001), and these mice express mouse *Htt* in mouse genetic context and do not contain any human sequences, and therefore these mice lack the proline-rich domain that has been shown to modify protein-protein interactions, aggregation and neuropathological phenotype (Saudou and Humbert, 2016; Zheng and Diamond, 2012). Levine and colleagues started z-series of mice, where both polyQ repeat mutation and the proline-rich stretch are humanized, whereas some of these lines unfortunately contain mutation of arginine in position 42), although this does not affect protein aggregation these mice are less studied (Levine et al., 1999; Menalled et al., 2000). The most used mouse lines of this series are zQ140 and zQ175 lines (no arginine mutation, but the latter has actually 190 CAG repeats (Menalled et al., 2003).

Compared to transgenic mice, disease progression is slower in the knock-in model mice. However, aggregation and behavioural disturbances caused by mutant huntingtin are more pronounced in the knock-in mice. Models with longer polyQ repeats are more widely used because the disease phenotype in mice with shorter repeat lengths is less apparent in mice. Although there are only few HD patients with homozygous mutant alleles (Lee et al., 2012), most of the research is done utilizing homozygous knock-in mice, as the phenotype is more robust and easier to measure. All these characteristics make knock-in mice models useful for more subtle HD phenotypes, as slowly progressing neuronal death, gliosis and myelin disruption or metabolic changes may not develop in short-lived transgenic mice (Ramaswamy et al., 2007; Zheng and Diamond, 2012).

In parallel with HD model mice, several cell lines were created that have facilitated studying HD. One of the first and most used series of cell lines was established from different *Hdh* knock-in mouse striatal precursor neurons (Zuccato et al., 2003). These lines are named *Hdh*^{7/7}, *Hdh*^{7/109} and *Hdh*^{109/109}, where the number shows CAG repeats in each allele of mouse huntingtin (*Hdh*, now denoted *Htt*) gene.

HD patient brain tissue and specific types of neural cells are limited and difficult to obtain. Therefore, the cellular reprogramming has become a valuable tool in neurodegenerative disease research (Rivetti di Val Cervo et al., 2021). In principle, the patient-derived neural progenitor cells can be obtained via direct transdifferentiation (Vierbuchen et al., 2010) or induced pluripotency followed by differentiation (Park et al., 2008). The genomic instability and epigenetic changes or loss of epigenetic marks and thereby the somatic memory of the cell create a high degree of variability in these cells and eventually in study results (Rivetti di Val Cervo et al., 2021). Additional shortcomings of the studies with reprogrammed cells are multitude of protocols, limited number of samples/lines in each study, and insufficient clinical data on patients (Guhr et al., 2018; Rivetti di Val Cervo et al., 2021). There are no therapies using iPSC for HD as the concerns of tumorigenicity of iPSC have remained, but embryonic stem cells (ESC) and induced pluripotent stem cells (iPSC) are found to be suitable for disease modelling (Geater et al., 2018). However, the full power of predictive modelling of disease progression and responsiveness to therapies require better integrative systems of *in vitro* iPSC and patient clinical data (Rivetti di Val Cervo et al., 2021). Three first ESC lines of HD were created from preimplantationally diagnosed IVF embryos in 2005 (Verlinsky et al., 2005). Although the HD iPSC Consortium has generated and made available several iPSC lines to overcome some problems indicated and to improve the quality of the HD research (The HD iPSC Consortium, 2012; The HD iPSC Consortium, 2017), many different cell lines exist, but the HD field is still missing an agreement on universal quality criteria for research and clinical grade iPSC cell lines that could path the way to more trustworthy research and cell-based therapy (Geater et al., 2018; Rivetti di Val Cervo et al., 2021).

1.3 Molecular mechanisms of Huntington's disease

Although extensively studied, a consensus about the causal mechanisms of Huntington's disease has not been reached. The proposed mechanisms include aggregation of mutant huntingtin, collapse of proteostasis network, impaired vesicle and organelle transport, mitochondrial dysfunction, excitotoxicity and transcriptional dysregulation among others. Extensive reviews on various aspects of HD have been written, the most recent ones are from Jimenes-Sanchez et al. (Jimenez-Sanchez et al., 2017) and Bates et al. (Bates et al., 2015). This overview focuses solely on transcriptional dysfunction observed in HD. The gene expression changes in different HD models are similar, lending support to the hypothesis of disturbed transcription being an essential factor in the pathogenesis of HD (Cha, 2007).

1.3.1 Transcriptional dysregulation

Hypothesis of transcriptional dysregulation in Huntington's disease arose from early neurochemical measurements in postmortem HD patient brains with specific cell loss and atrophy. Glutamate was one of the first neurotransmitters shown to be misregulated in HD, and was suggested to induce selective neuronal sensitivity to excitotoxicity in medium spiny neurons (MSN) of caudate putamen (Beal et al., 1986). Additionally, mRNA expression of N-methyl-D-aspartate (NMDA)-type glutamate receptor subunits, dopamine D1 and D2 receptors, glutamate transporter, neuronal nitric oxide synthase (nNOS) and proenkephalin and substance P among others were studied by *in situ* hybridization and were found mainly decreased in a cell-specific manner in HD postmortem brain tissue (reviewed in Cha, 2007). Decreased levels of neurotransmitter receptor mRNAs, neurotransmitters, and neurotransmitter metabolites were reported in HD, although it was under the debate whether these results might simply mirror the cell loss observed in the brain of HD patients. Whereas some of the results from that era may have been affected by the remarkable neural cell loss, the study by Augood and colleagues demonstrated decreased mRNA levels of neuropeptide enkephaline and substance P already in Vonsattel HD grade 0/1 HD brain without recognizable neuropathological abnormalities (Augood et al., 1996). Later, studies on transgenic HD mouse model R6/2 (Mangiarini et al. 1996) have established no widespread neuronal death in the otherwise fast-progressing HD disease model with altered neurotransmitter receptor expression similar to the pattern seen in human HD, therefore reinforcing transcriptional dysregulation as a separate feature of HD (Cha, 2007). Furthermore, many articles and reviews published to date still propose transcriptional dysregulation as one of the earliest features preceding neuronal death and therefore, possibly the most central mechanism in HD pathogenesis (Ament et al., 2018; Langfelder et al., 2016; Seredenina and Luthi-Carter, 2012; Sugars and Rubinsztein, 2003; Valor, 2015).

Advancements in methodology enabled to encapsulate the whole transcriptomic profile of specific organs, regions or timepoints in HD patients or HD models. The first microarray study came from Luthi-Carter et al., where distinctive set of signalling genes involved in striatal neuron function were found to be reduced in R6/2 mice as well as in N171-Q82 mice (Luthi-Carter, 2000). Scientists in the Huntington's Disease Array Group agreed on harmonizing array platforms and analysis tools, and on data sharing (Cha, 2007). Several studies on different HD models came to the conclusion that expression changes are similar between R6/2, R6/1, N171-82Q and HD190QG transgenic mice all expressing human *HTT* exon 1, and the affected genes were also in line with human HD microarray data (Desplats et al., 2006; Hodges et al., 2006; Luthi-Carter, 2002; Oyama

et al., 2006; Thomas et al., 2011). However, despite the fact that gene expression alterations seem to be a common theme in HD, the ratio of up- and downregulated genes may vary drastically and contradicting results have been published even in the same model system (Crocker et al., 2006; Luthi-Carter, 2000). Furthermore, different full-length *HTT* HD models have (YAC128, Hdh(Q92/Q92), CHL2(Q150/Q150)) or have not (YAC72, HD46, HD100) recapitulated the findings in transgenic mouse model expressing truncated *HTT*, suggesting that the details of the genetic context of *HTT* gene and specific codons of polyQ (CAG versus mixed CAA-CAG) might be involved in gene expression alterations (Becanovic et al., 2010; Chan, 2002; Kuhn et al., 2007; Luthi-Carter, 2002). Reproducibility of microarray results is established as a general problem, partially caused by small sample sizes and limited range of sensitivity, but is further affected by differences between HD models. To overcome this limitation and to ease comprehension of huge gene lists, meta-analysis of archival gene expression dataset of HD postmortem human brain regions and R6/2 and HdhQ150 mice were utilized in weighted correlation network analysis (Neueder and Bates, 2014). In that study, transcriptional dysregulation was also uncovered in HD cerebellum with gene expression changes similar to caudate nucleus and prefrontal cortex (BA4 region) in human. Additionally, the authors concluded that apart from alterations in immune system, HD mouse models closely mimic most of the characteristics of HD in humans. Collectively, the main outcomes from numerous microarray experiments were establishment of neural and/or striatal specificity of downregulated genes, confirmation of reduced mRNA levels of neurotransmitters, their receptors, Ca²⁺, Na⁺ and K⁺ channels, genes involved in secondary messengers system, nuclear receptors, genes of homeostasis and regulators of metabolism and chromatin remodelling factors (reviewed in (Cha, 2007; Seredenina and Luthi-Carter, 2012).

More recent RNA-seq, ChIP-seq and other sequencing and analysis methods have established more pathways involved in HD and major transcription factors responsible for transcriptional dysregulation in HD. The most thorough genomics and proteomics study to define huntingtin polyQ length-dependent gene networks in mice was published by Langerfelder and colleagues, and interactive online resource HDinHD.org was created that is maintained in collaboration with CHDI foundation to disseminate the data (Langfelder et al., 2016). Mutant *HTT* repeat length-dependent transcriptional signatures were clearly apparent in striatum, whereas the differences were smaller in cerebral cortex and liver (Langfelder et al., 2016). Their co-expression network analysis disclosed that top striatal modules contained medium spiny neuron identity genes, indicated by dysregulation of cyclic adenosine monophosphate (cAMP) signalling, cell death and protocadherin genes. Moreover, the authors validated 22 genes as modifiers of mutant *HTT* toxicity *in vivo* in a *D. melanogaster* HD model (Langfelder et al., 2016).

The heterogeneity of the complex manifestations of symptoms observed in HD patients are present also in mouse models (Gallardo-Orihuela et al., 2019). A study of transcriptional correlates of the motor and cognitive pathological phenotype traits revealed partial decrease of HD-associated genes (*Pde10a*, *Drd1*, *Drd2*, *Ppp1r1b*) in mice striatum that showed poor overall phenotypical score, whereas upregulation of transcripts (*Nfya*) associated with relatively better outcome were also observed (Gallardo-Orihuela et al., 2019). Of note, as authors discuss, the phenotype-transcription association cannot be explained by simple worsening of the transcriptional dysregulation in disease progression and an inherited and early-acquired epigenetic pattern may influence the manifestation of the disease in adulthood in otherwise isogenic mice.

The main limitation of many studies involving HD patients is the low number of samples. This is especially problematic, as HD is a progressive disease with varying age of onset. Furthermore, postmortem interval of sample collection and limitations of proper control group formation are also problematic. The biggest sample size up to date was used to study gene expression in prefrontal cortex of HD patients and pathologically normal controls. The identified differentially expressed genes were enriched for immune response, neuroinflammation, and developmental genes (Labadorf et al., 2015). Unexpectedly, the biggest changes were identified for a set of homeotic genes that had not been widely implicated in HD earlier (Labadorf et al., 2015). This study was followed by addition of more frontal cortex BA9 region HD disease samples and caudate nucleus samples at prodromal stage HD, and these neuronal tissues showed highly similar differentially expressed gene (DEG) profiles suggesting a common response to disease (Agus et al., 2019). The latter study revealed that caudate nucleus is affected prior to HD symptom onset, although a very small sample size used in the study may affect the conclusion (Agus et al., 2019). Therefore, meta-analysis of several studies may present more accurate results. Machine learning and comprehensive network biology approach were utilized on publicly available DNase-seq and brain transcriptomic and proteomic data from HD mouse models to investigate the roles of core transcription factors that drive gene expression changes in HD (Ament et al., 2018). The created transcriptional regulatory network enabled identification of 48 differentially expressed transcription factor target gene modules that help to explain previously published gene co-expression modules altered in HD. Furthermore, thirteen of those identified transcription factor modules were relevant in four different datasets from HD patients' striatum containing genes *GLI3*, *IRF2*, *KLF16*, *NPAS2*, *PAX6*, *RARB*, *RFX2*, *RXRG*, *SMAD3*, *TCF12*, *TEF*, *UBP1*, and *VEZ1*. Additionally, the authors noted that the targets of transcription factors in the downregulated sub-network were enriched for synaptic genes and seem to be essentially neuronal, whereas target genes of transcription factors from upregulated sub-network were enriched for stress response pathways including DNA damage repair and apoptosis (Ament et al., 2018).

Availability of brain tissue samples from HD patients is limited, therefore, in conjunction with the notion of transcriptional dysregulation in HD before disease onset, the usability of blood as an easily accessible tissue has been extensively studied, however, leading to inconclusive results (Borovecki et al., 2005; Lovrecic et al., 2009a; Mastrokolas et al., 2015; Runne et al., 2007). Two ongoing studies, namely Track-HD and Leiden HD cohort, follow HD carriers through disease pre-manifest, manifest and developed disease stage and gather a multitude of metrics. The most recent RNA-seq gene set enrichment analysis of the whole blood collected in these studies compared it with published correlation network analysis modules from HD and control brain datasets (Hensman Moss et al., 2017). This analysis identified dysregulated gene sets in the blood, which correlated with disease severity and with the most significantly dysregulated clusters of genes in the caudate nucleus in HD patients. Upregulated pathways were related to immune response and lipid metabolism and clusters of genes related to ion channels were downregulated (Hensman Moss et al., 2017). Therefore, these results suggest that mutant HTT induces common transcription disruption profiles in HD brain and blood, whereas at the level of specific genes, the correlation is weak as reported also in earlier publications (Borovecki et al., 2005; Lovrecic et al., 2009b; Mastrokolas et al., 2015; Runne et al., 2007).

Finally, in the future, genome-wide transcriptional profiling and RNA-seq could enable the usage of genome wide gene expression profiles as indicators of effectiveness in HD therapies (Cha, 2007; Valor, 2015).

1.3.2 Mechanisms of transcription dysregulation

The polyglutamine-expanded form of HTT may have a direct role in aberrant gene expression in HD, and this theory is reinforced by the data of transcriptional dysregulation in other polyQ tract diseases (Luthi-Carter, 2002). Transcription factors found to be altered in HD can be grouped based on whether the impairment detected is related to decrease of wild type HTT or expression of aggregation-prone mutant HTT. Therefore, both loss-of-function and gain-of-function hypothesis of HD have been proposed. Normal HTT binds better CA150, CtBP, LRXalpha, NRSF/REST, PRC1L, SP1, while increased association with mutant HTT has been detected for BCL11B, POU3F2 (alias BRN2), CBP/EP300/pCAF, NCOR1, NFYA/NFYB/NFYC, PQBP1, polycomb repressor complex proteins EZH2 and SUZ12, GTF2F2 (alias RAP30), TAF4 (alias TAFII130) (Seredenina and Luthi-Carter, 2012; Sugars and Rubinsztein, 2003). This suggests that imbalanced gene expression in HD could potentially be caused by the decreased levels of wild-type HTT and also by ectopic expression of polyQ-extended HTT protein. However, some HTT binding proteins like SIN3A, p53 and SETD2 (alias HYPB) seem not to have a clear preference and bind wt and mutant HTT with equal affinity (Seredenina and Luthi-Carter, 2012; Sugars and Rubinsztein, 2003). Interestingly, only some of these HTT-interacting transcription factors are found in polyQ aggregates and inclusion, and there is no correlation with whether the transcription factors involved contain a polyQ domain themselves. Factors that have been shown to be sequestered into mutant HTT inclusions include CBP, EP300, SIN3A, p53, SP1, TAF4 and TBP (extensive list can be found in Seredenina and Luthi-Carter, 2012).

Loss-of-function mechanisms impair specific pathways and processes where wild type HTT acts as a regulator. Participation of wild type HTT in gene expression regulation through neuron-restrictive silencing factor/ repressor element 1 silencing factor (REST/NRSF) was the first and is to date one of the most studied pathways altered in HD. Series of publications from Zuccato and colleagues have shown that wild-type HTT sequesters REST/NRSF in cytoplasm and thereby prevents inhibition of the neurotrophic factor *BDNF* gene (Zuccato, 2001; Zuccato et al., 2007, 2003). Their studies showed that this function is lost for mutant HTT. Moreover, many neuronal genes have been found to have REST/NRSF binding sites (RE-1/NRSE) and REST/NRSF also regulates expression of certain miRNAs relevant in nervous system (Bruce et al., 2004; Buckley et al., 2010; Conforti et al., 2013; Mortazavi et al., 2006; Rossbach, 2011). A negative feedback loop by mir-9/mir-9* regulates *REST* and *CoREST* (Packer et al., 2008). Therefore, increased concentration of REST/NRSF in cell nucleus in HD leads to altered expression of REST/NRSF-regulated genes, many of which are essential for neuronal development and maintenance. Additionally, it has been shown that wild type HTT binds directly mixed lineage kinase 2 (MLK2/MAP3K10) and through huntingtin associated protein 1 (HAP1) it binds NEUROD family members NeuroD1 and NeuroD2, and in sum, these bindings facilitate activation of NEUROD1 by phosphorylation (Marcora et al., 2003). Furthermore, it is plausible that HTT-HAP1 complex participates in the nuclear translocation of NeuroD (Saudou and Humbert, 2016) as it is shown for REST (Shimojo, 2008).

Both wild type and mutant HTT have been shown to bind to DNA in R6/2 mice brain and Hdh^{Q111} cells, whereas they display differential genomic distribution (Benn et al., 2008). Although the authors detected polyQ-dependent increased binding of mutant HTT

to recognition elements of transcription factors whose function is altered in HD, these binding events did not correlate with changes in target gene mRNA levels (Benn et al., 2008). Therefore these results suggest that HTT mediates association of large protein complexes instead of being itself a transcription factor and the formed complexes might alter genomic DNA conformation and transcription factor binding (Benn et al., 2008; Seredenina and Luthi-Carter, 2012). HTT also has functions in the regulation of miRNAs by binding AGO2 protein (Argonaute RISC Catalytic Component 2) and participation in the formation and/or functioning of P-bodys, which are perturbed by mutant HTT (Savas et al., 2008). This needs to be taken into account during development of allele-selective miRNA therapeutics for HD as mHTT may compromise participation of AGO family members and thereby productive cleavage of miRNAs (Ciesiolka et al., 2020; Hu et al., 2012). Since dynamic composition of miRISC (miRNA-induced silencing complex) plays a role in neurogenesis, differentiation, synapse formation and plasticity (Nawalpuri et al., 2020) impaired functionality of AGO2 due to expression of mHTT might be of relevance when studying neurodevelopmental aspects of HD.

Studying gain-of-functions of mHTT in the context of HD has have been more in focus than studying loss-of-functions. Direct gain-of-function mechanism of mutant HTT in transcriptional dysregulation arises from its ability to bind some transcription factors and components of the basal transcriptional machinery more avidly and sequester them into aggregates and inclusions. Specificity protein 1 (SP1)-dependent genes are especially impacted in R6/2 mice as reported in the first microarray analysis conducted to study HD (Luthi-Carter, 2000). Later, it was revealed that increased binding of SP1 to mutant HTT disrupted SP1 binding to TFIID subunit TAF4 (Dunah, 2002). Additional components of core transcriptional machinery adversely affected by mutant HTT are RNA polymerase II large subunit (RPB1) and subunits of TFIID (TBP, TAF4 and GTF2F2 (aliases TFIIF/RAP30)) (Dunah, 2002; Luthi-Carter, 2002; Zhai et al., 2005). Of note, despite the initial notions of SP1-dependent misregulation many SP1-regulated genes are expressed at normal levels in HD and the hypothesis of general downregulation of RNA polymerase II-dependent transcription is in contradiction to studies indicating mRNA and miRNA upregulation in HD (Desplats et al., 2006; Luthi-Carter, 2000; Seredenina and Luthi-Carter, 2012).

There has been a search for additional modifiers that could confer tissue specificity and/or affect disease progression in HD. Distinct epigenetic signatures of downregulated genes have been found to be partially responsible for the differences observed in different brain regions and patients. Transcriptionally repressed promoters are characterized by increased histone H3 lysine 4 trimethylation (H3K4me3) in R6/2 mice and human HD brain (Vashishtha et al., 2013). Reduction of demethylase levels effectively reversed down-regulation of key neuronal genes in R6/2, BACHD mice and *D. melanogaster* HD model (Vashishtha et al., 2013). Achour et al. studied R6/1 (with approx. 150Q repeats (officially R6/1 mice have 115Q repeats)) mice striatum and found reduced H3K27ac epigenetic marks at down-regulated genes in addition to decreased RNAPII occupancy. Moreover, they showed that striatal super-enhancers (regulating genes defining tissue identity and function) are characterized by temporally extended and high levels of H3K27ac, and that H3K27ac is reduced in these striatal enhancers in HD (Achour et al., 2015). Therefore, they proposed that these enhancers control genes (mainly) downregulated in R6/1 mice. Additionally, they showed that the level of CREB-binding protein (CBP) binding is higher at neuronal activity-regulated genes decreased in HD compared to activity-regulated genes increased in HD (Achour et al., 2015). In conclusion, the specific epigenetic signature of striatal genes downregulated in

HD are characterized by high levels of H3K4me3, H3K4me1, H3K27ac and RNAPII occupancy along genes and further rely on super-enhancers topography (Achour et al., 2015; Steffan et al., 2001; Valor, 2015; Vashishtha et al., 2013).

CBP is one factor that is affected in HD and may amplify detrimental effects of mHTT. Co-activator protein CBP acts as a bridge between CREB and the basal transcriptional machinery and contains also a polyQ tract (Lonze and Ginty, 2002; Sugars and Rubinsztein, 2003). CBP has acetyltransferase activity and acetylation of histones by CBP results in more open chromatin structure (Steffan et al., 2001). CBP functions are affected in HD by different mechanisms. First, CBP is included in HTT aggregates in HD cell culture models, HD transgenic mice, and human HD postmortem brain, and this interferes with CBP-activated gene transcription (Nucifora Jr., 2001; Steffan et al., 2000; Sugars and Rubinsztein, 2003). Second, increased proteasomal degradation of CBP has been described in PC12 cells expressing mutant *HTT* exon 1 (Cong et al., 2005). For comparison, this selective degradation of CBP is absent in spinocerebellar ataxia 3 (SCA3) cells, although mutant ataxin-3 attracts CBP into aggregates similar to mHTT (Chai et al., 2001; Cong et al., 2005). Third, acetyltransferase activity of CBP is abolished by direct binding of mutant HTT to CBP acetyltransferase domain (Steffan et al., 2001). The role of CBP dysfunction in HD is further supported by the demonstration that overexpression of CBP abolishes neuronal toxicity in HD models (Nucifora Jr., 2001). Collectively, these impairments of CBP by mHTT have an effect on the transcription of CBP-dependent genes.

Both tumour suppressor protein p53 and HTT possess polyproline moiety that has been shown to be additional modifier of mutant HTT fibril formation and cellular toxicity (Falk et al., 2020). Polyproline rich domain is essential for their interaction and it has been shown that mutant HTT binds p53 more efficiently, although contradictory outcomes of the binding have been reported (Bae et al., 2005; Steffan et al., 2000). At first, p53-dependent transcription was shown to be downregulated in HD (Steffan et al., 2000), whereas a later study revealed that mutant HTT disturbed interactions with the regulatory proteins of p53, thereby stabilizing p53, leading to upregulation of p53 and activation genes involved in cell-cycle control, apoptosis, cellular stress responses, and DNA repair (Bae et al., 2005). In addition to gain-of-function effect of mutant HTT on p53, a negative feed-back loop regulating *HTT* expression via p53 has been proposed (Feng et al., 2006). *HTT* gene itself contains multiple putative p53-response elements, and it has been shown that increased p53 levels induced *HTT* expression in human lung carcinoma cell line H1299/V138 and in mouse cerebral cortex and striatum (Feng et al., 2006). At the same time, studies on *TP53*-deficiency have provided inconsistent results, varying from beneficial changes like restoration of proenkephalin expression and aggregation of mutant HTT as a protective mechanism in Hdh^{Q140} mice and mHTT overexpressing MEF cells (Ryan et al., 2006), to no effect on *HTT* levels in human HEK 293 cells (De Souza et al., 2018). Therefore, participation of p53 in the regulation of *HTT* gene expression is currently unclear. Cell fate specified by the activation of stress sensor p53 depending on cell-type, environment and nature of the stressor may still play a role in HD (Bigan et al., 2020; Thomson and Leavitt, 2018).

In conclusion, both loss- and gain-of-functions of HTT are established in the dysregulation of transcription in HD, illustrating the complex role of HTT in both health and disease.

2 Transcription Factor TCF4

Transcription factor TCF4 belongs to the large and diverse helix-loop-helix (HLH) transcription factor (TF) family. It has been proposed that genes encoding for HLH proteins arose in unicellular organisms over 600 million years ago and duplication and diversification from ancestral genes occurred with multicellularity across the metazoan and plant kingdoms (Murre, 2019). Hundreds of HLH proteins have been identified with diverse functions in a wide variety of cell types (Massari and Murre, 2000; Murre, 2019).

Gene programs controlled by basic HLH (bHLH) transcription factors are lineage specification and commitment, self-renewal, proliferation, differentiation, and homing. Moreover, they also regulate circadian clock, protect against hypoxic stress, promote antigen receptor locus assembly, and program transdifferentiation (Murre, 2019). Additionally, roles of bHLH proteins have been shown in depositing or erasing epigenetic marks, activating noncoding transcription, and dictating enhancer–promoter communication and somatic recombination (Murre, 2019). The whole bHLH transcription factor family has emerged as a key determinant of neural cell fate specifications and differentiation in both development and disease (Dennis et al., 2019).

TCF4 is a member of the broadly expressed bHLH class I or E protein subfamily that binds Ephrussi box sequence (E-box) as homodimers or as heterodimers (Figure 1) with tissue specific class II bHLH proteins (Le Dréau et al., 2018; Murre, 2019). Additional members of E protein family are Transcription factor E2-alpha, also known as E12/E47 (encoded from *TCF3* gene (historical name *E2A*)) and TCF12 (encoded from *TCF12* gene (historical name *HEB*)). There is a single E protein in *Drosophila*, Daughterless (Da) and in *C. elegans*, hlh-2. DNA binding of TCF4 is inhibited through dimerization with HLH class V ID (Inhibitors of DNA-binding) proteins (Wang and Baker, 2015). TCF4 has been known by a multitude of names like ITF2, SEF2, ME2, E2-2, originating from the context of its discovery (Teixeira et al., 2021). Of note, the unfortunate parallel usage of the same name *TCF4* for transcription factor 7-like 2 (*TCF7L2*) gene, a member of the TCF/LEF family of transcription factors, has created confusion and misinterpretation of numerous results in the scientific literature.

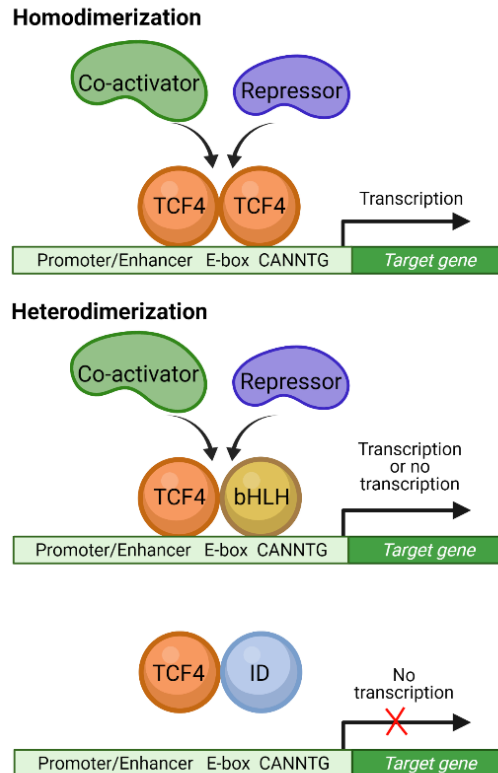


Figure 1. DNA-binding of transcription factor TCF4. TCF4 belongs to TF family of bHLHs that bind DNA as dimers. TCF4 dimers bind to Ephrussi box (E-box) with consensus sequence of CANNTG. TCF4 homodimers can be formed with all TCF4 isoforms. Heterodimerization partners of TCF4 are mainly transcription-activating bHLH class II tissue specific transcription factors (yellow) or other E proteins (TCF3 or TCF12). Dimerization with DNA-binding domain-deficient ID proteins (bHLH class V) disrupts DNA-binding and target gene transcription activation. bHLH – basic helix-loop-helix; E-box – Ephrussi box; ID – inhibitor of DNA binding. Created with BioRender.

Classical E-box is defined as CANNTG and TCF4 binding preference is thought to be adjusted by its dimerization partners (Wang and Baker, 2015). The strongest binding of TCF4 has been observed for the motif CAGGTGGT (Khund-Sayeed et al., 2016). Additionally, DNA binding of TCF4 in the context of E-box motifs ACATGTG and ACACGTG is decreased in the presence of 5-methyl-cytosine and increased in the presence of 5-hydroxymethyl-cytosine (modified cytosines are marked bold) (Khund-Sayeed et al., 2016). TCF4 DNA binding has also been studied in the context of an expanded consensus E-box 5'-⁰C(A/G)-¹CA²NNTG-3', with an added outer ⁰Cp(A/G) dinucleotide that can be methylated, successively oxidated and finally carboxylated (Yang et al., 2019). The study revealed that modification of the potential central E-box dinucleotide ²NN=²CG has very little effect, E-box dinucleotide ¹CA modification has a negative effect, whereas modifications of expanded E-box dinucleotide ⁰CG, particularly carboxylation, has a strong positive impact on TCF4 binding to DNA (Yang et al., 2019).

TCF4 haploinsufficiency causes Pitt-Hopkins syndrome (PTHS) (OMIM #610954) (Goodspeed et al., 2018; Sweatt, 2013; Zweier et al., 2007) and increased CTG trinucleotide repeat in intron 3 has been linked to Fuch's endothelial corneal dystrophy (OMIM #613267) (Fautsch et al., 2020; Ong Tone et al., 2021). Several genome-wide association studies (GWAS) have associated *TCF4* and SNPs in it with schizophrenia (SCZ) and other psychiatric conditions, although the direct mechanism has remained elusive (Doostparast Torshizi et al., 2019; Navarrete et al., 2013; Teixeira et al., 2021).

2.1 *TCF4* gene and protein structure and expression

TCF4 gene is located at 18q21.2 in human. *TCF4* gene expands approximately 0.365 Mb, has a complex gene structure, and is highly conserved in rodents and human (Sepp et al., 2011). Daughterless (*Da*) is studied in *D. melanogaster* as the sole orthologue of E proteins with highest similarity to *TCF4*, although very high sequence conservation is demonstrated only for the bHLH region (Tamberg et al., 2015).

Protein isoforms *TCF4-B*⁺ and *TCF4-B*⁻, *TCF4-A*, *TCF4-D* had been described before this study (Corneliussen et al., 1991; Liu et al., 1998; Skerjanc et al., 1996; Yoon and Chikaraishi, 1994). The calculated molecular weight of full length *TCF4* protein (*TCF4-B*) is 71 kDa. This isoform contains three transactivation domains AD1, AD2 and AD3 (Chen et al., 2013; Massari et al., 1996; Quong et al., 1993). In *TCF4* protein there are described also two repression domains – CE (Herbst and Kolligs, 2008) and Rep (Markus et al., 2002; Wong et al., 2008). Binding of DNA is facilitated by basic sequence (b) that precedes HLH domain and it coordinates dimerization (Tapscott et al., 1988). bHLH is followed by conserved C domain required for dimerization *in vivo* (Goldfarb et al., 1998). The illustrative schematic structure of *TCF4* protein with functional domains including ADs, NLS, NES, Rep, CE and C is shown on Figure 2 (data from Forrest et al., 2014, Sepp et al., 2011 and Greb-Markiewicz et al., 2019). However, interaction between these domains and other proteins that regulate the activity and functions of *TCF4 in vivo* has remained elusive.

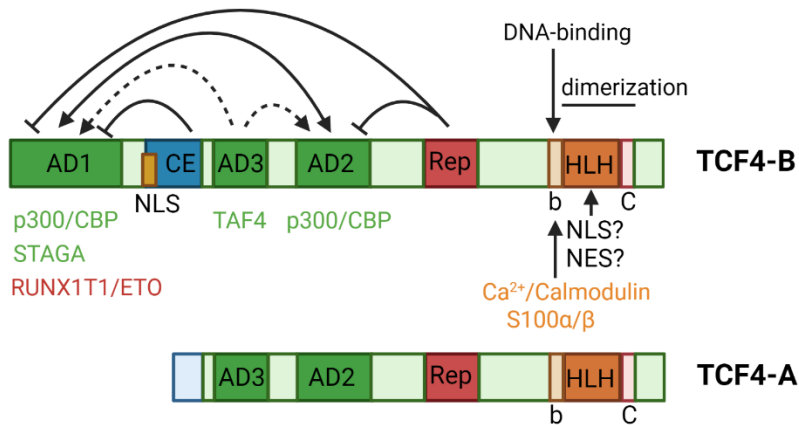


Figure 2. Protein domains of transcription factor TCF4. TCF4-B is the full length isoform and TCF4-A is the best studied short isoform (altogether, 18 N-terminally different protein isoforms have been identified to date). Shown are known domains of TCF4 and activation arrows and inhibition lines indicate the effects of different domains on ADs. Known co-activators (green) of TCF4-dependent transcription are p300/CBP, STAGA complex and TAF4 subunit of general transcription factor II D (enhancing the formation of the RNA polymerase II preinitiation complex at target genes). Binding of repressor protein (red) RUNX1T1/ETO promotes DNA condensation through recruitment of histone deacetylases and this binding competes with p300/CBP for the same site. Additionally, Ca²⁺-dependent calmodulin and S100 proteins binding to basic residue (b) affect binding of TCF4 to DNA and dimerization mediated by HLH domain. AD – activation domain; b – basic residues; C – conserved domain; CE – conserved element/ conserved repressor; HLH – helix-loop-helix motif; NES – nuclear export signal; NLS – nuclear localization signal; p300/CBP – E1A binding protein p300/ CREB binding protein; Rep – conserved repression domain; RUNX1T1/ETO/MTG8 – runt-related transcription factor 1/Eight Twenty One protein/myeloid translocation gene on chromosome 8; STAGA – SPT3-TAF(II)31-GCN5L acetylase; S100α/β – S100 Ca binding protein A/B; TAF4 – TATA-Box Binding Protein Associated Factor 4. Created with BioRender.

TCF4 is expressed in many human and murine tissues including heart, brain, lung, liver, placenta, skeletal muscle, kidney, pancreas, spleen and testis, and during murine embryonic development between gestational days 9.5 to 19.5 *post coitum* (Pscherer et al., 1996; Sepp et al., 2011; Skerjanc et al., 1996). Furthermore, high expression of *Tcf4* has been observed throughout the nervous system of adult mouse and in the developing brain (Chiamarello et al., 1995; de Pontual et al., 2009; Soosaar et al., 1994; Uittenbogaard and Chiamarello, 2000). Specific *TCF4* transcripts are upregulated in iPSC-derived human neural progenitor cells (NPCs) upon neural differentiation, although total *TCF4* mRNA levels remain unchanged (Hennig et al., 2017). Additionally, *TCF4* mRNA is expressed region-specifically in radial glia and stem cells of transient zones in both humans and mice embryos (H. Li et al., 2019). Recently, single cell RNA-seq was conducted to trace the transcriptional trajectories of successive generations of apical progenitors and their respective daughter neurons in mice from embryonic to early postnatal stages, and high expression of *Tcf4* was observed throughout neuronal development (Telley et al., 2019).

At protein level TCF4 is highly expressed in adult hippocampus, cerebellum, cerebral cortex, and nuclei in mouse and human amygdaloid complex (Jung et al., 2018), and in developing dorsal telencephalon in both human and mouse (Mesman et al., 2020).

Generation of *Tcf4* reporter mouse co-expressing GFP with TCF4 enabled to characterize high expression of TCF4 in most cortical and hippocampal cells, including excitatory and inhibitory neurons, as well as astrocytes and oligodendrocytes. The expression of TCF4 was restricted to interneurons and in cerebellum to granule neurons in striatum (Kim et al., 2020).

Very little is known about the regulation and activation of *TCF4* gene expression. Binding of transcription factors REST (NRSF), NFKB1, SPI1 (PU.1), and POU2F2 (previously known as OCT-2) to *TCF4* locus has been shown experimentally with ChIP (ENCODE Chip-seq data) (Euskirchen et al., 2007; Robertson et al., 2007; Rozowsky et al., 2009). Some of these factors are well known to be important in neurogenesis and neuronal plasticity (Masgutova et al., 2019; Theodorou et al., 2009; Zuccato et al., 2003). Additionally, an evolutionally conserved site (hs376) in a *TCF4* intron has been shown to induce reporter gene expression in the nervous system during mouse development (Navarrete et al., 2013). Pharmacological agents that alter the activity of the WNT signalling pathway regulate *TCF4* mRNA and protein expression, and histone deacetylase (HDAC) inhibitors enhance *TCF4* gene expression in human neuronal progenitor cells (Hennig et al., 2017). Furthermore, both WNT signalling activators and HDAC inhibitors upregulate *TCF4* gene expression in PTHS patient-derived fibroblasts, suggesting that these signalling pathways can be manipulated to alter *TCF4* gene expression in a therapeutically relevant manner (Hennig et al., 2017). Although the mechanism itself is not elusive, the therapy with HDAC inhibitors or HDAC knock-down has been beneficial in PTHS models (Kennedy et al., 2016). HDAC inhibitors normalize hippocampal long term potentiation (LTP) and memory recall. HDAC inhibitor vorinostat has been identified to modulate memory-associated genes dysregulated by *TCF4* haploinsufficiency (Kennedy et al., 2016). Furthermore, *Hdac2* isoform-selective knockdown is sufficient to rescue memory deficits in *Tcf4*^{+/-} mice (Kennedy et al., 2016).

A conserved distal enhancer in *TCF4* has been identified that binds TCF4 protein and mediates the exclusive upregulation of *TCF4-B* expression during plasmacytoid dendritic cell (pDC) lineage commitment, thus creating a positive feedback loop for TCF4 long isoforms (Grajkowska et al., 2017). This reveals the complex developmental regulation of E protein activity, which involves lineage-specific expression of E protein isoforms and feedback regulation through distal regulatory elements (Grajkowska et al., 2017). Recent research has demonstrated that TCF3 up-regulates *TCF4* by binding to the specific E-box sequence in an intron of the *TCF4* gene (H. Li et al., 2019). *Tcf4* levels are significantly reduced in the telencephalon of *Tcf3* knockout mice at embryonic day 12 (E12) but not at E14 or at birth, indicating that the regulation of *Tcf4* expression by TCF3 in the dorsal telencephalon is limited to the early embryonic stage and restoration of *Tcf4* expression at later stages depends on a mechanism yet to be discovered (H. Li et al., 2019).

2.2 Functions of TCF4 in the nervous system

The essentiality of TCF4 was first demonstrated by Zhuang et al showing that homozygous *Tcf4* mutant mice are born at extremely low frequency and die within the first week after birth (Zhuang et al., 1996). However, heterozygous *Tcf4* mutant mice appear normal and indistinguishable from wild type littermates (Zhuang et al., 1996). Loss of one copy of functional *TCF4* in human results in Pitt-Hopkins Syndrome (PTHS) that is described by developmental delay, mild to severe intellectual disability, language impairment, breathing pattern abnormalities and recurrent seizures (Whalen et al., 2012). Alterations in *TCF4* gene have been linked to schizophrenia, bipolar disorder and

non-syndromic intellectual disabilities (NSID), and to be responsible for developmental delay (Cross-Disorder Group of the Psychiatric Genomics Consortium, 2013; Genetic Risk and Outcome in Psychosis (GROUP) et al., 2009; Kalscheuer et al., 2008; Kharbanda et al., 2016; The Schizophrenia Psychiatric Genome-Wide Association Study (GWAS) Consortium, 2011). Recently, utilizing several CommonMind Consortium RNA-seq data of different tissues of schizophrenic patients the deconvolution of the regulatory processes mediating schizophrenia (SCZ) was done computationally, resulting in the identification of TCF4 as a master regulator in SCZ (Doostparast Torshizi et al., 2019). Furthermore, human-induced pluripotent stem cell (hiPSC)-derived neurons were used to empirically validate the role of TCF4 in orchestrating a schizophrenia-associated cellular transcriptional network (Doostparast Torshizi et al., 2019). As a result, TCF4 was suggested to contribute to SCZ susceptibility at early stages of neurodevelopment. Additionally, based on TCF4 protein expression patterns and TCF4-linked pathologies Kim and colleagues predicted that the prefrontal cortex and hippocampus are the pathophysiological loci for TCF4-linked disorders (Kim et al., 2020). Cognitive dysfunction and impaired memory function seem to be the common theme in disorders caused by or associated with mutations and variations in TCF4 gene.

The tissue- and cell type-specific roles of the broadly expressed TCF4 are largely determined via its dimerization with different class II bHLH partners. TCF4 has been shown to participate in hematopoiesis, myogenesis, melanogenesis, osteogenesis and neurogenesis, and in the differentiation of endothelial, mammary gland, placental, and Sertoli cells (reviewed by Teixeira et al., 2021). Participation of various class II bHLH proteins in the maintenance of neural progenitor cells (NPC) and their differentiation into neurons, oligodendrocytes and astrocytes is well known (Imayoshi and Kageyama, 2014). Since expression of TCF4 in the nervous system peaks during prenatal development and relatively high levels persist through adulthood (Kim et al., 2020; Li et al., 2018; Quednow et al., 2014), it has been postulated that TCF4 is relevant in both developing and adult nervous system development and physiology. Although there is evidence for dimerization of TCF4 with the proneural bHLH factors, systemic data on direct engagement of TCF4 in proneural bHLH-dependent processes are scarce. The study by Flora et al. identified the interaction of TCF4 with proneural bHLH factor ATOH1 (MATH1), and demonstrated disrupted development of pontine nucleus of *Tcf4*^{-/-} mice (of note, they did not observe embryonic lethality of null animals) (Flora et al., 2007). Furthermore, deletion of any of the additional E protein-encoding genes did not have detectable effects on ATOH1-dependent neurons, indicating a specific requirement of TCF4:ATOH1 heterodimers in this process (Flora et al., 2007).

TCF4 has been shown to participate in neurogenesis in mouse postnatal forebrain and in developing and adult hippocampus (Fischer et al., 2014; Jung et al., 2018). Furthermore, knocking out long transcripts of *Tcf4* in mice results in reduced cortical thickness and decreased dentate gyrus volume (Jung et al., 2018).

TCF4 has roles in neuronal migration, laminar layer formation, and dendrite and synapse formation in the developing cortex. These functions are impaired in *Tcf4* haploinsufficient mice (H. Li et al., 2019). Deletion of *Tcf4* results in mis-specification of CTIP2- and SATB2-expressing neurons in the mouse cerebral cortex, leading to defective development of the corpus callosum, anterior commissure, and the hippocampus (Mesman et al., 2020). In addition, *in utero* overexpression of TCF4 in mouse cerebral cortex severely disrupts the columnar organization of medial prefrontal cortex (Page et al., 2018). This phenomenon was dependent on transcription and neuronal activity, and

co-expression of TCF4 together with calmodulin and inwardly rectifying potassium channel Kir2.1 (that lowers the resting membrane potential and thereby reduces neuronal activity) rescues this morphological phenotype (Page et al., 2018). Besides migration and organization of neurons in the dorsal telencephalon, a role for TCF4 in the migration of the pontine nucleus neurons in anterior extramural migratory stream has also been described (Flora et al., 2007).

Enhanced hippocampal long term potentiation (LTP) has been described in several *TCF4* haploinsufficiency syndrome PTHS model mice (Thaxton et al., 2018). This synaptic phenotype might be linked to cognitive dysfunctions reported in PTHS patients (Thaxton et al., 2018). Reduction of TCF4 in prefrontal cortex layer 2/3 *in utero* alters the intrinsic excitability of neurons in this layer via repression of ion channel genes *Scn10a* and *Kcnq1* in rats (Rannals et al., 2016).

Besides the functions of TCF4 in neurons, studies in PTHS mouse models have revealed a cell-autonomous reductions of oligodendrocytes and myelination pointing to independent roles of TCF4 in oligodendrocytes (Phan et al., 2020).

2.3 Target genes of TCF4 in the nervous system

TCF4 binds DNA and regulates expression of its target genes in the context of different heterodimers, and this complicates identifying its direct target genes. Genome wide expression and chromatin binding profiling have been the main methods for TCF4 target gene analysis.

A few studies have analysed differentially expressed genes in human cell lines after knock-down of *TCF4*. Acute *TCF4* knock-down in SH-SY5Y cells resulted in altered expression of genes involved in TGF- β signalling, epithelial to mesenchymal transition (EMT) and apoptosis (Forrest et al., 2013). More precisely, the most significant DEGs were EMT regulators, *SNAI2* and *DEC1* and the proneural genes, *NEUROG2* and *ASCL1* (Forrest et al., 2013). Reduced *TCF4* in a neural progenitor cell line (derived from the developing human cerebral cortex) led to deregulation of genes involved in the cell cycle (Hill et al., 2017).

Tcf4-deficient mice have been used to identify TCF4 target genes *in vivo*. Notably, *Bmp7* is upregulated in *Tcf4*-deficient mice developing cerebral cortex and neuronal migration and deficits in these mice can be rescued via shRNA-mediated downregulation of *Bmp7* (Chen et al., 2016). The effect of reduced levels of TCF4 in neural progenitor cell line derived from the developing human cerebral cortex was analysed with microarray technology and results showed enrichment of genes involved in the cell cycle and proliferation of progenitor cell (Hill et al., 2017). RNA-seq performed with hippocampal CA1 tissue from naive *Tcf4*^(+/-) (PTHS model) mice identified over 400 differentially expressed genes associated with neuronal plasticity, including axon guidance, cell adhesion, calcium signalling, and most particularly with neurotransmitter receptors (Kennedy et al., 2016). The authors suggested that genes negatively regulated by TCF4 participate in the signalling of dopamine (*Drd1a*, *Cckbr*, and *Chrm4*), oxytocin (*Oxtr*), serotonin (*Htr2c*), glycine (*Gla2* and *Gla3*), and neuromedin B (*Nmbr*), whereas NMDA receptor (NMDAR) subunit 2a (*Grin2a*), neuropeptide Y receptor (*Npy2r*), and a pair of lysophospholipid receptors (*Lpar1* and *S1pr5*), that function in memory and learning, were positively regulated by TCF4 (Kennedy et al., 2016). This study additionally revealed DEGs dysregulated in *Tcf4*^(+/-) hippocampus only after threat recognition training (experiential learning), suggesting the involvement of TCF4 in transcriptional response to learning (Kennedy et al., 2016). In the latest RNA-seq studies, murine TCF4 has been

found to act as a transcriptional activator during cortical development and to regulate genes involved in neuronal differentiation and maturation (H. Li et al., 2019; Mesman et al., 2020). Mesman et al. compared the mice transcriptomes at E14.5 and P0 and concluded that TCF4 regulates some key genes of neural development like *Neurod1*, *Lpl*, *Kcna1* and *Id2* throughout neuronal development (Mesman et al., 2020). A mega-analysis of different adult *TCF4^{+/mut}* mice prefrontal cortex, hemibrain and hippocampal CA1 tissues indicated enrichment for processes associated with forebrain development, neuron projection, axon development, excitatory synapses, and postsynaptic density, and also for processes associated with axon ensheathment, and myelination (Phan et al., 2020). Interestingly, their bioinformatics analyses suggested that upregulated genes are predominantly associated with neuronal function while downregulated genes are associated with oligodendrocytes and myelination (Phan et al., 2020).

A cell type-specific analysis and deconvolution analysis of RNA-seq data determined a significant increase in the proportion of RNA coming from neurons and astrocytes and a significant decrease in myelinating oligodendrocytes in adult *TCF4^{+/mut}* mice and the latter was corroborated by reduced number of oligodendrocytes and impaired myelination in PTHS model mice (Phan et al., 2020).

More complex comparative and bioinformatics analysis have also been conducted and genome-wide chromatin immunoprecipitation assays have been used to identify direct target genes of TCF4. Moen et al. described by mass spectrometry the first transcription factor interaction network for flag-tagged TCF4 in mouse neural system mental disorders and found enrichment of proteins associated with neurodevelopmental diseases like intellectual disability, autism spectrum disorders and SCZ (Moen et al., 2017). Furthermore, they identified dozens of TCF4 target genes, which were bound by flag-tagged TCF4 and misregulated after *Tcf4* knockdown, e.g. mental disorder-linked genes *Foxp2*, *Shank3*, *Syngap1*, *Nrxn1*, intellectual disability genes *Gpr56*, *Tgfr2* and *Gli2*, and microcephaly-associated genes *Cenpj*, *Cdk5rap2*, *Mcph1* and *Wdr62*. Forrest et al, identified 10 604 TCF4 binding sites in the human SH-SY5Y neuroblastoma cells that were assigned to 5437 genes and, importantly, *de novo* motif enrichment showed that most TCF4 genomic binding sites contain at least one E-box (5'-CATcTG) (Forrest et al., 2018). Furthermore, approximately 77% of TCF4 binding sites overlapped with the H3K27ac histone modification that is characteristic for active enhancers and regulatory sequences, and target genes enriched belonged to functional clusters for pathways including nervous system development, ion transport and signal transduction (Forrest et al., 2018). TCF4 has also been found to bind to genes involved in neuronal development and SCZ risk in ChIP-seq conducted in SH-SY5Y neuroblastoma cells (Xia et al., 2018). Of note, one fifth of the binding sites were suggested to be situated in enhancers (Xia et al., 2018).

Enhancers are clearly involved in the regulation of target gene expression by the bHLH family of transcription factors (Powell and Jarman, 2008). For example, co-location of different bHLH binding sites within enhancers provide the important molecular context for bHLH protein function and determines whether a particular target gene responds to bHLH factors in a particular cellular context as shown for ATOH1 and NEUROG2 (Powell and Jarman, 2008), both of which dimerize with TCF4. Moreover, recent research has shown that TCF4 binds to the mediator complex with high affinity (Quevedo et al., 2019). TCF4 binding co-localizes with the binding of mediator complex in super-enhancers that regulate neurogenic transcription factor genes, including *TCF4* gene itself, and this positive feedback loop has been suggested to maintain the NPC pool (Quevedo et al., 2019).

2.4 Dimerization partners of TCF4

The molecular code of bHLH factors that determines both where and when the different types of neurons and glial cells are generated, has been proposed (Guillemot, 2007; Powell and Jarman, 2008). The notable mouse proneural bHLH factors are ASCL1 (MASH1), neurogenins 1-3 (NGN1-3/NEUROG1-3) and ATOH1 (MATH1) (Baker and Brown, 2018; Huang et al., 2014). bHLH factors involved in neuronal differentiation include NEUROD family (Miyata et al., 1999; Schwab et al., 2000; Tutukova et al., 2021). In contrast, HLH proteins from ID and HES families have anti-proneural and anti-oligodendrogenic activity, and bHLH factor OLIG2 is one of the patterning proteins providing positional identity along the dorsoventral axis of the neural tube (Guillemot, 2007).

It is generally thought that TCF4 and other E proteins act as obligatory binding partners of class II bHLH proteins (Massari and Murre, 2000; Murre, 2019; Wang and Baker, 2015). However, this notion has recently been challenged as new studies clearly show that homodimers of class II bHLH do form and may even be preferred and more active than heterodimers with E proteins (Le Dréau et al., 2018). Furthermore, neural cell reprogramming using ectopic expression of proneural and neural differentiation bHLH transcription factors without changing the levels of TCF4 or other E proteins have been shown (Dennis et al., 2019). However, one can speculate that E proteins are expressed in excess compared to class II bHLH factors and that could compensate for not being equally highly expressed.

Regardless of whether dimerization with TCF4 (or other E proteins) is an absolute necessity or not for bHLH proteins, several dimerization combinations and respective functional consequences have been described. TCF4 interactome includes ASCL1 (achaetes/scute complex homolog 1, also known as HASH1 or MASH1), ATOH1 (atonal homolog 1, also known as MATH1), ID1–4 (inhibitor of DNA binding 1–4), NEUROD1 (neurogenic differentiation 1) and MYOD1 (myogenic differentiation 1), LYL1 (lymphoblastic leukemia derived sequence 1), MSC (musculin) and TAL1/2 (T-cell acute lymphocytic leukaemia 1 and 2) (Blake et al., 2010). In HeLa cells, ASCL1 binds TCF4 with higher affinity compared to other E proteins and no ASCL1 homodimers form (Persson et al., 2000). However, transactivation of E-box in MCK enhancer-dependent reporter was lower in the case of TCF4-containing heterodimers compared to heterodimers with E12 and E47 in human SH-SY5Y neuroblastoma cells (Persson et al., 2000). Overexpressed TCF4 and other E proteins dimerize with NEUROD2 in P19 embryonal carcinoma cells, and these heterodimers bind to CAGATG E-box, a preferred binding site of NEUROD2, in *in vitro* assays, whereas NEUROD2 and NEUROD1 homodimers failed to do so. Of note, NEUROD2 dimerization with specific E proteins was suggested to depend on differential temporal expression of E proteins (Ravanpay and Olson, 2008).

Formation of homodimers of TCF4 has been demonstrated in many studies (Goldfarb and Lewandowska, 1995; Persson et al., 2000; Tanaka et al., 2008). Rep domain has been found to play a key role in maintaining E protein homodimers in an inactive state on myogenic enhancers (Markus et al., 2002). DNA binding of TCF4 homodimers is inhibited by calmodulin in increased Ca²⁺ environment, whereas heterodimers are not affected by Ca²⁺-calmodulin (Corneliussen et al., 1994; Saarikettu et al., 2004). To conclude, the formation of TCF4 hetero- and homodimers might occur simultaneously and most probably there is a mixture of different dimers of TCF4 at any given time in the cell.

3 Transcription Factor FOXO3 – a member of FOXO family

The transcription factor FOXO3 belongs to the transcription factor family of forkhead (FOX) proteins that is one of the largest classes of TFs in humans. FOX proteins participate in several cellular processes like development, differentiation, proliferation, metabolism, stress resistance and apoptosis (Golson and Kaestner, 2016). FOX family is named after its founding member the *D. melanogaster* fork head (*fkh*) gene product. FOX proteins are characterized by a conserved DNA-binding domain (DBD), also known as fork head box. This domain has helix-turn-helix motif that is made of three α -helices, two β -sheets and two large loops also called butterfly-like wings (Harel et al., 2021). Sequence homology of this DNA-binding domain among the 19 subfamilies/classes of FOX family (FOX A to S) is very high, whereas transactivation domains almost completely lack similarity. Studies of evolution of classical FOX protein binding core sequence RYAAAYA (R = purine, Y = pyrimidine) corroborate finding of helix 3 of DBD being highly conserved and sequence variability at the vicinity of the core sequence illustrates the recognition specificities among FOX proteins (Nakagawa et al., 2013; Schmitt-Ney, 2020). Binding of FOXNs and FOXO1 to less conserved (GACGC) consensus motifs has been reported, although the functional studies on the effects of this binding are lacking (Nakagawa et al., 2013).

In mammals, the Fox O box (FOXO) family contains FOXO1, FOXO3, FOXO4, and FOXO6, whereas there is only one member present in *D. melanogaster* and *C. elegans* – dFOXO and daf-16, respectively (Schmitt-Ney, 2020; Wang et al., 2009). FOXO proteins are ubiquitously expressed (Maiese, 2015). The DBD is nearly identical in FOXOs and they bind the same consensus sequence (5'-TTGTTAC-3'). Therefore, in general it has been suggested that FOXOs can regulate genes redundantly and specificity might be obtained by specific expression pattern or isoform-specific posttranslational regulation (Tsai et al., 2007; Weigelt et al., 2001). However, disruption of *FOXO* genes separately in mice revealed a functional diversification, as *Foxo1*-null embryos die in embryonic day 10.5, while *Foxo3*- and *Foxo4*-null mice are viable (Hosaka et al., 2004). Furthermore, abnormal ovarian follicular development was identified in *Foxo3*-null mice, whereas no consistent abnormalities were found in *Foxo4*-null mice (Golson and Kaestner, 2016). These results suggest different physiological roles of FOXOs in mammals (Schmitt-Ney, 2020).

FOXO TFs regulate diverse gene expression programs directing cell cycle, cell survival and metabolism, stem cell maintenance and lifespan in model organisms. Furthermore, FOXOs are linked to age-related diseases like cancer and diabetes (Eijkelenboom and Burgering, 2013; Jiramongkol and Lam, 2020; van den Berg and Burgering, 2011; van der Horst and Burgering, 2007).

3.1 Post-translational regulation of FOXOs

The role of FOXOs is limited under normal conditions, the main role of FOXOs seems to be to integrate signals from several pathways during stress and to maintain tissue homeostasis via fine-tuned target gene regulation (Schmitt-Ney, 2020). Post-translational modifications (PTMs) affect shuttling between nucleus and cytoplasm, and degradation of FOXOs (Burgering and Kops, 2002). Therefore, PTM of FOXOs has been extensively studied to dissect complex and tight control of FOXO activation (reviewed in Brown and Webb, 2018; Calnan and Brunet, 2008; Eijkelenboom and Burgering, 2013; Jiramongkol and Lam, 2020; van der Horst and Burgering, 2007). The current knowledge of PTM regulating FOXOs is depicted in Figure 3.

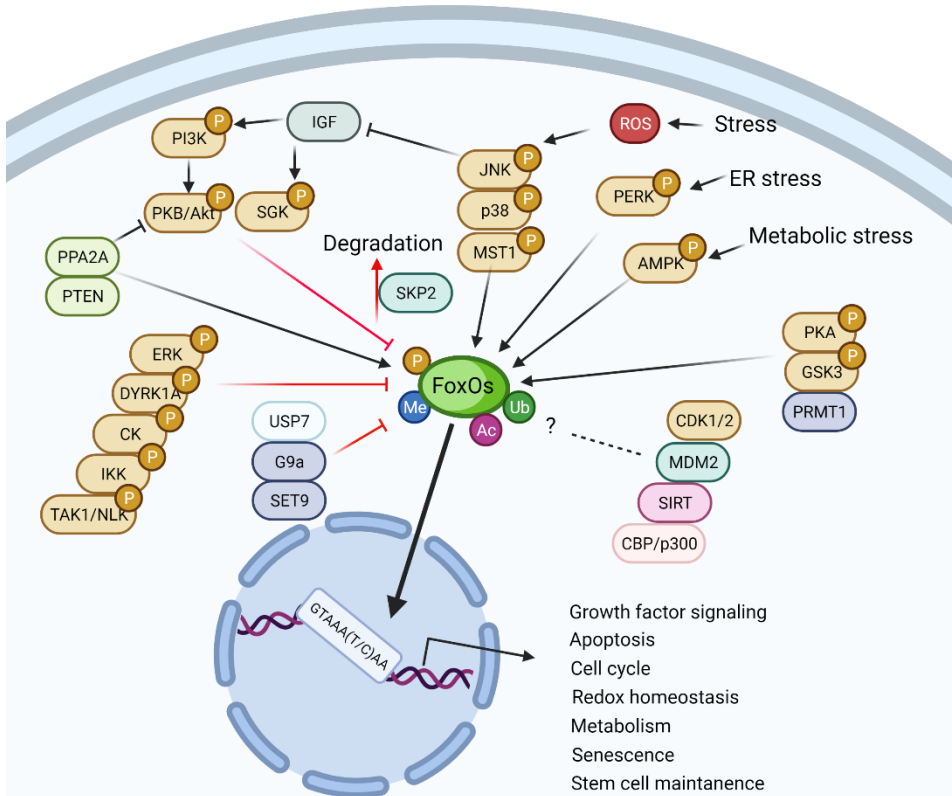


Figure 3. Post-translational modifications and nuclear translocation of FOXO proteins. Activity of FOXO transcription factors is co-ordinated via different post-translational modifications (PTMs). Effect of enzymes conveying inhibitory signals (are shown with red inhibitor lines) results in processes translocating FOXOs out from the nucleus and/or directing FOXOs to proteasomal degradation. Upon different stress signals several enzymes play a role in activation of FOXOs (shown with arrows) that is achieved via removing inhibitory PTM and enhancing nuclear translocation. Effect of enzymes with conflicting or limited evidence on activity of FOXOs is marked with dashed line. Kinases are coloured yellow, phosphatases are salad green, deacetylases are pink, acetylases are light pink, methyltransferase are blue, ubiquitin-ligases are ocean green, ubiquitin-specific protease is grey. Ac – acetylation; IGF – insulin-like growth factor; Me – methylation; P – phosphorylation; ROS – reactive oxygen species; Ub – ubiquitination. Created with BioRender.com

The first described and highly conserved pathway inactivating all FOXO family members is PI3K-PKB/AKT-directed phosphorylation that integrates insulin and growth factor signalling (Brunet et al., 1999; Burgering and Kops, 2002). Phosphorylation of FOXOs at three specific sites, namely T32, S253, and S315 in FOXO3, results in increased binding to shuttling protein 14-3-3 and translocation from nucleus to cytoplasm. Additionally, serum- and glucocorticoid-inducible kinases (SGKs) integrate insulin growth factor (IGF) survival signals similarly to PKB/AKT and phosphorylate FOXOs at the same serine and threonine residues, although with marked preference for S315 (Brunet et al., 2001). Recently, FOXO1 was found to be a direct target of PKA in endothelial and muscle cells, and the sites phosphorylated by PKA overlap with those phosphorylated by PKB/AKT (Lee et al., 2011; Silveira et al., 2020). In addition, glucagon-mediated PKA-specific phosphorylation at S276 of human FOXO1 in HepG2 cells increases its

nuclear translocation and protein stability (Wu et al., 2018). *In vivo* function of this PKA phosphorylation site was established in knock-in PKA phosphorylation resistant mice FOXO1-S273A and FOXO1-S273D (corresponding to S276 in human) that display impaired blood glucose homeostasis, linking the control of FOXO1 by PKA to metabolic diseases including diabetes (Wu et al., 2018).

Many other kinases have been shown to phosphorylate and inactivate FOXO family members. SGK and PKB/AKT phosphorylated FOXO1 at S319 functions as a docking site for casein kinase 1 (CK1), leading to the phosphorylation of additional serines, namely S322 and S325 (Rena, 2002). Additionally, dual-specificity tyrosine-phosphorylated and regulated kinase (DYRK1A) phosphorylates FOXO1 at S329. This phosphorylation appears to be constitutive, decreases the ability of FOXO1 to stimulate gene transactivation and reduces the proportion of FOXO1 present in the nucleus (Woods et al., 2001). Furthermore, mutation S329A led to the accumulation of FOXO1 in the nucleus and increased transactivation by FOXO1 in reporter assays (Woods et al., 2001). Next, phosphorylation by TAK1/NLK (transforming growth factor- β -activated kinase/Nemo-like kinase) inhibits transactivational activity of FOXO1 and directs its translocation from the nucleus (Kim et al., 2010). Fourth, I κ B kinase (IKK) phosphorylates human and mouse FOXO3 at S644, leading to ubiquitin-dependent proteolysis of FOXO3 (in a PKB-independent manner, of note, PKB/Akt positively regulates IKK via direct phosphorylation) (Hu et al., 2004; Nidai Ozes et al., 1999). Fifth, phosphorylation of FOXO1 and FOXO3 at several serine residues by stress-activated MAP kinase/extracellular signal-regulated kinase (ERK) promotes E3 ubiquitin ligase MDM2-mediated poly-ubiquitination and proteasomal degradation of FOXOs (Asada et al., 2007; Yang et al., 2008).

Besides the above-mentioned kinases that inactivate FOXOs, several kinases have been shown to have opposing or more complex effects on FOXO activity. ER-stress induced kinase PERK (protein kinase RNA (PKR)-like ER kinase) has context-specific effects on FOXO activity (Zhang et al., 2013). ER-stress induced kinase PERK (protein kinase RNA (PKR)-like ER kinase) activates FOXOs and overrides insulin-induced suppression of FOXOs by PKB/Akt. However, incoherent feed-forward regulation motif has also been found, where indirect action of PERK via AKT can lower FOXO activity. Whereas glycogen synthase kinase 3 (GSK3) positively regulates transactivation of FOXOs. Activation of FOXOs by GSK3 phosphorylation induces the expression of type I insulin-like growth factor receptor (IGF-IR) that promotes hepatoma cell proliferation, whereas in the endotoxin-induced myocardial injury model GSK3 β up-regulates FOXO3 levels that leads to apoptosis (Huo et al., 2014; Z. Li et al., 2019).

The regulation of FOXOs by mitogen-activated protein kinase (MAPK) family, STE20-like protein kinase (MST1), CDK family and AMPK are further discussed below to illustrate the different mechanisms of how FOXO activity is controlled. Among mitogen-activated protein kinase (MAPK) family kinases c-Jun NH2-terminal kinase (JNK) and p38 phosphorylate FOXOs under cellular stress conditions, leading to their translocation to the cell nucleus, activation of FOXO target genes and cell death (reviewed in van der Horst and Burgering, 2007). JNK inhibits insulin signalling and JNK-mediated phosphorylation induces release of FOXO from the shuttling protein 14-3-3. Several phospho-sites of p38 have been described in FOXO1 and FOXO3 that regulate translocation into the nucleus. Furthermore, these phospho-sites are involved in consequential FOXO-induced inhibition of cell proliferation and cell death (Asada et al., 2007; Ho et al., 2012; Marzi et al., 2016). In contrast, phosphorylation by ERK has an

inactivating effect on FOXOs, indicating that the outcome of MAPK signalling on the activity of FOXOs is controlled by the duration and magnitude of the integrated signals of ERK, JNK and p38 (Jiramongkol and Lam, 2020).

The mammalian ste20-like kinase 1 (MST1) is activated under conditions of oxidative stress and phosphorylates FOXO3 at S207 and FOXO1 at S212 (in forkhead domain) (Lehtinen et al., 2006). This induces FOXO proteins to release 14-3-3 and translocate into the nucleus, although dephosphorylation of this phospho-site is needed for effective DNA-binding and target gene activation in the nucleus (Lehtinen et al., 2006). MST1-FOXO signalling is conserved from nematodes to mammals and plausibly plays a role in regulating longevity via mediating oxidative stress response (Brown and Webb, 2018; Lehtinen et al., 2006).

Phosphorylation of FOXOs by CDK family can have opposing effects. On the one hand, the DNA damage-activated G1/S-phase checkpoint regulator CDK2 phosphorylates FOXO1 at S249 resulting in cytoplasmic localization and inhibition of FOXO1. This provides a mechanism that coordinates apoptotic cell death after DNA damage (Huang et al., 2006). On the other hand, the outcome of FOXO1 phosphorylation at S249 by CDK1 (responsible for G2/M transition) is dependent on cell type, with FOXO activation described in postmitotic neurons and NIH 3T3 cells and FOXO inhibition in a prostate carcinoma cell line (Liu et al., 2008; Yuan et al., 2008). Thus, it is plausible that the same phospho-site can be recognized by different components of cellular machinery depending on a cell cycle phase, cell type and/or additional unknown factors.

AMPK-induced phosphorylation of already nuclear FOXOs enhances binding of FOXOs to CBP/p300 and thereby increases FOXO transcriptional activity (Greer et al., 2007; Wang et al., 2012). Concurrent phosphorylation of FOXO3 by AMPK and MEK/ERK induces translocation of FOXO3 into the mitochondria to activate mitochondrial gene expression to sustain mitochondrial functionality in metabolic stress conditions (Celestini et al., 2018). Furthermore, starvation conditions activate AMPK that leads to phosphorylation of FOXO3 and up-regulation of autophagy genes (Greer et al., 2007).

A multitude of phospho-sites in FOXOs and explicit consequences on subcellular localization and transcriptional activity have led to the search for phosphatases that could enable dynamic integration of upstream signals. Several Ser/Thr phosphatases have been reported to dephosphorylate FOXOs. Phosphatase and tensin homolog (PTEN) was found to counteract phosphorylation by PKB in FOXOs (Nakamura et al., 2000). More recently protein phosphatase 2 (PP2A) was discovered to directly bind FOXOs and oppose PKB/AKT phosphorylation and the translocation of FOXOs by 14-3-3 (Singh et al., 2010; Yan et al., 2008). Furthermore, PP2A was also shown to regulate PKB/AKT and concerted action of PP2A on both FOXOs and PKB/Akt enhances FOXOs activity (Singh et al., 2010).

While the above-mentioned mechanisms are well established, many other PTMs of FOXOs mediate more context-specific complex outcomes. One example here is the acetylation of FOXOs. CBP/p300 directly acetylate FOXOs thereby inhibiting their DNA binding capability (Fukuoka et al., 2003). However, the total effect of CBP/p300 on FOXO-mediated transcription is additionally dependent on histone acetylation and co-activator activities of CBP/p300 that lead to activation of FOXO target genes (van der Horst and Burgering, 2007). Both of these processes can potentially occur at the same time. Moreover, in oxidative conditions Cys disulphide bonds form between FOXO4 and CBP/p300, which increases interaction and potentially sequesters these co-activators from other transcription factors, therefore further affecting gene expression profile (Dansen et al., 2009). Furthermore, deacetylase SIRT1 and other HDACs have been shown

to function similarly on FOXOs and CBP/p300 (van der Horst and Burgering, 2007). Therefore, both deacetylation and acetylation are not merely an 'on' or 'off' switches, but these processes orchestrate a complex regulatory mechanism that modifies transcriptional responses upon context (Brunet, 2004; Lin et al., 2018).

FOXO proteins are also regulated by methylation. Arginine methylation has been linked to activation of FOXOs. Protein arginine N-methyltransferase 1 (PRMT1) methylates R248 and R250 (in FOXO1) both of which situate near PKB consensus sequence in FOXOs, abrogating phosphorylation of FOXOs in oxidative stress condition, thereby preventing its nuclear exclusion, polyubiquitination, and proteasomal degradation (Yamagata et al., 2008). Contrarily, lysine methylation has been shown to promote inactivation of FOXOs. K270 in FOXO3 is methylated by methyltransferase Set9, and this modification disrupts FOXO3 DNA-binding activity and prevents neuronal apoptosis (Xie et al., 2012). FOXO1 can also be methylated at K273 by histone methyltransferase G9a (euchromatic histone-lysine N-methyltransferase 2 (EHMET2/G9a)), which enhances binding to E3 ligase SKP2 followed by poly-ubiquitination and decreased FOXO1 protein stability (Chae et al., 2019).

Mono- and poly-ubiquitinations affect the functioning and protein stability of FOXOs (reviewed in Huang and Tindall, 2011). S-phase kinase-associated protein 2 (SKP2) mediates poly-ubiquitination and degradation of FOXO1 following phosphorylation by PKB/AKT and several other kinases (Huang et al., 2005). E3 ligase murine double minute 2 (MDM2) binds ERK-phosphorylated FOXO3 and this poly-ubiquitination leads to proteasomal degradation of FOXO3 (Fu et al., 2009; Yang et al., 2008). In contrast, mono-ubiquitination of FOXO4 at K199 and K211 by MDM2 in response to oxidative stress directs FOXO4 into the nucleus and thereby potentially activates FOXO4-dependent gene expression (van der Horst et al., 2006). De-ubiquitination of FOXO4 is mediated by ubiquitin-specific protease 7 (USP7/HAUSP) (van der Horst et al., 2006). However, this does not affect FOXO4 protein half-life, but instead negatively regulates FOXO4 transcriptional activity (van der Horst et al., 2006).

It is less clear whether FOXO proteins are modified by less common post-translational modifications like glutathionylation, glycosylation, SUMOylation, hydroxylation, neddylation, citrullination, prenylation, palmitoylation, myristoylation and s-nitrosylation, and what might be the functional consequences of these modifications (Buuh et al., 2018; Jia et al., 2019).

Participation of microRNAs (miRNAs) in the regulation of FOXO expression have been mainly studied in cancer. The effect of most miRNAs studied to date is induction of mRNA degradation and translation inhibition of FOXOs, although whether the outcome is beneficial or detrimental depends on the cancer type and specific FOXO (reviewed by (Jiramongkol and Lam, 2020). Interestingly, circular FOXO3 pseudogene mRNA have been reported to sequester FOXO3-regulating miRNAs and thereby upregulate FOXO3 expression (Yang et al., 2016).

In conclusion, the activity of FOXOs is fine-tuned by the crosstalk between numerous PTMs indicating that FOXOs act as cellular integrators of different signals (Jiramongkol and Lam, 2020; van den Berg and Burgering, 2011; Wang et al., 2017).

3.2 Roles of FOXOs in Huntington's disease

In general, FOXOs function as tightly controlled integrators of environmental fluctuations and signals and this gives them an essential role in the regulation of metabolic homeostasis, redox balance, and the stress response via precisely regulated target gene expression (van der Horst et al., 2006). Studies in *C. elegans* and *D. melanogaster* have demonstrated a role for daf-16/dFOXO in oxidative stress-induced heat shock protein (HSP) expression, maintenance of proteostasis and longevity (Donovan and Marr, 2016; Hwangbo et al., 2004; Kenyon et al., 1993; Riddle et al., 1981). Gene programs coordinated by FOXOs are diverse, covering DNA damage response, apoptosis, proliferation, oxidative stress, cell metabolism, cell cycle regulation, and autophagy in order to maintain cellular homeostasis in development, aging and in disease (Burgering and Kops, 2002; Eijkelenboom and Burgering, 2013; Golson and Kaestner, 2016; van der Horst and Burgering, 2007). FOXO factors have been implicated in a variety of diseases including tumorigenesis and neurodegenerative diseases (Hornsveld et al., 2018; Hu et al., 2019). The roles of FOXO3 have been studied in different cancer types, where it was initially thought to function mainly as a tumour suppressor (Hornsveld et al., 2018). However, depending on the context, FOXO3 can also support tumour growth, suggesting that FOXO3 can affect various aspects of tumorigenesis (reviewed by (Hornsveld et al., 2018; Jiramongkol and Lam, 2020; Liu et al., 2018)). Similarly, FOXOs are thought to exert both detrimental and protective effects in neurodevelopmental diseases, including Huntington's disease (summarize in Figure 4) (Hu et al., 2019; Liu et al., 2017; Parker et al., 2012, 2005; Tourette et al., 2014).

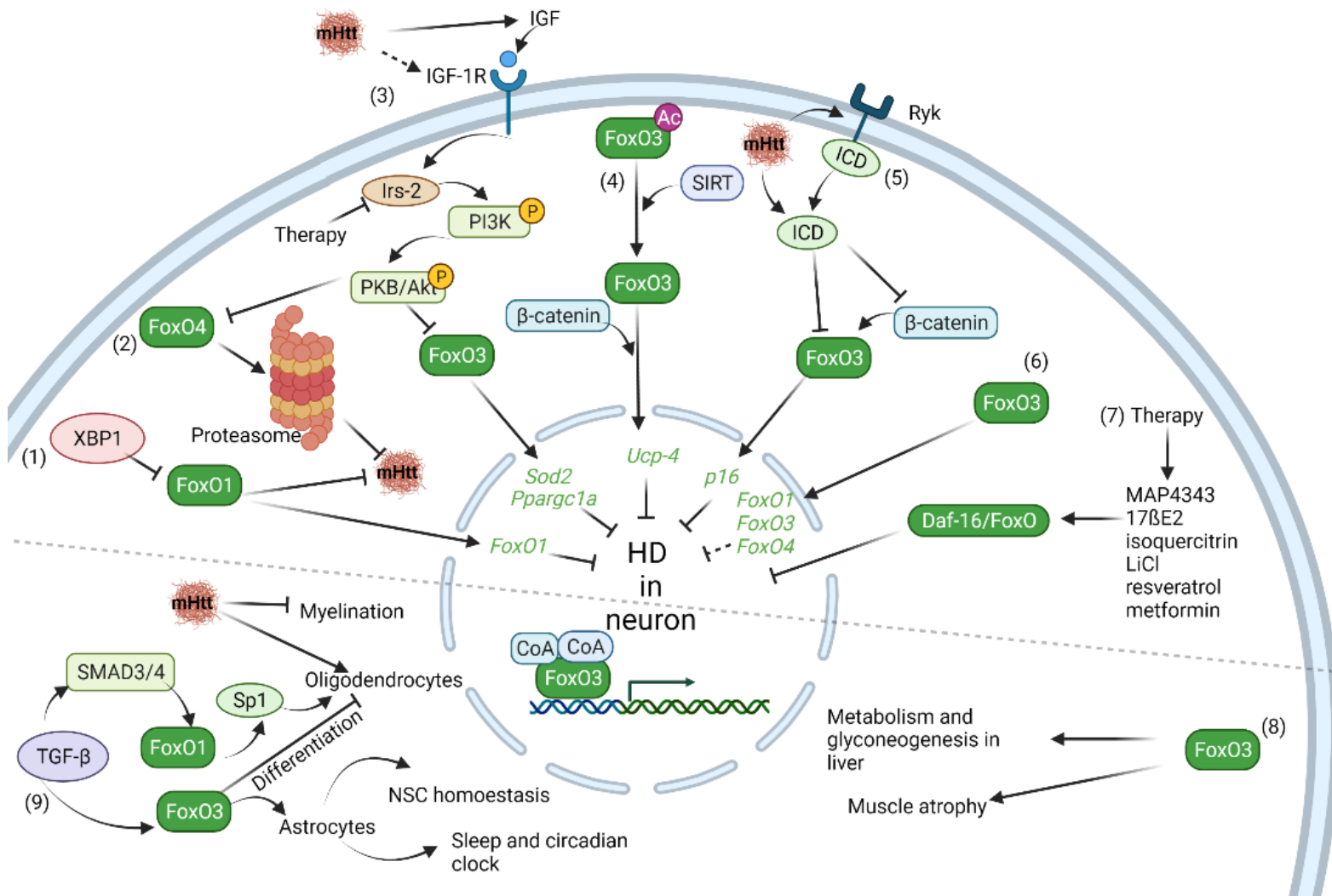


Figure 4. FOXO transcription factors in HD. The prevailing idea is that nuclear localization of FOXOs activates genes that regulate processes that reduce negative effects of mutant HTT (mHTT) and other HD processes. Several pathways affect levels and location of FOXO proteins and transcription of its target genes in HD neurons (upper part). (1) Deficiency of unfolded protein response protein XBP1 increases FOXO1 levels and enhance beneficial macroautophagy. (2) Ectopic expression of FOXO4 rescues proteasome activity in differentiated HD iPSC. (3) Expression of mHTT increases levels of insulin-like growth factor (IGF) which activates via IRS2 phosphorylation cascade of PI3K-PKB/AKT leading to phosphorylation of FOXOs and their translocation from nucleus and degradation. (4) De-acetylation of FOXOs by SIRT enables binding of β -catenin which enhances transcriptional activity of FOXOs. (5) Expression of mHTT induces cleavage of Wnt receptor Ryk-ICD fragment that binds to FOXOs' co-factor β -catenin and represses transcriptional activity of FOXOs reducing protection against cell death. (6) Autoregulation of FOXOs. (7) Several compounds showing promise as therapeutic agents in HD therapy have been shown to mediate beneficial effects via FOXO proteins. FOXO transcription factors have also functions in other cell types and processes found to be impaired in HD (lower part). (8) Muscle wasting and progressive impaired gluconeogenesis are characteristic to HD and FOXO3 has roles in these processes in liver and muscle tissue. (9) Pathway downstream of TGF β via FOXOs is responsible for oligodendrogenesis and myelinisation in oligodendrocytes, whereas in astrocytes the same pathway regulates NSC homeostasis and circadian rhythms. Ac – acetylated; CoA – co-activator; ICD – intracellular domain (fragment); IGF – insulin-like growth factor; IGF-1R – insulin-like growth factor 1 receptor; IRS2 – insulin receptor substrate 2; mHtt – mutant huntingtin protein; P – phosphorylated; Ryk – RTK subfamily with acronym from related to tyrosin kinase; SMAD3/4 – TGF- β signalling pathway proteins structurally similar to *C. elegans* Sma and *D. melanogaster* Mad proteins; TGF- β – transforming growth factor β ; XBP1 – X-box binding protein 1. Created with BioRender.com

FOXO3/FOXO1 have been postulated to be mainly neuroprotective in HD and various mechanisms for this have been shown. Studies on HD modelled in *C. elegans* and mouse cell lines have demonstrated that FOXOs convey protective signals in the early phases of mHTT toxicity, an effect achieved via activation of FOXO/daf-16 by sirtuin Sir2 (in mammals SIRT) and additionally requiring FOXO partner protein bar-1/ β -catenin (Parker et al., 2005) (Parker et al., 2012). Moreover, downregulation of FOXOs at early stages of HD in Q128 nematode HD model and in HD striatal cell line cells via non-canonical mechanism of Wnt receptor Ryk-ICD fragment binding to FOXO co-factor β -catenin, has been shown to be detrimental (Tourette et al., 2014).

In transgenic R6/2 mice reduction of insulin receptor substrate 2 (IRS2) levels, (except in β cells to prevent diabetes) in order to downregulate insulin signalling, resulted in improved motor performance, neuropathology and survival (Sadagurski et al., 2011). Furthermore, this slower disease progression was associated with nuclear localization of FOXO1 and increased expression of FOXO1-dependent genes (e.g. *Sod2* and *Ppargc1a*) affecting macroautophagy, mitochondrial function and oxidative stress resistance. Additionally, macroautophagy upregulated by unfolded protein response-related transcription factor XBP1-deficiency was associated with improved neuronal survival, motor performance, and drastic decrease in mHtt levels in cellular and animal models of HD, which was mechanistically linked to increased expression of FOXO1 (Vidal et al., 2012). In a follow-up study, FOXO3 functions were extended to regulating cellular senescence during neuronal differentiation in HD (Voisin et al., 2020).

Another line of evidence for the neuroprotective role of FOXOs in HD comes from iPSCs derived from HD patients (Liu et al., 2017). First, compared to wt controls HD-iPSCs are characterized by increased protective proteasome activity and higher levels of FOXOs, which protect the cells from mHTT toxicity (Liu et al., 2017). Second, HD-iPSC-derived NPCs exhibit lower proteasome activity than wt NPCs, and ectopic expression of FOXO4 rescues this detrimental lowering of proteasome activity (Liu et al., 2017). Finally, HD-iPSC-derived differentiated DARPP32-positive striatal medium spiny neurons demonstrated reduced FOXO4 levels and decreased proteasome activity, and were vulnerable to oxidative stress (Liu et al., 2017). In differentiated HD medium spiny neurons increase in PKB/AKT kinase activity was found, and inhibition of PKB/AKT improved proteasome activity and induced FOXO4 levels (Liu et al., 2017). Therefore, based on these results FOXOs were proposed to be a valuable therapeutic target in HD (Liu et al., 2017). FOXOs' role as a molecular target for therapy in HD gets further support from the study showing that daf-16/FOXO is essential for the effect of several therapeutic compounds (MAP4343, 17 β E2, isoquercitrin, resveratrol, GSK3 inhibitor lithium chloride, and AMPK activator metformin) that prolong the functioning of neurons in HD (Farina et al., 2017).

Although neuronal cell death is the main neuropathological sign of HD, glial cells are gaining increasing attention for their potential role in HD (Wilton and Stevens, 2020). In contrast to HD-induced loss of neurons, increase in oligodendrocyte abundance has been reported in low grade HD patients (Myers et al., 1991) mHtt expressed in oligodendrocytes directly affects myelinisation and hypomyelinisation is characteristic to HD (Huang et al., 2015; Osipovitch et al., 2019). SMAD3/4-FOXO1-Sp1 pathway downstream of TGF β has shown to function in cell cycle exit of oligodendrocyte progenitors, therefore playing a role in oligodendrogenesis and postnatal CNS myelinisation (Palazuelos et al., 2014). Psychiatric and sleep changes manifest in the prodromal stages of HD, and gene network analysis on human caudate nucleus

microarray data identified astrocyte-specific transcriptional network that was predicted to be regulated by FOXO3 (Scarpa et al., 2016). Moreover, this striatal astrocyte network correlates with sleep and stress traits described in (B6xA/J)F2 chronically stressed mice (Scarpa et al., 2016). Conserved TGF β -FOXO3-dependent striatal astrocyte network has been identified, and there is evidence for its relationship to neural stem cell homeostasis (Scarpa et al., 2016). It has also been hypothesized that astrocytes are a primary contributor to HD pathogenesis (Scarpa et al., 2016).

In addition to brain pathology, muscle wasting is apparent in symptomatic HD patients. No specific studies on FOXOs in HD muscles have been conducted, although it is known that FOXOs play a role in muscle atrophy in general by regulating proteasomal and autophagic pathways (Bondulich et al., 2017; Mammucari et al., 2007; Zhao et al., 2007). Similarly, body weight loss, liver dysfunction, and disturbances of metabolism and circadian clock are among additional alterations observed in HD (Morton, 2005; van der Burg et al., 2008). Supporting their involvement in HD, FOXOs are known to participate in the regulation of cell metabolism, hepatic gluconeogenesis and lipid metabolism, and circadian rhythms (Chaves et al., 2014; Kamagate et al., 2008; Nakae et al., 2001).

In conclusion, FOXOs have functions in many cellular processes that are disrupted in HD. Whether FOXOs are detrimental or protective in HD needs more thorough investigation. As FOXOs are integrators of numerous upstream signals they probably tip the balance very specifically depending on tissue type and disease stage, resulting in different outcomes.

4 Aims of the study

Dysregulation of transcription factors has been long established in Huntington's disease. Preliminary work of our research group with 200 unvalidated antibodies suggested alterations in subcellular localization of transcription factors FOXO3 and TCF4 in Huntington's disease model cells. Therefore, the aims of this thesis were to:

1. Validate localization disturbances of FOXO3 and TCF4 seen in an antibody screen conducted in Huntington's disease model cells;
2. Characterise mRNA and protein levels of FOXO3 in HD models and patients;
3. Elucidate the molecular mechanisms affecting FOXO3 in HD;
4. Analyse TCF4 gene and protein expression in human tissues and regulation of TCF4 and TCF4-dependent transcription in neurons;
5. Study mRNA and protein levels of different TCF4 isoforms in HD models and patients.

Altogether, this study addresses the roles of two transcription factors, FOXO3 and TCF4, in Huntington's disease.

5 Material and methods

I used the following experimental methods that are described in more detail in the publications specified in parentheses:

- Bioinformatics analysis of gene, mRNA and protein sequences (I, II, III, IV)
- Molecular cloning (II, III)
- Site-directed mutagenesis (II)
- Culturing of immortalized mammalian cells and rat primary cortical neurons (II, III, IV)
- Transfection of mammalian cells (II, III)
- siRNA design and transfection (II)
- Immunocytochemistry (II, IV)
- Preparation of cell lysates and immunoblotting (II, IV)
- Subcellular fractionation (II, IV)
- *In vitro* translation (IV)
- Primer design and optimization (I, II, IV)
- RNA isolation and reverse transcription followed by quantitative polymerase chain reaction (RT-qPCR) (I, II, IV)
- Luciferase reporter assay (II, III)
- Chromatin immunoprecipitation assay (II)

6 Results

Publication I

- Based on bioinformatics analysis, human *TCF4* gene contains 21 mutually exclusive 5' exons, generating transcripts that encode TCF4 protein isoforms with 18 different N-termini.
- Internal exons 8 and 15 have alternative splice acceptor sites that eventually lead to addition of glutamine and alanine to TCF4 protein sequence, respectively.
- In-frame alternative splicing of TCF4 utilizing alternative donor splice-sites in exon 18 creates + and - isoforms that contain or miss the amino acids RSRS. The + and – isoforms are expressed at roughly equal levels.
- Transcription is initiated at relatively similar levels from alternative transcription start sites within the *TCF4* gene in cerebellum and skeletal muscle tissue.
- The majority of alternative *TCF4* transcripts are expressed in most of the human tissues and brain regions, however, a few have a more limited expression pattern based on RT-PCR analysis.
- The expression of *TCF4* is ubiquitous, although the expression levels vary considerably between human tissues. The highest TCF4 mRNA levels are found in fetal brain, cerebellum and cerebral cortex.
- *TCF4* mRNA expression in the human hippocampus is detected in neurons of DG, CA1-CA3 subfields and subiculum, and in the cerebellum in cerebellar granule neurons, as assessed by *in situ* hybridization.
- Several TCF4 protein isoforms are expressed in human tissues as determined by Western blot analysis.
- All TCF4 protein isoforms that contain region coded by exons 8 and 9, display exclusively nuclear distribution.
- TCF4 contains a functional NLS sequence.
- All TCF4 isoforms can be transported to the nucleus by piggy-back mechanism through heterodimerization with NLS-containing bHLH partners (e.g. NEUROD2). TCF4 isoforms missing NLS can be exported from nucleus via heterodimerization with NES-containing partner proteins (e.g. ID2).
- TCF4 signal in immunohistochemical staining is mainly in neuronal nuclei, but also in the cytoplasm of neurons in CA3, DG and hilus regions of hippocampus and in the granule cell layer of the cerebellum in human brain.
- All TCF4 isoforms are capable of activating reporter gene transcription controlled by μ E5 E-boxes in HEK293 cells, although to a different extent. Transcriptional activity of TCF4 correlates with the presence of AD1, however, there is no significant correlation between isoform's ability to activate transcription and the presence of NLS, the presence of partial AD1 domain or the extra amino acids in the + isoforms.
- In HEK293 cells, the activation domains AD1 and AD2 mediate transactivation to a similar extent. However, the presence of both ADs in a single protein has a synergistic effect on transcriptional activity.

Publication II

- Immunocytochemical signal of FOXO3 differs between mouse striatal progenitor cell-derived wt Hdh^{7/7} cells and mutant Hdh^{7/109} and Hdh^{109/109} cells.
- FOXO3 protein levels are elevated in total cell lysates of mutant Hdh cells and both in the nuclear and cytosolic fractions.
- The levels and the phosphorylation of PKB/AKT and phosphorylation of FOXO3 at PKB/AKT phosphorylation site S253 are not changed in mutant Hdh cells.
- Levels of ERK1/2 are not changed in mutant Hdh cells, whereas a reduction of activated ERK1/2 is apparent in mutant Hdh cells.
- 3-NP treatment, a chemical model of HD, induces nuclear localization of overexpressed EGFP-FOXO3 and endogenous FOXO3 in rat cultured cortical neurons.
- 16 and 24 h 3-NP treatment increases levels of FOXO3 protein in rat cultured cortical neurons.
- *Foxo3* and FOXO3 target gene *FasL* mRNA levels are increased in both HD cellular models, namely mutant Hdh cells and in 3-NP treated neurons.
- *Foxo3* mRNA levels are increased in the cortex of R6/2 HD model mice and in the cortex and caudate nucleus tissue of HD patients.
- *FOXO3* promoter region contains four FHRE sequences based on bioinformatics analysis.
- Endogenous FOXO3 protein binds to its own promoter in Hdh^{7/7}, Hdh^{109/109} and in rat primary cortical neurons based on chromatin immunoprecipitation assay.
- FHRE 3 (TAACA) is to a large extent responsible for the transcriptional autoregulation of FOXO3 in Hdh^{7/7}, Hdh^{109/109} cells and in rat primary cortical neurons.

Publication III

- TCF4-dependent transcription is regulated by neural activity in neurons.
 - TCF4 protein isoforms induce E-box-dependent reporter gene expression in rat primary neurons upon membrane depolarization with KCl to mimic neuronal activity.
 - Membrane depolarization-induced rise in TCF4-mediated transcription requires Ca²⁺ influx through L-type voltage-gated Ca²⁺ channels (VGCCs).
 - Increase in excitatory synaptic activity by bicuculline/4-AP treatment also results in upregulation of TCF4-regulated transcription through both NMDARs and L-type VGCCs.
- Endogenous and overexpressed TCF4 proteins localize in the nucleus of primary neurons. Overexpressed TCF4 isoforms lacking NLS localize both to the nucleus and cytoplasm.
- The region between AD2 and bHLH is essential for neuronal-activity-dependent regulation of TCF4 functions
 - TCF4-mediated transactivation in neurons requires AD2, although AD2 is not sufficient for neural activity-dependent regulation of TCF4 activity.
 - bHLH domain together with the TCF4 region between amino acids M430 and P498 is essential for activity-dependent regulation of TCF4 in neurons

- Signalling via sAC and PKA regulates neuronal activity-dependent functions of TCF4
 - KCl-induced E-box-dependent reporter gene expression is reduced by Calcium/calmodulin dependent protein kinase II (CAMK2) inhibitor KN-62 and the PKA inhibitor H89, but not by treatment with Calcium/calmodulin-dependent protein kinase kinase (CAMKK) inhibitor STO-609, Ca²⁺-dependent PKC isoform inhibitor Go6976 and unrelated casein kinase (CK) inhibitor TBB.
 - Overexpression of constitutively active forms of PKA-Cα and PKCα, and treatment with PKA activator dbcAMP, but not PKC activator PDBu, activate TCF4-dependent transcription in reporter assay.
 - Co-expression of the dominant negative (DN) PKA-regulative subunit R1 and not DN PKCα reduces TCF4-dependent transcription in KCl-treated neurons.
 - Inhibition of soluble adenylyl cyclase (sAC) by KH7 interferes with the induction of TCF4-dependent transcription upon membrane depolarization.
- TCF4 S448 is phosphorylated by PKA upon neuronal activity and this phosphorylation is needed for full induction of TCF4-dependent transcription in neurons.
- *In vivo* overexpression of wt TCF4-A⁻ but not TCF4-A⁻ mutant S448A by *in utero* electroporation results in formation of cellular aggregates in rat layer 2/3 the medial prefrontal cortex (mPFC).
- TCF4 participates in activating *GADD45G* transcription following membrane depolarization
 - Overexpressed TCF4-A⁻ and ASCL1 co-operatively induce transcription from *GADD45G* promoter in membrane-depolarized neurons in reporter assay.
 - Silencing *TCF4* with siRNAs reduces ASCL1-mediated transcription from *GADD45G* promoter in rat primary neurons.
 - *GADD45G* promoter contains two potential E-box sequences based on *in silico* analysis. Mutating the E-box sequences proximal to the transcription start site in *GADD45G* promoter abolishes reporter induction in depolarized neurons.
 - Based on chromatin immunoprecipitation assay, TCF4 binds to endogenous *Gadd45g* promoter in rat neurons.
 - TCF4 regulates the expression of endogenous *Gadd45g* gene in rat primary neurons
 - Overexpression of VP16-TCF4-I⁻ increases both basal and depolarization-induced levels of endogenous *Gadd45g*.
 - Silencing of *Tcf4* via AAV-mediated *Tcf4* shRNA expression decreases *Gadd45g* transcription only in depolarized neurons.
- TCF4 missense variations P299S and G428V identified in SCZ patients alter the transcriptional activity of TCF4-B⁻ in unstimulated or both in unstimulated and depolarized neurons, respectively.

Publication IV

- Immunoreactive signal of polyclonal TCF4 antibodies is changed in HD model mutant Hdh cells, suggesting altered subcellular localization and/or nuclear levels of the protein.
- Based on data mining from publicly available databases, the gene structure of mouse *Tcf4* is similar to human *TCF4*, encoding multiple protein isoforms mostly conserved in both species.
- Both low (probably TCF4-D/A/H/I) and high (probably TCF4-B/C) molecular weight TCF4 protein isoforms are reduced in mutant Hdh cells, in total cell lysates and also in both cytosolic and nuclear fractions.
- Different sets of TCF4 isoforms are expressed in cytoplasmic and nuclear fraction of Hdh cells.
- Levels of *Tcf4* transcripts encoding TCF4-B, -C, and -A are reduced in Hdh^{109/109} cells.
- 3-NP treatment decreases the levels of *Tcf4* transcripts encoding TCF4-B, -C, -D and -A in rat primary cortical neurons.
- Specific *Tcf4* transcripts are changed in R6/1 mice brain tissues
 - The transcript levels of *Tcf4-D (8c-II)*, *Tcf4-A* and *Tcf4-I* are reduced and *TCF4-D (7b-I)* is increased in R6/1 mice cortex compared to wt mice.
 - The levels of *Tcf4-I* are decreased in R6/1 mice striatum.
 - The total level of *Tcf4* mRNA are decreased in hippocampus of R6/1 mice compared to wt mice. More precisely, the transcript levels of *Tcf4-B/C*, *Tcf4-B*, *Tcf4-D (8c-II)*, *Tcf4-A* and *Tcf4-I* are decreased, whereas mRNA levels of *Tcf4-D (7b-I)* are increased.
 - *Tcf4* mRNA levels in R6/1 cerebellum are not changed compared to wt mice.
- Protein levels of specific TCF4 isoforms are changed in R6/1 mice brain tissues
 - TCF4-A isoform levels are lower in R6/1 mice cortex compared to wt mice.
 - There is no significant change in R6/1 striatum compared to wt mice.
 - TCF4-B/C and TCF4-D isoforms are decreased in R6/1 mice hippocampus.
- TCF4-B/C protein isoform levels are decreased in the CA1 region of hippocampus and cerebral cortex in HD patients compared to health controls.
- *Bdnf* mRNA levels are decreased in cortex, hippocampus and cerebellum of R6/1 mice.
- mRNA levels of TCF4 binding partners *Neurod1* and *Ascl1* are changed in R6/1 mice brain tissue
 - *Neurod1* mRNA levels are upregulated and *Ascl1* levels downregulated in cortex of R6/1 mice.
 - *Neurod1* mRNA levels are unchanged and *Ascl1* mRNA levels were increased in striatum of R6/1 compared to wt mice.
 - No change in mRNA levels of *Neurod1* and *Ascl1* were detected in hippocampus.
 - *Neurod1* levels are reduced in cerebellum of R6/1 mice, whereas levels of *Ascl1* mRNA are unchanged.

- TCF4 and ASCL1 activate E-box-dependent gene transcription synergistically in rat cortical and hippocampal neurons.
 - Different TCF4 isoforms induce E-box-dependent reporter gene transcription to relatively same extent, except TCF4-I⁻ which shows lower induction.
 - TCF4- and E-box-dependent reporter gene transcription is enhanced by membrane depolarization and the induction is essentially similar for all major TCF4 isoforms.
 - The total induction of the reporter gene transcription is higher in cortical neurons than in hippocampal neurons overexpressing TCF4.
 - TCF4 isoforms show different activation of the reporter gene transcription when co-expressed with ASCL1. The induction is minimal for co-expression of TCF4-B⁻ and ASCL1 and the highest for TCF4-I⁻ and ASCL1.
 - Membrane depolarization further increases the co-expression induced transcription activation in both cortical and hippocampal neurons.
 - There is synergy between TCF4 and ASCL1, both in unstimulated and in depolarized neurons, however, the extent of the synergy varies considerably depending on the TCF4 isoform.
 - The synergy between TCF4 and ASCL1 upon membrane depolarization is greater in hippocampal neurons than in cortical neurons.

7 Discussion

7.1 Identification of transcription factors with altered subcellular localization and/or expression in Huntington's disease

The global dysregulation of gene expression has been long noted in Huntington's disease (Sugars and Rubinsztein, 2003; Valor, 2015; Xiang et al., 2018). Results of our immunocytochemical assays indicated that the nuclear localization of forkhead transcription factor family member FOXO3 is increased in genetic and 3-NP-treatment HD model cells. The immunocytochemical signal observed with the antibodies targeting the bHLH transcription factor TCF4 was also altered in mutant HTT expressing cells, but given the of the limited specificity of the used antibodies we were not able to differentiate between changes in TCF4 subcellular localization and expression level in these assays. Nevertheless, our results, together with previous studies on mislocalized transcription factors in HD (Valenza, 2005; Zuccato et al., 2003) suggest that changes in the subcellular distribution of transcription factors is among the mechanisms that underlie dysregulation of gene expression in HD. It would be of interest in future studies to elucidate whether these changes could be attributable to impaired nucleocytoplasmic transport or dysregulated functioning of nucleoporins described in several HD models and patients (Grima et al., 2017).

7.2 FOXO3 in Huntington's disease

The observed change in the subcellular localization of FOXO3 in HD cells led us to further study FOXO3 and its regulation in HD. We observed increased levels of FOXO3 protein in cell-based HD models. Furthermore, subcellular fractionation revealed parallel increase in FOXO3 levels in both nuclear and cytosolic fractions of mutant Hdh cells. FOXOs are vital integrators of survival and stress signals and their cellular distribution, activation and degradation is under stringent control that is achieved via complex post-translational modifications (PTMs) (Brown and Webb, 2018; Calnan and Brunet, 2008; Eijkelenboom and Burgering, 2013; Fasano et al., 2019; van der Horst and Burgering, 2007). PKB/AKT is one of the best described kinases regulating subcellular localization and degradation of FOXO3 (Brunet et al., 1999; Burgering and Kops, 2002). There are a number of studies showing conflicting results of PKB/AKT activity in various HD models and tissues (Ahmed et al., 2015; Colin et al., 2005; Gines et al., 2003; Ginés et al., 2010; Gratuze et al., 2015; Martín-Flores et al., 2020). Here we show that PKB/AKT signalling is not compromised in mutant Hdh cells, therefore increased levels of FOXO3 in the nucleus of mutant Hdh cells could not be explained by deranged PKB/AKT signalling. However, a possibility exists that the amount of PKB/AKT in HD cells is not sufficient for regulating increased amount of FOXO3 protein. In addition to PKB/AKT, MAPK kinases ERK 1/2 are known to phosphorylate and thereby promote degradation of FOXOs (Yang et al., 2008). We did not detect significant changes in the total levels of ERK 1/2, but we observed a drastic reduction in the levels of phosphorylation activated ERK 1/2 in mutant Hdh cells. This decrease might be dependent on the dose of mHtt since in homozygous Hdh^{109/109} cells the reduction is greater than in Hdh^{7/109} cells. To elucidate whether and how the reduced activity of ERK1/2 is linked to the increased levels of FOXO3 in HD cells, further studies on ERK 1/2 specific phosphorylation of FOXO3 in HD are warranted. Compromised ERK 1/2 signalling in HD has been shown to affect the resilience of the cells to oxidative stress

(Ginés et al., 2010) and FOXO3 is one of the key factors regulating the response to various types of stress (Eijkelenboom and Burgering, 2013). ERK signalling pathway is considered neuroprotective in HD as compounds upregulating decreased ERK rescue from cell death in HD models (Bodai and Marsh, 2012; Maher et al., 2011; Sarantos et al., 2012; Szlachcic et al., 2015; Yusuf et al., 2018). However, few publications state the contrary and show that increased levels of phosphorylated ERK 1/2 is related to neuronal vulnerability (Fusco et al., 2012) or exemplify the complexity and contrasting effects of ERK functions in neurodegenerative diseases (Blum et al., 2015; Rai et al., 2019). Phosphorylation of additional serine-residues by CK1 and SGK kinases aid the export of FOXO3 from the nucleus by 14-3-3 that induces its proteolysis (Brunet et al., 2001; Rena, 2002). Furthermore, PTM are not limited to phosphorylation and there exists a term “the FOXO code” to illustrate the whole complexity of modifications (Brown and Webb, 2018; Calnan and Brunet, 2008). Therefore, further elucidation of PTM of FOXO3 in HD context is needed to understand which roles of FOXO3 could be affected.

The observed nuclear localization of FOXO3 with concurrent increased FOXO3 protein levels led us to study *Foxo3* mRNA levels in HD model cells. Utilizing RT-qPCR we detected nearly 2-fold upregulation of *FOXO3* mRNA in cell-based HD models and a small increase in transgenic R6/2 mice and postmortem HD patient brain tissue. However, an integrated genomics and proteomics study on different HD knock-in mice with varying repeat size did not find significantly changed FOXO3 levels (Langfelder et al., 2016). This discrepancy might be due to different HD model animals used, small effect size and stringent false discovery rate (FDR) cut-off applied. Nevertheless, our study additionally revealed increased mRNA levels of FOXO3 target gene *FasL* in Hdh cells and in 3-NP treated primary neurons. However, Fas receptor and FasL levels are decreased in postmortem HD patient caudate and putamen (Ferrer et al., 2000), contradicting our results obtained in cellular HD model, whereas FAS receptor levels are increased in inducible HD cell-line (Sipione, 2002) that together may suggest dependence on disease stage. We additionally observed a difference in upregulation dynamics of *FasL* and *Foxo3* mRNA in response to 3-NP treatment. We hypothesise that fast up-regulation of *FasL* may rely on nuclear translocation of already synthesized FOXO3, whereas, slower up-regulation of *Foxo3* suggests an autoregulation or more complex process requiring additional factors. We demonstrated in chromatin immunoprecipitation (ChIP) experiments that FOXO3 binds to its own promoter and identified a Forkhead Response Element (FHRE) site that is to a large extent responsible for autoregulation of *Foxo3*. This is in line with previous studies showing the ability of FOXO factors to directly activate *Foxo1* and *Foxo4* transcription (Essaghir et al., 2009; Mubarak et al., 2009). Our work is also in agreement with study of Lützner *et al.* suggesting positive feedback mechanism in the regulation of *Foxo3* expression (Lützner et al., 2012). Of the potential FHREs analyzed by Lützner *et al.* by electrophoretic mobility shift assay, the highest affinity of FOXO3 was shown for site 1–2 FHREs (according to our numbering), and the site 3 FHRE, found to be functional in our study, was also bound by FOXO3 *in vitro*. However, the functionality of these sites in cells was not demonstrated in their study. In conclusion, we show that FOXO3 levels are increased in HD as a result of an overactivated positive autofeedback loop and together with previous studies suggest that this kind of loop might be characteristic for all FOXO family members and helps to sustain the stress response of FOXOs.

The outcome of elevated FOXO3 levels most probably depends on accompanying cellular signals and factors. Upon growth factor deprivation and oxidative stress activation of FOXOs induces apoptosis in neurons (Hu et al., 2019; Neri, 2012). Decreased BDNF levels

and increased oxidative stress have been reported in HD (Browne and Beal, 2006; Zuccato, 2001) and we further detected increased levels of apoptosis-triggering *FasL* mRNA levels and up-regulated *FOXO3* levels, that were previously suggested to induce motor neuron death (Barthélémy et al., 2004). Therefore, increased levels of FOXO3 may be detrimental to cortical and striatal neurons in HD. Furthermore, it has been noted that HD-related skeletal muscle atrophy is accompanied with increased FOXO3 levels (Mielcarek et al., 2015). On the other hand, there are publications suggesting participation of FOXOs in vital signalling pathways that protect from mutant Htt toxicity (Parker et al., 2012; Tourette et al., 2014; Vidal et al., 2012). Tourette et al. showed that *Hdh*^{7/7} cells are resistant to changes in *Foxo3* levels, whereas reduced *Foxo3* levels increase and overexpression decrease cell death in mutant *Hdh*^{109/109} cells (Tourette et al., 2014). More recent data indicate that FOXO3 is needed to prolong the functioning of the neurons in HD (Farina et al., 2017). Additionally, FOXO3 may antagonize the progression of cellular senescence in HD patient-derived neural stem cells (NSCs) and differentiated medium spiny neurons (MSNs), and reducing *FOXO3* expression strongly potentiates the mortality of HD NSCs (Voisin et al., 2020). Proteins containing coiled-coil structure with extended polyQ tracts interact with nuclear FOXOs and that was suggested to impair the functions of FOXOs leading to transcriptional dysregulation of dendrite morphogenesis and behavioural defects in *D. melanogaster* expressing polyQ proteins (Kwon et al., 2018). Therefore, increased levels of FOXO3 could be beneficial for rescuing this adverse interaction.

In addition to neurons, other neural cell types have gained attention in the context of HD. The RNA-seq-based computed astrocyte-specific transcriptional network was found to be the most relevant to HD pathology in the caudate nucleus (Scarpa et al., 2016). Furthermore, this HD-astrocyte-specific transcriptional network was shown to be regulated by FOXO3. A recent study revealed that white matter failure and hypomyelination are characteristic of HD in human (Osipovitch et al., 2019). This might be a result of a cell-autonomous defect in the terminal glial differentiation of mHTT-expressing human glial progenitor cells (hGPCs (bipotential oligodendrocyte-astrocytes)), instead of being secondary to neuronal loss as initially hypothesized, and may be central to the pathogenesis and neurological manifestations of HD. The role of FOXO1 in myelination has been previously established (Palazuelos et al., 2014). However, a direct link between FOXOs and oligodendrocytes has not been made yet in the context of HD. We studied immortalized striatal progenitor cells, cultured primary cortical neurons and brain tissues of R6/2 and postmortem HD patients. None of them enabled dissecting FOXO3 levels in the different HD-relevant cell populations, a task that could be achieved in the future with single-cell RNA-seq analysis of brain tissue.

Lastly, the participation of FOXO3 and other FOXOs in HD has been substantiated in a ChIP-seq study by HD Consortium, where FOXO binding sequences were among the top 10 motifs found under H3K27ac peaks enriched in HD versus non-disease samples (The HD iPSC Consortium, 2017). To conclude, the current knowledge on the involvement of FOXOs in HD suggests that activated FOXOs decrease progression of HD via suppressing the expression of mHtt, induction of autophagy and upregulation of genes encoding ROS scavengers and master regulators of mitochondrial biogenesis (Hu et al., 2019). Nevertheless, conflicting results have been published and the exact role of FOXO3 in HD and other neurodegenerative diseases and whether it's up-regulation is beneficial or detrimental is under continuous debate. Most probably it is dependent on multiple factors like cell type, disease state, age of onset and concurrent additional stressors, and therefore requires further investigation.

7.3 TCF4 in health

Little was known about the TCF4 at the time of our initial observation of TCF4 as a potentially misregulated transcription factor in HD model cells. Therefore, we first described the complex human *TCF4* gene structure with numerous alternative 5' exons and subsequently also characterized the mouse *Tcf4* gene. In general, the *TCF4* gene structure and internal exons are highly conserved between species, however, there are fewer transcripts and TCF4 isoforms in mice than in humans. By immunocytochemical assays we demonstrated mainly nuclear localization of longer TCF4-encoded isoforms and a more equal distribution between subcellular compartments of shorter TCF4-encoding isoforms. This nuclear translocation of the long isoforms relies on NLS sequence we identified. Functional bHLH domain is required for efficient nucleo-cytoplasmic redistribution of TCF4 short isoforms, which is achieved by binding with heterodimerization partners with NLS or NES sequences. Greb-Markiewicz et al. suggested additional highly conserved potential NLS and NES signal sequences in TCF4 bHLH domain (Greb-Markiewicz et al., 2019). However, we find that high conservation reported may arise from the fact that these sequences reside in canonical bHLH domain, moreover, the context used to study these signals do not allow dimerization (only part of bHLH was included) that potentially cause unnatural conformation of the domain, therefore may conceivably lead to misinterpretation of the results.

Thorough studies by Jung et al. on developing and adult mice brain and by Kim et al. on mice brain at the level of neural cell types have extended the knowledge of the spatio-temporal and cell type-specific expression patterns of TCF4 in the brain (Jung et al., 2018; Kim et al., 2020). Knowing that multitude of alternative TCF4 isoforms can be produced, we first demonstrated that the various TCF4 isoforms with different molecular weight are expressed in human cortex, hippocampus, cerebellum and other tissues by western blotting. However, it might be technically problematic to distinguish all isoforms or even the major isoforms TCF4-B and TCF4-A; of note, many commercial TCF4 antibodies are not properly validated. We validated TCF4 antibodies used and compared tissue bands with the bands of overexpressed TCF4 isoforms or *in vitro* translated TCF4 isoforms (including +/- isoforms). Nevertheless, this method of analysis is circumferential and creating TCF4 isoform-specific knock-out models may help to clarify this matter in the future.

The existence of a number of different TCF4 protein isoforms raised an intriguing question whether the isoforms have functional differences in target gene activation. This issue has not been addressed thoroughly (Liu et al., 1998; Skerjanc et al., 1996; Sobrado et al., 2009; Yoon and Chikaraishi, 1994). Our studies demonstrated that while all TCF4 isoforms can activate E-box-controlled reporter gene transcription, there is a disparity between TCF4 isoforms. Furthermore, functional differences of short and long TCF4 isoforms have been shown recently in oligodendrocyte differentiation and in plasmacytoid dendritic cell development (Grajkowska et al., 2017; Wedel et al., 2020). Additionally, we revealed that TCF4-controlled transcription is regulated by neural activity in neurons. While both AD1 and AD2 were able to mediate transcriptional activation and function synergistically in non-neural HEK293 cells, only transactivation domain AD2, and not AD1 separately, activated reporter gene transcription in neurons. Additionally, essentiality of AD2 has been noted in the developing prefrontal cortex *in vivo* (Page et al., 2018). Intriguingly, we found AD2 not to be involved in neuronal-activity-dependent regulation of TCF4 that is mediated by the region between AD2 and bHLH instead. This suggests that neural activity-dependent activation of

TCF4-mediated transcription might not be essential during the development of the nervous system, but rather in the later phases and for neuronal plasticity. These findings reveal fundamental differences between TCF4 isoforms as AD1 domain exists only in long isoforms, whereas AD2 and bHLH domains are universal to all TCF4 isoforms. In addition to AD1 and AD2, there is also AD3 (Chen et al., 2013) that is present in almost all TCF4 isoforms, and only TCF4-I⁻ misses the 6 initial amino acid residues of this domain. TAF4 binds to AD3 as a co-activator to facilitate TFIID complex binding potentially enhancing transcription initiation this way (Chen et al., 2013). Furthermore, this domain functions synergistically with AD1 and AD2 in E proteins HEB and E2A (Chen et al., 2013). However, proper analysis of TCF4 AD3 in different cellular contexts remains to be done.

We showed that TCF4 is regulated by neuronal activity predominantly via cAMP-PKA pathway, more precisely by phosphorylation of S448 by PKA. Increased expression of TCF4 severely disrupts the distribution of pyramidal cells in the mPFC (Page et al., 2018) and we showed that mutation S448A in TCF4-A⁻ rescues this phenotype of rat cortical 2/3 layer pyramidal neurons overexpressing TCF4-A⁻ *in vivo*. The significance of cAMP-PKA pathway was substantiated by our finding that soluble adenylyl cyclase (sAC) and not transmembrane AC (tmAC) is required for depolarization-induced TCF4-dependent transcription in neurons. Phosphorylation of bHLH proteins has been shown to affect their stability (Jo et al., 2011; Lin and Lee, 2012), dimerization specificity (Lluís et al., 2005) and temporal dynamics of their expression (Quan et al., 2016). However, the exact mechanism how phosphorylation of TCF4 by PKA regulates TCF4 transactivational capacity remains elusive. Neural activity initiates Ca²⁺ influx through voltage gated calcium channels and N-methyl D-aspartate receptors in neurons, which, in addition to PKA, activates also Ca²⁺/calmodulin-dependent protein kinase II (CAMKII) and protein kinase C (PKC) (Hagenston and Bading, 2011). Although we did not find the involvement of CAMKII and PKC in our experiments, their role cannot be completely ruled out in the regulation of activity-dependent TCF4 activation. Of note, binding of calmodulin to E protein dimers in the presence of Ca²⁺ restricts heterodimer formation with other bHLH proteins, inhibits the DNA-binding activity of E protein homodimers and therefore directly affects E protein-mediated transcription (Corneliussen et al., 1994; Hauser et al., 2008; Onions et al., 2000; Saarikettu et al., 2004). These post-translational regulatory mechanisms and Ca²⁺-affected formation of dimers likely enable signal-responsive regulation of target genes by specific bHLH dimers.

The effect of *TCF4* gene is dosage-dependent as illustrated by *TCF4*-associated diseases. Heterozygous mutations in *TCF4* lead to the haploinsufficiency of TCF4 causing a neurodevelopmental Pitt-Hopkins syndrome (PTHS) (Amiel et al., 2007; de Pontual et al., 2009; Sepp et al., 2012; Zweier et al., 2007), while partial deletions affecting only long isoforms of TCF4 lead to mild intellectual disability (Kharbanda et al., 2016). Several common variations in *TCF4* are linked to schizophrenia (Cross-Disorder Group of the Psychiatric Genomics Consortium, 2013; Genetic Risk and Outcome in Psychosis (GROUP) et al., 2009; The Schizophrenia Psychiatric Genome-Wide Association Study (GWAS) Consortium, 2011). The causal relationship of *TCF4* genetic variants and schizophrenia has not been established, nevertheless, TCF4 is strongly related with gating endophenotypes of schizophrenia and is susceptible to environmental impacts and in sum the role of TCF4 would be in line with neurodevelopmental hypothesis of schizophrenia and models like repeated-hit model and Gene X Environment model (Quednow et al., 2014). TCF4 has been suggested to be the master regulator of schizophrenia (Doostparast Torshizi et al., 2019). We tested the ability of TCF4 missense

variants found in patients with SCZ to activate E-box-controlled gene transcription in neurons as one possible mean of an effect of otherwise seemingly unarmful mutations. Small, yet significant increase in reporter gene expression was shown with variants P299S and G428V in untreated neurons and higher activity compared to wt was also detected in depolarized neurons. There is more research done on PTHS mutations that decrease TCF4 protein levels or its transcriptional activity (de Pontual et al., 2009; Sepp et al., 2012; Zweier et al., 2007), whereas accumulating evidence suggest that increased levels of TCF4 might be detrimental as well (Page et al., 2018; Talkowski et al., 2012; Ye et al., 2012). Comparative study of mice slightly over-expressing TCF4 and mice with decreased expression of long TCF4 isoforms described unchanged basic neurotransmission, but revealed *Tcf4* gene-dose mediated impact to increase LTD and LTP, respectively, in hippocampal neural networks (Badowska et al., 2020). It was suggested that disturbed synaptic plasticity has profound impact on higher order cognition of these *TCF4* mutant models. We hypothesize that impaired synaptic plasticity can be partially caused by aberrant TCF4-dependent transcriptional response to neuronal activity affecting neuronal connectivity and/or excitatory-inhibitory balance. Future work will further elucidate the role of TCF4 in the pathophysiology of schizophrenia.

Dimerization of TCF4 and ASCL1 has been shown previously (Persson et al., 2000), and synergism between ASCL1 and TCF4-B⁻ was proposed by de Pontual et al. in reporter gene assay with *DeltaM* promoter E-box constructs (de Pontual et al., 2009). Here we show that endogenous TCF4 binds to neuronal activity-regulated *Gadd45g*-promoter in rat primary cortical neurons. Furthermore, reporter assay with *GADD45G*-promoter constructs revealed synergistic effect of overexpressed TCF4-A⁻ and ASCL1 both in resting and depolarized neurons, and downregulation of *Tcf4* reduces endogenous *Gadd45g* mRNA levels. We then set out to determine transcriptional capacity of all TCF4 isoforms alone and when dimerized with ASCL1, and to elucidate the effect of neuronal activity on these dimers in neurons. Our results of reporter gene assays in rat primary cortical and hippocampal neurons showed that there is a synergistic effect between all studied TCF4 protein isoforms and ASCL1, although the extent varies several times depending on TCF4 protein isoform. However, no known domain or regulatory sequence seems to be responsible for that. In addition, membrane depolarization by KCl-treatment further increased the reporter gene transcription by these heterodimers. Hypothetically, this effect can be mediated by increased affinity of calmodulin to TCF4 dimers at high Ca²⁺ concentrations that inhibits homodimer binding and enables binding of heterodimers to DNA that has been shown with MyoD and E12 (Hauser et al., 2008). Our results demonstrate that low transactivation capability of a TCF4 isoform (homodimers) can be compensated when heterodimerized with ASCL1, whereas highly active full length TCF4-B⁻ showed limited synergism with ASCL1 in neurons. Parallel experiments in cortical and hippocampal neurons revealed interesting differences, as the synergy between TCF4 and ASCL1 increases only in hippocampal neurons upon membrane depolarization, TCF4-dependent transcription is in general higher in cortical neurons compared to hippocampal. This suggests differences of these neurons and brain regions that need to be considered for example for the development of gene therapies for PTHS. We have studied TCF4 partnership with ASCL1, but the E proteins (and TCF4 as one of them) have been considered to be the obliged dimerization partners to many other bHLH proteins for DNA binding (Massari and Murre, 2000). Therefore, based on our data, we can hypothesize that levels of TCF4 and specific TCF4 isoforms may have differential effects on target gene activation by dimerizing with various bHLH proteins, and thereby

influence neural development, potentially play a role in different disorders and diseases and have a potential in regenerative medicine as co-factors for cell reprogramming (Dennis et al., 2019; Le Dréau et al., 2018; Wang and Baker, 2015).

7.4 TCF4 in Huntington's disease

To follow up on our initial observations on the altered immunocytochemical signal of TCF4 in HD cells, we studied TCF4 in different cell and mouse HD models and in postmortem tissue from HD patients, and revealed misregulated TCF4 expression in HD. Regulation at transcriptional level was suggested by our RT-qPCR data, where the expression of various *Tcf4* transcripts was reduced in Hdh cells and in the brain of R6/1 mouse model of HD. However, we observed differences in *Tcf4* expression between the studied brain areas that included cerebral cortex, hippocampus, striatum and cerebellum. The levels of specific *Tcf4* transcripts as well as total *Tcf4* mRNA were reduced in R6/1 hippocampus, while almost unchanged total *Tcf4* mRNA levels hid significant reduction of specific transcripts in cortex (*Tcf4-D*, *-A* and *-I*) and striatum (*Tcf4-I*) of R6/1 mice. Although TCF4-I might be a marginal isoform, as could be extrapolated from a recent splice-site junction-based analysis of RNA-seq data from Fuchs' corneal dystrophy patient and control corneas, however, cornea is a very specialized tissue and may not replicate TCF4 isoform-encoding transcript ratios in different regions of the brain (Sirp et al., 2020). On the other hand, we showed that transcriptional activity of TCF4-I⁻ isoform is very high in neural activity induced neurons.

Although nuclear levels of TCF4 seemed to be decreased in mutant Hdh cells, the antibodies used in the immunocytochemical analysis did not enable us to elucidate whether the affected TCF4 isoforms were NLS-containing long isoforms, which preferentially reside in the nucleus, or smaller isoforms, which rely on NLS-containing binding partners for their nuclear import (Sepp et al., 2017, 2011). By Western blot analysis of total lysates and cellular fractions from striatal progenitor-derived Hdh cells we demonstrated that both high and lower molecular weight TCF4 isoforms are reduced in the nucleus and cytoplasm of mutant Hdh cells. However, the isoform-specific expression of TCF4 is more complex in different brain tissues of R6/1 HD model mice at various ages. The most prominent reduction of TCF4 protein was detected in the hippocampus (TCF4-B/C and TCF4-D), and in the cortex (TCF4) of R6/1 mice. The finding of decreased TCF4-B/C protein isoforms was recapitulated in HD patient CA1 region of the hippocampus and cerebral cortex. Our RT-qPCR results showed decline of respective mRNA transcripts in R6/1 suggesting that misregulation of *Tcf4* gene expression is the underlying cause of reduced TCF4 protein levels. Although, we have validated the TCF4 antibodies used in this study and made effort to annotate several TCF4-like bands by comparing them to *in vitro* translated TCF4 isoform bands, some uncertainty for this annotation remains since a) not all TCF4 isoforms are expressed at comparable levels in different brain regions as highlighted in our experiments with R6/1 mice (e.g. TCF4 isoforms in cortex vs striatum); b) +/- isoforms progress differently in gel; c) the expression patterns are divergent also between mouse and human hippocampus. Nevertheless, our results confidently show that TCF4 is downregulated in HD. Future studies are warranted to elucidate the causal mechanisms of this downregulation in different brain regions and in the context of alternative TCF4 isoforms.

TCF4 can bind DNA as a homodimer (Blake et al., 2010) but its transcriptional capacity is higher in the context of heterodimers with bHLH proteins from other classes (Nurm et al., 2021; Persson et al., 2000; Sepp et al., 2017). Here we measured mRNA levels of

Neurod1 and *Ascl1* in different brain regions of wt and R6/1 mice and found a) no change in hippocampus (coupled with decreased TCF4 mRNA and protein levels); b) significant up-regulation of *Neurod1* and down-regulation of *Ascl1* mRNA in cerebral cortex (coupled with decreased TCF4-A transcripts); c) down-regulation of *Neurod1* in cerebellum (coupled with unchanged levels of *Tcf4* mRNA). Previously, reduced levels of NEUROD1 in the hippocampus of R6/2 and in HD patient iPSC lines have been reported in conjunction with impaired neurogenesis (Fedele et al., 2011; The HD iPSC Consortium, 2017). NEUROD1 is essential for the survival and maturation of adult-born neurons in hippocampus (Gao et al., 2009). Furthermore, wild type HTT mediates activation of NEUROD1 leading to phosphorylation of NEUROD1 via forming a scaffold to enable complex forming of HAP1, kinase MLK2 and NEUROD1 (Marcora et al., 2003). This activation may be altered by the expression of mHTT, and, although it has not been directly studied, it may add an extra layer to misregulation of bHLH transcription factors in HD. A RNA-seq study in HD patient-derived iPSCs identified *NEUROD1* as a hub in the HD network and several other genes in this network encode proteins that regulate *NEUROD1* expression, such as *ASCL1*, *NEUROG2*, *POU4F* and *REST/NRSF* (The HD iPSC Consortium, 2017). Therefore, in addition to TCF4 itself, TCF4 dimerization partners also seem to be dysregulated in HD and potentially further affect TCF4-dependent transcription. Furthermore, our results from reporter assays about differential synergy of TCF4 isoforms with *ASCL1* in rat cortical and hippocampal neurons illustrate the interplay between the bHLH proteins and emphasize the importance of considering all TCF4 isoforms when elucidating the functions and effects of TCF4 in health and disease.

In addition to downregulated TCF4 expression in HD, activation of transcription by TCF4 may be further impaired because of misregulated co-activators (Seredenina and Luthi-Carter, 2012). The aggregation prone mHTT sequesters CBP and TAF4/TAFII130 into aggregates, decreasing their availability (Dunah, 2002; Nucifora Jr., 2001) and CBP and TAF4/TAFII130 have been shown to bind AD1 and AD2 or AD3 in TCF4, respectively (Bayly et al., 2004; Chen et al., 2013). TAF4 is required for TFIID binding to TCF4-regulated promoters, enabling formation of RNAPol II complex. Additionally, TAF4 binds transcription factor SP1 to this complex, and enhanced aggregation of SP1 with mHTT has been shown to inhibit this binding (Chen et al., 2013; Dunah, 2002). Together, these observations illustrate the complexity and vulnerability of transcription activation in HD.

Here, we also showed that TCF4-dependent transcription is induced by neuronal activity that increases intracellular Ca^{2+} levels. Widespread dysregulation of genes involved in Ca^{2+} signalling pathways has been described in HD, including genes for several subunits of the voltage gated Ca^{2+} channel *CACNA1* and the plasma membrane Ca^{2+} -ATPases, and downstream effectors *CAMKII*, *CALM* (calmodulin) and *CREB* (The HD iPSC Consortium, 2017). Functionally, it has been shown that mHTT binds both calmodulin and transglutaminase TG2 with higher affinity than wt HTT and mHTT increases interaction between calmodulin and TG2, which has a role in mHTT aggregate stabilisation (Zainelli, 2004). Moreover, interruption of binding between calmodulin and mHTT is protective in the context of HD (Dai et al., 2009; Dudek et al., 2008). As mentioned above, increased intracellular Ca^{2+} can inhibit E protein-dependent transcriptional activation by preferable binding of calmodulin to E protein homodimers (Hauser et al., 2008; Hermann et al., 1998; Saarikettu et al., 2004). The total effect of these misregulations on TCF4, its heterodimerization partners and consequential target gene activation needs to be elucidated in the future.

Studies have revealed that prodromal HD patients have poorer performance in many neurocognitive functions (Stout et al., 2011) such as learning and memory that rely on neuronal plasticity and neurogenesis in the hippocampus among others (Aimone et al., 2009, 2006; Chambers et al., 2004; Eriksson et al., 1998; reviewed in Gonçalves et al., 2016). However, the hippocampus remains relatively unaffected from neurodegeneration in HD patients (Ramirez-Garcia et al., 2019). On the other hand, reduced hippocampal adult neurogenesis in subgranular zone (SGZ) of the dentate gyrus (DG) of the hippocampus has been reported in R6/2, R6/1 and YAC128 transgenic HD model mice (Gil et al., 2005; Lazic et al., 2004; Simpson et al., 2011). Furthermore, impaired synaptic vesicle functions have been identified in several brain regions of HD patients and hippocampal synaptic plasticity deficits have been thoroughly studied in mouse models of HD (Neueder and Bates, 2014; Quirion and Parsons, 2019). Developmental basis for HD has been proposed based on the critical functions of huntingtin in the developing nervous system and reinforced by the decline of cognitive functions and emergence of psychiatric disturbances at early stages of HD preceding the classical motor symptoms by many years (Bates et al., 2015; Zuccato and Cattaneo, 2014). Recently, it has been shown that slight downregulation of *Tcf4* expression levels does not alter basic neurotransmission, but increases long-term potentiation and thereby shapes long-term plasticity in hippocampal neuronal networks (Badowska et al., 2020). Furthermore, *Tcf4* conditional KO mice display abnormal migration of neural progenitor cells, which leads to disruption of integrity and hypoplasia in the dentate gyrus and impairs the social memory, therefore revealing a critical role for TCF4 in regulating DG development (Wang et al., 2020). Additionally, BDNF is one of the master regulators of synaptic plasticity (Park and Poo, 2013). Misregulation of BDNF and its downstream signalling pathways are well-described in HD (Smith-Dijak et al., 2019), and enhancing BDNF signalling restores synaptic plasticity and memory in HD mice (Anglada-Huguet et al., 2016; Lynch et al., 2007). Here we showed that decreased TCF4 in R6/1 mice hippocampus and cortex coincide with reduced levels of *Bdnf* in these tissues. A recent study shows that TCF4 directly binds an enhancer of *Bdnf* suggesting that the expression of *Bdnf* is potentially regulated by TCF4 (Tuvikene et al., 2021). This could provide a complementary mechanism of BDNF dysregulation in addition to downregulation of BDNF as a result of the inability of mHTT to regulate REST/NRSF activity (Gauthier et al., 2004; Zuccato, 2001; Zuccato et al., 2003).

The role of neuronal activity in the process of axon myelination and its role in plasticity, cognitive functions and learning has been established (Choi et al., 2019; Fields, 2008; Nickel and Gu, 2018). TCF4 is a critical partner for OLIG2 in oligodendrocytes in curating terminal differentiation and myelination process (Wedel et al., 2020). Furthermore, studies in PTHS mice models linked myelin-related transcriptomic profile and reduced number of oligodendrocytes and myelination deficits functionally with TCF4 (Phan et al., 2020). Therefore, TCF4 might be a vital player in neural plasticity and cognitive functions via participation in neurogenesis, migration and myelination among other process.

Collectively, altered expression of TCF4 and its binding partners in HD, especially in hippocampus, opens the possibility that misregulation of TCF4-dependent transcription could contribute to the decline of cognitive function in HD.

8 Conclusions

The main findings of this thesis are as follows:

- Transcription factor FOXO3 is overactivated in Huntington's disease via a positive auto-feedback loop.
- bHLH transcription factor TCF4 is expressed in various tissues in human but not at equal levels. TCF4 isoforms are generated by alternative 5' exons usage and splicing; some TCF4 protein isoforms have functional NLS motif.
- TCF4 is a neuronal activity-regulated transcription factor and its activation is mediated by soluble adenylyl cyclase and protein kinase A.
- TCF4 isoforms differ in their capacity to activate gene transcription.
- There is transactivational synergy between TCF4 and ASCL1, although the effect size is different for specific TCF4 isoforms and this synergy is further affected by neural activity in hippocampal neurons.
- The levels of different TCF4 isoforms are reduced in cell-based and in animal HD models and in postmortem HD patient brain. The most drastical decrease occurs in HD patient hippocampus tissue.

References

- Achour M, Le Gras S, Keime C, Parmentier F, Lejeune F-X, Boutillier A-L, Neri C, Davidson I, Merienne K (2015) Neuronal identity genes regulated by super-enhancers are preferentially down-regulated in the striatum of Huntington's disease mice. *Hum Mol Genet* 24:3481–3496.
- Agus F, Crespo D, Myers RH, Labadorf A (2019) The caudate nucleus undergoes dramatic and unique transcriptional changes in human prodromal Huntington's disease brain. *BMC Med Genomics* 12:137.
- Ahmed I, Sbodio JI, Harraz MM, Tyagi R, Grima JC, Albacarys LK, Hubbi ME, Xu R, Kim S, Paul BD, Snyder SH (2015) Huntington's disease: Neural dysfunction linked to inositol polyphosphate multikinase. *Proc Natl Acad Sci* 112:9751–9756.
- Aimone JB, Wiles J, Gage FH (2009) Computational Influence of Adult Neurogenesis on Memory Encoding. *Neuron* 61:187–202.
- Aimone JB, Wiles J, Gage FH (2006) Potential role for adult neurogenesis in the encoding of time in new memories. *Nat Neurosci* 9:723–727.
- Ament SA, Pearl JR, Cattle JP, Bragg RM, Skene PJ, Coffey SR, Bergey DE, Wheeler VC, MacDonald ME, Baliga NS, Rosinski J, Hood LE, Carroll JB, Price ND (2018) Transcriptional regulatory networks underlying gene expression changes in Huntington's disease. *Mol Syst Biol* 14.
- Amiel J, Rio M, Pontual L de, Redon R, Malan V, Boddaert N, Plouin P, Carter NP, Lyonnet S, Munnich A, Colleaux L (2007) Mutations in TCF4, Encoding a Class I Basic Helix-Loop-Helix Transcription Factor, Are Responsible for Pitt-Hopkins Syndrome, a Severe Epileptic Encephalopathy Associated with Autonomic Dysfunction. *Am J Hum Genet* 80:988–993.
- Andrew SE, Paul Goldberg Y, Kremer B, Telenius H, Theilmann J, Adam S, Starr E, Squitieri F, Lin B, Kalchman MA, Graham RK, Hayden MR (1993) The relationship between trinucleotide (CAG) repeat length and clinical features of Huntington's disease. *Nat Genet* 4:398–403.
- Anglada-Huguet M, Vidal-Sancho L, Giralto A, García-Díaz Barriga G, Xifró X, Alberch J (2016) Prostaglandin E2 EP2 activation reduces memory decline in R6/1 mouse model of Huntington's disease by the induction of BDNF-dependent synaptic plasticity. *Neurobiol Dis* 95:22–34.
- Asada S, Daitoku H, Matsuzaki H, Saito T, Sudo T, Mukai H, Iwashita S, Kako K, Kishi T, Kasuya Y, Fukamizu A (2007) Mitogen-activated protein kinases, Erk and p38, phosphorylate and regulate Foxo1. *Cell Signal* 19:519–527.
- Augood SJ, Faull RLM, Love DR, Emson PC (1996) Reduction in enkephalin and substance P messenger RNA in the striatum of early grade Huntington's disease: A detailed cellular in situ hybridization study. *Neuroscience* 72:1023–1036.
- Badowska DM, Brzózka MM, Kannaiyan N, Thomas C, Dibaj P, Chowdhury A, Steffens H, Turck CW, Falkai P, Schmitt A, Papiol S, Scheuss V, Willig KI, Martins-de-Souza D, Rhee JS, Malzahn D, Rossner MJ (2020) Modulation of cognition and neuronal plasticity in gain- and loss-of-function mouse models of the schizophrenia risk gene Tcf4. *Transl Psychiatry* 10:343.
- Bae B-I, Xu H, Igarashi S, Fujimuro M, Agrawal N, Taya Y, Hayward SD, Moran TH, Montell C, Ross CA, Snyder SH, Sawa A (2005) p53 Mediates Cellular Dysfunction and Behavioral Abnormalities in Huntington's Disease. *Neuron* 47:29–41.

- Baker NE, Brown NL (2018) All in the family: proneural bHLH genes and neuronal diversity. *Development* 145:dev159426.
- Bañez-Coronel M, Porta S, Kagerbauer B, Mateu-Huertas E, Pantano L, Ferrer I, Guzmán M, Estivill X, Martí E (2012) A Pathogenic Mechanism in Huntington's Disease Involves Small CAG-Repeated RNAs with Neurotoxic Activity. *PLoS Genet* 8:e1002481.
- Barthélémy C, Henderson CE, Pettmann B (2004) [No title found]. *BMC Neurosci* 5:48.
- Bates GP, Dorsey R, Gusella JF, Hayden MR, Kay C, Leavitt BR, Nance M, Ross CA, Scahill RI, Wetzel R, Wild EJ, Tabrizi SJ (2015) Huntington disease. *Nat Rev Dis Primer* 1:15005.
- Bayly R, Chuen L, Currie RA, Hyndman BD, Casselman R, Blobel GA, LeBrun DP (2004) E2A-PBX1 Interacts Directly with the KIX Domain of CBP/p300 in the Induction of Proliferation in Primary Hematopoietic Cells. *J Biol Chem* 279:55362–55371.
- Beal M, Brouillet E, Jenkins B, Ferrante R, Kowall N, Miller J, Storey E, Srivastava R, Rosen B, Hyman B (1993) Neurochemical and histologic characterization of striatal excitotoxic lesions produced by the mitochondrial toxin 3-nitropropionic acid. *J Neurosci* 13:4181–4192.
- Beal MF (1992) Does impairment of energy metabolism result in excitotoxic neuronal death in neurodegenerative illnesses? *Ann Neurol* 31:119–130.
- Beal MF, Kowall NW, Ellison DW, Mazurek MF, Swartz KJ, Martin JB (1986) Replication of the neurochemical characteristics of Huntington's disease by quinolinic acid. *Nature* 321:168–171.
- Becanovic K, Pouladi MA, Lim RS, Kuhn A, Pavlidis P, Luthi-Carter R, Hayden MR, Leavitt BR (2010) Transcriptional changes in Huntington disease identified using genome-wide expression profiling and cross-platform analysis. *Hum Mol Genet* 19:1438–1452.
- Benn CL, Sun T, Sadri-Vakili G, McFarland KN, DiRocco DP, Yohrling GJ, Clark TW, Bouzou B, Cha J-HJ (2008) Huntingtin Modulates Transcription, Occupies Gene Promoters In Vivo, and Binds Directly to DNA in a Polyglutamine-Dependent Manner. *J Neurosci* 28:10720–10733.
- Bigan E, Sasidharan Nair S, Lejeune F-X, Fragnaud H, Parmentier F, Mégret L, Verny M, Aaronson J, Rosinski J, Neri C (2020) Genetic cooperativity in multi-layer networks implicates cell survival and senescence in the striatum of Huntington's disease mice synchronous to symptoms. *Bioinformatics* 36:186–196.
- Blake DJ, Forrest M, Chapman RM, Tinsley CL, O'Donovan MC, Owen MJ (2010) TCF4, Schizophrenia, and Pitt-Hopkins Syndrome. *Schizophr Bull* 36:443–447.
- Blum D, Herrera F, Francelle L, Mendes T, Basquin M, Obriot H, Demeyer D, Sergeant N, Gerhardt E, Brouillet E, Buée L, Outeiro TF (2015) Mutant huntingtin alters Tau phosphorylation and subcellular distribution. *Hum Mol Genet* 24:76–85.
- Bodai L, Marsh JL (2012) A novel target for Huntington's disease: ERK at the crossroads of signaling: The ERK signaling pathway is implicated in Huntington's disease and its upregulation ameliorates pathology. *BioEssays* 34:142–148.
- Bondulich MK et al. (2017) Myostatin inhibition prevents skeletal muscle pathophysiology in Huntington's disease mice. *Sci Rep* 7:14275.
- Borlongan C (1997) 3-Nitropropionic acid animal model and Huntington's disease. *Neurosci Biobehav Rev* 21:289–293.

- Borovecki F, Lovrecic L, Zhou J, Jeong H, Then F, Rosas HD, Hersch SM, Hogarth P, Bouzou B, Jensen RV, Krainc D (2005) Genome-wide expression profiling of human blood reveals biomarkers for Huntington's disease. *Proc Natl Acad Sci U S A* 102:11023–11028.
- Brouillet E, Hantraye P, Ferrante RJ, Dolan R, Leroy-Willig A, Kowall NW, Beal MF (1995) Chronic mitochondrial energy impairment produces selective striatal degeneration and abnormal choreiform movements in primates. *Proc Natl Acad Sci* 92:7105–7109.
- Brouillet E, Jacquard C, Bizat N, Blum D (2005) 3-Nitropropionic acid: a mitochondrial toxin to uncover physiopathological mechanisms underlying striatal degeneration in Huntington's disease. *J Neurochem* 95:1521–1540.
- Brown AK, Webb AE (2018) Regulation of FOXO Factors in Mammalian Cells In: *Current Topics in Developmental Biology*, pp165–192. Elsevier.
- Browne SE, Beal MF (2006) Oxidative Damage in Huntington's Disease Pathogenesis. *Antioxid Redox Signal* 8:2061–2073.
- Bruce AW, Donaldson IJ, Wood IC, Yerbury SA, Sadowski MI, Chapman M, Gottgens B, Buckley NJ (2004) Genome-wide analysis of repressor element 1 silencing transcription factor/neuron-restrictive silencing factor (REST/NRSF) target genes. *Proc Natl Acad Sci* 101:10458–10463.
- Brunet A (2004) Stress-Dependent Regulation of FOXO Transcription Factors by the SIRT1 Deacetylase. *Science* 303:2011–2015.
- Brunet A, Bonni A, Zigmond MJ, Lin MZ, Juo P, Hu LS, Anderson MJ, Arden KC, Blenis J, Greenberg ME (1999) Akt Promotes Cell Survival by Phosphorylating and Inhibiting a Forkhead Transcription Factor. *Cell* 96:857–868.
- Brunet A, Park J, Tran H, Hu LS, Hemmings BA, Greenberg ME (2001) Protein Kinase SGK Mediates Survival Signals by Phosphorylating the Forkhead Transcription Factor FKHL1 (FOXO3a). *Mol Cell Biol* 21:952–965.
- Buckley NJ, Johnson R, Zuccato C, Bithell A, Cattaneo E (2010) The role of REST in transcriptional and epigenetic dysregulation in Huntington's disease. *Neurobiol Dis* 39:28–39.
- Burgering BMT, Kops GJPL (2002) Cell cycle and death control: long live Forkheads. *Trends Biochem Sci* 27:352–360.
- Buuh ZY, Lyu Z, Wang RE (2018) Interrogating the Roles of Post-Translational Modifications of Non-Histone Proteins: Miniperspective. *J Med Chem* 61: 3239–3252.
- Calnan DR, Brunet A (2008) The FoxO code. *Oncogene* 27:2276–2288.
- Celestini V et al. (2018) Uncoupling FoxO3A mitochondrial and nuclear functions in cancer cells undergoing metabolic stress and chemotherapy. *Cell Death Dis* 9:231.
- Cha J-HJ (2007) Transcriptional signatures in Huntington's disease. *Prog Neurobiol* 83:228–248.
- Chae Y-C, Kim J-Y, Park JW, Kim K-B, Oh H, Lee K-H, Seo S-B (2019) FOXO1 degradation via G9a-mediated methylation promotes cell proliferation in colon cancer. *Nucleic Acids Res* 47:1692–1705.
- Chai Y, Wu L, Griffin JD, Paulson HL (2001) The role of protein composition in specifying nuclear inclusion formation in polyglutamine disease. *J Biol Chem* 276: 44889–44897.

- Chambers RA, Potenza MN, Hoffman RE, Miranker W (2004) Simulated Apoptosis/Neurogenesis Regulates Learning and Memory Capabilities of Adaptive Neural Networks. *Neuropsychopharmacology* 29:747–758.
- Chan EYW (2002) Increased huntingtin protein length reduces the number of polyglutamine-induced gene expression changes in mouse models of Huntington's disease. *Hum Mol Genet* 11:1939–1951.
- Chaves I, van der Horst GTJ, Schellevis R, Nijman RM, Koerkamp MG, Holstege FCP, Smidt MP, Hoekman MFM (2014) Insulin-FOXO3 Signaling Modulates Circadian Rhythms via Regulation of Clock Transcription. *Curr Biol* 24:1248–1255.
- Chen T, Wu Q, Zhang Y, Lu T, Yue W, Zhang D (2016) Tcf4 Controls Neuronal Migration of the Cerebral Cortex through Regulation of Bmp7. *Front Mol Neurosci* 9.
- Chen W-Y, Zhang J, Geng H, Du Z, Nakadai T, Roeder RG (2013) A TAF4 coactivator function for E proteins that involves enhanced TFIIID binding. *Genes Dev* 27:1596–1609.
- Chiang C et al. (2012) Complex reorganization and predominant non-homologous repair following chromosomal breakage in karyotypically balanced germline rearrangements and transgenic integration. *Nat Genet* 44:390–397.
- Chiamarello A, Soosaar A, Neuman T, Zuber MX (1995) Differential expression and distinct DNA-binding specificity of ME1a and ME2 suggest a unique role during differentiation and neuronal plasticity. *Mol Brain Res* 29:107–118.
- Choi EH, Blasiak A, Lee J, Yang IH (2019) Modulation of Neural Activity for Myelination in the Central Nervous System. *Front Neurosci* 13:952.
- Ciesiolka A, Stroynowska-Czerwinska A, Joachimiak P, Ciolak A, Kozłowska E, Michalak M, Dabrowska M, Olejniczak M, Raczynska KD, Zielinska D, Wozna-Wysocka M, Krzyzosiak WJ, Fiszler A (2020) Artificial miRNAs targeting CAG repeat expansion in ORFs cause rapid deadenylation and translation inhibition of mutant transcripts. *Cell Mol Life Sci*.
- Colin E, Régulier E, Perrin V, Dürr A, Brice A, Aebischer P, Déglon N, Humbert S, Saudou F (2005) Akt is altered in an animal model of Huntington's disease and in patients. *Eur J Neurosci* 21:1478–1488.
- Conforti P, Mas Montey A, Zuccato C, Buckley NJ, Davidson B, Cattaneo E (2013) In vivo delivery of DN:REST improves transcriptional changes of REST-regulated genes in HD mice. *Gene Ther* 20:678–685.
- Cong S-Y, Pepers BA, Evert BO, Rubinsztein DC, Roos RAC, van Ommen G-JB, Dorsman JC (2005) Mutant huntingtin represses CBP, but not p300, by binding and protein degradation. *Mol Cell Neurosci* 30:560–571.
- Corneliusson B, Holm M, Waltersson Y, Onions J, Hallberg B, Thornell A, Grundström T (1994) Calcium/calmodulin inhibition of basic-helix-loop-helix transcription factor domains. *Nature* 368:760–764.
- Corneliusson B, Thornell A, Hallberg B, Grundström T (1991) Helix-loop-helix transcriptional activators bind to a sequence in glucocorticoid response elements of retrovirus enhancers. *J Virol* 65:6084–6093.
- Crocker SF, Costain WJ, Robertson HA (2006) DNA microarray analysis of striatal gene expression in symptomatic transgenic Huntington's mice (R6/2) reveals neuroinflammation and insulin associations. *Brain Res* 1088:176–186.
- Cross-Disorder Group of the Psychiatric Genomics Consortium (2013) Identification of risk loci with shared effects on five major psychiatric disorders: a genome-wide analysis. *Lancet Lond Engl* 381:1371–1379.

- Cummings DM, Alaghband Y, Hickey MA, Joshi PR, Hong SC, Zhu C, Ando TK, André VM, Cepeda C, Watson JB, Levine MS (2012) A critical window of CAG repeat-length correlates with phenotype severity in the R6/2 mouse model of Huntington's disease. *J Neurophysiol* 107:677–691.
- Dai Y, Dudek NL, Li Q, Fowler SC, Muma NA (2009) Striatal Expression of a Calmodulin Fragment Improved Motor Function, Weight Loss, and Neuropathology in the R6/2 Mouse Model of Huntington's Disease. *J Neurosci* 29:11550–11559.
- Dansen TB, Smits LMM, van Triest MH, de Keizer PLJ, van Leenen D, Koerkamp MG, Szybowska A, Meppelink A, Brenkman AB, Yodoi J, Holstege FCP, Burgering BMT (2009) Redox-sensitive cysteines bridge p300/CBP-mediated acetylation and FoxO4 activity. *Nat Chem Biol* 5:664–672.
- de Pontual L et al. (2009) Mutational, functional, and expression studies of the *TCF4* gene in Pitt-Hopkins syndrome. *Hum Mutat* 30:669–676.
- De Souza RAG, Kosior N, Thomson SB, Mathelier A, Zhang AW, Bečanović K, Wasserman WW, Leavitt BR (2018) Computational Analysis of Transcriptional Regulation Sites at the HTT Gene Locus. *J Huntingt Dis* 7:223–237.
- Dennis DJ, Han S, Schuurmans C (2019) bHLH transcription factors in neural development, disease, and reprogramming. *Brain Res* 1705:48–65.
- Desplats PA, Kass KE, Gilmartin T, Stanwood GD, Woodward EL, Head SR, Sutcliffe JG, Thomas EA (2006) Selective deficits in the expression of striatal-enriched mRNAs in Huntington's disease. *J Neurochem* 96:743–757.
- Donovan MR, Marr MT (2016) dFOXO Activates Large and Small Heat Shock Protein Genes in Response to Oxidative Stress to Maintain Proteostasis in Drosophila. *J Biol Chem* 291:19042–19050.
- Doostparast Torshizi A, Armoskus C, Zhang H, Forrest MP, Zhang S, Souaiaia T, Evgrafov OV, Knowles JA, Duan J, Wang K (2019) Deconvolution of transcriptional networks identifies TCF4 as a master regulator in schizophrenia. *Sci Adv* 5:eaau4139.
- Dudek NL, Dai Y, Muma NA (2008) Protective Effects of Interrupting the Binding of Calmodulin to Mutant Huntingtin. *J Neuropathol Exp Neurol* 67:355–365.
- Dunah AW (2002) Sp1 and TAFII130 Transcriptional Activity Disrupted in Early Huntington's Disease. *Science* 296:2238–2243.
- Eijkelenboom A, Burgering BMT (2013) FOXOs: signalling integrators for homeostasis maintenance. *Nat Rev Mol Cell Biol* 14:83–97.
- El-Daher M, Hangen E, Bruyère J, Poizat G, Al-Ramahi I, Pardo R, Bourg N, Souquere S, Mayet C, Pierron G, Lévêque-Fort S, Botas J, Humbert S, Saudou F (2015) Huntingtin proteolysis releases non-polyQ fragments that cause toxicity through dynamin 1 dysregulation. *EMBO J* 34:2255–2271.
- Eriksson PS, Perfilieva E, Björk-Eriksson T, Alborn A-M, Nordborg C, Peterson DA, Gage FH (1998) Neurogenesis in the adult human hippocampus. *Nat Med* 4:1313–1317.
- Essaghir A, Dif N, Marbehan CY, Coffey PJ, Demoulin J-B (2009) The transcription of FOXO genes is stimulated by FOXO3 and repressed by growth factors. *J Biol Chem* 284:10334–10342.
- Euskirchen GM, Rozowsky JS, Wei C-L, Lee WH, Zhang ZD, Hartman S, Emanuelsson O, Stolc V, Weissman S, Gerstein MB, Ruan Y, Snyder M (2007) Mapping of transcription factor binding regions in mammalian cells by ChIP: Comparison of array- and sequencing-based technologies. *Genome Res* 17:898–909.

- Falk AS, Bravo-Arredondo JM, Varkey J, Pacheco S, Langen R, Siemer AB (2020) Structural Model of the Proline-Rich Domain of Huntingtin Exon-1 Fibrils. *Biophys J* 119:2019–2028.
- Farina F, Lambert E, Commeau L, Lejeune F-X, Roudier N, Fonte C, Parker JA, Boddaert J, VERNY M, Baulieu E-E, Neri C (2017) The stress response factor daf-16/FOXO is required for multiple compound families to prolong the function of neurons with Huntington’s disease. *Sci Rep* 7:4014.
- Fasano C, Disciglio V, Bertora S, Lepore Signorile M, Simone C (2019) FOXO3a from the Nucleus to the Mitochondria: A Round Trip in Cellular Stress Response. *Cells* 8:1110.
- Fautsch MP, Wieben ED, Baratz KH, Bhattacharyya N, Sadan AN, Hafford-Tear NJ, Tuft SJ, Davidson AE (2020) TCF4-mediated Fuchs endothelial corneal dystrophy: Insights into a common trinucleotide repeat-associated disease. *Prog Retin Eye Res* 100883.
- Fedele V, Roybon L, Nordström U, Li JY, Brundin P (2011) Neurogenesis in the R6/2 mouse model of Huntington’s disease is impaired at the level of NeuroD1. *Neuroscience* 173:76–81.
- Feng Z, Jin S, Zupnick A, Hoh J, de Stanchina E, Lowe S, Prives C, Levine AJ (2006) p53 tumor suppressor protein regulates the levels of huntingtin gene expression. *Oncogene* 25:1–7.
- Ferrer I, Blanco R, Cutillas B, Ambrosio S (2000) Fas and Fas-L expression in Huntington’s disease and Parkinson’s disease: Fas and Fas-L expression. *Neuropathol Appl Neurobiol* 26:424–433.
- Fields RD (2008) White matter in learning, cognition and psychiatric disorders. *Trends Neurosci* 31:361–370.
- Fischer B, Azim K, Hurtado-Chong A, Ramelli S, Fernández M, Raineteau O (2014) E-proteins orchestrate the progression of neural stem cell differentiation in the postnatal forebrain. *Neural Develop* 9:23.
- Flora A, Garcia JJ, Thaller C, Zoghbi HY (2007) The E-protein Tcf4 interacts with Math1 to regulate differentiation of a specific subset of neuronal progenitors. *Proc Natl Acad Sci* 104:15382–15387.
- Forrest MP, Hill MJ, Kavanagh DH, Tansey KE, Waite AJ, Blake DJ (2018) The Psychiatric Risk Gene Transcription Factor 4 (TCF4) Regulates Neurodevelopmental Pathways Associated With Schizophrenia, Autism, and Intellectual Disability. *Schizophr Bull* 44:1100–1110.
- Forrest MP, Waite AJ, Martin-Rendon E, Blake DJ (2013) Knockdown of Human TCF4 Affects Multiple Signaling Pathways Involved in Cell Survival, Epithelial to Mesenchymal Transition and Neuronal Differentiation. *PLoS ONE* 8:e73169.
- Fu W, Ma Q, Chen L, Li P, Zhang M, Ramamoorthy S, Nawaz Z, Shimojima T, Wang H, Yang Y, Shen Z, Zhang Yingtao, Zhang X, Nicosia SV, Zhang Yanping, Pledger JW, Chen J, Bai W (2009) MDM2 Acts Downstream of p53 as an E3 Ligase to Promote FOXO Ubiquitination and Degradation. *J Biol Chem* 284:13987–14000.
- Fukuoka M, Daitoku H, Hatta M, Matsuzaki H, Umemura S, Fukamizu A (2003) Negative regulation of forkhead transcription factor AFX (Foxo4) by CBP-induced acetylation. *Int J Mol Med* 12:503–508.

- Fusco FR, Anzilotti S, Giampà C, Dato C, Laurenti D, Leuti A, Colucci D'Amato L, Perrone L, Bernardi G, Melone MAB (2012) Changes in the expression of extracellular regulated kinase (ERK 1/2) in the R6/2 mouse model of Huntington's disease after phosphodiesterase IV inhibition. *Neurobiol Dis* 46:225–233.
- Gallardo-Orihuela A, Hervás-Corpión I, Hierro-Bujalance C, Sanchez-Sotano D, Jiménez-Gómez G, Mora-López F, Campos-Caro A, Garcia-Alloza M, Valor LM (2019) Transcriptional correlates of the pathological phenotype in a Huntington's disease mouse model. *Sci Rep* 9:18696.
- Gao Z, Ure K, Ables JL, Lagace DC, Nave K-A, Goebbels S, Eisch AJ, Hsieh J (2009) Neurod1 is essential for the survival and maturation of adult-born neurons. *Nat Neurosci* 12:1090–1092.
- Gauthier LR, Charrin BC, Borrell-Pagès M, Dompierre JP, Rangone H, Cordelières FP, De Mey J, MacDonald ME, Leßmann V, Humbert S, Saudou F (2004) Huntingtin Controls Neurotrophic Support and Survival of Neurons by Enhancing BDNF Vesicular Transport along Microtubules. *Cell* 118:127–138.
- Geater C, Hernandez S, Thompson L, Mattis VB (2018) Cellular Models: HD Patient-Derived Pluripotent Stem Cells In: Huntington's Disease, *Methods in Molecular Biology* (Precious SV, Rosser AE, Dunnett SB eds), pp41–73. New York, NY: Springer New York.
- Genetic Risk and Outcome in Psychosis (GROUP) et al. (2009) Common variants conferring risk of schizophrenia. *Nature* 460:744–747.
- Gil JMAC, Mohapel P, Araújo IM, Popovic N, Li J-Y, Brundin P, Petersén Å (2005) Reduced hippocampal neurogenesis in R6/2 transgenic Huntington's disease mice. *Neurobiol Dis* 20:744–751.
- Gines S, Ivanova E, Seong I-S, Saura CA, MacDonald ME (2003) Enhanced Akt Signaling Is an Early Pro-survival Response That Reflects N -Methyl-D-aspartate Receptor Activation in Huntington's Disease Knock-in Striatal Cells. *J Biol Chem* 278:50514–50522.
- Ginés S, Paoletti P, Alberch J (2010) Impaired TrkB-mediated ERK1/2 Activation in Huntington Disease Knock-in Striatal Cells Involves Reduced p52/p46 Shc Expression. *J Biol Chem* 285:21537–21548.
- Godin JD, Colombo K, Molina-Calavita M, Keryer G, Zala D, Charrin BC, Dietrich P, Volvert M-L, Guillemot F, Dragatsis I, Bellaïche Y, Saudou F, Nguyen L, Humbert S (2010) Huntingtin Is Required for Mitotic Spindle Orientation and Mammalian Neurogenesis. *Neuron* 67:392–406.
- Goldfarb A, Lewandowska K (1995) Inhibition of cellular differentiation by the SCL/tal oncoprotein: transcriptional repression by an Id-like mechanism. *Blood* 85:465–471.
- Goldfarb AN, Lewandowska K, Pennell CA (1998) Identification of a Highly Conserved Module in E Proteins Required for in Vivo Helix-loop-helix Dimerization. *J Biol Chem* 273:2866–2873.
- Golson ML, Kaestner KH (2016) Fox transcription factors: from development to disease. *Development* 143:4558–4570.
- Gonçalves JT, Schafer ST, Gage FH (2016) Adult Neurogenesis in the Hippocampus: From Stem Cells to Behavior. *Cell* 167:897–914.
- Goodspeed K, Newsom C, Morris MA, Powell C, Evans P, Golla S (2018) Pitt-Hopkins Syndrome: A Review of Current Literature, Clinical Approach, and 23-Patient Case Series. *J Child Neurol* 33:233–244.

- Grajkowska LT, Ceribelli M, Lau CM, Warren ME, Tiniakou I, Nakandakari Higa S, Bunin A, Haecker H, Mirny LA, Staudt LM, Reizis B (2017) Isoform-Specific Expression and Feedback Regulation of E Protein TCF4 Control Dendritic Cell Lineage Specification. *Immunity* 46:65–77.
- Gratuze M, Noël A, Julien C, Cisbani G, Milot-Rousseau P, Morin F, Dickler M, Goupil C, Bezeau F, Poitras I, Bissonnette S, Whittington RA, Hébert SS, Cicchetti F, Parker JA, Samadi P, Planel E (2015) Tau hyperphosphorylation and deregulation of calcineurin in mouse models of Huntington’s disease. *Hum Mol Genet* 24:86–99.
- Greb-Markiewicz B, Kazana W, Zarebski M, Ozyhar A (2019) The subcellular localization of bHLH transcription factor TCF4 is mediated by multiple nuclear localization and nuclear export signals. *Sci Rep* 9:15629.
- Greer EL, Oskoui PR, Banko MR, Maniar JM, Gygi MP, Gygi SP, Brunet A (2007) The Energy Sensor AMP-activated Protein Kinase Directly Regulates the Mammalian FOXO3 Transcription Factor. *J Biol Chem* 282:30107–30119.
- Grima JC et al. (2017) Mutant Huntingtin Disrupts the Nuclear Pore Complex. *Neuron* 94:93-107.e6.
- Guhr A, Kobold S, Seltmann S, Seiler Wulczyn AEM, Kurtz A, Löser P (2018) Recent Trends in Research with Human Pluripotent Stem Cells: Impact of Research and Use of Cell Lines in Experimental Research and Clinical Trials. *Stem Cell Rep* 11:485–496.
- Guillemot F (2007) Spatial and temporal specification of neural fates by transcription factor codes. *Development* 134:3771–3780.
- Hagenston AM, Bading H (2011) Calcium Signaling in Synapse-to-Nucleus Communication. *Cold Spring Harb Perspect Biol* 3:a004564–a004564.
- Harel M, Berchansky A, Canner D (2021) Forkhead box protein.
- Hauser J, Saarikettu J, Grundström T (2008) Calcium Regulation of Myogenesis by Differential Calmodulin Inhibition of Basic Helix-Loop-Helix Transcription Factors. *Mol Biol Cell* 19:2509–2519.
- Hennig KM, Fass DM, Zhao W-N, Sheridan SD, Fu T, Erdin S, Stortchevoi A, Lucente D, Cody JD, Sweetser D, Gusella JF, Talkowski ME, Haggarty SJ (2017) WNT/ β -Catenin Pathway and Epigenetic Mechanisms Regulate the Pitt-Hopkins Syndrome and Schizophrenia Risk Gene TCF4. *Mol Neuropsychiatry* 3:53–71.
- Hensman Moss DJ, Flower MD, Lo KK, Miller JRC, van Ommen G-JB, ’t Hoen PAC, Stone TC, Guinee A, Langbehn DR, Jones L, Plagnol V, van Roon-Mom WMC, Holmans P, Tabrizi SJ (2017) Huntington’s disease blood and brain show a common gene expression pattern and share an immune signature with Alzheimer’s disease. *Sci Rep* 7:44849.
- Herbst A, Kolligs FT (2008) A conserved domain in the transcription factor ITF-2B attenuates its activity. *Biochem Biophys Res Commun* 370:327–331.
- Hermann S, Saarikettu J, Onions J, Hughes K, Grundström T (1998) Calcium regulation of basic helix-loop-helix transcription factors. *Cell Calcium* 23:135–142.
- Hill MJ, Killick R, Navarrete K, Maruszak A, McLaughlin GM, Williams BP, Bray NJ (2017) Knockdown of the schizophrenia susceptibility gene TCF4 alters gene expression and proliferation of progenitor cells from the developing human neocortex. *J Psychiatry Neurosci* 42:181–188.
- Ho K-K, McGuire VA, Koo C-Y, Muir KW, de Olano N, Maifoshie E, Kelly DJ, McGovern UB, Monteiro LJ, Gomes AR, Nebreda AR, Campbell DG, Arthur JSC, Lam EW-F (2012) Phosphorylation of FOXO3a on Ser-7 by p38 Promotes Its Nuclear Localization in Response to Doxorubicin. *J Biol Chem* 287:1545–1555.

- Hodges A et al. (2006) Regional and cellular gene expression changes in human Huntington's disease brain. *Hum Mol Genet* 15:965–977.
- Hornsveld M, Dansen TB, Derksen PW, Burgering BMT (2018) Re-evaluating the role of FOXOs in cancer. *Semin Cancer Biol* 50:90–100.
- Hosaka T, Biggs WH, Tieu D, Boyer AD, Varki NM, Cavenee WK, Arden KC (2004) Disruption of forkhead transcription factor (FOXO) family members in mice reveals their functional diversification. *Proc Natl Acad Sci* 101:2975–2980.
- Hu J, Liu J, Yu D, Chu Y, Corey DR (2012) Mechanism of allele-selective inhibition of huntingtin expression by duplex RNAs that target CAG repeats: function through the RNAi pathway. *Nucleic Acids Res* 40:11270–11280.
- Hu MC-T, Lee D-F, Xia W, Golfman LS, Ou-Yang F, Yang J-Y, Zou Y, Bao S, Hanada N, Saso H, Kobayashi R, Hung M-C (2004) I κ B Kinase Promotes Tumorigenesis through Inhibition of Forkhead FOXO3a. *Cell* 117:225–237.
- Hu W, Yang Z, Yang W, Han M, Xu B, Yu Z, Shen M, Yang Y (2019) Roles of forkhead box O (FoxO) transcription factors in neurodegenerative diseases: A panoramic view. *Prog Neurobiol* 181:101645.
- Huang B, Wei W, Wang G, Gaertig MA, Feng Y, Wang W, Li X-J, Li S (2015) Mutant Huntingtin Downregulates Myelin Regulatory Factor-Mediated Myelin Gene Expression and Affects Mature Oligodendrocytes. *Neuron* 85:1212–1226.
- Huang C, Chan JA, Schuurmans C (2014) Proneural bHLH Genes in Development and Disease In: *Current Topics in Developmental Biology*, pp75–127. Elsevier.
- Huang H, Regan KM, Lou Z, Chen J, Tindall DJ (2006) CDK2-Dependent Phosphorylation of FOXO1 as an Apoptotic Response to DNA Damage. *Science* 314:294–297.
- Huang H, Regan KM, Wang F, Wang D, Smith DI, van Deursen JMA, Tindall DJ (2005) Skp2 inhibits FOXO1 in tumor suppression through ubiquitin-mediated degradation. *Proc Natl Acad Sci* 102:1649–1654.
- Huang H, Tindall DJ (2011) Regulation of FOXO protein stability via ubiquitination and proteasome degradation. *Biochim Biophys Acta BBA - Mol Cell Res* 1813:1961–1964.
- Huo X, Liu S, Shao T, Hua H, Kong Q, Wang J, Luo T, Jiang Y (2014) GSK3 Protein Positively Regulates Type I Insulin-like Growth Factor Receptor through Forkhead Transcription Factors FOXO1/3/4. *J Biol Chem* 289:24759–24770.
- Hwangbo DS, Gersham B, Tu M-P, Palmer M, Tatar M (2004) Drosophila dFOXO controls lifespan and regulates insulin signalling in brain and fat body. *Nature* 429:562–566.
- Imayoshi I, Kageyama R (2014) bHLH Factors in Self-Renewal, Multipotency, and Fate Choice of Neural Progenitor Cells. *Neuron* 82:9–23.
- Jia X et al. (2019) Neddylation inactivation facilitates FOXO3a nuclear export to suppress estrogen receptor transcription and improve fulvestrant sensitivity. *Clin Cancer Res clincanres.2434.2018*.
- Jimenez-Sanchez M, Licitra F, Underwood BR, Rubinsztein DC (2017) Huntington's Disease: Mechanisms of Pathogenesis and Therapeutic Strategies. *Cold Spring Harb Perspect Med* 7:a024240.
- Jiramongkol Y, Lam EW-F (2020) FOXO transcription factor family in cancer and metastasis. *Cancer Metastasis Rev* 39:681–709.
- Jo C, Cho S-J, Jo SA (2011) Mitogen-activated Protein Kinase Kinase 1 (MEK1) Stabilizes MyoD through Direct Phosphorylation at Tyrosine 156 During Myogenic Differentiation. *J Biol Chem* 286:18903–18913.

- Jung M, Häberle BM, Tschakowsky T, Wittmann M-T, Balta E-A, Stadler V-C, Zweier C, Dörfler A, Gloeckner CJ, Lie DC (2018) Analysis of the expression pattern of the schizophrenia-risk and intellectual disability gene *TCF4* in the developing and adult brain suggests a role in development and plasticity of cortical and hippocampal neurons. *Mol Autism* 9:20.
- Kalscheuer VM, Feenstra I, Van Ravenswaaij-Arts CMA, Smeets DFCM, Menzel C, Ullmann R, Musante L, Ropers H-H (2008) Disruption of the *TCF4* gene in a girl with mental retardation but without the classical Pitt-Hopkins syndrome. *Am J Med Genet A* 146A:2053–2059.
- Kamagate A, Qu S, Perdomo G, Su D, Kim DH, Slusher S, Meseck M, Dong HH (2008) FoxO1 mediates insulin-dependent regulation of hepatic VLDL production in mice. *J Clin Invest* JCI32914.
- Kennedy AJ, Rahn EJ, Paulukaitis BS, Savell KE, Kordasiewicz HB, Wang J, Lewis JW, Posey J, Strange SK, Guzman-Karlsson MC, Phillips SE, Decker K, Motley ST, Swayze EE, Ecker DJ, Michael TP, Day JJ, Sweatt JD (2016) Tcf4 Regulates Synaptic Plasticity, DNA Methylation, and Memory Function. *Cell Rep* 16:2666–2685.
- Kenyon C, Chang J, Gensch E, Rudner A, Tabtiang R (1993) A *C. elegans* mutant that lives twice as long as wild type. *Nature* 366:461–464.
- Keryer G, Pineda JR, Liot G, Kim J, Dietrich P, Benstaali C, Smith K, Cordelières FP, Spassky N, Ferrante RJ, Dragatsis I, Saudou F (2011) Ciliogenesis is regulated by a huntingtin-HAP1-PCM1 pathway and is altered in Huntington disease. *J Clin Invest* 121:4372–4382.
- Kharbanda M, Kannike K, Lampe A, Berg J, Timmusk T, Sepp M (2016) Partial deletion of *TCF4* in three generation family with non-syndromic intellectual disability, without features of Pitt-Hopkins syndrome. *Eur J Med Genet* 59:310–314.
- Khund-Sayeed S, He X, Holzberg T, Wang J, Rajagopal D, Upadhyay S, Durell SR, Mukherjee S, Weirauch MT, Rose R, Vinson C (2016) 5-Hydroxymethylcytosine in E-box motifs ACAT|GTG and ACAC|GTG increases DNA-binding of the B-HLH transcription factor *TCF4*. *Integr Biol* 8:936–945.
- Kim H, Berens NC, Ochandarena NE, Philpot BD (2020) Region and Cell Type Distribution of *TCF4* in the Postnatal Mouse Brain. *Front Neuroanat* 14:42.
- Kim S, Kim Y, Lee J, Chung J (2010) Regulation of FOXO1 by TAK1-Nemo-like Kinase Pathway. *J Biol Chem* 285:8122–8129.
- Kotliarova S et al. (2005) Decreased expression of hypothalamic neuropeptides in Huntington disease transgenic mice with expanded polyglutamine-EGFP fluorescent aggregates. *J Neurochem* 93:641–653.
- Kremer B, Goldberg P, Andrew SE, Theilmann J, Telenius H, Zeisler J, Squitieri F, Lin B, Bassett A, Almqvist E, Bird TD, Hayden MR (1994) A Worldwide Study of the Huntington's Disease Mutation: The Sensitivity and Specificity of Measuring CAG Repeats. *N Engl J Med* 330:1401–1406.
- Kuhn A et al. (2007) Mutant huntingtin's effects on striatal gene expression in mice recapitulate changes observed in human Huntington's disease brain and do not differ with mutant huntingtin length or wild-type huntingtin dosage. *Hum Mol Genet* 16:1845–1861.
- Labadorf A, Hoss AG, Lagomarsino V, Latourelle JC, Hadzi TC, Bregu J, MacDonald ME, Gusella JF, Chen J-F, Akbarian S, Weng Z, Myers RH (2015) RNA Sequence Analysis of Human Huntington Disease Brain Reveals an Extensive Increase in Inflammatory and Developmental Gene Expression. *PLOS ONE* 10:e0143563.

- Landwehrmeyer GB et al. (1995) Huntington's disease gene: Regional and cellular expression in brain of normal and affected individuals. *Ann Neurol* 37:218–230.
- Langfelder P et al. (2016) Integrated genomics and proteomics define huntingtin CAG length-dependent networks in mice. *Nat Neurosci* 19:623–633.
- Lazic SE, Grote H, Armstrong RJE, Blakemore C, Hannan AJ, van Dellen A, Barker RA (2004) Decreased hippocampal cell proliferation in R6/1 Huntington's mice: *NeuroReport* 15:811–813.
- Le Dréau G, Escalona R, Fueyo R, Herrera A, Martínez JD, Usieto S, Menendez A, Pons S, Martínez-Balbas MA, Martí E (2018) E proteins sharpen neurogenesis by modulating proneural bHLH transcription factors' activity in an E-box-dependent manner. *eLife* 7:e37267.
- Lee J-M et al. (2012) CAG repeat expansion in Huntington disease determines age at onset in a fully dominant fashion. *Neurology* 78:690–695.
- Lee J-W, Chen H, Pullikotil P, Quon MJ (2011) Protein Kinase A- α Directly Phosphorylates FoxO1 in Vascular Endothelial Cells to Regulate Expression of Vascular Cellular Adhesion Molecule-1 mRNA. *J Biol Chem* 286:6423–6432.
- Lehtinen MK, Yuan Z, Boag PR, Yang Y, Villén J, Becker EBE, DiBacco S, de la Iglesia N, Gygi S, Blackwell TK, Bonni A (2006) A Conserved MST-FOXO Signaling Pathway Mediates Oxidative-Stress Responses and Extends Life Span. *Cell* 125:987–1001.
- Levine MS, Klapstein GJ, Koppel A, Gruen E, Cepeda C, Vargas ME, Jokel ES, Carpenter EM, Zanjani H, Hurst RS, Efstratiadis A, Zeitlin S, Chesselet MF (1999) Enhanced sensitivity to N-methyl-D-aspartate receptor activation in transgenic and knockin mouse models of Huntington's disease. *J Neurosci Res* 58:515–532.
- Li H, Zhu Y, Morozov YM, Chen X, Page SC, Rannals MD, Maher BJ, Rakic P (2019) Disruption of TCF4 regulatory networks leads to abnormal cortical development and mental disabilities. *Mol Psychiatry* 24:1235–1246.
- Li M et al. (2018) Integrative functional genomic analysis of human brain development and neuropsychiatric risks. *Science* 362:eaat7615.
- Li S-H, Schilling G, Young WS, Li X-, Margolis RL, Stine OC, Wagster MV, Abbott MH, Franz ML, Ranen NG, Folstein SE, Hedreen JC, Ross CA (1993) Huntington's disease gene (IT15) is widely expressed in human and rat tissues. *Neuron* 11:985–993.
- Li Z, Zhu H, Liu C, Wang Y, Wang D, Liu H, Cao W, Hu Y, Lin Q, Tong C, Lu M, Sachinidis A, Li L, Peng L (2019) GSK-3 β inhibition protects the rat heart from the lipopolysaccharide-induced inflammation injury via suppressing FOXO3A activity. *J Cell Mol Med* 23:7796–7809.
- Lin C-H (2001) Neurological abnormalities in a knock-in mouse model of Huntington's disease. *Hum Mol Genet* 10:137–144.
- Lin CH, Lee EHY (2012) JNK1 Inhibits GluR1 Expression and GluR1-Mediated Calcium Influx through Phosphorylation and Stabilization of Hes-1. *J Neurosci* 32:1826–1846.
- Lin X-X, Sen I, Janssens GE, Zhou X, Fonslow BR, Edgar D, Stroustrup N, Swoboda P, Yates JR, Ruvkun G, Riedel CG (2018) DAF-16/FOXO and HLH-30/TFEB function as combinatorial transcription factors to promote stress resistance and longevity. *Nat Commun* 9:4400.
- Liot G, Bossy B, Lubitz S, Kushnareva Y, Sejbuk N, Bossy-Wetzel E (2009) Complex II inhibition by 3-NP causes mitochondrial fragmentation and neuronal cell death via an NMDA- and ROS-dependent pathway. *Cell Death Differ* 16:899–909.

- Liu P, Kao TP, Huang H (2008) CDK1 promotes cell proliferation and survival via phosphorylation and inhibition of FOXO1 transcription factor. *Oncogene* 27:4733–4744.
- Liu Y, Ao X, Ding W, Ponnusamy M, Wu W, Hao X, Yu W, Wang Y, Li P, Wang J (2018) Critical role of FOXO3a in carcinogenesis. *Mol Cancer* 17:104.
- Liu Y, Qiao F, Leiferman PC, Ross A, Schlenker EH, Wang H (2017) FOXOs modulate proteasome activity in human-induced pluripotent stem cells of Huntington's disease and their derived neural cells. *Hum Mol Genet* 26:4416–4428.
- Liu Y, Ray SK, Yang X-Q, Luntz-Leybman V, Chiu I-M (1998) A Splice Variant of E2–2 Basic Helix-Loop-Helix Protein Represses the Brain-specific Fibroblast Growth Factor 1 Promoter through the Binding to an Imperfect E-box. *J Biol Chem* 273:19269–19276.
- Lluís F, Ballestar E, Suelves M, Esteller M, Muñoz-Cánoves P (2005) E47 phosphorylation by p38 MAPK promotes MyoD/E47 association and muscle-specific gene transcription. *EMBO J* 24:974–984.
- Lonze BE, Ginty DD (2002) Function and Regulation of CREB Family Transcription Factors in the Nervous System. *Neuron* 35:605–623.
- Lovrecic L, Kastrin A, Kobal J, Pirtosek Z, Krainc D, Peterlin B (2009a) Gene expression changes in blood as a putative biomarker for Huntington's disease. *Mov Disord* 24:2277–2281.
- Lovrecic L, Kastrin A, Kobal J, Pirtosek Z, Krainc D, Peterlin B (2009b) Gene expression changes in blood as a putative biomarker for Huntington's disease. *Mov Disord* 24:2277–2281.
- Ludolph AC, He F, Spencer PS, Hammerstad J, Sabri M (1991) 3-Nitropropionic Acid - Exogenous Animal Neurotoxin and Possible Human Striatal Toxin. *Can J Neurol Sci J Can Sci Neurol* 18:492–498.
- Luthi-Carter R (2002) Polyglutamine and transcription: gene expression changes shared by DRPLA and Huntington's disease mouse models reveal context-independent effects. *Hum Mol Genet* 11:1927–1937.
- Luthi-Carter R (2000) Decreased expression of striatal signaling genes in a mouse model of Huntington's disease. *Hum Mol Genet* 9:1259–1271.
- Lützner N, Kalbacher H, Krones-Herzig A, Rösl F (2012) FOXO3 Is a Glucocorticoid Receptor Target and Regulates LKB1 and Its Own Expression Based on Cellular AMP Levels via a Positive Autoregulatory Loop. *PLoS ONE* 7:e42166.
- Lynch G, Kramar EA, Rex CS, Jia Y, Chappas D, Gall CM, Simmons DA (2007) Brain-Derived Neurotrophic Factor Restores Synaptic Plasticity in a Knock-In Mouse Model of Huntington's Disease. *J Neurosci* 27:4424–4434.
- Maher P, Dargusch R, Bodai L, Gerard PE, Purcell JM, Marsh JL (2011) ERK activation by the polyphenols fisetin and resveratrol provides neuroprotection in multiple models of Huntington's disease. *Hum Mol Genet* 20:261–270.
- Maiese K (2015) FoxO Proteins in the Nervous System. *Anal Cell Pathol* 2015:1–15.
- Mammucari C, Milan G, Romanello V, Masiero E, Rudolf R, Del Piccolo P, Burden SJ, Di Lisi R, Sandri C, Zhao J, Goldberg AL, Schiaffino S, Sandri M (2007) FoxO3 Controls Autophagy in Skeletal Muscle In Vivo. *Cell Metab* 6:458–471.
- Mangiarini L, Sathasivam K, Seller M, Cozens B, Harper A, Hetherington C, Lawton M, Trotter Y, Lehrach H, Davies SW, Bates GP (1996) Exon 1 of the HD Gene with an Expanded CAG Repeat Is Sufficient to Cause a Progressive Neurological Phenotype in Transgenic Mice. *Cell* 87:493–506.

- Marcora E, Gowan K, Lee JE (2003) Stimulation of NeuroD activity by huntingtin and huntingtin-associated proteins HAP1 and MLK2. *Proc Natl Acad Sci* 100: 9578–9583.
- Markus M, Du Z, Benezra R (2002) Enhancer-specific Modulation of E Protein Activity. *J Biol Chem* 277:6469–6477.
- Martín-Flores N, Pérez-Sisqués L, Creus-Muncunill J, Masana M, Ginés S, Alberch J, Pérez-Navarro E, Malagelada C (2020) Synaptic RTP801 contributes to motor-learning dysfunction in Huntington’s disease. *Cell Death Dis* 11:569.
- Marzi L, Combes E, Vié N, Ayrolles-Torro A, Tosi D, Desigaud D, Perez-Gracia E, Larbouret C, Montagut C, Iglesias M, Jarlier M, Denis V, Linares LK, Lam EW-F, Martineau P, Del Rio M, Gongora C (2016) FOXO3a and the MAPK p38 are activated by cetuximab to induce cell death and inhibit cell proliferation and their expression predicts cetuximab efficacy in colorectal cancer. *Br J Cancer* 115:1223–1233.
- Masgutova G, Harris A, Jacob B, Corcoran LM, Clotman F (2019) Pou2f2 Regulates the Distribution of Dorsal Interneurons in the Mouse Developing Spinal Cord. *Front Mol Neurosci* 12:263.
- Massari ME, Jennings PA, Murre C (1996) The AD1 transactivation domain of E2A contains a highly conserved helix which is required for its activity in both *Saccharomyces cerevisiae* and mammalian cells. *Mol Cell Biol* 16:121–129.
- Massari ME, Murre C (2000) Helix-Loop-Helix Proteins: Regulators of Transcription in Eucaryotic Organisms. *Mol Cell Biol* 20:429–440.
- Mastrokolas A, Ariyurek Y, Goeman JJ, van Duijn E, Roos RA, van der Mast RC, van Ommen GB, den Dunnen JT, ’t Hoen PA, van Roon-Mom WM (2015) Huntington’s disease biomarker progression profile identified by transcriptome sequencing in peripheral blood. *Eur J Hum Genet* 23:1349–1356.
- McColgan P, Tabrizi SJ (2018) Huntington’s disease: a clinical review. *Eur J Neurol* 25:24–34.
- Menalled L, Lutz C, Ramboz S, Brunner D, Lager B, Noble S, Park L, Howland D (2014) A Field Guide to Working with Mouse Models of Huntington’s Disease.
- Menalled L, Zanjani H, MacKenzie L, Koppel A, Carpenter E, Zeitlin S, Chesselet M-F (2000) Decrease in Striatal Enkephalin mRNA in Mouse Models of Huntington’s Disease. *Exp Neurol* 162:328–342.
- Menalled LB (2005) Knock-in mouse models of Huntington’s disease. *NeuroRX* 2:465–470.
- Menalled LB, Sison JD, Dragatsis I, Zeitlin S, Chesselet M-F (2003) Time course of early motor and neuropathological anomalies in a knock-in mouse model of Huntington’s disease with 140 CAG repeats. *J Comp Neurol* 465:11–26.
- Mesman S, Bakker R, Smidt MP (2020) Tcf4 is required for correct brain development during embryogenesis. *Mol Cell Neurosci* 106:103502.
- Mielcarek M, Toczek M, Smeets CJLM, Franklin SA, Bondulich MK, Jolinon N, Muller T, Ahmed M, Dick JRT, Piotrowska I, Greensmith L, Smolenski RT, Bates GP (2015) HDAC4-Myogenin Axis As an Important Marker of HD-Related Skeletal Muscle Atrophy. *PLOS Genet* 11:e1005021.
- Miyata T, Maeda T, Lee JE (1999) NeuroD is required for differentiation of the granule cells in the cerebellum and hippocampus. *Genes Dev* 13:1647–1652.
- Moen MJ, Adams HHH, Brandsma JH, Dekkers DHW, Akinci U, Karkampouna S, Quevedo M, Kockx CEM, Ozgür Z, van IJcken WFJ, Demmers J, Poot RA (2017) An interaction network of mental disorder proteins in neural stem cells. *Transl Psychiatry* 7:e1082–e1082.

- Mortazavi A, Thompson ECL, Garcia ST, Myers RM, Wold B (2006) Comparative genomics modeling of the NRSF/REST repressor network: From single conserved sites to genome-wide repertoire. *Genome Res* 16:1208–1221.
- Morton AJ (2005) Disintegration of the Sleep-Wake Cycle and Circadian Timing in Huntington's Disease. *J Neurosci* 25:157–163.
- Mubarak B, Soriano FX, Hardingham GE (2009) Synaptic NMDAR activity suppresses FOXO1 expression via a cis-acting FOXO binding site: FOXO1 is a FOXO target gene. *Channels* 3:233–239.
- Murre C (2019) Helix–loop–helix proteins and the advent of cellular diversity: 30 years of discovery. *Genes Dev* 33:6–25.
- Myers RH, Vonsattel JP, Paskevich PA, Kiely DK, Stevens TJ, Cupples LA, Richardson EP, Bird ED (1991) Decreased Neuronal and Increased Oligodendroglial Densities in Huntington's Disease Caudate Nucleus. *J Neuropathol Exp Neurol* 50:729–742.
- Nakae J, Kitamura T, Silver DL, Accili D (2001) The forkhead transcription factor Foxo1 (Fkhr) confers insulin sensitivity onto glucose-6-phosphatase expression. *J Clin Invest* 108:1359–1367.
- Nakagawa S, Gisselbrecht SS, Rogers JM, Hartl DL, Bulyk ML (2013) DNA-binding specificity changes in the evolution of forkhead transcription factors. *Proc Natl Acad Sci* 110:12349–12354.
- Nakamura N, Ramaswamy S, Vazquez F, Signoretti S, Loda M, Sellers WR (2000) Forkhead Transcription Factors Are Critical Effectors of Cell Death and Cell Cycle Arrest Downstream of PTEN. *Mol Cell Biol* 20:8969–8982.
- Nasir J, Floresco SB, O'Kusky JR, Diewert VM, Richman JM, Zeisler J, Borowski A, Marth JD, Phillips AG, Hayden MR (1995) Targeted disruption of the Huntington's disease gene results in embryonic lethality and behavioral and morphological changes in heterozygotes. *Cell* 81:811–823.
- Navarrete K, Pedrosa I, De Jong S, Stefansson H, Steinberg S, Stefansson K, Ophoff RA, Schalkwyk LC, Collier DA (2013) *TCF4* (*e2-2; ITF2*): A schizophrenia-associated gene with pleiotropic effects on human disease. *Am J Med Genet B Neuropsychiatr Genet* 162:1–16.
- Nawalpuri B, Ravindran S, Muddashetty RS (2020) The Role of Dynamic miRISC During Neuronal Development. *Front Mol Biosci* 7:8.
- Neri C (2012) Role and Therapeutic Potential of the Pro-Longevity Factor FOXO and Its Regulators in Neurodegenerative Disease. *Front Pharmacol* 3.
- Neueder A, Bates GP (2014) A common gene expression signature in Huntington's disease patient brain regions. *BMC Med Genomics* 7:60.
- Nickel M, Gu C (2018) Regulation of Central Nervous System Myelination in Higher Brain Functions. *Neural Plast* 2018:1–12.
- Nidai Ozes O, Mayo LD, Gustin JA, Pfeiffer SR, Pfeiffer LM, Donner DB (1999) NF- κ B activation by tumour necrosis factor requires the Akt serine–threonine kinase. *Nature* 401:82–85.
- Nucifora Jr. FC (2001) Interference by Huntingtin and Atrophin-1 with CBP-Mediated Transcription Leading to Cellular Toxicity. *Science* 291:2423–2428.
- Nurm K, Sepp M, Castany-Pladevall C, Creus-Muncunill J, Tuvikene J, Sirp A, Vihma H, Blake DJ, Perez-Navarro E, Timmusk T (2021) Isoform-specific reduction of the basic helix-loop-helix transcription factor TCF4 levels in Huntington's disease. *eneuro* ENEURO.0197-21.2021.

- Oliveira JMA (2010) Nature and cause of mitochondrial dysfunction in Huntington's disease: focusing on huntingtin and the striatum: Mutant huntingtin and striatal mitochondria. *J Neurochem* no-no.
- Ong Tone S, Kocaba V, Böhm M, Wylegala A, White TL, Jurkunas UV (2021) Fuchs endothelial corneal dystrophy: The vicious cycle of Fuchs pathogenesis. *Prog Retin Eye Res* 80:100863.
- Onions J, Hermann S, Grundström T (2000) A Novel Type of Calmodulin Interaction in the Inhibition of Basic Helix–Loop–Helix Transcription Factors [†]. *Biochemistry* 39:4366–4374.
- Osipovitch M, Asenjo Martinez A, Mariani JN, Cornwell A, Dhaliwal S, Zou L, Chandler-Militello D, Wang S, Li X, Benraiss S-J, Agate R, Lampp A, Benraiss A, Windrem MS, Goldman SA (2019) Human ESC-Derived Chimeric Mouse Models of Huntington's Disease Reveal Cell-Intrinsic Defects in Glial Progenitor Cell Differentiation. *Cell Stem Cell* 24:107-122.e7.
- Oyama F, Miyazaki H, Sakamoto N, Becquet C, Machida Y, Kaneko K, Uchikawa C, Suzuki T, Kurosawa M, Ikeda T, Tamaoka A, Sakurai T, Nukina N (2006) Sodium channel beta4 subunit: down-regulation and possible involvement in neuritic degeneration in Huntington's disease transgenic mice. *J Neurochem* 98: 518–529.
- Packer AN, Xing Y, Harper SQ, Jones L, Davidson BL (2008) The Bifunctional microRNA miR-9/miR-9* Regulates REST and CoREST and Is Downregulated in Huntington's Disease. *J Neurosci* 28:14341–14346.
- Page SC, Hamersky GR, Gallo RA, Rannals MD, Calcaterra NE, Campbell MN, Mayfield B, Briley A, Phan BN, Jaffe AE, Maher BJ (2018) The schizophrenia- and autism-associated gene, transcription factor 4 regulates the columnar distribution of layer 2/3 prefrontal pyramidal neurons in an activity-dependent manner. *Mol Psychiatry* 23:304–315.
- Palazuelos J, Klingener M, Aguirre A (2014) TGF Signaling Regulates the Timing of CNS Myelination by Modulating Oligodendrocyte Progenitor Cell Cycle Exit through SMAD3/4/FoxO1/Sp1. *J Neurosci* 34:7917–7930.
- Palfi S, Ferrante RJ, Brouillet E, Beal MF, Dolan R, Guyot MC, Peschanski M, Hantraye P (1996) Chronic 3-Nitropropionic Acid Treatment in Baboons Replicates the Cognitive and Motor Deficits of Huntington's Disease. *J Neurosci* 16:3019–3025.
- Park H, Poo M (2013) Neurotrophin regulation of neural circuit development and function. *Nat Rev Neurosci* 14:7–23.
- Park I-H, Arora N, Huo H, Maherali N, Ahfeldt T, Shimamura A, Lensch MW, Cowan C, Hochedlinger K, Daley GQ (2008) Disease-Specific Induced Pluripotent Stem Cells. *Cell* 134:877–886.
- Parker JA, Arango M, Abderrahmane S, Lambert E, Tourette C, Catoire H, Néri C (2005) Resveratrol rescues mutant polyglutamine cytotoxicity in nematode and mammalian neurons. *Nat Genet* 37:349–350.
- Parker JA, Vazquez-Manrique RP, Tourette C, Farina F, Offner N, Mukhopadhyay A, Orfila A-M, Darbois A, Menet S, Tissenbaum HA, Neri C (2012) Integration of β -catenin, sirtuin, and FOXO signaling protects from mutant huntingtin toxicity. *J Neurosci Off J Soc Neurosci* 32:12630–12640.
- Persson P, Jögi A, Grynfeld A, Pålman S, Axelson H (2000) HASH-1 and E2-2 Are Expressed in Human Neuroblastoma Cells and Form a Functional Complex. *Biochem Biophys Res Commun* 274:22–31.

- Phan BN et al. (2020) A myelin-related transcriptomic profile is shared by Pitt–Hopkins syndrome models and human autism spectrum disorder. *Nat Neurosci* 23: 375–385.
- Pouladi MA, Morton AJ, Hayden MR (2013) Choosing an animal model for the study of Huntington’s disease. *Nat Rev Neurosci* 14:708–721.
- Powell LM, Jarman AP (2008) Context dependence of proneural bHLH proteins. *Curr Opin Genet Dev* 18:411–417.
- Pscherer A, Dörflinger U, Kirfel J, Gawlas K, Rüschoff J, Buettner R, Schüle R (1996) The helix-loop-helix transcription factor SEF-2 regulates the activity of a novel initiator element in the promoter of the human somatostatin receptor II gene. *EMBO J* 15:6680–6690.
- Quan X-J, Yuan L, Tiberi L, Claeys A, De Geest N, Yan J, van der Kant R, Xie WR, Klisch TJ, Shymkowitz J, Rousseau F, Bollen M, Beullens M, Zoghbi HY, Vanderhaeghen P, Hassan BA (2016) Post-translational Control of the Temporal Dynamics of Transcription Factor Activity Regulates Neurogenesis. *Cell* 164:460–475.
- Quednow BB, Brzózka MM, Rossner MJ (2014) Transcription factor 4 (TCF4) and schizophrenia: integrating the animal and the human perspective. *Cell Mol Life Sci* 71:2815–2835.
- Quevedo M, Meert L, Dekker MR, Dekkers DHW, Brandsma JH, van den Berg DLC, Özgür Z, van IJcken WFJ, Demmers J, Fornerod M, Poot RA (2019) Mediator complex interaction partners organize the transcriptional network that defines neural stem cells. *Nat Commun* 10:2669.
- Quirion JG, Parsons MP (2019) The Onset and Progression of Hippocampal Synaptic Plasticity Deficits in the Q175FDN Mouse Model of Huntington Disease. *Front Cell Neurosci* 13:326.
- Quong MW, Massari ME, Zwart R, Murre C (1993) A new transcriptional-activation motif restricted to a class of helix-loop-helix proteins is functionally conserved in both yeast and mammalian cells. *Mol Cell Biol* 13:792–800.
- Rai SN, Dilnashin H, Birla H, Singh SS, Zahra W, Rathore AS, Singh BK, Singh SP (2019) The Role of PI3K/Akt and ERK in Neurodegenerative Disorders. *Neurotox Res* 35:775–795.
- Ramaswamy S, McBride JL, Kordower JH (2007) Animal Models of Huntington’s Disease. *ILAR J* 48:356–373.
- Ramirez-Garcia G, Galvez V, Diaz R, Bayliss L, Fernandez-Ruiz J, Campos-Romo A (2019) Longitudinal atrophy characterization of cortical and subcortical gray matter in Huntington’s disease patients. *Eur J Neurosci* ejn.14617.
- Rannals MD, Hamersky GR, Page SC, Campbell MN, Briley A, Gallo RA, Phan BN, Hyde TM, Kleinman JE, Shin JH, Jaffe AE, Weinberger DR, Maher BJ (2016) Psychiatric Risk Gene Transcription Factor 4 Regulates Intrinsic Excitability of Prefrontal Neurons via Repression of SCN10a and KCNQ1. *Neuron* 90:43–55.
- Ravanpay AC, Olson JM (2008) E protein dosage influences brain development more than family member identity. *J Neurosci Res* 86:1472–1481.
- Rawlins MD, Wexler NS, Wexler AR, Tabrizi SJ, Douglas I, Evans SJW, Smeeth L (2016) The Prevalence of Huntington’s Disease. *Neuroepidemiology* 46:144–153.
- Reiner A, Del Mar N, Meade CA, Yang H, Dragatsis I, Zeitlin S, Goldowitz D (2001) Neurons Lacking Huntingtin Differentially Colonize Brain and Survive in Chimeric Mice. *J Neurosci* 21:7608–7619.

- Rena G (2002) Two novel phosphorylation sites on FKHR that are critical for its nuclear exclusion. *EMBO J* 21:2263–2271.
- Riddle DL, Swanson MM, Albert PS (1981) Interacting genes in nematode dauer larva formation. *Nature* 290:668–671.
- Rivetti di Val Cervo P, Besusso D, Conforti P, Cattaneo E (2021) hiPSCs for predictive modelling of neurodegenerative diseases: dreaming the possible. *Nat Rev Neurol*.
- Robertson G, Hirst M, Bainbridge M, Bilenky M, Zhao Y, Zeng T, Euskirchen G, Bernier B, Varhol R, Delaney A, Thiessen N, Griffith OL, He A, Marra M, Snyder M, Jones S (2007) Genome-wide profiles of STAT1 DNA association using chromatin immunoprecipitation and massively parallel sequencing. *Nat Methods* 4: 651–657.
- Rosbach M (2011) Non-Coding RNAs in Neural Networks, REST-Assured. *Front Genet* 2.
- Rozowsky J, Euskirchen G, Auerbach RK, Zhang ZD, Gibson T, Bjornson R, Carriero N, Snyder M, Gerstein MB (2009) PeakSeq enables systematic scoring of ChIP-seq experiments relative to controls. *Nat Biotechnol* 27:66–75.
- Runne H, Kuhn A, Wild EJ, Pratyaksha W, Kristiansen M, Isaacs JD, Régulier E, Delorenzi M, Tabrizi SJ, Luthi-Carter R (2007) Analysis of potential transcriptomic biomarkers for Huntington’s disease in peripheral blood. *Proc Natl Acad Sci* 104:14424.
- Ryan AB, Zeitlin SO, Scrabble H (2006) Genetic interaction between expanded murine Hdh alleles and p53 reveal deleterious effects of p53 on Huntington’s disease pathogenesis. *Neurobiol Dis* 24:419–427.
- Saarikettu J, Sveshnikova N, Grundström T (2004) Calcium/Calmodulin Inhibition of Transcriptional Activity of E-proteins by Prevention of Their Binding to DNA. *J Biol Chem* 279:41004–41011.
- Sadagurski M, Cheng Z, Rozzo A, Palazzolo I, Kelley GR, Dong X, Krainc D, White MF (2011) IRS2 increases mitochondrial dysfunction and oxidative stress in a mouse model of Huntington disease. *J Clin Invest* 121:4070–4081.
- Sarantos MR, Papanikolaou T, Ellerby LM, Hughes RE (2012) Pizotifen Activates ERK and Provides Neuroprotection in vitro and in vivo in Models of Huntington’s Disease. *J Huntingt Dis* 1:195–210.
- Saudou F, Finkbeiner S, Devys D, Greenberg ME (1998) Huntingtin Acts in the Nucleus to Induce Apoptosis but Death Does Not Correlate with the Formation of Intranuclear Inclusions. *Cell* 95:55–66.
- Saudou F, Humbert S (2016) The Biology of Huntingtin. *Neuron* 89:910–926.
- Savas JN, Makusky A, Ottosen S, Baillat D, Then F, Krainc D, Shiekhhattar R, Markey SP, Tanese N (2008) Huntington’s disease protein contributes to RNA-mediated gene silencing through association with Argonaute and P bodies. *Proc Natl Acad Sci* 105:10820–10825.
- Scarpa JR, Jiang P, Losic B, Readhead B, Gao VD, Dudley JT, Vitaterna MH, Turek FW, Kasarskis A (2016) Systems Genetic Analyses Highlight a TGFβ-FOXO3 Dependent Striatal Astrocyte Network Conserved across Species and Associated with Stress, Sleep, and Huntington’s Disease. *PLOS Genet* 12:e1006137.
- Schilling G (1999) Intranuclear inclusions and neuritic aggregates in transgenic mice expressing a mutant N-terminal fragment of huntingtin [published erratum appears in *Hum Mol Genet* 1999 May;8(5):943]. *Hum Mol Genet* 8:397–407.

- Schmitt-Ney M (2020) The FOXO's Advantages of Being a Family: Considerations on Function and Evolution. *Cells* 9.
- Schwab MH, Bartholomae A, Heimrich B, Feldmeyer D, Druffel-Augustin S, Goebbels S, Naya FJ, Zhao S, Frotscher M, Tsai M-J, Nave K-A (2000) Neuronal Basic Helix-Loop-Helix Proteins (NEX and BETA2/Neuro D) Regulate Terminal Granule Cell Differentiation in the Hippocampus. *J Neurosci* 20:3714–3724.
- Sepp M, Kannike K, Eesmaa A, Urb M, Timmusk T (2011) Functional Diversity of Human Basic Helix-Loop-Helix Transcription Factor TCF4 Isoforms Generated by Alternative 5' Exon Usage and Splicing. *PLoS ONE* 6:e22138.
- Sepp M, Pruunsild P, Timmusk T (2012) Pitt–Hopkins syndrome-associated mutations in TCF4 lead to variable impairment of the transcription factor function ranging from hypomorphic to dominant-negative effects. *Hum Mol Genet* 21: 2873–2888.
- Sepp M, Vihma H, Nurm K, Urb M, Page SC, Roots K, Hark A, Maher BJ, Pruunsild P, Timmusk T (2017) The Intellectual Disability and Schizophrenia Associated Transcription Factor TCF4 Is Regulated by Neuronal Activity and Protein Kinase A. *J Neurosci* 37:10516–10527.
- Seredenina T, Luthi-Carter R (2012) What have we learned from gene expression profiles in Huntington's disease? *Neurobiol Dis* 45:83–98.
- Shimojo M (2008) Huntingtin regulates RE1-silencing transcription factor/neuron-restrictive silencer factor (REST/NRSF) nuclear trafficking indirectly through a complex with REST/NRSF-interacting LIM domain protein (RILP) and dynactin p150 Glued. *J Biol Chem* 283:34880–34886.
- Siebzehnrübl FA et al. (2018) Early postnatal behavioral, cellular, and molecular changes in models of Huntington disease are reversible by HDAC inhibition. *Proc Natl Acad Sci* 115:E8765–E8774.
- Silveira WA, Gonçalves DA, Machado J, Lautherbach N, Lustrino D, Paula-Gomes S, Pereira MG, Miyabara EH, Sandri M, Kettelhut IC, Navegantes LC (2020) cAMP-dependent protein kinase inhibits FoxO activity and regulates skeletal muscle plasticity in mice. *FASEB J* 34:12946–12962.
- Simpson JM, Gil-Mohapel J, Pouladi MA, Ghilan M, Xie Y, Hayden MR, Christie BR (2011) Altered adult hippocampal neurogenesis in the YAC128 transgenic mouse model of Huntington disease. *Neurobiol Dis* 41:249–260.
- Singh A, Ye M, Bucur O, Zhu S, Tanya Santos M, Rabinovitz I, Wei W, Gao D, Hahn WC, Khosravi-Far R (2010) Protein Phosphatase 2A Reactivates FOXO3a through a Dynamic Interplay with 14-3-3 and AKT. *Mol Biol Cell* 21:1140–1152.
- Sipione S (2002) Early transcriptional profiles in huntingtin-inducible striatal cells by microarray analyses. *Hum Mol Genet* 11:1953–1965.
- Sirp A, Leite K, Tuvikene J, Nurm K, Sepp M, Timmusk T (2020) The Fuchs corneal dystrophy-associated CTG repeat expansion in the TCF4 gene affects transcription from its alternative promoters. *Sci Rep* 10:18424.
- Skerjanc IS, Truong J, Filion P, McBurney MW (1996) A Splice Variant of the ITF-2 Transcript Encodes a Transcription Factor That Inhibits MyoD Activity. *J Biol Chem* 271:3555–3561.
- Smith-Dijak AI, Sepers MD, Raymond LA (2019) Alterations in synaptic function and plasticity in Huntington disease. *J Neurochem* 150:346–365.
- Sobrado VR, Moreno-Bueno G, Cubillo E, Holt LJ, Nieto MA, Portillo F, Cano A (2009) The class I bHLH factors E2-2A and E2-2B regulate EMT. *J Cell Sci* 122:1014–1024.

- Soosaar A, Chiaramello A, Zuber MX, Neuman T (1994) Expression of basic-helix-loop-helix transcription factor ME2 during brain development and in the regions of neuronal plasticity in the adult brain. *Mol Brain Res* 25:176–180.
- Steffan JS, Bodai L, Pallos J, Poelman M, McCampbell A, Apostol BL, Kazantsev A, Schmidt E, Zhu Y-Z, Greenwald M, Kurokawa R, Housman DE, Jackson GR, Marsh JL, Thompson LM (2001) Histone deacetylase inhibitors arrest polyglutamine-dependent neurodegeneration in *Drosophila*. *Nature* 413:739–743.
- Steffan JS, Kazantsev A, Spasic-Boskovic O, Greenwald M, Zhu Y-Z, Gohler H, Wanker EE, Bates GP, Housman DE, Thompson LM (2000) The Huntington's disease protein interacts with p53 and CREB-binding protein and represses transcription. *Proc Natl Acad Sci* 97:6763–6768.
- Stout JC, Paulsen JS, Queller S, Solomon AC, Whitlock KB, Campbell JC, Carlozzi N, Duff K, Beglinger LJ, Langbehn DR, Johnson SA, Biglan KM, Aylward EH, The PREDICT-HD Investigators and Coordinators of the Huntington Study Group (2011) Neurocognitive signs in prodromal Huntington disease. *Neuropsychology* 25: 1–14.
- Strong TV, Tagle DA, Valdes JM, Elmer LW, Boehm K, Swaroop M, Kaatz KW, Collins FS, Albin RL (1993) Widespread expression of the human and rat Huntington's disease gene in brain and nonneural tissues. *Nat Genet* 5:259–265.
- Sugars KL, Rubinsztein DC (2003) Transcriptional abnormalities in Huntington disease. *Trends Genet* 19:233–238.
- Sweatt JD (2013) Pitt–Hopkins Syndrome: intellectual disability due to loss of TCF4-regulated gene transcription. *Exp Mol Med* 45:e21–e21.
- Szlachcic WJ, Switonski PM, Krzyzosiak WJ, Figlerowicz M, Figiel M (2015) Huntington disease iPSCs show early molecular changes in intracellular signaling, the expression of oxidative stress proteins and the p53 pathway. *Dis Model Mech* 8:1047–1057.
- Talkowski ME et al. (2012) Sequencing Chromosomal Abnormalities Reveals Neurodevelopmental Loci that Confer Risk across Diagnostic Boundaries. *Cell* 149:525–537.
- Tamberg L, Sepp M, Timmusk T, Palgi M (2015) Introducing Pitt-Hopkins syndrome-associated mutations of TCF4 to *Drosophila* daughterless. *Biol Open* 4: 1762–1771.
- Tanaka A, Itoh F, Itoh S, Kato M (2008) TAL1/SCL Relieves the E2-2-Mediated Repression of VEGFR2 Promoter Activity. *J Biochem (Tokyo)* 145:129–135.
- Tapscott S, Davis R, Thayer M, Cheng P, Weintraub H, Lassar A (1988) MyoD1: a nuclear phosphoprotein requiring a Myc homology region to convert fibroblasts to myoblasts. *Science* 242:405–411.
- Teixeira JR, Szeto RA, Carvalho VMA, Muotri AR, Papes F (2021) Transcription factor 4 and its association with psychiatric disorders. *Transl Psychiatry* 11:19.
- Telley L, Agirman G, Prados J, Amberg N, Fièvre S, Oberst P, Bartolini G, Vitali I, Cadilhac C, Hippenmeyer S, Nguyen L, Dayer A, Jabaudon D (2019) Temporal patterning of apical progenitors and their daughter neurons in the developing neocortex. *Science* 364:eaav2522.
- Thaxton C, Kloth AD, Clark EP, Moy SS, Chitwood RA, Philpot BD (2018) Common Pathophysiology in Multiple Mouse Models of Pitt–Hopkins Syndrome. *J Neurosci* 38:918–936.

- The HD iPSC Consortium (2012) Induced Pluripotent Stem Cells from Patients with Huntington's Disease Show CAG-Repeat-Expansion-Associated Phenotypes. *Cell Stem Cell* 11:264–278.
- The HD iPSC Consortium (2017) Developmental alterations in Huntington's disease neural cells and pharmacological rescue in cells and mice. *Nat Neurosci* 20:648–660.
- The Huntington's Disease Collaborative Research Group (1993) A novel gene containing a trinucleotide repeat that is expanded and unstable on Huntington's disease chromosomes. *Cell* 72:971–983.
- The Schizophrenia Psychiatric Genome-Wide Association Study (GWAS) Consortium (2011) Genome-wide association study identifies five new schizophrenia loci. *Nat Genet* 43:969–976.
- Theodorou E, Dalembert G, Heffelfinger C, White E, Weissman S, Corcoran L, Snyder M (2009) A high throughput embryonic stem cell screen identifies Oct-2 as a bifunctional regulator of neuronal differentiation. *Genes Dev* 23:575–588.
- Thomas EA, Coppola G, Tang B, Kuhn A, Kim S, Geschwind DH, Brown TB, Luthi-Carter R, Ehrlich ME (2011) In vivo cell-autonomous transcriptional abnormalities revealed in mice expressing mutant huntingtin in striatal but not cortical neurons. *Hum Mol Genet* 20:1049–1060.
- Thomson SB, Leavitt BR (2018) Transcriptional Regulation of the Huntingtin Gene. *J Huntingt Dis* 7:289–296.
- Tourette C et al. (2014) The Wnt Receptor Ryk Reduces Neuronal and Cell Survival Capacity by Repressing FOXO Activity During the Early Phases of Mutant Huntingtin Pathogenicity. *PLoS Biol* 12:e1001895.
- Tsai K-L, Sun Y-J, Huang C-Y, Yang J-Y, Hung M-C, Hsiao C-D (2007) Crystal structure of the human FOXO3a-DBD/DNA complex suggests the effects of post-translational modification. *Nucleic Acids Res* 35:6984–6994.
- Túnez I, Tasset I, Pérez-De La Cruz V, Santamaría A (2010) 3-Nitropropionic Acid as a Tool to Study the Mechanisms Involved in Huntington's Disease: Past, Present and Future. *Molecules* 15:878–916.
- Tutukova S, Tarabykin V, Hernandez-Miranda LR (2021) The Role of Neurod Genes in Brain Development, Function, and Disease. *Front Mol Neurosci* 14:662774.
- Tuvikene J, Esvald E-E, Rähni A, Uustalu K, Zhuravskaya A, Avarlaid A, Makeyev EV, Timmusk T (2021) Intronic enhancer region governs transcript-specific Bdnf expression in rodent neurons. *eLife* 10:e65161.
- Uittenbogaard M, Chiaramello A (2000) Differential expression patterns of the basic Helix-Loop-Helix transcription factors during aging of the murine brain. *Neurosci Lett* 280:95–98.
- Valenza M (2005) Dysfunction of the Cholesterol Biosynthetic Pathway in Huntington's Disease. *J Neurosci* 25:9932–9939.
- Valor LM (2015) Transcription, Epigenetics and Ameliorative Strategies in Huntington's Disease: a Genome-Wide Perspective. *Mol Neurobiol* 51:406–423.
- van den Berg MCW, Burgering BMT (2011) Integrating Opposing Signals Toward Forkhead Box O. *Antioxid Redox Signal* 14:607–621.
- van der Burg JMM, Bacos K, Wood NI, Lindqvist A, Wierup N, Woodman B, Wamsteeker JI, Smith R, Deierborg T, Kuhar MJ, Bates GP, Mulder H, Erlanson-Albertsson C, Morton AJ, Brundin P, Petersén Å, Björkqvist M (2008) Increased metabolism in the R6/2 mouse model of Huntington's disease. *Neurobiol Dis* 29:41–51.

- van der Horst A, Burgering BMT (2007) Stressing the role of FoxO proteins in lifespan and disease. *Nat Rev Mol Cell Biol* 8:440–450.
- van der Horst A, de Vries-Smits AMM, Brenkman AB, van Triest MH, van den Broek N, Colland F, Maurice MM, Burgering BMT (2006) FOXO4 transcriptional activity is regulated by monoubiquitination and USP7/HAUSP. *Nat Cell Biol* 8:1064–1073.
- Vashishtha M et al. (2013) Targeting H3K4 trimethylation in Huntington disease. *Proc Natl Acad Sci* 110:E3027–E3036.
- Verlinsky Y, Strelchenko N, Kukhareno V, Rechitsky S, Verlinsky O, Galat V, Kuliev A (2005) Human embryonic stem cell lines with genetic disorders. *Reprod Biomed Online* 10:105–110.
- Vidal RL, Figueroa A, Court FA, Thielen P, Molina C, Wirth C, Caballero B, Kiffin R, Segura-Aguilar J, Cuervo AM, Glimcher LH, Hetz C (2012) Targeting the UPR transcription factor XBP1 protects against Huntington’s disease through the regulation of FoxO1 and autophagy. *Hum Mol Genet* 21:2245–2262.
- Vierbuchen T, Ostermeier A, Pang ZP, Kokubu Y, Südhof TC, Wernig M (2010) Direct conversion of fibroblasts to functional neurons by defined factors. *Nature* 463:1035–1041.
- Voisin J, Farina F, Naphade S, Fontaine M, Tshilenge K, Galicia Aguirre C, Lopez-Ramirez A, Dancourt J, Ginisty A, Sasidharan Nair S, Lakshika Madushani K, Zhang N, Lejeune F, Verny M, Campisi J, Ellerby LM, Neri C (2020) FOXO3 targets are reprogrammed as Huntington’s disease neural cells and striatal neurons face senescence with p16^{INK4a} increase. *Aging Cell* 19.
- Vonsattel J-P, Myers RH, Stevens TJ, Ferrante RJ, Bird ED, Richardson EP (1985) Neuropathological Classification of Huntington’s Disease: *J Neuropathol Exp Neurol* 44:559–577.
- Wang F, Marshall CB, Yamamoto K, Li G-Y, Gasmi-Seabrook GMC, Okada H, Mak TW, Ikura M (2012) Structures of KIX domain of CBP in complex with two FOXO3a transactivation domains reveal promiscuity and plasticity in coactivator recruitment. *Proc Natl Acad Sci U S A* 109:6078–6083.
- Wang L-H, Baker NE (2015) E Proteins and ID Proteins: Helix-Loop-Helix Partners in Development and Disease. *Dev Cell* 35:269–280.
- Wang M, Zhang X, Zhao H, Wang Q, Pan Y (2009) FoxO gene family evolution in vertebrates. *BMC Evol Biol* 9:222.
- Wang X, Hu S, Liu L (2017) Phosphorylation and acetylation modifications of FOXO3a: Independently or synergistically? *Oncol Lett* 13:2867–2872.
- Wang Y, Lu Z, Zhang Yilan, Cai Y, Yun D, Tang T, Cai Z, Wang C, Zhang Yandong, Fang F, Yang Z, Behnisch T, Xie Y (2020) Transcription Factor 4 Safeguards Hippocampal Dentate Gyrus Development by Regulating Neural Progenitor Migration. *Cereb Cortex* 30:3102–3115.
- Wedel M, Fröb F, Elsesser O, Wittmann M-T, Lie DC, Reis A, Wegner M (2020) Transcription factor Tcf4 is the preferred heterodimerization partner for Olig2 in oligodendrocytes and required for differentiation. *Nucleic Acids Res* 48:4839–4857.
- Weigelt J, Climent I, Dahlman-Wright K, Wikström M (2001) Solution Structure of the DNA Binding Domain of the Human Forkhead Transcription Factor AFX (FOXO4)[†]. *Biochemistry* 40:5861–5869.

- Whalen S et al. (2012) Novel comprehensive diagnostic strategy in Pitt-Hopkins syndrome: Clinical score and further delineation of the TCF4 mutational spectrum. *Hum Mutat* 33:64–72.
- Wheeler V (1999) Length-dependent gametic CAG repeat instability in the Huntington's disease knock-in mouse. *Hum Mol Genet* 8:115–122.
- Wheeler VC, White JK, Gutekunst CA, Vrbanac V, Weaver M, Li XJ, Li SH, Yi H, Vonsattel JP, Gusella JF, Hersch S, Auerbach W, Joyner AL, MacDonald ME (2000) Long glutamine tracts cause nuclear localization of a novel form of huntingtin in medium spiny striatal neurons in HdhQ92 and HdhQ111 knock-in mice. *Hum Mol Genet* 9:503–513.
- White JK, Auerbach W, Duyao MP, Vonsattel J-P, Gusella JF, Joyner AL, MacDonald ME (1997) Huntingtin is required for neurogenesis and is not impaired by the Huntington's disease CAG expansion. *Nat Genet* 17:404–410.
- Wilton DK, Stevens B (2020) The contribution of glial cells to Huntington's disease pathogenesis. *Neurobiol Dis* 143:104963.
- Wong M-C, Castanon I, Baylies MK (2008) Daughterless dictates Twist activity in a context-dependent manner during somatic myogenesis. *Dev Biol* 317:417–429.
- Woods YL, Rena G, Morrice N, Barthel A, Becker W, Guo S, Unterman TG, Cohen P (2001) The kinase DYRK1A phosphorylates the transcription factor FKHR at Ser329 in vitro, a novel in vivo phosphorylation site. *Biochem J* 355:597–607.
- Wu Y et al. (2018) Novel Mechanism of Foxo1 Phosphorylation in Glucagon Signaling in Control of Glucose Homeostasis. *Diabetes* 67:2167–2182.
- Xia H, Jahr FM, Kim N-K, Xie L, Shabalin AA, Bryois J, Sweet DH, Kronfol MM, Palasuberniam P, McRae M, Riley BP, Sullivan PF, van den Oord EJ, McClay JL (2018) Building a schizophrenia genetic network: transcription factor 4 regulates genes involved in neuronal development and schizophrenia risk. *Hum Mol Genet* 27:3246–3256.
- Xiang C, Zhang S, Dong X, Ma S, Cong S (2018) Transcriptional Dysregulation and Post-translational Modifications in Polyglutamine Diseases: From Pathogenesis to Potential Therapeutic Strategies. *Front Mol Neurosci* 11:153.
- Xie Q, Hao Y, Tao L, Peng S, Rao C, Chen H, You H, Dong M, Yuan Z (2012) Lysine methylation of FOXO3 regulates oxidative stress-induced neuronal cell death. *EMBO Rep* 13:371–377.
- Yamagata K, Daitoku H, Takahashi Y, Namiki K, Hisatake K, Kako K, Mukai H, Kasuya Y, Fukamizu A (2008) Arginine Methylation of FOXO Transcription Factors Inhibits Their Phosphorylation by Akt. *Mol Cell* 32:221–231.
- Yan L, Lavin VA, Moser LR, Cui Q, Kanies C, Yang E (2008) PP2A Regulates the Pro-apoptotic Activity of FOXO1. *J Biol Chem* 283:7411–7420.
- Yang J, Horton JR, Li J, Huang Y, Zhang X, Blumenthal RM, Cheng X (2019) Structural basis for preferential binding of human TCF4 to DNA containing 5-carboxylcytosine. *Nucleic Acids Res* 47:8375–8387.
- Yang J-Y et al. (2008) ERK promotes tumorigenesis by inhibiting FOXO3a via MDM2-mediated degradation. *Nat Cell Biol* 10:138–148.
- Yang W, Du WW, Li X, Yee AJ, Yang BB (2016) Foxo3 activity promoted by non-coding effects of circular RNA and Foxo3 pseudogene in the inhibition of tumor growth and angiogenesis. *Oncogene* 35:3919–3931.

- Ye T, Lipska BK, Tao R, Hyde TM, Wang L, Li C, Choi KH, Straub RE, Kleinman JE, Weinberger DR (2012) Analysis of Copy Number Variations in Brain DNA from Patients with Schizophrenia and Other Psychiatric Disorders. *Biol Psychiatry* 72:651–654.
- Yoon SO, Chikaraishi DM (1994) Isolation of two E-box binding factors that interact with the rat tyrosine hydroxylase enhancer. *J Biol Chem* 269:18453–18462.
- Yuan Z, Becker EBE, Merlo P, Yamada T, DiBacco S, Konishi Y, Schaefer EM, Bonni A (2008) Activation of FOXO1 by Cdk1 in Cycling Cells and Postmitotic Neurons. *Science* 319:1665–1668.
- Yusuf IO, Cheng P-H, Chen H-M, Chang Y-F, Chang C-Y, Yang H-I, Lin C-W, Tsai S-J, Chuang J-I, Wu C-C, Huang B-M, Sun HS, Yang S-H (2018) Fibroblast Growth Factor 9 Suppresses Striatal Cell Death Dominantly Through ERK Signaling in Huntington’s Disease. *Cell Physiol Biochem* 48:605–617.
- Zainelli GM (2004) Calmodulin Regulates Transglutaminase 2 Cross-Linking of Huntingtin. *J Neurosci* 24:1954–1961.
- Zeitlin S, Liu J-P, Chapman DL, Papaioannou VE, Efstratiadis A (1995) Increased apoptosis and early embryonic lethality in mice nullizygous for the Huntington’s disease gene homologue. *Nat Genet* 11:155–163.
- Zhai W, Jeong H, Cui L, Krainc D, Tjian R (2005) In Vitro Analysis of Huntingtin-Mediated Transcriptional Repression Reveals Multiple Transcription Factor Targets. *Cell* 123:1241–1253.
- Zhang W, Hietakangas V, Wee S, Lim SC, Gunaratne J, Cohen SM (2013) ER stress potentiates insulin resistance through PERK-mediated FOXO phosphorylation. *Genes Dev* 27:441–449.
- Zhao J, Brault JJ, Schild A, Cao P, Sandri M, Schiaffino S, Lecker SH, Goldberg AL (2007) FoxO3 Coordinately Activates Protein Degradation by the Autophagic/Lysosomal and Proteasomal Pathways in Atrophying Muscle Cells. *Cell Metab* 6:472–483.
- Zheng Z, Diamond MI (2012) Huntington Disease and the Huntingtin Protein In: *Progress in Molecular Biology and Translational Science*, pp189–214. Elsevier.
- Zhuang Y, Cheng P, Weintraub H (1996) B-lymphocyte development is regulated by the combined dosage of three basic helix-loop-helix genes, E2A, E2-2, and HEB. *Mol Cell Biol* 16:2898–2905.
- Zuccato C (2001) Loss of Huntingtin-Mediated BDNF Gene Transcription in Huntington’s Disease. *Science* 293:493–498.
- Zuccato C, Belyaev N, Conforti P, Ooi L, Tartari M, Papadimou E, MacDonald M, Fossale E, Zeitlin S, Buckley N, Cattaneo E (2007) Widespread Disruption of Repressor Element-1 Silencing Transcription Factor/Neuron-Restrictive Silencer Factor Occupancy at Its Target Genes in Huntington’s Disease. *J Neurosci* 27:6972–6983.
- Zuccato C, Cattaneo E (2014) *Normal Function of Huntingtin*. Oxford University Press.
- Zuccato C, Tartari M, Crotti A, Goffredo D, Valenza M, Conti L, Cataudella T, Leavitt BR, Hayden MR, Timmusk T, Rigamonti D, Cattaneo E (2003) Huntingtin interacts with REST/NRSF to modulate the transcription of NRSE-controlled neuronal genes. *Nat Genet* 35:76–83.
- Zweier C et al. (2007) Haploinsufficiency of TCF4 Causes Syndromal Mental Retardation with Intermittent Hyperventilation (Pitt-Hopkins Syndrome). *Am J Hum Genet* 80:994–1001.

Acknowledgements

First and foremost, I want to thank my supervisors, professor Tõnis Timmusk and research scientist Mari Sepp, for believing in me, encouraging me and enabling to continue the journey after receiving Master's degree. I'm thankful to Mari for patient guidance and clear vision of what needs to be done to achieve the goals and it was great to see how brilliant mind works. I'm grateful to Tõnis creating a very good and collaborative working environment that enabled me to focus totally on my scientific goals in the lab without the need to forget that we have lives outside the lab as well. Understanding and support from Tõnis made impossible possible - to have children and work towards a doctoral degree at the same time.

I will miss all the Neurobiology lab members – old and new - and always cherish the good atmosphere in the lab. We all felt the desire to be the best but it was fueled by the mentality that there is a solution to every scientific problem and we can conquer those together without demotivating competition. I'm honored that I had opportunity to work with so smart and brave minds for so many years.

I appreciate that I had opportunity to supervise Bachelor's and Master's degree students and together we develop each other skills to guide, to study, to read and write, and to do the best research we could do.

I thank all the co-authors for their contributions to the publications and I'm especially grateful to Alex the Finisher who finalized and repeated the last experiments and was fast and efficient wizard in Illustrator enabling transformation of my last manuscript to published article before the defense of this thesis. As they say it is the darkest before the dawn and without "coach" Jürgen's kind words, calmness, honest critique and strong belief that I will manage, this thesis would not have been finished.

Finally, I want to thank my parents, Leonora and Aavo, and my husband, Mihkel, and also my friends and relatives for the support and interest in my research. I feel that they have never questioned my ability to achieve what I have put my mind on but I'm thankful that they understood or at least accepted my urge to prove it to myself as well 😊 .

I thank all the funding agencies that supported this work: Estonian Ministry of Education and Research (Grant 0140143) and Estonian Science Foundation (Grants 7257 and 8844), Wellcome Trust Grant 067952, Estonian Research Council Institutional Research Funding Grant IUT19-18 and Grant PRG805, funds from the Estonian Academy of Sciences, the National R&D program "Health" (Grant AR12098), the European Union through the European Regional Development Fund (Project No. 2014-2020.4.01.15-0012) and H2020-MSCA-RISE-2016 (EU734791), the Pitt Hopkins Research Foundation and Million Dollar Bike Ride Pilot Grant Program for Rare Disease Research at UPenn Orphan Disease Center (Grants MDBR-16-122-PHP and MDBR-17-127-Pitt Hopkins). This work has also been partially supported by "TUT Institutional Development Program for 2016–2022" Graduate School in clinical medicine receiving funding from the European Regional Development Fund under Program ASTRA 2014-2020.4.01.16-0032 in Estonia.

Abstract

Molecular mechanisms of Huntington's disease

Huntington's disease is a devastating hereditary neurodegenerative disease affecting 3-5 persons in 100 000 worldwide. Despite the efforts of 30 last years since the initial discovery of the mutation in huntingtin gene as the molecular cause for HD in 1993, there is still no effective cure for this disease. From the fundamental neuropathological findings of atrophic striatum and cortex at the onset of HD, numerous studies on susceptibility to apoptosis and neuronal cell death occurring in these brain regions and discovering balancing factors counteracting it have been conducted. However, recent research on pre-symptomatic and prodromal HD patients have revealed impaired cognition and memory, disturbances in specific sets of neuron precursors and realization that wt HTT is playing a role in neurogenesis has led to recognition of HD as potentially neurodevelopmental disease.

Dysregulation of transcription is well studied in HD models and in HD patients utilizing microarray and RNA-seq techniques and is a widely accepted molecular mechanism having an effect in HD. Transcription factors exert their function in nucleus and here we showed subcellular misregulation and/or expression level change of two transcription factors FOXO3 and TCF4. FOXO3 has known functions in balancing stress signals and regulating cell survival or apoptosis pathways and TCF4 plays a role in neurogenesis and neuronal differentiation. Both of these processes have been implicated in HD. Therefore, both TF have potential to modulate the progress of HD. By immunocytochemical staining we confirmed increased nuclear localization of FOXO3 in HD cells, whereas levels of nuclear TCF4 were decreased in a cell-based HD model.

Next, we showed that in addition to the change in FOXO3 localization, FOXO3 mRNA and protein levels were increased in HD. Furthermore, we detected increased levels of FOXO3 in both nuclear and cytosolic fractions. FOXO3 localization and activation is tightly controlled by post-translational modifications and phosphorylation by protein kinase B (PKB/Akt) is considered the most influential. We report unaffected total and activated PKB/Akt protein levels in mutant *Hdh* cells and unchanged levels of phosphorylated pFOXO3-S253 as a PKB/Akt target. Therefore, results of Akt-mediated phosphorylation are not coupled with FOXO3 shuttling from cytoplasm to nucleus. In contrast, levels of phosphorylated ERK1/2 kinases were significantly reduced in HD model cells. Furthermore, we detected binding of FOXO3 to its own promoter and described a forkhead response element (FHRE) essential to elicit FOXO3-dependent transcription of *Foxo3*. In sum, we propose an over-activated positive feedback loop for FOXO3 in HD, although the scientific debate is still ongoing whether increased levels of FOXO3 is beneficial or detrimental in HD.

The finding of subcellular mislocalization of TCF4 was the starting point to our quest to find the roles and regulation of this relatively unknown bHLH TF at that time. Therefore, first we described the human *TCF4* gene structure and showed that TCF4 isoforms are generated by alternative 5' exons usage and splicing. Then we determined that bHLH transcription factor TCF4 was ubiquitously, but not equally expressed in human tissues. We discovered an NLS sequence in TCF4 and studied functionality of activation domains AD1 and AD2 on gene transcription activation in HEK293 and in rat primary neurons. Subsequently, we found that TCF4 is neuronal activity regulated transcription factor and that this activity-dependence is mediated by cAMP-PKA pathway and phosphorylation of S448 in TCF4. Dimerization of TCF4 is required for E-box binding

on target gene promoter (as is for all bHLH TF) and functional DNA-binding homo- and heterodimers with class II bHLH proteins can be formed (dimerization with class V bHLH (ID) protein impairs DNA binding). First, we showed synergy between TCF4 isoform A and ASCL1 on *GADD45G* promoter and μ E5 E-box promoter construct in rat primary neurons. However, in total 18 N-terminally different TCF4 isoforms with varying internal exon and functional domain composition could be expressed that raised the question of their potentially different capacity on target gene transcription. Here we report differential transactivational capacity of five TCF4 isoforms and revealed also differences in co-operation with dimerization partner ASCL1 in resting and in depolarized rat primary cortical and hippocampal neurons. Therefore, our results highlight functional differences between TCF4 isoforms and suggest including all TCF4 isoforms in studies elucidating TCF4 participation and functions in health and disease.

Subsequently, we continued to study the role of transcription factor TCF4 in HD. We report downregulated TCF4 in HD cell-based and animal models and in HD patients. We detected mainly decreased levels of specific TCF4 isoform-encoding transcripts in different brain regions of HD transgenic mouse model R6/1 compared to wt mice at four ages. Decreased levels were confirmed on protein level in R6/1 mice hippocampus and cortex and were further corroborated with decreased TCF4-B/C protein levels in postmortem HD patient CA1 region. In addition to TCF4, we determined mRNA levels of *Bdnf* and TCF4 dimerization partners with known functions in nervous system development. *Bdnf* mRNA levels were decreased in hippocampus, cortex and cerebellum of R6/1 mice and we hypothesize that this reduction may be TCF4-dependent in cortex and hippocampus as binding of TCF4 to a enhancer of *Bdnf* has been reported recently. mRNAs of *Ascl1* and *Neurod1* were differentially expressed in specific brain regions of R6/1 mice. A tightly controlled amount of TCF4 is required for normal neurogenesis and development as illustrated by the PTHS that is caused by haploinsufficiency of *TCF4*. Many class II bHLH proteins require dimerization with TCF4 for efficient DNA binding. Therefore, we can hypothesize that disruption of delicate balance of both TCF4 and its dimerization partners may lead to detrimental outcomes described in HD brain. Our results of decreased TCF4 levels in hippocampus may suggest a link between the following observations: a) cognitive impairments take place in pre-symptomatic and prodromal HD patients, b) TCF4 regulates neurogenesis in hippocampus, c) decreased levels of TCF4 have an effect on memory function. Our study is the first to report complex dysregulation of TCF4 in HD that may help to advance the neurodevelopmental hypothesis of HD.

To conclude, we studied in depth two transcription factors found to be mislocalized in preliminary screen with panel of antibodies raised against more than 200 transcription factors in HD cells. Our results suggest a novel molecular mechanism responsible for upregulation of FOXO3 in HD and functional differences of TCF4 protein isoforms in health and in HD.

Lühikokkuvõte

Huntingtoni tõve molekulaarsed mehhanismid

Huntingtoni tõbi on pärilik neurodegeneratiivne haigus, mille all kannatab maailmas keskmiselt 3-5 inimest 100 000-st. Huntingtoni tõbe põhjustav geenimutatsioon tuvastati 1993. aastal, kuid sellest hoolimata pole arstide ja teadlaste viimase ligemale 30 aasta pingutused vilja kandnud ning paraku pole turule toodud ühtegi Huntingtoni tõve ravimit, mis ei piirduks vaid sümptomite leevendamisega. Neuropatoloogiliselt iseloomustab Huntingtoni tõbe ajukoore ja juttkeha neuronite massiline suremine ja atroofia, seepärast on varasemad arvukad uuringud keskendunud eelkõige apoptoosi ja spetsiifiliste neuronite surmasignaalidele vastuvõtlikkuse uurimisele lootuses tuvastada faktorid, mis võimaldaksid vastu seista Huntingtoni tõvele iseloomulikele kahjustavatele mõjuritele. Kuna geneetilised testid võimaldavad nüüd haigust tuvastada aastaid enne klassikaliste sümptomite ilmnemist, siis on viimasel ajal hakatud uurima ka pre-sümptomaatilisi ja väga varajases sümptomite ilmnemise faasis Huntingtoni tõve patsiente, kellel on märgatud kognitiivsete võimete muutuseid, mälu- ning emotsioonide kontrollihäireid. Lisaks on kinnitust leidnud metsiktüüpi huntingtiini roll neurogeneesis ning katsed Huntingtoni tõve erinevates mudelites on kinnitanud vähenenud neuronite eellasrakkude hulka spetsiifilistes ajuosades, mis kokkuvõttes viitab sellele, et Huntingtoni tõbi võib olla lisaks neurodegeneratiivsele haigusele ka neuropaalse arengu häire.

Mikrokiibi ja RNA sekveneerimise tehnoloogia abil tuvastati Huntingtoni tõves tõsised transkriptsiooni regulatsiooni häired ning hetkel on see laialdaselt aktsepteeritud molekulaarne mehhanism, mis mängib olulist rolli Huntingtoni tõve arengus. Transkriptsioonifaktorid on regulatoorsed valgud, mis täidavad oma funktsiooni raku tuumas. Sellele doktoritööle eelnevas uuringus märkasime ja selle doktoritöö käigus kinnitasime immuunotsüokeemilist meetodit kasutades transkriptsioonifaktorite FOXO3 ja TCF4 muutunud rakusisese paiknemise ja/või tuumasisese valgutaseme muutuse HD mudelrakuliinis. Olulisemate funktsioonidena võib FOXO3 korral välja tuua rolli stressi- ja ellujäämissignaali integraatori ja tasakaalustatud rakuvastuse tekitajana, samas TCF4 on tihedalt seotud neurogeneesi ja diferentseerumisega. Kõik need mainitud protsessid on häirunud Huntingtoni tõve korral.

Järgmiseks uurisime FOXO3 mRNA ja valgutasemeid, mis mõlemad olid olulisel määral kõrgenenud Huntingtoni tõve korral nii kasutatud raku- ja loomudelites kui ka HD patsientides. Lisaks selgus, et FOXO3 valgu hulk on suurenenud nii tsütosooli kui ka tuuma fraktsioonis. FOXO3 lokalisatsioon, aktiivsus ja hulk on rangelt kontrollitud mitmesuguste post-translaatorsete modifikatsioonide abil ning neist olulisimaks on peetud proteiin kinaas B (PKB/Akt). Me ei tuvastanud muutusi PKB/Akt valgu tasemetes ega muutunud fosfo-aktiveeritud PKB/Akt osakaalu mutantsetes Hdh rakkudes ega ka oluliselt muutunud PKB/Akt poolt fosforüleeritud FOXO3 tasemeid. Seega ei seleta need tulemused FOXO3 muutunud asukohta Hdh rakkudes. Lisaks uurisime ERK1/2 kinaaside tasemeid ning kuigi üldtasemed olid võrreldavad metsiktüüpi ja mutantsetes Hdh rakkudes, siis fosfo-aktiveeritud ERK1/2 tasemed olid mutantsetes Hdh rakkudes märgatavalt langenud. Vähenenud fosfo-ERK ei pruugi FOXO3 piisavalt fosforüleerida, mis võib häirida FOXO3 lagundamist ja tema transporti tuumast mitokondrisse ning lõpptulemusena põhjustada FOXO3 kogunemise tuuma. Järgnevalt uurisime võimalust, et FOXO3 transkriptsioon on autoreguleeritud ning bioinformaatilisel analüüsil tuvastasime mitu võimalikku FOXO3 seondumisjärjestust ehk FHRE-d (ingl. *fork head*

response element) *FOXO3* promootoris. Kromatiin-immunopretsipitatsiooni, lutsifraasi reporter katsete ja mutageneesi abil kinnitasime *FOXO3*-sõltuva FHRE olemasolu *FOXO3* promootoris. Sellest lähtuvalt väidame, et *FOXO3* tasemed on Huntingtoni tõves tõusnud positiivse auto-tagasisidestus mehhanismi tõttu, samas suurenenud *FOXO3* kasulikkus või kahjulikkus Huntingtoni tõves vajab edasisi põhjalikumaid uuringuid.

Huntingtoni tõve mudelrakkudes tuvastatud muutunud rakusisene paiknemine tõi TCF4 meie uurimisgrupi huviorbiiti ning sellest leiust sai alguse meie teadusgrupi TCF4 uurimise teekond. Kuna TCF4 oli sel hetkel üsnagi vähetuntud, siis kirjeldasime esmakordselt inimese *TCF4* geeni struktuuri ning näitasime, et TCF4 erinevad isovorme kodeerivad mRNAd luuakse kasutades alternatiivseid 5' eksoneid ning sisemist splaissimist. Pöördtranskriptsiooniga kvantitatiivset polümeraasi ahelreaktsiooni meetodit (RT-qPCR) kasutades kirjeldasime *TCF4* laialdase, kuid mitte samaväärse ekspressiooni paljudes inimese kudedes. Lisaks tuvastasime tuuma lokalisatsiooni signaaljärjestuse (ingl. *NLS*) ning uurisime TCF4 aktivatsioonidomäänide AD1 ja AD2 efekti E-boks-sõltuva transkriptsiooni aktivatsioonile (E-boks on DNA järjestus, millele TCF4 seob) nii HEK293 rakkudes kui ka roti primaarsetes närvirakkudes. Järgnevalt leidsime, et TCF4-st sõltuv transkriptsioon on neuraalse aktiivsuse poolt reguleeritav ning see toimub tsüklilise adenosiinmonofosfaadi (ingl. *cAMP*) ja proteiini kinaas A (PKA) signaaliraja vahendusel, mille tulemusena fosforüleeritakse TCF4 valgu positsioonis 448 asuv seriini jääk (S448). On teada, et sihtmärkgeeni promootoris asuvale reguleeritavale E-boks järjestusele seondumiseks on vajalik TCF4 dimeriseerumine ning TCF4 võib moodustada nii homodimeere (TCF4 isovormid paarduvad omavahel) kui heterodimeere aluselise heeliks-ling-heeliks (ingl. *bHLH*) klass II valkudega (bHLH klass V valkudega (ID ingl. *inhibitors of differentiation*) dimeriseerumine takistab DNA-le seondumist). Oma katsetes näitasime TCF4 ja ASCL1 omavahelist sünergiaid transkriptsiooni aktivatsioonile *GADD45G* promootori ja kunstlikke μ E5 E-boks järjestusi sisaldava promootori korral roti primaarsetes neuronites. Kuna *TCF4* geenilt on võimalik lõpptulemusena ekspresseerida 18 N-terminaalselt erinevat TCF4 isovormi, mis varieeruvad sisemiste eksonite ja nende poolt kodeeritavate funktsionaalsete domäänide poolest, siis tõstatas küsimus TCF4 isovormide võimalikest erinevustest transkriptsiooni aktiveerida. Me näitasime, et TCF4 erinevatel isovormidel on tõepoolest erinev transaktivatsiooniline võimekus ning lisaks leidsime, esineb erinevusi ka dimeriseerumispartneriga ko-opereerumisel nii neuraalselt aktiiveeritud kui aktiveerimata roti primaarsetes ajukoore ja hippokampuse närvirakkudes. Kokkuvõtvalt toovad meie tulemused esile, et *TCF4* geeni keerukas struktuur on aluseks paljudele TCF4 valgu isovormidele, mis erinevad omavahel funktsionaalselt. Seetõttu on vaja uurida komplekselt kõiki TCF4 isovorme ja nende osalemist organismi normaalses funktsioneerimises ja ka haiguste kontekstis.

Järgnevalt uurisimegi transkriptsioonifaktorit TCF4 Huntingtoni tõves. Lisaks varem mainitud lokalisatsiooni muutusele leidsime, et TCF4 tasemed on vähenenud nii Huntingtoni tõve mudelites kui ka patsientides. Me uurisime RT-qPCRi kasutades põhjalikult erinevaid TCF4 isovorme kodeerivaid mRNAsid Huntingtoni tõve transgeense hiire mudeli R6/1 erinevates ajuosades ja seda neljas erinevas vanusegrupis. Me tuvastasime ajuosa- ja TCF4 isovorm-spetsiifilised allaregulatsioonid võrreldes metsiktüüpi hiirtega. Vähenenud *TCF4* isovorm-spetsiifilised mRNA tasemed leidsid kinnitust valgu tasemel hippokampuses ja ajukoores ning veelgi enam, TCF4-B/C valgu hulk on langenud ka Huntingtoni tõve patsientide *post mortem* hippokampuse CA1 regioonis ja ajukoores. Lisaks TCF4-le määrasime RT-qPCR meetodil ka kahe närvisüsteemi arengus olulist rolli täitva TCF4 dimerisatsioonipartneri mRNA tasemed.

Transkriptsioonifaktorid *Ascl1* ja *Neurod1* olid erinevalt ekspresseeritud spetsiifilistes R6/1 hiire ajuosades ning need muutused ei olnud korrelatsioonis TCF4 muutustega. TCF4 valgu täpsed tasemed on vajalikud närvisüsteemi normaalseks arenguks. Seda illustreerib *TCF4* haplopuudulikkusest tulenev Pitt-Hopkinsi sündroom (PTHS), mida iseloomustavad intellektipuue, alaareng ja hingamisraskused. Lisaks on teada, et paljud klass II bHLH valgud vajavad efektiivseks DNA-le seondumiseks dimeriseerumist TCF4-ga. Seetõttu võiks püstitada hüpoteesi, et õrna tasakaalu rikkumine nii TCF4 kui partnerite häiritud ekspressiooni tõttu võib viia kahjulike tagajärgedeni, mida on kirjeldatud Huntingtoni tõve mudelloomadega ja patsientide ajus. Hiljuti on lisandunud veel andmeid TCF4 regulatsiooni osas hippokampuse neurogeneesis ja mälu funktsioonides ning sarnased kognitiivsed ja mäluhäired on tuvastatud ka presümptomaatilistes Huntingtoni tõve patsientides. Kui lisada juurde käesoleva töö tulemused, milles näitasime, et TCF4 on drastiliselt vähenenud hippokampuses, siis võibki see olla varem teadmata ühendusliik, mis võiks aidata osaliselt seletada täheldatud häirete tekkimist. Meie uuring on esimene, milles näidatakse TCF4 keerukat regulatsioonihäiret Huntingtoni tõves ning need teadmised võivad aidata edasi liikuda Huntingtoni tõve neuro-arengulise hüpoteesi uurimisel.

Kokkuvõtteks, me uurisime põhjalikult kahte transkriptsioonifaktorit, mille tuvastasime rohkem kui 200 transkriptsioonifaktori vastase antikehaga tehtud eeluuringus kui häirunud paiknemisega valgud Huntingtoni tõve mudelrakkudes. Me leidsime molekulaarse mehhanismi, mis vastutab FOXO3 ülesreguleerimise eest Huntingtoni tõves ning laiendasime olulisel määral teadmisi *TCF4* geeni ning TCF4 valgu isovormide funktsionaalsete erisuste kohta nii organismi normaalses arengus ja toimimises kui ka Huntingtoni tõves.

Appendix 1

Publication I

Mari Sepp, **Kaja Kannike**, Ave Eesmaa, Mari Urb and Tõnis Timmusk (2011). Functional Diversity of Human Basic Helix-Loop-Helix Transcription Factor TCF4 Isoforms Generated by Alternative 5' Exon Usage and Splicing. *PLoS ONE* 6(7): e22138. doi: 10.1371/journal.pone.0022138.

Functional Diversity of Human Basic Helix-Loop-Helix Transcription Factor TCF4 Isoforms Generated by Alternative 5' Exon Usage and Splicing

Mari Sepp, Kaja Kannike, Ave Eesmaa, Mari Urb, Tõnis Timmusk*

Department of Gene Technology, Tallinn University of Technology, Tallinn, Estonia

Abstract

Background: Transcription factor 4 (TCF4 alias ITF2, E2-2, ME2 or SEF2) is a ubiquitous class A basic helix-loop-helix protein that binds to E-box DNA sequences (CANNTG). While involved in the development and functioning of many different cell types, recent studies point to important roles for TCF4 in the nervous system. Specifically, human *TCF4* gene is implicated in susceptibility to schizophrenia and *TCF4* haploinsufficiency is the cause of the Pitt-Hopkins mental retardation syndrome. However, the structure, expression and coding potential of the human *TCF4* gene have not been described in detail.

Principal Findings: In the present study we used human tissue samples to characterize human *TCF4* gene structure and *TCF4* expression at mRNA and protein level. We report that although widely expressed, human *TCF4* mRNA expression is particularly high in the brain. We demonstrate that usage of numerous 5' exons of the human *TCF4* gene potentially yields in TCF4 protein isoforms with 18 different N-termini. In addition, the diversity of isoforms is increased by alternative splicing of several internal exons. For functional characterization of TCF4 isoforms, we overexpressed individual isoforms in cultured human cells. Our analysis revealed that subcellular distribution of TCF4 isoforms is differentially regulated: Some isoforms contain a bipartite nuclear localization signal and are exclusively nuclear, whereas distribution of other isoforms relies on heterodimerization partners. Furthermore, the ability of different TCF4 isoforms to regulate E-box controlled reporter gene transcription is varied depending on whether one or both of the two TCF4 transcription activation domains are present in the protein. Both TCF4 activation domains are able to activate transcription independently, but act synergistically in combination.

Conclusions: Altogether, in this study we have described the inter-tissue variability of TCF4 expression in human and provided evidence about the functional diversity of the alternative TCF4 protein isoforms.

Citation: Sepp M, Kannike K, Eesmaa A, Urb M, Timmusk T (2011) Functional Diversity of Human Basic Helix-Loop-Helix Transcription Factor TCF4 Isoforms Generated by Alternative 5' Exon Usage and Splicing. PLoS ONE 6(7): e22138. doi:10.1371/journal.pone.0022138

Editor: Fatah Kashanchi, George Mason University, United States of America

Received: February 28, 2011; **Accepted:** June 16, 2011; **Published:** July 15, 2011

Copyright: © 2011 Sepp et al. This is an open-access article distributed under the terms of the Creative Commons Attribution License, which permits unrestricted use, distribution, and reproduction in any medium, provided the original author and source are credited.

Funding: This work was supported by Estonian Ministry of Education and Research (Grant 0140143) and Estonian Science Foundation (Grants 7257 and 8844). The funders had no role in study design, data collection and analysis, decision to publish, or preparation of the manuscript.

Competing Interests: The authors have declared that no competing interests exist.

* E-mail: tonis.timmusk@ttu.ee

Introduction

TCF4 (Gene 6925), alias ITF2 (immunoglobulin transcription factor 2), SEF2 (leukemia virus SL3-3 enhancer factor 2), E2-2 and ME2 (mouse E2), is one of the widely expressed class A basic helix-loop-helix (bHLH) transcription factors (TFs) that are homologous to *Drosophila melanogaster* protein daughterless (Gene 34413) [1,2]. The bHLH factor TCF4 discussed here should not be confused with the high mobility group box transcription factor 7-like 2 (TCF7L2; Gene 6934) that is a downstream effector of the β -catenin signaling pathway and is also known as TCF4 (T-cell specific factor 4).

Class A bHLH factors in mammals include TCF4, HEB (TCF12; Gene 6938) and E2A (TCF3, ITF1; Gene 6929) alternative isoforms E12 and E47 [3]. These proteins are referred to as E-proteins since they bind to Ephrussi box (E-box) sequence (CANNTG) as homodimers or as heterodimers with tissue-specific bHLH factors [3,4]. Dimerization is mediated by the C-terminal HLH motif that together with the preceding stretch of basic amino acids is required also for DNA binding. Structurally related Id proteins (inhibitors of

differentiation) hinder DNA binding of E-proteins by heterodimerization, whereas Ca^{2+} -calmodulin specifically inhibits DNA binding of E-protein homodimers [5–7]. Three amino-terminally distinct TCF4 isoforms have been described – TCF4-A, TCF4-B and TCF4-D [2]. All these isoforms contain the bHLH domain and a transcription activation domain (AD2) [8]. TCF4-B has an additional transcription activation domain in its N-terminus (AD1) [9].

In *Drosophila* the only E-protein, daughterless, is involved in sex determination and neurogenesis [10,11]. In mammals, substantial functional overlap among E-proteins has hampered deciphering their exact roles. However, it is known that TCF4 is required for postnatal survival in mice [12,13] and has many cell lineage specific functions. For instance, TCF4 regulates development of B-, T- and plasmacytoid dendritic cells [13–15], development of Sertoli cells [16] and pontine nucleus neurons [17], myogenesis [18], melanogenesis [19] and epithelial-mesenchymal transition [20]. The importance of TCF4 in human nervous system development is underscored by the association of a TCF4 allele with schizophrenia [21] and identification of *TCF4*

haploinsufficiency as the cause for Pitt-Hopkins syndrome (OMIM 610954), a rare disease featuring mental retardation, hyperventilation and seizures [22–24].

In this study we show that *TCF4* is widely, but not equally expressed and its levels are particularly high in the nervous system. We demonstrate that usage of alternative 5' exons for transcribing the human *TCF4* gene potentially yields in numerous *TCF4* protein isoforms that differ in their subcellular localization and capacity to activate transcription.

Results

TCF4 gene contains many mutually exclusive 5' exons

To describe the structure and alternative splicing of the human *TCF4* gene we performed bioinformatic analysis of mRNA and expressed sequence tag (EST) sequences available in public databases and sequences of RT-PCR products from this study. In estimation of transcription start sites we relied on publicly available data from sequencing of oligo-cap, cap-trapping and SMART cDNA libraries [25–28]. *TCF4* gene is located on chromosome 18q21.2 and spans 437 kbs. It has 41 exons of which 21 are alternative 5' exons situated at various positions throughout the gene (Figure 1). In this study *TCF4* exons are named as follows: initial 5' exons are designated with a lowercase letter preceded by a number that shows the following internal exon in the gene; internal exons are numbered from 1 to 20; exon 21 is the only terminal 3' exon. *TCF4* transcripts are named according to the initial exon they contain. Initial exons 1a and 1b are located upstream of internal exon 1. Exons 3a–3d precede and 4a–4c follow internal exon 3. 4c is a 5' extension of internal exon 4. There are three 5' exons (5a–5c) in front of exon 5; two (7a, 7b) in front of exon 7; four (8a–8d) in front of exon 8; and three (10a–10c) in front of exon 10. Generally, 5' exons are spliced together with the next internal exon in the gene, apart from the cases when the following internal exon is a cassette exon and can be skipped (exons 1 or 2, exon 3, exons 8–9; see below). As an exception 5' exon 1a is never used together with internal exons 1 or 2 and is always joined to internal exon 3 or 4. We identified several alternative splice donor sites in the 5' exons: two (I–II) in exons 5a, 8b and 8c; three (I–III) in exons 4a and 7a. In case of exon 7b the intron between 7b-I and internal exon 7 can be retained giving rise to 7b-II transcripts. Different usage of splice sites sometimes affects the coding potential of a transcript (Figure 1C). In addition, the reading frame shifts with alternative splicing of internal cassette exons 1 or 2 and exon 3. Examination of open reading frames and search for possible translation start codons demonstrated that, altogether, *TCF4* transcripts potentially code for 18 N-terminally distinct protein isoforms named TCF4-A – TCF4-R (Figures 1C and S1) of which only isoforms TCF4-A, TCF4-B and TCF4-D have been described previously as SEF2-1A or ITF2-A, SEF2-1B or ITF2-B, and SEF2-1D, respectively [2,18]. Most of the *TCF4* isoforms have a stretch of unique amino acids in their N-termini and the whole aminoterminal transactivation domain AD1 (coded by exons 3–6) is present only in isoforms with the longest N-termini such as TCF4-J, -K, -L and TCF4-B (Figures 1C and S1). Other *TCF4* isoforms contain parts of AD1 or are completely devoid of it. More precisely, isoforms TCF4-C, -E, -M, -O and -P contain a region of AD1 coded by exons 4–6, isoforms TCF4-F, -N and -R contain a region coded by exons 5–6, isoform TCF4-Q has only a short sequence coded by exon 6, and the rest of the isoforms (TCF4-D, -G, -A, -H and -I) lack AD1.

Apart from differences in the N-termini, the number of *TCF4* isoforms is increased by in-frame alternative splicing of internal exons (Figures 1C and S1). Firstly, simultaneous skipping of

internal cassette exons 8 and 9 gives rise to *TCF4* Δ isoforms, as opposed to full-length isoforms that contain the amino acids coded by exons 8–9. Secondly, at exon 18 there are two alternative splice donor sites that enable to splice in or out a 12 bps sequence encoding amino acid sequence RSRG present in + isoforms and absent in – isoforms. Thirdly, exons 8 and 15 contain two alternative splice acceptor sites that lead to optional inclusion of the first three nucleotides (CAG) of an exon in mRNA and a glutamine or alanine residue, respectively, in the corresponding position in protein sequence (Figure S1). All *TCF4* isoforms, regardless of their N-terminal or internal differences, contain transactivation domain AD2 (coded by exons 14–16) and the bHLH domain (coded by exon 19).

The overall structure of *TCF4* gene is conserved in the mouse genome. The identity between human and mouse sequences for internal exons 3–20 and 3' exon 21 is 92%. Out of the 21 *TCF4* 5' exons in human genome at least 13 are also transcribed in mouse as assessed by the presence of respective ESTs in public databases (Table S1). Sequences of most human 5' exons align to the respective region in the mouse genome with approximately 70–99% identity (Figure S2). Exons 1b, 3c, 5b and 5c are more divergent and for exons 1a, 1 and 2 no alignment between human and mouse genes was obtained. Five out of the seven non-conserved human *TCF4* exons indicated above originate from exonization of various transposable elements. Namely, exon 1a overlaps with two LTR repeats, exon 1b overlaps with DNA transposon MER5B, exon 1 consists of SINE (Alu) and LINE repeat sequences, exon 2 consists of Alu repeat sequence and exon 5c consists of SINE (MIR) element sequence. In addition, 5' exon 3a immediately follows a SINE (MIR) element in the genome (Figure S2).

In order to determine the relative abundance of mRNAs initiated at different positions within the *TCF4* gene, we carried out ribonuclease protection assays with the probe spanning internal exons 3–11 (Figure 2A). Transcripts containing different number of internal exons were detected in human cerebellum and muscle (Figure 2B). The longest protected fragment, containing exons 3–11, corresponds to transcripts initiated at 5' exons 1a, 1b and 3a–3d. The fragment comprising exons 4–11 represents the sum of transcripts containing the above mentioned 5' exons in case of exon 3 skipping and transcripts initiated at 4a–4c. The fragments comprising exons 5–11, 7–11 and 8–11 rise from transcripts initiated at 5a–5c, 7a–7b and 8a–8d, correspondingly. The fragments comprising exons 3–7, 4–7 and 5–7 represent transcripts that are initiated at the same sites as fragments 3–11, 4–11 and 5–11, respectively, but that lack the cassette exons 8–9 as a result of alternative splicing. All Δ 8–9 transcripts additionally give rise to the fragment containing exons 10–11 and this fragment also includes transcripts initiated at exons 10a–10c. Densitometric quantification of the protected fragments showed that the levels of *TCF4* transcripts spanning different number of internal exons were comparable in both human cerebellum and muscle (Figure 2C). From these data we concluded that transcription is initiated at relatively similar levels from alternative sites within the *TCF4* gene.

TCF4 mRNAs are ubiquitously but not equally expressed

We studied the usage of different 5' exons in a variety of human tissues and brain regions by reverse transcription polymerase chain reaction (RT-PCR). Our results showed that although the majority of the alternative *TCF4* transcripts were present in most tissues analyzed, there were a few that had a more limited expression pattern (Figure 3A). For instance we detected transcripts containing exon 1a only in testis, prostate and placenta. The use of 5' exons 1b, 3a and 5c was restricted to testis, prostate and trachea. Furthermore, there were several transcripts, most remarkably 8d transcripts, that

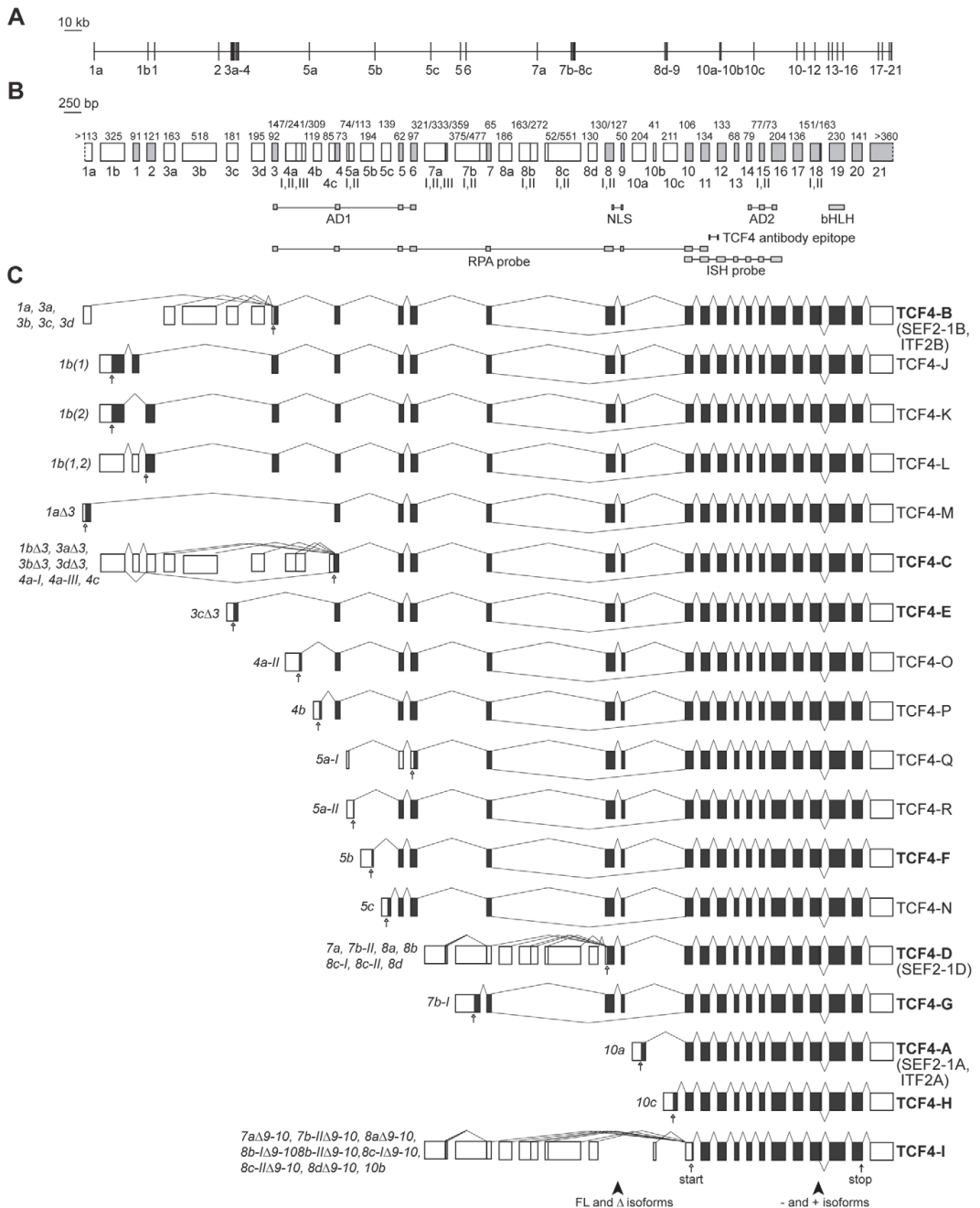


Figure 1. Structure and alternative splicing of the human *TCF4* gene. *TCF4* genomic organization with (A) introns drawn in scale or (B) exons drawn in scale. White boxes mark 5' exons and light grey boxes represent internal or 3' exons. Exon names are shown below the boxes. Roman numerals designate alternative splice donor or acceptor sites. Numbers above the exons indicate their sizes in bps. The regions encoding the respective domains of *TCF4*, the NLS identified in this study and the epitope of the used *TCF4* antibody are indicated below the gene structure. Locations of RPA and ISH riboprobes used in this study are also shown. AD, transcription activation domain; bHLH, basic helix-loop-helix domain; NLS, nuclear localization signal; RPA,

ribonuclease protection assay; ISH, *in situ* hybridization. (C) *TCF4* alternative transcripts grouped together according to the encoded TCF4 protein isoform. Translated and untranslated regions are indicated as dark grey and white boxes, respectively. Transcripts are designated with the name of the 5' exon and, if needed, with the number of the splice site used in the 5' exon. Excluded internal exons are shown with the symbol Δ and included internal exons in parentheses, if necessary. The names of the protein isoforms are shown at the right. The isoforms cloned in this study are brought in bold. The position of the first in-frame start codon for each transcript and stop codon are shown with empty and filled arrows, respectively. Arrowheads at the bottom of the panel point to the regions of alternative splicing giving rise to full-length (FL) and Δ , - and + isoforms. doi:10.1371/journal.pone.0022138.g001

featured considerably higher expression levels in the nervous system than in other tissues. RT-PCR analysis also provided information about the occurrence of alternative splicing. The skipping of exon 3 ($\Delta 3$) was a minor event in case of transcripts 1b, 3a, 3c, and 3d, whereas comparable levels of full-length and $\Delta 3$ mRNAs were present in case of transcripts 1a and 3b. Several general observations were made concerning the usage of alternative splice donor sites at 5' exons. Firstly, the prevalence of splice site utilization at exon 7a decreased in the row of II, III, I. Secondly, the levels of 7b-I transcripts were higher than those of 7b-II transcripts in most of the tissues analyzed, except in the nervous system where nearly equal levels of 7b-I and 7b-II transcripts were detected. Thirdly, 8b-I transcripts were present only in the cerebellum, whereas in all other tissues and brain regions splice donor site II of exon 8b was exclusively used. Fourthly, splice site II was predominantly used at exon 8c. The levels of 5a and 8c-I transcripts were too low for reliable

expression analysis; nevertheless, the respective PCR amplification products were consistently detected in the brain samples (data not shown). Our analysis did not reveal the usage of splice donor site II at exon 4a in any of the tissues studied.

Next, we examined in-frame alternative splicing of *TCF4* internal exons (Figure 3B). To monitor the splicing of cassette exons 8–9, we performed PCR with forward and reverse primers in exon 5 and 11, respectively. To evaluate the usage of two alternative splice donor sites at exon 18, we amplified the region spanning exons 10–20 and analyzed the PCR product by restriction with BglII, that has a unique recognition site in the 12 bp region present only in transcripts coding for the + isoforms. As shown in Figure 3B inclusion of exons 8–9 was prevalent and skipping of exons 8–9 a rare event in most tissues analyzed. Comparable amounts of full-length and $\Delta 8-9$ transcripts were present only in the *corpus callosum*. The levels of transcripts containing or lacking the extra 12 bps of exon 18 were roughly equal in most tissues analyzed (Figure 3B).

To compare *TCF4* expression levels in different human tissues more precisely, we performed quantitative PCR with three pairs of primers designed to amplify all *TCF4* transcripts (products spanning exons 10–11, 17–18 or 19–20). The obtained relative values were normalized to the expression levels of four house-keeping genes as described in Materials and Methods. We found that *TCF4* mRNA levels were considerably elevated in fetal brain and adult cerebellum – approximately 200 and 100 times above the levels measured in colon, respectively (Figure 4A). Compared to the levels in colon, about 40-fold higher levels were detected in cerebral cortex and spleen and more than 10-fold higher levels were seen in uterus, lung, thymus and placenta. The lowest quantities of *TCF4* transcripts were present in fetal liver, pancreas and colon. From these results we concluded that although the expression of *TCF4* is ubiquitous, its levels vary considerably between tissues. Particularly, we turned our attention to high expression levels of *TCF4* in the nervous system and carried out *in situ* hybridization experiments on sections from human hippocampus and cerebellum to characterize *TCF4* expression at cellular level. As shown in Figure 4B *TCF4* mRNA was detected in hippocampal neurons in dentate gyrus and CA1-CA3 regions, neurons of subiculum and parahippocampal gyrus of the cortex, and cerebellar granule neurons.

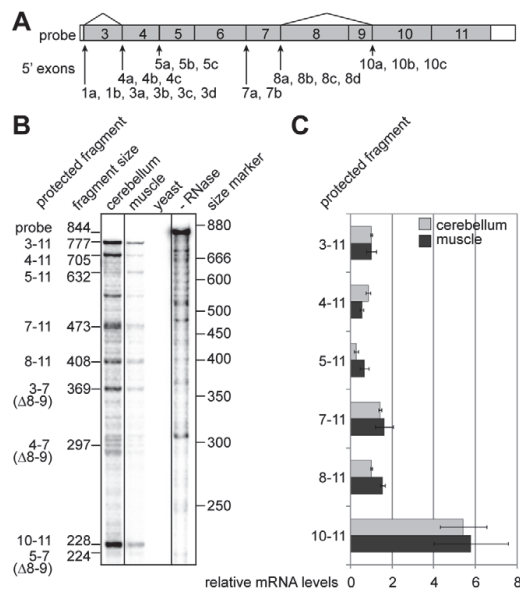


Figure 2. Initiation of transcription from alternative sites within the *TCF4* gene. (A) Schematic representation of the ribonuclease protection assay probe complementary to *TCF4* exons 3–11. Location of the *TCF4* 5' exons relative to the probe is shown with arrows and the sites of alternative splicing with lines. (B) Autoradiograph of the probe fragments protected by human cerebellum or muscle RNA and fragments obtained from control reactions with yeast RNA or without RNase treatment. The expected sizes of the protected fragments in bps and the exons they span are shown at the left and the location of the size markers at the right. (C) Densitometric quantification of the protected fragments in B from two assays. The values are given in relation to the levels of the fragment spanning exons 3–11 for both tissues. Error bars indicate standard deviations. doi:10.1371/journal.pone.0022138.g002

Several TCF4 protein isoforms are expressed in human tissues

We next asked whether and which of the different TCF4 protein isoforms are translated *in vivo*. To address this question we monitored the expression of endogenous TCF4 isoforms in different human tissue extracts by western blotting with TCF4-specific antibodies that recognize an epitope present in all described TCF4 isoforms. As shown in Figure 5A multiple TCF4 isoforms were present in human lung, liver, kidney, muscle and testis. In these tissues we detected three prominent bands that were assigned as high, medium and low molecular weight (Mw) TCF4. In case of frontal cortex, hippocampus and cerebellum low molecular weight TCF4 band was predominant and the signals of medium and high Mw TCF4 were very low. The levels of high or

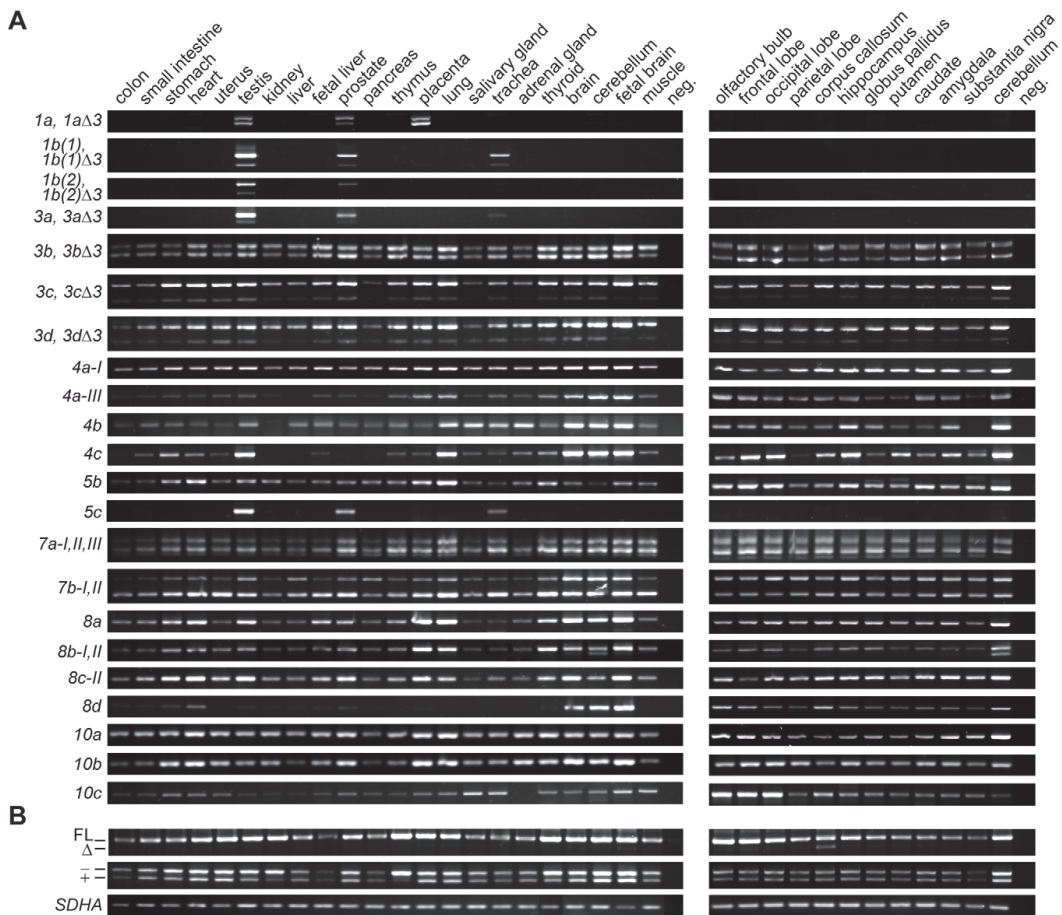


Figure 3. Expression of alternative *TCF4* mRNAs in human tissues and brain regions. (A) RT-PCR analysis of *TCF4* transcripts with different 5' exons and (B) with alternative internal splicing. Transcripts are designated as in Figure 1C. The positions of bands respective to the transcripts encoding the full-length (FL) and Δ isoforms, + and - isoforms are indicated at the left on panel B. mRNAs with longer exon 18 (+) give rise to RT-PCR product that has a unique BglII restriction site enabling discrimination from RT-PCR products amplified from mRNAs not containing the 12 bps insert (-). House-keeping gene *SDHA* mRNA expression is shown at the bottom of the panel. PCR with no template was performed as a negative control (neg) with each primer pair. doi:10.1371/journal.pone.0022138.g003

medium Mw TCF4 were elevated relative to other forms of TCF4 in testis or lung, respectively. To validate the specificity of the TCF4 antibodies, we implemented a RNAi based approach in Neuro2A mouse neuroblastoma cells. Similarly to the human tissue extracts, high, medium and low Mw bands were detected in the lysates of Neuro2A cells by western blotting with the TCF4 antibodies. Compared to mock and scrambled siRNA transfected cells the levels of all three forms were reduced in cells transfected with three different siRNAs targeting *TCF4* exon 12 or 20 that are present in all described *TCF4* transcripts (Figure 5B), thus verifying that the TCF4 antibodies used in the current study specifically recognize TCF4 proteins.

In order to define the nature of the three bands, we cloned the coding regions of isoforms TCF4-A – TCF4-I into pCDNA mammalian expression vector. In addition, we cloned variants coding for + and - isoforms, full-length and Δ isoforms. We

transfected the obtained plasmids into HEK293 cells and detected the overexpressed proteins by western blotting with TCF4-specific antibodies. The different TCF4 isoforms were expressed at variable levels (Figure 5C). The levels of isoforms TCF4-B⁺, -B⁻, -BA⁺, -BA⁻, -CA⁻, -A⁺, -A⁻, -H⁻ and -I⁻ were high, those of TCF4-C⁻ and -D⁻ medium, and those of TCF4-E⁻ and -F⁻ low. Expression of TCF4-G⁻ was not detected by western blotting. Although it was not possible to distinguish all isoforms from each other by size, we compared side by side the bands detected in human muscle and testis to different TCF4 isoforms translated *in vitro* (Figure 5D) and made the following conclusions about the nature of the three bands in human tissue extracts: the high Mw TCF4 fractionates similarly to TCF4-B and -C, the medium Mw TCF4 similarly to TCF4-D, and low Mw TCF4 to TCF4-A and TCF4-H. In addition, a few proteins with smaller molecular weight than any of the cloned TCF4 isoforms were detected in

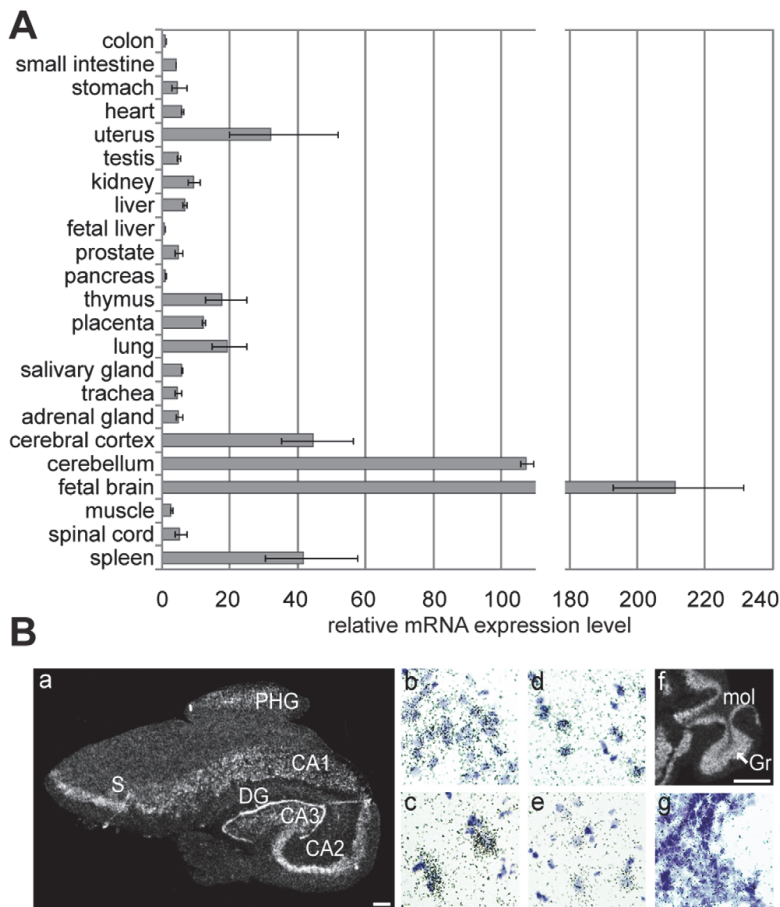


Figure 4. Inter-tissue variability of *TCF4* mRNA levels. (A) Quantitative RT-PCR analysis of *TCF4* expression in human tissues. Levels of *TCF4* transcripts were determined using three different primer pairs and the results were normalized to the expression levels of four house-keeping genes (*SDHA*, *HMBS*, *GAPDH* and *UBC*). Shown are the means relative to the *TCF4* expression level measured in colon that was arbitrarily set as 1. Error bars indicate standard deviations. (B) *In situ* hybridization analysis of *TCF4* expression in human hippocampus and cerebellum. Autoradiographs from (a) a coronal section of the hippocampus and (f) a sagittal section of the cerebellum are shown. Scale bar 1 mm. Bright-field higher magnification images of emulsion-dipped and hematoxylin-stained sections of (b) the granular cell layer of the dentate gyrus, (c) pyramidal cell layer of the CA2 region, (d) subiculum and (e) PHG region of the cortex. CA1, CA2, CA3, respective regions of the hippocampus; DG, dentate gyrus; Gr, granular cell layer of the cerebellum; mol, molecular layer of the cerebellum; PHG, parahippocampal gyrus; S, subiculum.
doi:10.1371/journal.pone.0022138.g004

several tissues (Figure 5A). These could be non-specific signals, represent *TCF4* proteolytic fragments or undescribed *TCF4* isoforms. In sum, the above described *TCF4* gene structure and expression data demonstrate that multiple *TCF4* isoforms are present in human tissues and suggest that the isoforms could potentially differ in their functional properties.

TCF4 is imported to the nucleus due to its NLS or via a piggy-back mechanism

To gain insight into possible functional variation amongst the *TCF4* isoforms we first investigated, by indirect immunofluorescence, the intracellular localization of *TCF4* isoforms overexpressed in HEK293 cells (Figure 6A). We observed two patterns of

distribution – exclusively nuclear and nuclear plus cytoplasmic. Full-length *TCF4* isoforms that have longer N-termini (*TCF4*-B⁺, -B⁻, -C⁻, -D⁻, -E⁻, -F⁻ and -G⁻) were restricted to cell nucleus whereas isoforms with shorter N-termini (*TCF4*-A⁻, -H⁻ and -I⁻) and Δ isoforms (*TCF4*-BA⁺, -BA⁻ and -CA⁻) localized to the nucleus and, in addition, to the cytoplasm.

Since all isoforms with exclusively nuclear distribution contain the amino acids coded by exons 8–9 and the isoforms with broader intracellular localization are devoid of these amino acids, we searched for possible nuclear localization signal (NLS) in this region. Using PSORT software we identified a potential bipartite NLS that contains two clusters of basic amino acids (RRR and KKVRK) separated by a linker of 11 amino acids. The two clusters are conserved in *TCF4* of *Mus musculus*, *Xenopus laevis* and

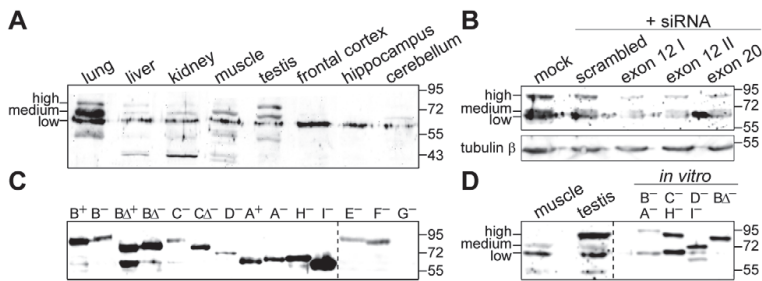


Figure 5. Expression of TCF4 protein isoforms. (A) Western blot analysis of different human tissues and brain regions with TCF4 antibodies. (B) The effect of TCF4 targeting siRNAs on the levels of proteins detected by TCF4 antibodies in extracts of Neuro2A cells. Three different siRNAs specific for TCF4 exon 12 or 20 were transfected into Neuro2A cells; mock and scrambled siRNA transfections were performed in control. Tubulin β levels were determined to demonstrate equal loading. (C) Western blot analysis of TCF4 isoforms overexpressed in HEK293 cells using TCF4 antibodies. (D) Comparison of fractionation of proteins recognized by TCF4 antibodies in human muscle and testis extracts to *in vitro* translated selected human TCF4 isoforms. The localization of endogenous TCF4 with high, medium or low molecular weight is indicated at the left in A, B and D; the dashed line in C and D separates different exposures; molecular mass (in kDa) marker bands are shown at the right on all panels.
doi:10.1371/journal.pone.0022138.g005

Danio rerio, and also in two other E-proteins E2A and HEB (Figure 6B). To validate the NLS we performed site-directed mutagenesis in the context of TCF4-B⁻ isoform and replaced the basic amino acids in cluster 1, 2 or both with alanines. As shown in Figure 6C mutagenesis of either cluster 1 (M1) or 2 (M2) produced a protein that is partly cytoplasmic, but even when both clusters were mutated (M1+2) a substantial portion of the protein remained nuclear, similarly to the genuine TCF4 isoforms not containing the region coded by exons 8–9. As a next step we fused the NLS to the C-terminus of EGFP and monitored its localization in HEK293 cells. EGFP-NLS fusion protein was confined to the nucleus whereas control EGFP was distributed diffusely all over the cell (Figure 6D). From these results we concluded that the identified NLS is functional, but additional region(s) responsible for nuclear import of isoforms lacking the amino acids coded by exons 8–9 exist in TCF4 protein.

Another region with high basic charge density is located in the DNA-binding domain of TCF4. To test whether this part of the protein is able to mediate nuclear import we constructed different fusion proteins where the entire bHLH domain or its N-terminal or C-terminal part is fused with EGFP. The fusion proteins were overexpressed in HEK293 cells and their localization was studied by direct EGFP fluorescence (Figure 6D). EGFP-bHLH was present in the nucleus and cytoplasm indicating that the bHLH domain was to some extent able to direct the protein to the nucleus, since in contrast to EGFP (29 kDa), the EGFP-bHLH (43 kDa) fusion protein cannot be transported to the nucleus by passive mechanisms due to its higher molecular mass. At the same time EGFP-bHLH-N (36 kDa) and EGFP-bHLH-C (37 kDa) were detected only in the cytoplasm, meaning that neither part alone was able to mediate nuclear import. These data led us to hypothesize that structural integrity of the bHLH domain is necessary for EGFP-bHLH nuclear localization mediated by heterodimerization with endogenous NLS bearing HLH-proteins. To test this assumption, we co-expressed EGFP and the described fusion proteins together with known TCF4 dimerization partners: E2-tagged NeuroD2 (Gene 18013), that features nuclear localization, and mCherry-fused Id2 (Gene 15902), that bears a nuclear export signal (NES) and is similarly to the described EGFP-Id2 fusion protein [29] predominantly cytoplasmic. The results of this assay showed that NeuroD2-E2 did not influence the distribution of EGFP and EGFP-bHLH-N, but was able to direct EGFP-

bHLH and to lesser extent also EGFP-bHLH-C to the nucleus. Co-expression of mCherry-Id2 altered only the localization of EGFP-bHLH by excluding it from the nucleus (Figure 6D). We additionally monitored the effects of NeuroD2-E2 and mCherry-Id2 co-expression on the localization of genuine NLS-lacking TCF4 isoform A⁻. Similarly to EGFP-bHLH, the distribution of TCF4-A⁻ was guided by its heterodimerization partner (Figure 6E). Altogether these results demonstrate that TCF4 can be directed to the nucleus by two mechanisms. Firstly, isoforms that bear the NLS independently translocate to the nucleus. Secondly, all TCF4 isoforms can be transported to the nucleus by a piggy-back mechanism through heterodimerization with NLS containing bHLH partners. Additionally, isoforms lacking NLS can be exported from the nucleus by heterodimerization with NES containing partner proteins.

Subsequently, we examined the intracellular distribution of endogenous TCF4. For this we chose to study human hippocampus and cerebellum because of high TCF4 expression levels in these brain regions. We performed immunohistochemical staining of the sections using TCF4 and neuronal marker NeuN or glial marker GFAP specific antibodies, followed by confocal microscopy. As shown in Figure 6F, TCF4 signal was found mainly in the neuronal nuclei but also in the cytoplasm of neurons in different hippocampal regions (CA, dentate gyrus, hilus) and cerebellar granular layer. Of note, the TCF4 antibody additionally marked processes of GFAP-positive cells in tissues and rat primary cultures, but to our knowledge this glial cytoplasmic signal is non-specific as no such staining was observed when tagged TCF4 isoforms were overexpressed in cultured rat glial cells and stained with tag-specific antibodies (data not shown).

TCF4 isoforms activate transcription differentially

As a next step in functional characterization of TCF4 isoforms we performed reporter assays with a construct carrying 12 μ E5 (CACCTG) E-boxes [1] in front of a minimal promoter controlling the expression of firefly luciferase gene *luc2P* (Figure 7A). The reporter construct was transfected into HEK293 cells together with expression plasmids encoding different TCF4 isoforms and a vector with the minimal promoter in front of *Renilla* luciferase *hRlucP* gene. Compared to empty vector transfected cells the normalized luciferase activity was approximately 250 or 150 times higher in cells expressing TCF4-

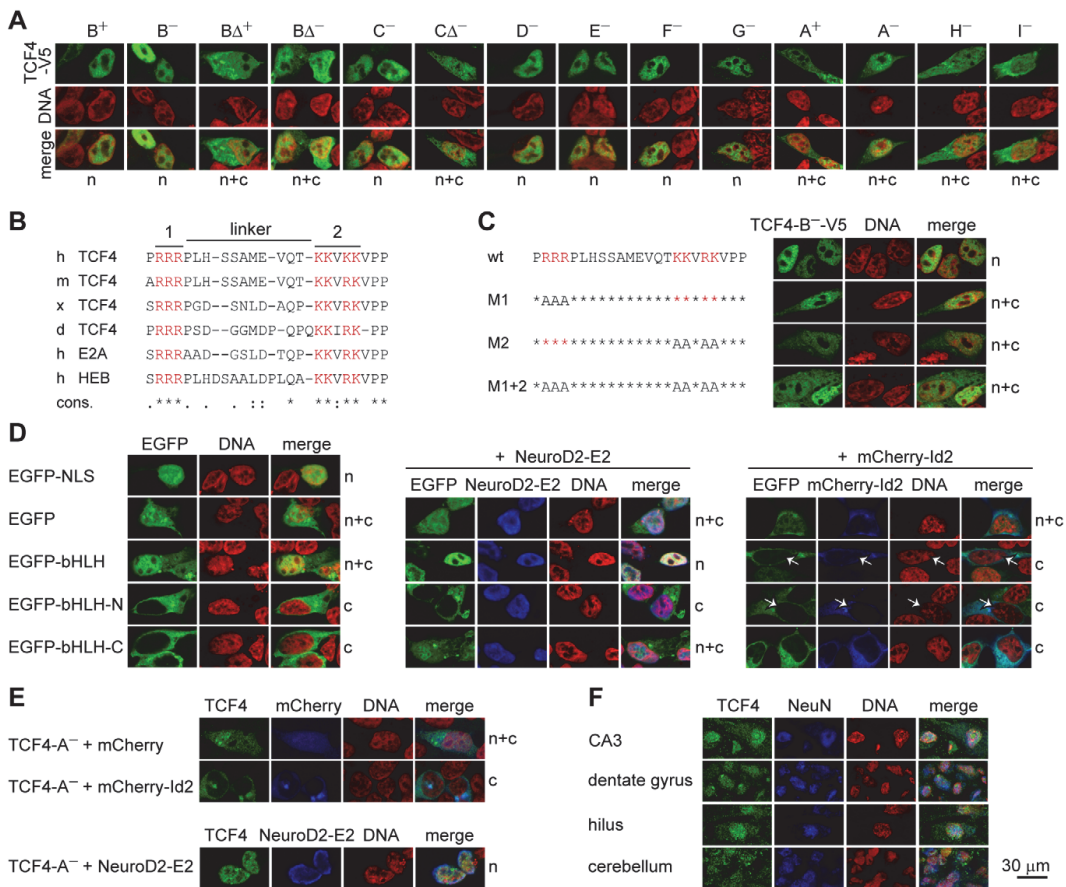


Figure 6. TCF4 intracellular localization. (A) Immunocytochemical analysis of V5-tagged TCF4 isoforms overexpressed in HEK293 cells. Isoforms analyzed are indicated at the top and localization pattern at the bottom of the panel. n, nuclear; c, cytoplasmic; n+c, nuclear and cytoplasmic. DNA was counterstained with DAPI (pseudocoloured red) to visualize nuclei. (B) Alignment of the identified bipartite NLS in TCF4 of *Homo sapiens* (h), *Mus musculus* (m), *Xenopus laevis* (x) and *Danio rerio* (d); in E2A and HEB of *Homo sapiens*. Two clusters of basic amino acids (in red, 1 and 2) and the linker are indicated with lines at the top. Conservation is indicated at the bottom. *, identity; :, conserved; ;, semi-conserved substitution. (C) The effect of site-directed mutagenesis of the NLS on the localization of TCF4 in HEK293 cells. Basic amino acids in cluster 1 (M1), 2 (M2) or both (M1+2) were replaced with alanines in the context of TCF4-B⁻ΔV5 and the localization of the proteins was monitored by immunocytochemistry. (D) Localization of EGFP fusion proteins with TCF4 NLS, bHLH, N-terminal (N) or C-terminal (C) half of TCF4 bHLH domain in HEK293 cells. NeuroD2-E2 or mCherry-Id2 encoding plasmid was cotransfected when indicated. White arrows indicate cells expressing mCherry-Id2. (E) Effect of mCherry-Id2 or NeuroD2-E2 co-expression on subcellular distribution of TCF4-A⁻. The localization patterns of overexpressed TCF4 proteins are indicated at the right of the panels in C, D and E. (F) Immunohistochemical analysis of endogenous TCF4 in human hippocampal and cerebellar sections. NeuN staining was used to identify neurons. doi:10.1371/journal.pone.0022138.g006

B⁺ or -B⁻, respectively. More than 650-fold increase was observed with TCF4-B Δ⁺ and -B Δ⁻ isoforms. TCF4-C⁻ activated reporter gene transcription over 10 and TCF4-C Δ⁻ almost 50 times. The increased luciferase activity in Δ isoforms expressing cells compared to the respective full-length isoform expressing cells could reflect higher levels of Δ isoforms in HEK293 cells (Figure 5C). The two isoforms with low expression level, TCF4-E⁻ and -F⁻, activated reporter gene transcription about 7- and 21-fold, correspondingly. Isoforms completely lacking AD1 elevated luciferase activity approximately 20 (TCF4-D⁻, -A⁺ and -A⁻) or 70 times (TCF4-H⁻ and -I⁻). Search for correlations

revealed a strong positive relationship between the presence of full-length AD1 and isoform's ability to transactivate in HEK293 cells (point biserial correlation coefficient r = 0.87, p < 0.00011). There were no significant correlations between the isoform's capacity to activate transcription and the presence of NLS, presence of only the C-terminal part of AD1 or presence of the extra four amino acids in the + isoforms. These results indicate that, although to a different extent, all TCF4 isoforms analyzed are able to activate transcription controlled by μE5 E-boxes in HEK293 cells.

To study further the individual role of TCF4 transcription activation domains AD1 and AD2, we took two approaches.

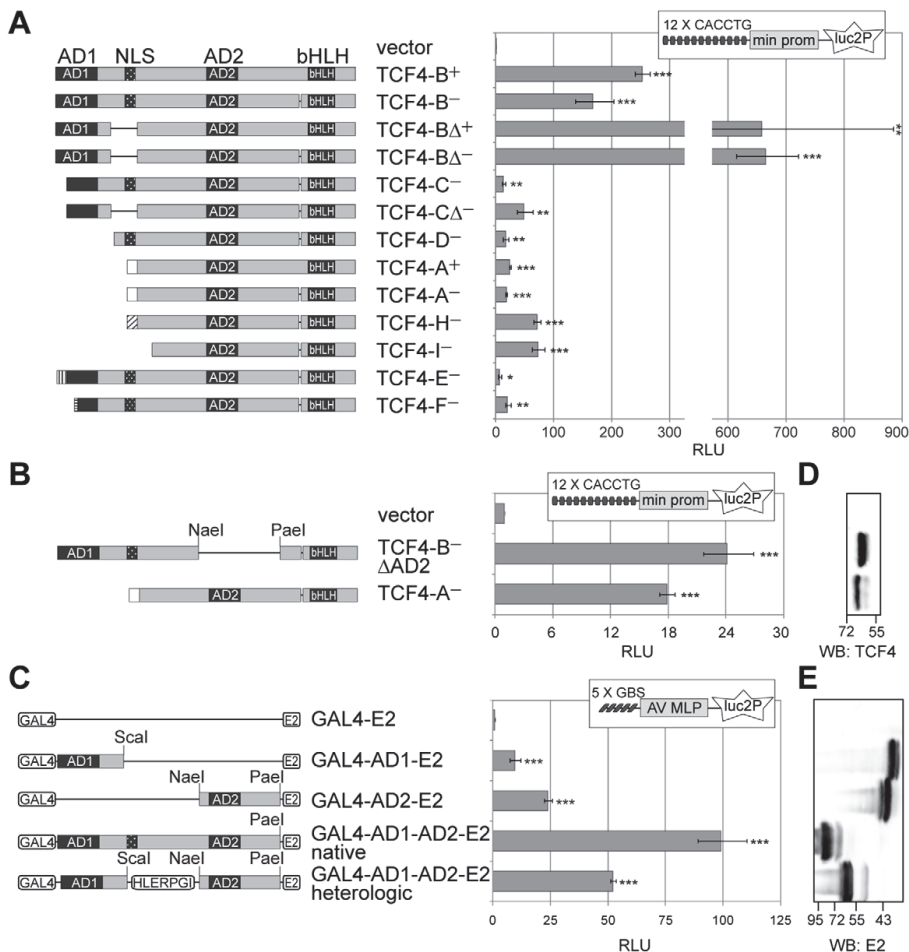


Figure 7. Transcription activation by alternative TCF4 isoforms. (A) Reporter assay with HEK293 cells transfected with firefly luciferase construct carrying 12 μ E5 E-boxes in front of a minimal (min) promoter along with the indicated TCF4 isoform encoding plasmid or an empty vector. (B) Reporter assay with HEK293 cells transfected with luciferase constructs and TCF4-B⁻ ΔAD2 or TCF4-A⁻ encoding plasmid or empty vector as indicated. (C) Reporter assay with HEK293 cells transfected with firefly luciferase construct carrying 5 GAL4 binding sites (GBS) in front of adenovirus major late promoter (AV MLP) along with the indicated E2-tagged GAL4 fusion proteins. (A, B and C) For normalization *Renilla* luciferase construct with minimal promoter was cotransfected. Luciferase activities were measured and data are presented as fold induced levels above the signals obtained from empty vector transfected cells. Shown are the mean results from at least three independent experiments performed in duplicates, error bars indicate standard deviations. Statistical significance shown with asterisks is relative to the luciferase activity measured from empty vector transfected HEK293 cells (*, p<0.05; **, p<0.01; ***, p<0.001; t-test). RLU, relative luciferase units. Schematic representation of the expressed TCF4 proteins with the locations of restriction enzymes used for the generation of the respective plasmids is shown at the left. (D) Western blot analysis of TCF4-B⁻ ΔAD2 and TCF4-A⁻ expressed in HEK293 cells. (E) Western blot analysis of E2-tagged GAL4 fusion proteins expressed in HEK293 cells. (D and E) Localization of molecular mass (in kDa) marker bands is indicated at the bottom and the order of samples is as in B and C, respectively. doi:10.1371/journal.pone.0022138.g007

Firstly, we compared the abilities of artificial TCF4-B⁻ without AD2 (ΔAD2) and native TCF4-A⁻ to regulate E-box controlled transcription. TCF4-B⁻ ΔAD2 and native TCF4-A⁻ the AD2 domain, both have the bHLH domain. Secondly, we used heterologic constructs where AD1 or AD2 is fused with GAL4 DNA binding domain and E2 epitope-tag. We assessed the ability of the GAL4 fusion proteins to activate reporter transcription from pG5luc vector that carries GAL4 binding sites in front of firefly luciferase *luc* gene. As shown in Figures 7B and

7C similar reporter gene activation levels were achieved with TCF4-B⁻ ΔAD2 compared to TCF4-A⁻, and GAL4-AD1-E2 compared to GAL4-AD2-E2 in HEK293 cells. When joined to native bHLH DNA binding domain, 24 or 18 fold upregulation of reporter gene transcription were seen with AD1 or AD2 containing proteins, respectively (Figure 7B) When fused with heterologic GAL4 DNA binding domain, AD1 activated transcription about 10 times and AD2 about 24 times (Figure 7C). We noted that when both activation domains are present in a single

protein as is the case for TCF4-B isoforms, the activation of transcription exceeds the additive effect of AD1 and AD2, suggesting that the two domains may act synergistically in HEK293 cells. To test this we studied the transactivation capacity of GAL4 fusion proteins that contain both TCF4 activation domains joined by native or heterologic amino acids. As shown in Figure 7C these proteins activated reporter transcription approximately 100 and 50 times, respectively. In both cases the activation fold exceeded the additive effect of single TCF4 activation domain containing GAL4 fusion proteins. All the compared proteins were expressed at similar levels in HEK293 cells as determined by western blotting with TCF4 or E2-specific antibodies (Figures 7D and 7E). Altogether these data show that the two activation domains are capable of mediating transactivation to a similar extent in HEK293 cells. Additionally, the results indicate that when both activation domains are present in a single protein, the two domains act synergistically in HEK293 cells.

Discussion

Large-scale human transcriptome analyses have revealed that more than 90% of protein-coding genes undergo alternative splicing and around half have two or more alternative promoters [26,30–32]. Additionally, over-representation of alternative promoters has been attributed to genes involved in development and regulation of transcription [32]. Here, we demonstrate that the human gene for the transcription factor TCF4 is transcribed using 21 mutually exclusive 5' initial exons, many of which contain more than one transcription start sites and/or splice donor sites. These 5' exons are located at various positions in the gene interspersed with internal exons 1–9, followed by constitutive internal exons 10–20 and 3' exon 21. Therefore, *TCF4* transcripts containing different number of internal exons are generated and, according to our data, these are expressed at comparable levels in human tissues and potentially encode for TCF4 protein isoforms with 18 different N-termini. We named the isoforms TCF4-A – TCF4-R in agreement with the previous studies that have described three N-terminally distinct isoforms, i.e. TCF4-A, -B and -D [2,18]. Additionally, several studies have described TCF4 isoforms differing by the presence or absence of four amino acids (RSRS) N-terminal to the bHLH domain [2,18,33,34], which are denoted here as + and – isoforms, respectively. These isoforms result from alternative splice donor site selection at exon 18 and their mRNAs are present at comparable levels in most human tissues analyzed here. We show that in human *TCF4* gene there is another site of alternative splicing at internal exons 8–9. Transcripts lacking these exons are expressed at low levels in human tissues and code for protein isoforms indicated with Δ in this study.

One by one analysis of alternative 5' exons containing *TCF4* transcripts' expression and quantitative analysis of overall *TCF4* expression in human tissues corroborated the concept of TCF4 being a ubiquitous transcription factor. Most alternative 5' exons containing transcripts were broadly expressed. Nevertheless, expression of transcripts containing 5' exons 1a, 1b, 3a and 5c was detected only in a few tissues including testis and prostate. These exons originate from exonization of different transposable elements (TEs) or are located immediately behind a TE in the human genome. Incorporation of TE-derived sequences into promoters or UTR or coding regions of genes has been documented by many studies [35–37]. In accordance with the restricted expression of TE-dependent *TCF4* transcripts, TEs are known to be transcriptionally silenced in most mammalian tissues as a defense mechanism against potentially deleterious effects of their activity [38,39]. TE-dependent *TCF4* transcripts code for 5 unique TCF4

protein isoforms with long N-termini (TCF4-J – TCF4-N). Since it was not possible to distinguish all TCF4 isoforms from each other by SDS-PAGE fractionation, we were not able to conclusively determine which protein isoforms are expressed in human tissues; nevertheless, we detected three prominent TCF4 forms of different molecular weight. Notably, high Mw TCF4 protein was relatively more abundant in testis, medium Mw TCF4 in lung and low Mw TCF4 was the major form in the brain tissue, insinuating that the ratio of different TCF4 isoforms with distinct N-termini is varied between human tissues.

Our report reveals that although broadly expressed, *TCF4* transcript levels differ greatly between tissues. The highest levels are present in fetal brain, but expression remains elevated also in adult brain where we detected *TCF4* mRNA and protein in neurons. These findings are consistent with earlier studies that have demonstrated TCF4 expression in human or rodent nervous system [18,40–44] and further support the important role for TCF4 in the development and functioning of the nervous system as exemplified by involvement of TCF4 in the pontine nucleus development in mice, association of *TCF4* with schizophrenia and identification of *TCF4* haploinsufficiency as the cause of Pitt-Hopkins mental retardation syndrome [17,21–24]. Interestingly, translocation that results in a *TCF4* allele without at least 6 upper 5' exons has been described in a patient with mild mental retardation [45]. Possibly, in this patient, initiation of *TCF4* transcription at downstream 5' exons still takes place, explaining the less severe phenotype than in classical Pitt-Hopkins syndrome patients. Nevertheless, it seems that for production of sufficient amounts of TCF4 protein and normal development, the presence of all transcription initiation sites is critical. Based on experiments with *HEB* and *E2A* knockout mice, it has been suggested that the overall E-protein dosage is more crucial in the development of nervous system than family member identity [46]. However, since even slight disturbances in *TCF4* expression in human cause a neurodevelopmental disorder and *TCF4* knockout mice display disrupted pontine nucleus development [17], it is apparent that other E-proteins are not able to compensate for the loss of TCF4 in all aspects of the nervous system development. Additionally, transgenic mice with mild overexpression of *TCF4* in forebrain display deficits in contextual and cued fear conditioning and sensorimotor gating [47], indicating that precise regulation of *TCF4* expression is crucial for correct brain function and deviations in either way result in cognitive disturbances. All this substantiates the complex structure and the high number of 5' exons in *TCF4* gene, as these probably enable proper amounts of TCF4 protein to be synthesized. It is noteworthy that according to the *TCF4* gene structure described here, the SNP rs9960767 associated with susceptibility to schizophrenia [21] is located in *TCF4* intronic sequence between 5' exons 5b and 5c. However, whether and how this marker is coupled to dysregulation of *TCF4* expression remains to be elucidated.

The variety of TCF4 isoforms raises a question – are they produced only for sufficient amount of TCF4 proteins or are the functions of different isoforms divergent? In the present study we have shown that the alternative TCF4 isoforms differ in two aspects: first, their intracellular distribution is differentially regulated depending on the presence or absence of a nuclear localization signal; second, their ability to activate E-box controlled transcription is varied depending mainly on whether they contain one or two functional transcription activation domains. We discovered in the region coded by exons 8–9, upstream of AD2, a bipartite NLS that is responsible for nuclear localization of TCF4 isoforms with longer N-termini. This NLS is conserved among E-proteins and mutating the second half of the NLS has been demonstrated to reduce nuclear import of E2A [48].

TCF4 isoforms with shorter N-termini (TCF4-A, -H and -L) and Δ isoforms do not contain the NLS. Our analysis shows that these proteins are transported to the nucleus via heterodimerization with NLS-bearing partners and directed to the cytoplasm by forming dimers with NES-containing proteins. As substantial amount of NLS-lacking TCF4 isoforms overexpressed in HEK293 cells is localized to the nuclei, there must be abundance of NLS-containing heterodimerization partners expressed endogenously. This is not surprising since TCF4 is able to form dimers with a variety of class B bHLH factors [3]. In addition, we noticed that NLS-bearing TCF4-B isoform was not able to mediate nuclear redirection of NLS-lacking TCF4-A isoform (data not shown), suggesting that TCF4 homodimers are not efficiently formed in HEK293 cells.

E-proteins function as transcription activators or repressors [49]. In our reporter assays all TCF4 isoforms were able to activate transcription from a promoter containing μ E5 E-boxes in HEK293 cells whereas TCF4-B isoforms were more potent transactivators than other isoforms. All the studied isoforms contain the AD2 domain, but only TCF4-B isoforms contain full-length AD1, including exon 3 encoded LDFS motif that is known to be required for AD1 mediated transactivation by recruiting histone acetyltransferases [50,51]. This motif is present also in some of the TE-dependent isoforms (TCF4-J, -K, and -L) that were not included in our reporter assays. We suggest that the AD1 acts synergistically with the AD2, since the additive effect of individual capacities of these domains to activate transcription is surpassed by proteins that contain both TCF4 activation domains. Similar synergism between two activation domains has been described in bHLH-zipper protein TFE3 and POU homeodomain protein Oct-2 [52,53]. In contrast to a study on *FGF-1* promoter that proposed differential roles for TCF4 + and - isoforms [33], we saw no differences between the + and - isoforms in ability to activate transcription from μ E5 E-boxes controlled promoter. However, we noticed higher reporter gene transcription in the presence of Δ isoforms than the respective full-length isoforms, probably due to higher expression levels of Δ isoforms compared to full-length isoforms. This indicates that NLS coding region absent in Δ isoforms could affect the stability of TCF4 proteins. In sum, we show that differences in the functioning of alternative TCF4 isoforms do exist. In the light of the knowledge that an isoform of HEB, homologous to TCF4-A, is specifically required for the generation of T-cell precursors *in vivo* and this function cannot be carried out by the HEB isoform homologous to TCF4-B [54], it would be of importance to study the distinct functions of TCF4 isoforms by rescue experiments with different TCF4 isoforms in *TCF4* knockout background.

Materials and Methods

Ethics statement

All experiments with human postmortem tissues were approved by the ethics committee of medical studies at National Institute for Health Development of Estonia (Permit Number: 402). The protocols involving animals were approved by the ethics committee of animal experiments at Ministry of Agriculture of Estonia (Permit Number: 45).

Bioinformatic analyses

Human *TCF4* gene structure and mRNAs were identified by analyzing genomic, mRNA and expressed sequence tag (EST) databases using tools available at <http://www.ncbi.nlm.nih.gov> and <http://genome.ucsc.edu>. The locations of transposable elements were determined by RepeatMasker track in UCSC Genome browser. Nuclear localization signal (NLS) was predicted

using software at <http://wolfsort.org>. Sequence alignments were prepared with tools available at <http://www.ebi.ac.uk/Tools>. The nucleotide sequences have been deposited in the EMBL Nucleotide Sequence Database under Accession Numbers FR748202-FR748223.

Constructs

Standard methods of recombinant DNA technology were used for generation of all constructs. Full-length coding regions of TCF4 isoforms were PCR-amplified from human brain cDNA and cloned into pcDNA3.1 (Invitrogen). Both, constructs coding for native TCF4 and C-terminally V5/His-tagged TCF4 isoforms, were created. TCF4-B⁻ amino acid sequence is used as a reference for the description of following TCF4 constructs. pEGFP-C1-C3 (Clontech) were used for generation of pEGFP-NLS, pEGFP-bHLH, pEGFP-bHLH-N and pEGFP-bHLH-C that code for EGFP fusion proteins containing TCF4 amino acids P156-P178, I541-M667, I541-K585 and E586-M667, respectively. Mutagenesis of TCF4 NLS was performed using complementary primers against the target sequence containing the respective mutation using Phusion High-Fidelity DNA Polymerase (Finnzymes). pcDNA-TCF4B⁻AD2 codes for TCF4-B⁻ without amino acids G316-M497. GAL4 DNA-binding domain was obtained from pBind vector (Promega) and inserted into pQM-CMV-E2-C vector (Icosagen). TCF4 activation domains AD1 (M1-Y148), AD2 (G316-G496), AD1-AD2 (M1-G469) and AD1 plus AD2 with heterologic linker (M1-Y148, HLERPGI, G316-G496) were cloned in-frame between GAL4 DNA-binding domain and E2-tag. Full-length coding regions of NeuroD2 and Id2 were PCR-amplified from mouse brain cDNA and inserted into pQM-CMV-E2-C (Icosagen) in front of E2 tag and pmCherry-C (Clontech) behind mCherry sequence, respectively. For E-box reporter vector pGL4.29[luc2P/12 μ E5/Hygro], the CRE binding-site in pGL4.29[luc2P/CRE/Hygro] (Promega) was replaced with 12 μ E5 E-boxes by tandem insertion of annealed oligonucleotides. For pGL4[hRlucP/min/Hygro], the 12 μ E5 E-boxes were removed from pGL4.29[luc2P/12 μ E5/Hygro] and firefly luciferase encoding *luc2P* was replaced with *Renilla* luciferase encoding *hRlucP* gene from pGL4.83[hRlucP/Puro] (Promega). For pBluescript-TCF4(3F-11R) and pSC-A-TCF4(10F-16R) used for cRNA probe synthesis, PCR amplified TCF4 cDNA fragments spanning exons 3-11 and 10-16 were ligated into EcoRV linearized pBluescriptKS+ vector or cloned into pSC-A vector (Stratagene), respectively. Sequences of all oligonucleotides used are listed in Supporting Table S2.

Ribonuclease protection assay

EcoRI linearized pBluescript-TCF4(3F-11R) was subjected to *in vitro* transcription using MAXIscript Kit and T3 polymerase (Ambion). The concentration of limiting nucleotide (UTP) was 10 μ M of which 1/6 was [α -³²P]UTP (specific activity 3000 Ci/mmol; Hartmann analytics). 10 μ g of total RNA and 2.5 \times 10⁵ CPM of radiolabeled probe were used for hybridization and the assay was performed with the RPA III Kit (Ambion) as suggested by the manufacturer. The protected fragments were separated in 5% acrylamid urea gel, visualized by autoradiography and quantified with ImageQuant T4 software (Amersham Biosciences).

RNA isolation and RT-PCR

Total RNAs from postmortem adult human brain regions and muscle were purified using RNAwiz reagent (Ambion) and treated with TURBO DNase (Ambion). Other human tissue RNAs were obtained from Clontech. First-strand cDNAs were synthesized from 5 μ g of total RNA with Superscript III reverse transcriptase

(Invitrogen) with oligo(dT) primers according to manufacturer's recommendations. PCR amplification was performed using HotFire polymerase (Solis Biodyne). For quantitative PCR, LightCycler 2.0 engine (Roche), qPCR Core kit for SYBR R Green I No ROX (Eurogentec) and polycarbonate qPCR capillaries (Bioron) were used. The reactions were carried out in a volume of 10 μ l containing 1/80 of reverse transcription reaction as a template. In control, PCR with primers specific for the ubiquitously expressed hypoxanthine-guanine phosphoribosyltransferase (HPRT), succinate dehydrogenase complex subunit A (SDHA), ubiquitin C (UBC), hydroxymethylbilane synthase (HMBS) and glyceraldehyde-3-phosphate dehydrogenase (GAPDH) were performed. For normalization of quantitative PCR data the geometric mean of four selected housekeeping genes (SDHA, UBC, HMBS and GAPDH) with high expression stability ($M < 1.5$) was calculated using geNorm software [55]. For quantification of *TCF4* mRNA expression, three different primer pairs detecting all *TCF4* transcripts were designed (products spanning exons 10–11, 17–18 and 19–20). The results obtained with each primer pair were normalized with the geNorm calculated factor, log-transformed and standardized as described [56]. Means and standard deviations (SD) were calculated and the data were back-transformed to the original scale for graphical representation. The bars represent geometric means and error bars represent upper and lower limits back-transformed as mean+SD and mean-SD, respectively. All products from the RT-PCR reactions were verified by sequencing. The primers together with the used annealing temperatures, cycle numbers and product sizes are listed in Supporting Table S2. When indicated PCR amplified DNA was diluted three times and subjected to restriction with BglII (Fermentas).

In situ hybridization

cRNA probes were synthesized from BamHI linearized pSC-A-TCF4(10F-16R) with MAXIScript *in vitro* Transcription Kit and T3 polymerase (Ambion), using [α -³⁵S]UTP (Amersham Biosciences) for labeling. Serial coronal sections (16 μ m) from fresh-frozen adult male human hippocampus and cerebellum were subjected to *in situ* hybridization following the protocol described earlier [57]. Emulsion-dipped sections were developed after 3 weeks using D-19 developer (Eastman Kodak), fixed (sodium fixer; Kodak), and counterstained with hematoxylin (Shandon).

Cell culture and transfection

Human embryonic kidney HEK293 cells and mouse neuroblastoma Neuro2A cells were grown in MEM (Minimum Essential Medium Eagle; PAA) or DMEM (Dulbecco's modified Eagle's medium; PAA), respectively, supplemented with 10% fetal bovine serum (PAA), 100 U/ml penicillin (PAA) and 0.1 mg/ml streptomycin (PAA) at 37°C in 5% CO₂. For transfection of DNA constructs 0.375 μ g DNA and 0.75 μ l of LipoD293 reagent (SigmaGen) were used per well of a 48-well plate or scaled up accordingly. In case of cotransfections, equal amounts of all plasmids were used. For transfection of siRNAs 24 pmol siRNA and 4 μ l of Lipofectamine RNAiMAX (Invitrogen) were used per well of a 6-well plate. siRNAs were ordered from Ambion and their sequences are brought in Supporting Table S2.

Protein extracts and Western blotting

In vitro translation was performed using ThT Quick Coupled Transcription/Translation System (Promega) according to manufacturer's instructions. Cell and tissue extracts were prepared in RIPA buffer (50 mM Tris HCl pH 8.0, 150 mM NaCl, 1% NP-40, 0.5% Na-DOC, 0.1% SDS, 1 mM DTT, 1 mM PMSF, protease inhibitors cocktail Complete (Roche)). Protein concentrations were determined using BCA assay (Pierce). Equal amounts

of proteins were separated in 8% SDS-PAGE and transferred to PVDF membrane (Biorad). For western blotting the antibodies were diluted in 2% skim milk and 0.1% Tween 20 in PBS as following: rabbit polyclone anti TCF4/ITF2 (CeMines) 1:1000, mouse monoclonal anti E2 (Icosagen; 5E11) 1:5000, mouse monoclonal anti tubulin β (Developmental Studies Hybridoma Bank) 20 ng/ml, HRP-conjugated goat anti mouse/rabbit IgG (Pierce) 1:5000. Chemiluminescent signal was detected using SuperSignal West Femto Chemiluminescent Substrate (Pierce).

Cyto- and histochemical immunostaining

For cytochemistry, cells were grown on poly-L-lysine (Sigma) coated coverslips and fixed with 4% paraformaldehyde for 15 minutes, treated with 50 mM NH₄Cl in PBS for 10 minutes and permeabilized in 0.5% Triton X-100 in PBS for 15 minutes. Cells were blocked with 2% bovine serum albumin (BSA) in PBS. The reactions with primary and secondary antibodies were carried out in 0.2% BSA and 0.1% Tween 20 in PBS at room temperature. For histochemistry, 16 μ m coronal sections from fresh-frozen adult male human hippocampus and cerebellum were fixed with 4% paraformaldehyde for 30 minutes and blocked in 0.25% Triton X-100, 0.5% Tween 20, 3% goat serum in PBS. Primary antibody reactions were carried out in blocking buffer overnight at 4°C. The antibodies were diluted as following: rabbit polyclone anti TCF4/ITF2 (CeMines) 1:200, mouse monoclonal anti V5 (Invitrogen) 1:500, mouse monoclonal anti E2 (Icosagen, 5E11) 1:500, mouse monoclonal anti NeuN 1:100 (Chemicon), mouse monoclonal anti GFAP 1:800 (Chemicon), Alexa 488 or Alexa 568 conjugated goat anti mouse/rabbit IgG (Molecular Probes) 1:2000. The samples were mounted in ProLong Gold antifade reagent with DAPI (Molecular Probes) and analyzed by confocal microscopy (LSM Duo, Zeiss).

Luciferase assays

Cells on 48-well plates were lysed 24 hours post-transfection in 50 μ l Passive Lysis Buffer (Promega). Dual-Glo Luciferase assay (Promega) was performed following manufacturer's instructions and luminescence was measured with GENios pro (Tecan) plate reader. For data analysis background signals from untransfected cells were subtracted and firefly luciferase signal values were normalized to *Renilla* luciferase signals. The obtained data were log-transformed, autoscaled, means and standard deviations (SD) were calculated and t-tests for analyses of statistical significance were performed. For graphical representation, the data were back-transformed to the original scale. Error bars represent upper and lower limits back-transformed as mean+SD and mean-SD, respectively. Correlation analysis was performed with tools at <http://faculty.vassar.edu/lowry/pbcorr.html>.

Supporting Information

Figure S1 Alignment of TCF4 isoforms. Amino acids different from the consensus are in blue. Localization of functional domains is indicated with lines above the sequence. Amino acid(s) in parentheses are absent from (1) isoforms coded by transcripts spliced at acceptor II of exon 8, (2) Δ isoforms coded by transcripts without exons 8–9, (3) isoforms coded by transcripts spliced at acceptor II of exon 15, (4) – isoforms (as opposed to + isoforms) coded by transcripts spliced at donor I of exon 18. AD, activation domain; NLS, nuclear localization signal; bHLH, basic helix-loop-helix domain. (PDF)

Figure S2 Multiple alignment of *Homo sapiens* (h) genomic DNA regions containing *TCF4* 5' exons and internal exons 1–2 with the respective regions in *Pan troglodytes* (c), *Mus musculus* (m), *Rattus*

norvegicus (r) and/or *Macaca mulatta* genomes (rh). The exons' names are given above each aligned region. The nucleotides in the aligned regions are numbered according to human genome assembly March 2006 NCBI36/hg18, chimp genome assembly March 2006 CGSC 2.1/panTro2, mouse genome assembly July 2007 NCBI37/mm9, rat genome assembly November 2004 Baylor 3.4/rn4 and rhesus genome assembly January 2006 MGSC merged 1.0/rheMac2. Alignments were produced with ClustalW and the percentages of identity were calculated between human TCF4 5' exon sequence and the respective mouse sequence using Needleman-Wunsch global alignment. The exon sequences are in bold case, internal exons are in blue and sequences of primers used for expression analysis are underlined. Dotted blue lines above the sequences indicate transposable elements. Arabic numerals above exonic sequences indicate the number of human ESTs starting at the respective position and obtained from oligo-cap, cap-trapping and SMART libraries available in public databases through UCSC genome browser as of 3rd of November 2010. Possible in-frame translation start codons are shaded in gray. For each in-frame ATG codon NetStart translation start score is shown above the start codon. When needed the locations of alternative splice donor sites are indicated

References

- Henthorn P, Kiledjian M, Kadesch T (1990) Two distinct transcription factors that bind the immunoglobulin enhancer microE5/kappa 2 motif. *Science* 247: 467–470.
- Cornelissen B, Thornell A, Hallberg B, Grundstrom T (1991) Helix-loop-helix transcriptional activators bind to a sequence in glucocorticoid response elements of retrovirus enhancers. *J Virol* 65: 6084–6093.
- Massari ME, Murre C (2000) Helix-loop-helix proteins: regulators of transcription in eucaryotic organisms. *Mol Cell Biol* 20: 429–440.
- Ephrussi A, Church GM, Tonegawa S, Gilbert W (1985) B lineage-specific interactions of an immunoglobulin enhancer with cellular factors in vivo. *Science* 227: 134–140.
- Benezra R, Davis RL, Lockshon D, Turner DL, Weintraub H (1990) The protein Id: a negative regulator of helix-loop-helix DNA binding proteins. *Cell* 61: 49–59.
- Saarikettu J, Sveshnikova N, Grundstrom T (2004) Calcium/calmodulin inhibition of transcriptional activity of E-proteins by prevention of their binding to DNA. *J Biol Chem* 279: 41004–41011.
- Hauser J, Sveshnikova N, Wallenius A, Baradaran S, Saarikettu J, et al. (2008) B-cell receptor activation inhibits AID expression through calmodulin inhibition of E-proteins. *Proc Natl Acad Sci U S A* 105: 1267–1272.
- Quong MW, Massari ME, Zwart R, Murre C (1993) A new transcriptional-activation motif restricted to a class of helix-loop-helix proteins is functionally conserved in both yeast and mammalian cells. *Mol Cell Biol* 13: 792–800.
- Massari ME, Jennings PA, Murre C (1996) The AD1 transactivation domain of E2A contains a highly conserved helix which is required for its activity in both *Saccharomyces cerevisiae* and mammalian cells. *Mol Cell Biol* 16: 121–129.
- Cronmiller C, Cline TW (1986) The relationship of relative gene dose to the complex phenotype of the daughterless locus in *Drosophila*. *Dev Genet* 7: 205–221.
- Caudy M, Grell EH, Dambly-Chaudiere C, Ghysen A, Jan LY, et al. (1988) The maternal sex determination gene *daughterless* has zygotic activity necessary for the formation of peripheral neurons in *Drosophila*. *Genes Dev* 2: 843–852.
- Zhuang Y, Cheng P, Weintraub H (1996) B-lymphocyte development is regulated by the combined dosage of three basic helix-loop-helix genes, E2A, E2-2, and HEB. *Mol Cell Biol* 16: 2898–2905.
- Bergqvist I, Eriksson M, Saarikettu J, Eriksson B, Cornelissen B, et al. (2000) The basic helix-loop-helix transcription factor E2-2 is involved in T lymphocyte development. *Eur J Immunol* 30: 2857–2863.
- Cisse B, Caton ML, Lehner M, Maeda T, Scheu S, et al. (2008) Transcription factor E2-2 is an essential and specific regulator of plasmacytoid dendritic cell development. *Cell* 135: 37–48.
- Nagasawa M, Schmidlin H, Hazekamp MG, Schotte R, Blom B (2008) Development of human plasmacytoid dendritic cells depends on the combined action of the basic helix-loop-helix factor E2-2 and the Ets factor Spi-B. *Eur J Immunol* 38: 2389–2400.
- Muir T, Sadler-Riggelman I, Stevens JD, Skinner MK (2006) Role of the basic helix-loop-helix protein ITF2 in the hormonal regulation of Sertoli cell differentiation. *Mol Reprod Dev* 73: 491–500.
- Flora A, Garcia JJ, Thaller C, Zoghbi HY (2007) The E-protein Tcf4 interacts with Math1 to regulate differentiation of a specific subset of neuronal progenitors. *Proc Natl Acad Sci U S A* 104: 15382–15387.
- Skerjanc IS, Truong J, Filion P, McBurney MW (1996) A splice variant of the ITF-2 transcript encodes a transcription factor that inhibits MyoD activity. *J Biol Chem* 271: 3555–3561.
- Furumura M, Potterf SB, Toyofuku K, Matsunaga J, Muller J, et al. (2001) Involvement of ITF2 in the transcriptional regulation of melanogenic genes. *J Biol Chem* 276: 28147–28154.
- Sobrado VR, Moreno-Bueno G, Cubillo E, Holt IJ, Nieto MA, et al. (2009) The class I bHLH factors E2-2A and E2-2B regulate EMT. *J Cell Sci* 122: 1014–1024.
- Stefansson H, Ophoff RA, Steinberg S, Andreassen OA, Cichon S, et al. (2009) Common variants conferring risk of schizophrenia. *Nature* 460: 744–747.
- Zweier C, Peippo MM, Hoyer J, Sousa S, Bottani A, et al. (2007) Haploinsufficiency of TCF4 causes syndromal mental retardation with intermittent hyperventilation (Pitt-Hopkins syndrome). *Am J Hum Genet* 80: 994–1001.
- Brockschmidt A, Todt U, Ryu S, Hoischen A, Landwehr C, et al. (2007) Severe mental retardation with breathing abnormalities (Pitt-Hopkins syndrome) is caused by haploinsufficiency of the neuronal bHLH transcription factor TCF4. *Hum Mol Genet* 16: 1488–1494.
- Amiel J, Rio M, de Pontual L, Redon R, Malan V, et al. (2007) Mutations in TCF4, encoding a class I basic helix-loop-helix transcription factor, are responsible for Pitt-Hopkins syndrome, a severe epileptic encephalopathy associated with autonomic dysfunction. *Am J Hum Genet* 80: 988–993.
- Maruyama K, Sugano S (1994) Oligo-capping: a simple method to replace the cap structure of eukaryotic mRNAs with oligoribonucleotides. *Gene* 138: 171–174.
- Kimura K, Wakamatsu A, Suzuki Y, Ota T, Nishikawa T, et al. (2006) Diversification of transcriptional modulation: large-scale identification and characterization of putative alternative promoters of human genes. *Genome Res* 16: 55–65.
- Carninci P, Sandelin A, Lenhard B, Katayama S, Shimokawa K, et al. (2006) Genome-wide analysis of mammalian promoter architecture and evolution. *Nat Genet* 38: 626–635.
- Zhu YY, Machleder EM, Chenchik A, Li R, Siebert PD (2001) Reverse transcriptase template switching: a SMART approach for full-length cDNA library construction. *Biotechniques* 30: 892–897.
- Kurooka H, Yokota Y (2005) Nucleo-cytoplasmic shuttling of Id2, a negative regulator of basic helix-loop-helix transcription factors. *J Biol Chem* 280: 4313–4320.
- Gustincich S, Sandelin A, Plessy C, Katayama S, Simone R, et al. (2006) The complexity of the mammalian transcriptome. *J Physiol* 575: 321–332.
- Wang ET, Sandberg R, Luo S, Khrebukova I, Zhang L, et al. (2008) Alternative isoform regulation in human tissue transcriptomes. *Nature* 456: 470–476.
- Back D, Davis C, Ewing B, Gordon D, Green P (2007) Characterization and predictive discovery of evolutionarily conserved mammalian alternative promoters. *Genome Res* 17: 145–155.
- Liu Y, Ray SK, Yang XQ, Luntz-Leyman V, Chiu IM (1998) A splice variant of E2-2 basic helix-loop-helix protein represses the brain-specific fibroblast growth factor 1 promoter through the binding to an imperfect E-box. *J Biol Chem* 273: 19269–19276.

34. Yoon SO, Chikaraishi DM (1994) Isolation of two E-box binding factors that interact with the rat tyrosine hydroxylase enhancer. *J Biol Chem* 269: 18453–18462.
35. Wu M, Li L, Sun Z (2007) Transposable element fragments in protein-coding regions and their contributions to human functional proteins. *Gene* 401: 165–171.
36. Jordan IK, Rogozin IB, Glazko GV, Koonin EV (2003) Origin of a substantial fraction of human regulatory sequences from transposable elements. *Trends Genet* 19: 68–72.
37. van de Lagemaat LN, Landry JR, Mager DL, Medstrand P (2003) Transposable elements in mammals promote regulatory variation and diversification of genes with specialized functions. *Trends Genet* 19: 530–536.
38. Yoder JA, Walsh CP, Bestor TH (1997) Cytosine methylation and the ecology of intragenomic parasites. *Trends Genet* 13: 335–340.
39. Zamudio N, Bourc'his D (2005) Transposable elements in the mammalian germline: a comfortable niche or a deadly trap? *Heredity* 105: 92–104.
40. Pscherer A, Dorflinger U, Kirfel J, Gawlas K, Ruschoff J, et al. (1996) The helix-loop-helix transcription factor SEF-2 regulates the activity of a novel initiator element in the promoter of the human somatostatin receptor II gene. *Embo J* 15: 6680–6690.
41. Uittenbogaard M, Chiaramello A (2000) Differential expression patterns of the basic helix-loop-helix transcription factors during aging of the murine brain. *Neurosci Lett* 280: 95–98.
42. Soosaar A, Chiaramello A, Zuber MX, Neuman T (1994) Expression of basic-helix-loop-helix transcription factor ME2 during brain development and in the regions of neuronal plasticity in the adult brain. *Brain Res Mol Brain Res* 25: 176–180.
43. Chiaramello A, Soosaar A, Neuman T, Zuber MX (1995) Differential expression and distinct DNA-binding specificity of ME1a and ME2 suggest a unique role during differentiation and neuronal plasticity. *Brain Res Mol Brain Res* 29: 107–118.
44. de Pontual L, Mathieu Y, Golzio C, Rio M, Malan V, et al. (2009) Mutational, functional, and expression studies of the TCF4 gene in Pitt-Hopkins syndrome. *Hum Mutat* 30: 669–676.
45. Kalscheuer VM, Feenstra I, Van Ravenswaaij-Arts CM, Smeets DF, Menzel C, et al. (2008) Disruption of the TCF4 gene in a girl with mental retardation but without the classical Pitt-Hopkins syndrome. *Am J Med Genet A* 146A: 2053–2059.
46. Ravanpay AC, Olson JM (2008) E protein dosage influences brain development more than family member identity. *J Neurosci Res* 86: 1472–1481.
47. Brzozka MM, Radyushkin K, Wichert SP, Ehrenreich H, Rossner MJ (2010) Cognitive and sensorimotor gating impairments in transgenic mice overexpressing the schizophrenia susceptibility gene Tcf4 in the brain. *Biol Psychiatry* 68: 33–40.
48. Lingbeck JM, Trausch-Azar JS, Ciechanover A, Schwartz AL (2005) E12 and E47 modulate cellular localization and proteasome-mediated degradation of MyoD and Id1. *Oncogene* 24: 6376–6384.
49. Murre C (2005) Helix-loop-helix proteins and lymphocyte development. *Nat Immunol* 6: 1079–1086.
50. Qiu Y, Sharma A, Stein R (1998) p300 mediates transcriptional stimulation by the basic helix-loop-helix activators of the insulin gene. *Mol Cell Biol* 18: 2957–2964.
51. Massari ME, Grant PA, Pray-Grant MG, Berger SL, Workman JL, et al. (1999) A conserved motif present in a class of helix-loop-helix proteins activates transcription by direct recruitment of the SAGA complex. *Mol Cell* 4: 63–73.
52. Artandi SE, Merrell K, Avitahl N, Wong KK, Calame K (1995) TFE3 contains two activation domains, one acidic and the other proline-rich, that synergistically activate transcription. *Nucleic Acids Res* 23: 3865–3871.
53. Tanaka M, Clouston WM, Herr W (1994) The Oct-2 glutamine-rich and proline-rich activation domains can synergize with each other or duplicates of themselves to activate transcription. *Mol Cell Biol* 14: 6046–6055.
54. Wang D, Claus CL, Vaccarelli G, Braunstein M, Schmitt TM, et al. (2006) The basic helix-loop-helix transcription factor HEBAlt is expressed in pro-T cells and enhances the generation of T cell precursors. *J Immunol* 177: 109–119.
55. Vandesompele J, De Preter K, Pattyn F, Poppe B, Van Roy N, et al. (2002) Accurate normalization of real-time quantitative RT-PCR data by geometric averaging of multiple internal control genes. *Genome Biol* 3: research0034.0031–research0034.0011.
56. Willems E, Leyns L, Vandesompele J (2008) Standardization of real-time PCR gene expression data from independent biological replicates. *Anal Biochem* 379: 127–129.
57. Timmusk T, Palm K, Metsis M, Reintam T, Paalme V, et al. (1993) Multiple promoters direct tissue-specific expression of the rat BDNF gene. *Neuron* 10: 475–489.

Appendix 2

Publication II

Kaja Kannike, Mari Sepp, Chiara Zuccato, Elena Cattaneo, and Tõnis Timmusk (2014). Forkhead Transcription Factor FOXO3a Levels Are Increased in Huntington Disease Because of Overactivated Positive Autofeedback Loop. *J. Biol. Chem.* 289: 32845–32857. doi: 10.1074/jbc.M114.612424.

Forkhead Transcription Factor FOXO3a Levels Are Increased in Huntington Disease Because of Overactivated Positive Autoregulation Loop*

Received for publication, September 18, 2014, and in revised form, September 30, 2014. Published, JBC Papers in Press, September 30, 2014, DOI:10.1074/jbc.M114.612424

Kaja Kannike[‡], Mari Sepp[‡], Chiara Zuccato[§], Elena Cattaneo[§], and Tõnis Timmusk^{‡1}

From the [‡]Department of Gene Technology, Tallinn University of Technology, Tallinn 12618, Estonia and the [§]Department of Pharmacological Sciences and Center for Stem Cell Research, University of Milan, Milano 20133, Italy

Background: Forkhead box O (FOXO) transcription factors, integrators of stress and survival signals, have been implicated in neurodegenerative diseases including Huntington disease (HD).

Results: FOXO3a regulates its own transcription and its levels are increased in HD.

Conclusion: Positive autoregulation loop contributes to elevated FOXO3a activity in HD.

Significance: Autoregulation of FOXO3a adds complexity to transcription dysregulation in HD.

Huntington disease (HD) is a fatal autosomal dominant neurodegenerative disorder caused by an increased number of CAG repeats in the *HTT* gene coding for huntingtin. Decreased neurotrophic support and increased mitochondrial and excitotoxic stress have been reported in HD striatal and cortical neurons. The members of the class O forkhead (FOXO) transcription factor family, including FOXO3a, act as sensor proteins that are activated upon decreased survival signals and/or increased cellular stress. Using immunocytochemical screening in mouse striatal Hdh^{7/7} (wild type), Hdh^{7/109} (heterozygous for HD mutation), and Hdh^{109/109} (homozygous for HD mutation) cells, we identified FOXO3a as a differentially regulated transcription factor in HD. We report increased nuclear FOXO3a levels in mutant Hdh cells. Additionally, we show that treatment with mitochondrial toxin 3-nitropropionic acid results in enhanced nuclear localization of FOXO3a in wild type Hdh^{7/7} cells and in rat primary cortical neurons. Furthermore, mRNA levels of *Foxo3a* are increased in mutant Hdh cells compared with wild type cells and in 3-nitropropionic acid-treated primary neurons compared with untreated neurons. A similar increase was observed in the cortex of R6/2 mice and HD patient post-mortem caudate tissue compared with controls. Using chromatin immunoprecipitation and reporter assays, we demonstrate that FOXO3a regulates its own transcription by binding to the conserved response element in *Foxo3a* promoter. Altogether, the findings of this study suggest that FOXO3a levels are increased in HD cells as a result of overactive positive feedback loop.

tive decline. Genetically, HD is an autosomal dominant disease caused by a CAG repeat expansion in the *HTT* (*huntingtin*) gene, which translates into a polyglutamine tract in HTT protein (1). Neuropathologically, HD is characterized by loss of medium sized spiny neurons in the striatum and pyramidal neurons in the cerebral cortex (2). Several pathogenic mechanisms have been described that mediate neuronal dysfunction and death; these mechanisms include transcriptional dysregulation, loss of neurotrophic support, mitochondrial impairment, cellular stress, and excitotoxicity (3, 4). A number of transcriptional pathways are disrupted in HD including decreased expression of genes involved in growth factor, neurotransmitter and calcium signaling, and up-regulation of some genes associated with cellular stress (5). Notably, reduced brain-derived neurotrophic factor (BDNF) expression and its delivery to striatal targets in addition to decreased levels of TrkB receptors have been described in HD (6–9). Mitochondrial dysfunction hypothesis is supported by the fact that 3-nitropropionic acid (3-NP), an irreversible inhibitor of mitochondrial complex II, induces striatal degeneration similar to HD in rodents and primates (10–12). Additionally, mutant huntingtin disrupts mitochondrial Ca²⁺ homeostasis, promotes formation of reactive oxygen species, and sensitizes cells to excitotoxic stimuli and apoptosis (13–15). The relative importance of different disease mechanisms is unclear, but overall imbalance between activation of prosurvival and apoptotic pathways has been suggested.

Forkhead box O (FOXO) family proteins FOXO1, FOXO3a, FOXO4, and FOXO6 act as cellular sensors of stress and survival signals. They regulate transcriptional programs that affect differentiation, survival, longevity, cell cycle, metabolism, stress resistance, autophagy, and tumor suppression (16). The activity of FOXO proteins is precisely controlled by post-translational modifications, mainly phosphorylation, acetylation, ubiquitylation, and methylation (17–19). Growth factor-induced phosphorylation of FOXOs by AKT/PKB (protein kinase b) leads to inactivation and redistribution of FOXOs from nucleus to cyto-

Huntington disease (HD)² is a neurodegenerative disorder that manifests in chorea, psychiatric disturbances, and cogni-

* This work was supported by Wellcome Trust Grant 067952, Estonian Ministry of Education and Research Targeted Funding Grant 0140143 and Institutional Research Funding Grant IUT19-18, Estonian Science Foundation Grants 7257 and 8844, and funds from the Estonian Academy of Sciences.

✂ Author's Choice—Final version full access.

¹ To whom correspondence should be addressed: Akadeemia tee 15, 12618 Tallinn, Estonia. Tel.: 3726204444; Fax: 3726204401; E-mail: tonis.timmusk@ttu.ee.

² The abbreviations used are: HD, Huntington disease; 3-NP, 3-nitropropionic acid; BDNF, brain-derived neurotrophic factor; qPCR, quantitative PCR;

This is an Open Access article under the CC BY license.

HDAC, histone deacetylase; FHRE, Forkhead response elements; AcH, acetyl histone; URR, unrelated untranscribed region; TM, triple mutant; AMPK, AMP-activated protein kinase.

Increased FOXO3a Activity in Huntington Disease

sol, a mechanism mediating also the neuroprotective signaling of BDNF (20–23). Another pathway activated by BDNF is Ras/MAPK/ERK1/2, which results in phosphorylation of FOXO3a and directs it to proteasomal degradation (24). FOXO mRNAs are widely expressed at varying levels in mammalian tissues; compared with *Foxo1* and *Foxo4*, *Foxo3a* displays the highest expression in the brain (25, 26).

Here we screened for transcription factors dysregulated in HD, using a panel of over 200 antibodies. One of the transcription factors identified was FOXO3a. We examined localization, expression, and regulation of FOXO3a using different HD models: striatal cell lines from mutant *Htt* knock-in mice, 3-NP-treated rat primary cortical neurons, and R6/2 transgenic mice. Additionally, we analyzed mRNA levels of *FOXO3a* in post-mortem caudate and cerebral cortex of HD patients. Our results suggest that activity of FOXO3a is increased in HD models and in HD patients through mechanisms involving positive autoregulation.

MATERIALS AND METHODS

Human Samples—Post-mortem human brain tissues were obtained from the Harvard Brain Tissue Resource Center. Cortex tissues were from controls 5074, 5936, 5959, 08704, and 13574 and from HD patients 5570, 6121, 0497, 0950, and 18590. Caudate nucleus tissues were from controls 5936, 5959, and 6142 and from HD patients 5507, 6010, and 6183. Distribution by disease grade is as follows: HD grade 2: 6051 and 6121; HD grade 3: 0950, 5570, 6010, 6183, and 18590; and HD grade 4: 0497 and 5507. All diagnoses were based on clinical assessment and histopathological evaluation by experienced neuropathologists according to Vonsattel classification. The use of these tissues has been approved by the Università degli Studi Milano ethical board following the guidelines of the Declaration of Helsinki.

Animal Procedures—All animal procedures were performed in compliance with the local ethics committee. The R6/2 and control mice were housed using a normal light/dark cycle. After overnight starvation, the 6-week-old animals were sacrificed and dissected to separate the different neuronal areas. Sprague-Dawley rats were mated, and females were sacrificed in a CO₂ chamber on day 23 of gestation for isolation of the fetuses.

Constructs—pFLAG-FOXO3A-WT (Addgene plasmid no. 8360) and pFLAG-FOXO3A-TM (Addgene plasmid no. 8361) have been described previously (27). For pEGFP-FOXO3A construct, the KspAI and EcoRI fragment of pFLAG-FOXO3A-WT containing the entire FOXO3A coding sequence was cloned into pEGFP-C1 vector (Clontech). For *Foxo3a* promoter constructs FL, Δ4, Δ3–4, Δ1–4, FLmut3 mouse genomic DNA regions chr10:41996473–41998267, 41996471–41998135, 41996471–41997927, and 41996471–41997399 (according to mouse genome assembly NCBI37/mm9) were PCR-amplified and inserted into pGL4.15[luc2P/Hygro] vector (Promega). For pGL4.83[hRlucP/PGK1/Puro] mouse 3-phosphoglycerate kinase 1 (*PGK1*) promoter sequence (ChrX:103382066–103382573 according to NCBI37/mm9 genome assembly) was inserted into pGL4.83[hRlucP/Puro] (Promega). The *Renilla* luciferase encoding vector with *EF1α* promoter pGL4.83[hRlucP/EF1α/Puro] has been described previously (28).

In silico analysis of potential FHREs in *Foxo3a* promoter sequence was performed using MatInspector software (Genomatix). For site-directed mutagenesis of FHRE in region 3 of the *Foxo3a* FL promoter construct, complementary primers against the target sequence containing the respective mutation (5′-CACACACGTGTGCTGGgtACAAGCGCGCCAG-3′) and Phusion high fidelity DNA polymerase (Thermo Scientific) were used.

Cell Culture and Transfections—The conditionally immortalized striatal progenitor Hdh^{7/7}, Hdh^{7/109}, and Hdh^{109/109} cells have been described previously (29). Briefly, these cells are derived from primary striatal cells from mice with different *Htt* genotypes and immortalized with temperature-sensitive large T antigen. Hdh^{7/7} cells are from wild type mice carrying two copies of the endogenous *Htt* allele with 7 CAG repeats; Hdh^{7/109} are from heterozygous, and Hdh^{109/109} are from homozygous knock-in mice with one or both *Htt* alleles having 109 CAG repeats, respectively. Hdh cells were propagated in DMEM (Invitrogen) supplemented with 10% fetal bovine serum (PAA Laboratories), 100 units/ml penicillin, and 0.1 mg/ml streptomycin (PAA Laboratories) at 33 °C in 5% CO₂. Hdh cells cultured on 48-well plates were transfected using Lipofectamine 2000 (Invitrogen) at reagent:DNA ratio 2:1. For luciferase assays, 0.125 μg of effector protein construct, 0.125 μg of firefly luciferase construct, and 10 ng of *Renilla* luciferase construct pGL4.83[hRlucP/PGK1/Puro] were used. When indicated, Hdh^{7/7} cells were treated with 1 mM 3-NP (Sigma-Aldrich) for 48 h.

HEK293 cells were propagated in MEM (Invitrogen) supplemented with 10% fetal bovine serum (PAA), 100 units/ml penicillin, and 0.1 mg/ml streptomycin (PAA). LipoD293 (Signagen) and RNAiMAX (Invitrogen) were utilized for plasmid and siRNA transfections, respectively, in HEK293 cells according to the manufacturers' protocols. Predesigned Silencer Select siRNAs against FOXO3a s80658 (siRNA1) and s1408638 (siRNA2) and negative control 1 siRNA (scrambled) were purchased from Ambion.

For rat cortical neuronal cultures the cortical hemispheres from embryonic day 22.5 embryos of Sprague-Dawley rats were dissected, and the underlying diencephalons, hippocampi, and striata were trimmed away. The obtained cortices were treated as described previously (30). Neuronal cultures were used for analyses at 6–8 days *in vitro*. Neurons cultured on 48-well plates were transfected at days 5 and 6 *in vitro* using Lipofectamine 2000 (Invitrogen) at reagent:DNA ratio 2:1. For cytochemical analysis, 0.5 μg of pEGFP-FOXO3A-WT encoding vector was used, and for luciferase assays, 0.25 μg of effector protein construct, 0.25 μg of firefly luciferase construct, and 10 ng of *Renilla* luciferase construct pGL4.83[hRlucP/EF1α/Puro] were used. When indicated, neurons were treated with 0.5 mM 3-NP for 2–24 h.

Immunocytochemistry—Cells grown on poly-L-lysine-coated coverslips were fixed in 4% paraformaldehyde in PBS for 15 min, treated with 50 mM NH₄Cl in PBS for 10 min, permeabilized in 0.5% Triton X-100 in PBS for 15 min, and blocked with 2% bovine serum albumin in PBS. Incubations with rabbit polyclonal anti-FOXO3a 1:200 (1112; Cermes, epitope SADDSP-SLSKWPGS) and Alexa 488- or Alexa 546-conjugated goat

anti-rabbit IgG 1:2000 (Molecular Probes) antibodies were carried out in 0.2% BSA and 0.1% Tween 20 in PBS at room temperature for 1.5 h each. The samples were mounted in ProLong Gold antifade reagent with 4'-6-diamidino-2-phenylindole (Molecular Probes) and analyzed by confocal microscopy (LSM Duo; Zeiss).

Western Blotting—Cells were lysed in radioimmune precipitation assay buffer (50 mM Tris-HCl, pH 8, 150 mM NaCl, 1% Nonidet P-40, 0.5% sodium deoxycholate, 0.1% SDS, 1 mM dithiothreitol, and protease inhibitors mixture Complete mini (Roche)); if necessary, phosphatase inhibitors mixture (Roche) was added. Cell lysates were sonicated for 15 s with 30% amplitude on Sonics VibraCell and centrifuged at 16,100 × *g* for 15 min at 4 °C. Nuclear and cytosolic fractions were prepared as described previously (29). Protein concentrations in lysates were measured with BCA assay (Pierce). Equal amounts of protein were separated in 8% SDS-PAGE and transferred to PVDF membrane (Bio-Rad). Membranes were blocked overnight at 4 °C in 5% skim milk and 0.1% Tween 20, incubated with primary antibodies and secondary antibodies in 0.1% Tween 20 with 2% skim milk in PBS or 5% BSA in TBS (in case of phospho-site specific antibodies). Antibodies were diluted as follows: rabbit polyclonal anti-FOXO3a 1:1000 (1112; CeMines), rabbit polyclonal anti-Flag 1:1000 (F7425; Sigma-Aldrich), mouse monoclonal anti-tubulin β to a final concentration of 30 ng/ml (E-7; Developmental Studies Hybridoma Bank), rabbit polyclonal anti-HDAC2 1:1000 (sc-7899; Santa Cruz), rabbit polyclonal anti-pFOXO3a(Ser-253) 1:1000 (06-953; Upstate/Millipore), rabbit polyclonal anti-pFOXO3a(Ser-294) 1:1000 (A16693; Life Technologies), rabbit polyclonal anti-AKT1/2/3 1:2000 (sc-8312; Santa Cruz), rabbit polyclonal anti-pAKT(Ser-473) 1:2000 (9271; Cell Signaling), mouse monoclonal anti-ERK1/2 1:1000 (sc-135900; Santa Cruz), mouse monoclonal anti-pERK 1:1000 (sc-7383; Santa Cruz), mouse monoclonal anti-GAPDH 1:2000 (MAB374; Chemicon), and HRP-conjugated goat anti-mouse/rabbit IgG 1:2500 (Thermo Scientific). Chemoluminescent signal was detected using SuperSignal West Femto chemoluminescent substrate (Thermo Scientific) and ImageQuant 400 imaging system (Amersham Biosciences). Images were quantified with ImageQuant T4 v2005 software (Amersham Biosciences).

RNA Extraction and Reverse Transcription—Total RNAs from 200–300 mg of human cortex and/or striatum tissue of samples 5074, 5936, 5959, 6142, 6051, 6121, 5570, 6010, 6183, and 5507 were isolated by using 2 ml of TRIzol reagent (Invitrogen), after the tissues had been homogenized in liquid nitrogen with a mortar and pestle. The concentration of RNA was evaluated spectrophotometrically, and its quality was verified by means of agarose gel electrophoresis of 1 μ g of each sample. Genomic DNA was digested using 1 unit of rDNase I (Applied Biosystems) per 1 μ g/ml of total RNA at 37 °C for 10 min following the manufacturer's instructions. From human cortex tissue samples 08704, 13574, 00497, 00950, and 18590, the total RNAs were extracted from 50 mg of tissue using RNeasy lipid tissue mini kit (Qiagen) following the manufacturer's instructions. The RNA integrity number and concentrations were assessed by a RNA 6000 Nano Kit (Agilent) according to the

manufacturer's instructions; all samples used had RNA integrity numbers above 6.

Total RNA from R6/2 mice tissue was extracted by lipid tissue mini kits (Qiagen) from 100 mg of tissue and treated with 2 units of Turbo DNase (Invitrogen) following the manufacturer's instructions. Total RNAs from Hdh cells and primary cortical neurons were extracted using a RNeasy micro kit (Qiagen) following the manufacturer's instructions. First strand cDNAs were synthesized from 0.3–5 μ g of total RNA with Superscript III first strand synthesis system (Invitrogen) with oligo(dT) or with combination of oligo(dT) and random decamer primers.

Chromatin Immunoprecipitation—Cells on 100-mm dishes were cross-linked in 1% formaldehyde, 100 mM NaCl, 0.5 mM EGTA, 50 mM HEPES (pH 8.0) for 10 min at room temperature. One-tenth volume of 1.25 M glycine was added for quenching, and cells were washed twice with PBS and lysed in buffer containing 1% SDS, 10 mM EDTA, 50 mM Tris-HCl (pH 8.0) and protease inhibitors cocktail (Roche). Lysates were sonicated five times for 5 s at 50% amplitude on Sonics VibraCell to obtain 200–1000-bp fragments of genomic DNA, and insoluble material was spun down for 5 min at maximum speed in a tabletop centrifuge at 4 °C. 400 μ g of the primary neuron lysates or 1000 μ g of Hdh^{7/7} and Hdh^{109/109} cell lysates were diluted 1:9 with dilution buffer (1% Triton X-100, 150 mM NaCl, 2 mM EDTA, 20 mM Tris-HCl, pH 8.0, protease inhibitors cocktail (Roche)) and incubated with 5 μ g FOXO3a antibodies (1112; CeMines), acetyl-histone H4 antibodies (06-866; Millipore) or without antibodies overnight at 4 °C. 60 μ l of 50% protein A-Sepharose slurry (GE Healthcare), preabsorbed in 200 μ g/ml BSA and 10 μ g/ml sheared salmon sperm DNA, was added per reaction for 6–8 h. Sepharose-chromatin complexes were washed 3 times with wash buffer (1% Triton X-100, 0.1% SDS, 150 mM NaCl, 2 mM EDTA, 20 mM Tris-HCl (pH 8.0), protease inhibitors cocktail (Roche)) and once with wash buffer containing 500 mM NaCl. The immune complexes were eluted two times by addition of 75 μ l of elution buffer (1% SDS, 100 mM NaHCO₃, 1 mM EDTA), and the eluates of the same sample were combined. Cross-links were reversed by incubating the eluates in 200 mM NaCl at 65 °C overnight. DNA was purified with QIAquick PCR purification kit (Qiagen): 500 μ l of QIAquick binding buffer, 100 μ l of water, and sodium acetate to 60 mM concentration were added to the eluates, and the mixtures were subjected to columns as described in the manufacturer's protocol. DNA was eluted with 50 μ l of 10 mM Tris-Cl (pH 8.5).

Quantitative PCR—LightCycler 2.0 engine (Roche), qPCR Core kit for SYBR® Green I No ROX (Eurogentec) and polycarbonate qPCR capillaries (Bioron GmbH) were used to perform quantitative PCR. The reactions were carried out in triplicate in a volume of 10 μ l containing 1/80 of reverse transcription reaction or 1/50 of DNA from chromatin immunoprecipitation eluate. The following cycling conditions were used: 95 °C for 5 min, 45 cycles of 95 °C for 10–15 s, 55–62 °C for 10–20 s, and 72 °C for 10–20 s. Melting curve analysis was performed at the end of each reaction to confirm amplification of a single PCR product. The primers for expression analysis of mouse *Foxo3a* were 5'-TACGAGTGGATGGTGCCTG-3' and 5'-AGGTTGTGCCGGATGGAGTTC-3'; rat *Foxo3a* 5'-TACGAGTGGATGGTGCCTG-3' and 5'-AGGTTGTGCCGGATGGAG-

Increased FOXO3a Activity in Huntington Disease

TTC-3'; and human *FOXO3a* 5'-TTCAAGGATAAGGGCG-ACAGCAAC-3' and 5'-CTGCCAGGCCACTTGGAGAG-3'. Primers for mouse and rat *FasL* were 5'-AAGGAAGTGGCA-GAACTCCGTG-3' and 5'-GTTGCAAGACTGACCCCGG-AAG-3'. Target gene mRNA expression levels in mouse and rat were normalized to the levels of hypoxanthine-guanine phosphoribosyltransferase (*HPRT1*) transcripts detected with primers 5'-CAGTCCCAGCGTCGTGATTA-3' and 5'-AGC-AAGTCTTTCAGTCCTGTC-3'. Results from human HD post-mortem material were normalized to geometric mean of mRNA levels of three normalizing genes: *HPRT1*, 5'-GCCAG-ACCTTGTGGATTG-3' and 5'-CTCTCATCTTAGGCT-TTGTATTTT-3'; *SDHA* (succinate dehydrogenase complex, subunit A), 5'-TGGGAACAAGAGGGCATCTG-3' and 5'-CCACCACTGCATCAAATTCATG-3'; and *HMBS* (hydroxymethylbilane synthase), 5'-GGCAATGCGGCTGCAA-3' and 5'-GGGTACCCACGCGAATCAC-3'. The primers used were 5'-TCCTTCCCCTCCCTGC-3' and 5'-ACGCCTC-TCGCTCCTCT-3' for mouse *Foxo3a* promoter and 5'-CCAGCCTCACATTCCATTTC-3' and 5'-GCGCTTGTTT-ACCAGCACAC-3' for rat *Foxo3a* promoter. Primers against unrelated region for mouse were 5'-GTGGCTATGTGGTGT-TTCAGGT-3' and 5'-TGTGGGAGCAGAGAAGCCTA-3' and for rat 5'-TAGACCCAGGAGGGAGTTATTTAA-GAG-3' and 5'-TTGGGAATGCAATGCGAGTGTGTAC-3'.

Luciferase Assay—48 h post-transfection cells on 48-well plates were lysed in 50 μ l of passive lysis buffer (Promega), and reporter activities were measured using Dual-Glo luciferase assay (Promega) and GENios Pro multifunction microplate reader (Tecan). The reactions were carried out in duplicate. Background signals from untransfected cells were subtracted, and firefly luciferase signal values were normalized to *Renilla* luciferase signals.

Statistics—qPCR data were analyzed essentially as described previously (31). Briefly, data were log-transformed and auto-scaled, means and S.D. values were calculated, and two-tailed paired *t* tests were performed. In case of analysis of mRNA levels in post-mortem human tissues, two-tailed equal variance *t* tests were used. The data were back-transformed into the original scale for graphical depiction. The error bars represent upper and lower limits backtransformed as mean + S.D. and mean - S.D., respectively. Western blot and luciferase assay data were log-transformed to ensure normal distribution, means and S.D. values were calculated, and two-tailed paired *t* tests and unpaired *t* tests were used as appropriate. The numbers of experiments are indicated under "Results."

RESULTS

Immunocytochemical Screening Reveals Differential FOXO3a Signal in Hdh Cells—The hypothesis of transcriptional dysregulation in HD is reinforced by several studies demonstrating pathological alterations in nuclear translocation of transcription factors. For example, subcellular distribution of neuron-restrictive silencer factor (REST/NRSF) and sterol regulatory element-binding protein (SREBP) has been demonstrated to be changed in mutant huntingtin-expressing cells (29, 32). To identify mislocalized transcription factors in HD, we immunostained mouse striatal Hdh^{7/7} (wild type), Hdh^{7/109} (heterozy-

gous for HD mutation), and Hdh^{109/109} (homozygous for HD mutation) cells with a panel of 200 antibodies against various transcription factors. One of the antibodies identified by the screening was an antibody generated against a peptide in FOXO3a. As shown in Fig. 1A FOXO3a-like immunoreactive signal in Hdh^{7/7} cells was mainly cytoplasmic, whereas in heterozygous and homozygous mutant Hdh cells, the signal was detected also in the nucleus. To validate this observation in a different cell stress condition, we tested whether 3-NP-induced mitochondrial stress, widely used to mimic HD in rodents and in non-human primates (10, 33), is able to influence the distribution of FOXO3a-like immunoreactive signal in Hdh^{7/7} cells. As demonstrated in Fig. 1B, treatment with 1 mM 3-NP for 48 h considerably increased the amount of FOXO3a-like immunoreactive signal in the nuclei of Hdh^{7/7} cells. Thus, mitochondrial toxin 3-NP induced Hdh^{109/109}-like nuclear staining with FOXO3a antibodies in Hdh^{7/7} cells.

To determine the target specificity of the FOXO3a antibodies used, we transfected HEK293 cells with constructs encoding EGFP- or Flag-tagged FOXO3a and with scrambled or FOXO3a-specific siRNAs. By cytochemistry we observed co-localization of signals visualized by direct EGFP fluorescence or by indirect immunolabeling with FOXO3a antibodies in cells expressing EGFP-FOXO3a fusion protein (Fig. 1C). Western blotting revealed that FOXO3a antibodies recognized overexpressed Flag-FOXO3a protein, as well as an endogenous protein of similar molecular mass (Fig. 1D). Compared with untransfected control or scrambled siRNA transfected cells, the intensity of the endogenous signal obtained by immunoblotting with FOXO3a antibodies was reduced to 39 or 13% in cells transfected with FOXO3a-specific siRNA 1 or 2, respectively (Fig. 1, D and E). Similar reduction was seen in FOXO3a mRNA levels by RT-PCR analysis performed in parallel (Fig. 1F). Collectively, the above results verify the specificity of the antibodies and suggest that the control of FOXO3a localization is disturbed in HD cells.

FOXO3a Protein Levels Are Elevated in Mutant Hdh Cells—To compare FOXO3a protein expression levels in Hdh^{7/7}, Hdh^{7/109}, and Hdh^{109/109} cells, we prepared total cell lysates from all three cell lines and estimated the relative amount of FOXO3a protein by immunoblotting using antibodies against FOXO3a (Fig. 2A). FOXO3a-specific signal intensities were quantified densitometrically and normalized to the amount of tubulin β measured from the same extracts. Protein levels of FOXO3a showed significantly more than 2-fold increase in mutant Hdh^{7/109} and Hdh^{109/109} cell lines, respectively, compared with FOXO3a protein level in wild type Hdh^{7/7} cells (Fig. 2B; *n* = 4, *p* = 0.035 and *p* = 0.026, respectively).

Elevated levels of FOXO3a protein seen in total lysates and differential immunocytochemical staining in mutant Hdh cells raised the question of distribution of excess FOXO3a in those cells. To answer this, nuclear and cytosolic fractions were prepared, and equal amounts of protein extracts were resolved by SDS-PAGE and analyzed by Western blotting with FOXO3a antibodies (Fig. 2C). To assess the quality of fractionation and monitor loading, histone deacetylase 2 (HDAC2) and tubulin β were detected as nuclear and cytosolic markers, correspondingly. Protein levels of FOXO3a

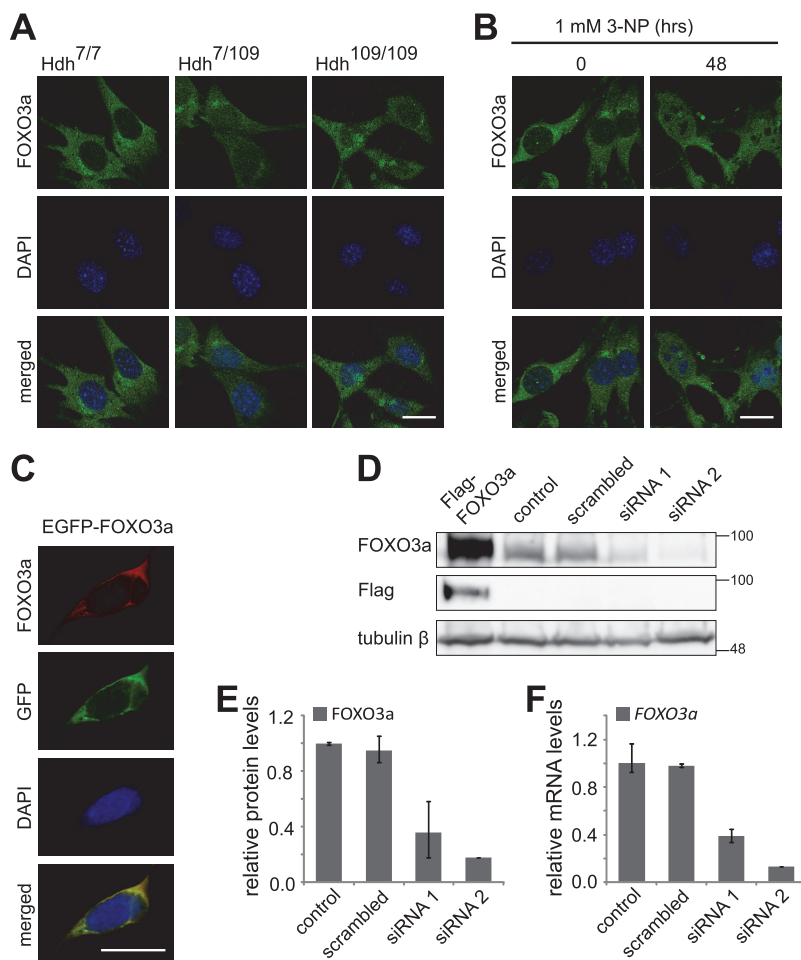


FIGURE 1. Localization of FOXO3a-like immunoreactive signal in Hdh cells and validation of FOXO3a antibody. *A*, representative micrographs demonstrating differential distribution of FOXO3a antibody staining in Hdh^{7/7}, Hdh^{7/109}, and Hdh^{109/109} cells. *B*, immunocytochemical analysis with FOXO3a antibodies in Hdh^{7/109} cells left untreated or treated with 1 mM 3-NP for 48 h. *C*, co-localization of EGFP signal and FOXO3a antibody staining in HEK293 cells transfected with EGFP-FOXO3a encoding construct. In *A–C*, DNA was counterstained with DAPI. Scale bar, 20 μ m. *D*, Western blot analysis with FOXO3a antibodies of HEK293 cells left untransfected (control) or transfected with Flag-FOXO3a encoding construct, scrambled siRNA, or siRNAs 1 and 2 against FOXO3a. Flag-specific antibodies were used for verification of Flag-FOXO3a expression and tubulin β served as loading control. *E*, quantification of the data in *D*. FOXO3a signals were normalized to tubulin β signals. *F*, RT-qPCR analysis of FOXO3a mRNA levels in siRNAs transfected HEK293 cells performed in parallel with Western blotting. In *E* and *F*, the mean results from two independent experiments are shown.

were increased \sim 2-fold in both nuclear (Fig. 2*D*) and cytosolic fractions (Fig. 2*E*) of Hdh^{109/109} cells compared with WT cells ($n = 4$, $p = 0.012$ and $p = 0.035$, respectively). In Hdh^{7/109} cells, a 1.4-fold borderline increase was detected in both fractions (Fig. 2, *D* and *E*; $n = 4$). Collectively, these results indicate that the overall elevated FOXO3a protein content in mutant Hdh cells is associated with its increased levels both in the cytoplasm and nuclei.

Activation of AKT Is Not Reduced in Mutant Hdh Cells—The main kinase responsible for phosphorylation and nuclear export of FOXO3a protein is AKT (20). Because increased nuclear FOXO3a was present in HD cells, we asked whether AKT signaling might be compromised in these cells. First, we determined the levels of total AKT and activated AKT (phos-

phorylated at Ser-473) in Hdh cells by immunoblotting (Fig. 3*A*). Signal intensities were quantified densitometrically and normalized to the amount of tubulin β . Levels of total AKT did not change dramatically in Hdh cell lines, and a 20% reduction in Hdh^{7/109} cells compared with Hdh^{7/7} cells was observed (Fig. 3*B*; $n = 4$, $p = 0.045$). Protein levels of pAKT1/2/3(Ser-473) in heterozygous and homozygous mutant cells did not differ from the levels in WT cells (Fig. 3*B*; $n = 3$). Second, we measured the levels of FOXO3a phosphorylated at an AKT site in the forkhead domain (Ser-253) in Hdh cells (Fig. 3*C*). Compared with Hdh^{7/7} cells there was a tendency for increased pFOXO3a(S253) levels in Hdh^{7/109} cells and for decreased pFOXO3a(S253) levels in Hdh^{109/109} cells (Fig. 3, *C* and *D*; $n = 3$, 1.7-fold and 0.7-fold, respectively). Altogether, these results

Increased FOXO3a Activity in Huntington Disease

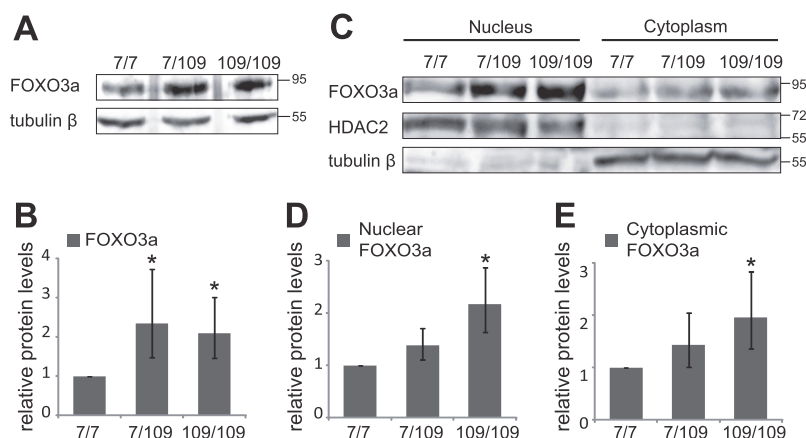


FIGURE 2. Levels of FOXO3a protein in Hdh cells. *A*, Western blot analysis of FOXO3a and tubulin β expression in total extracts of Hdh cells. *B*, quantification of data in *A*. FOXO3a levels were normalized to tubulin β levels. *C*, Western blot analysis of FOXO3a in nuclear and cytoplasmic fractions of Hdh cells. HDAC2 and tubulin β served as controls for nuclear and cytoplasmic fractions, respectively. *D* and *E*, quantification of FOXO3a levels in nuclear (*D*) and cytoplasmic fractions (*E*) of Hdh cells. For normalization, FOXO3a signal intensities were normalized to HDAC2 or tubulin β signal intensities for nuclear or cytoplasmic fractions, respectively, of each Hdh cell line. The relative FOXO3a levels in Hdh^{7/7} cells were arbitrarily set as 1. The statistical significance shown with asterisks is relative to the levels measured from Hdh^{7/7} cells. *, $p < 0.05$; $n = 4$

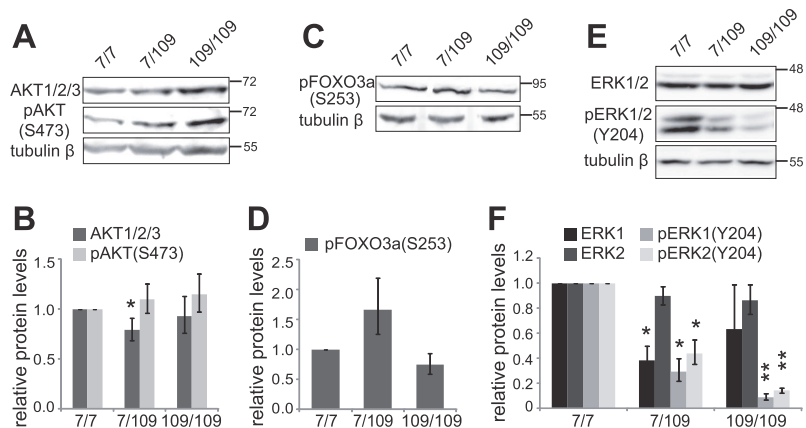


FIGURE 3. AKT and ERK activity in Hdh cells. *A*, Western blot analysis of AKT1/2/3 proteins and AKT1/2/3 phosphorylated at serine 473 (pAKT1/2/3(Ser-473)) in Hdh cells. Tubulin β served as a loading control. *B*, quantification of the signals of AKT1/2/3 and pAKT1/2/3(Ser-473) in *A*. Signals were normalized to the levels of tubulin β . *C*, Western blot analysis of FOXO3a phosphorylated at serine 273 (pFOXO3a(Ser-273)) in Hdh cells. Tubulin β levels were determined in control. *D*, quantification of the data in *C*. pFOXO3a(Ser-273) signals were normalized to the levels of tubulin β . *E*, Western blot analysis of ERK1/2 and ERK1/2 phosphorylated at tyrosine 204 (pERK1/2(Tyr-204)) in Hdh cells. Tubulin β was utilized for loading control. *F*, quantification of the signals of both ERK isoforms and phosphorylated isoforms in *E*. Signals were normalized to the levels of tubulin β or HDAC2. The statistical significance shown with asterisks is relative to the levels measured from Hdh^{7/7} cells. *, $p < 0.05$; **, $p < 0.01$; ***, $p < 0.001$; $n = 3$

indicate that increased nuclear levels of FOXO3a cannot be attributed to reduced AKT signaling in HD cells.

Levels of Activated ERK Are Reduced in Mutant Hdh Cells—The ERK kinase phosphorylates FOXO3a initiating its translocation from nucleus to cytoplasm, reducing its transcriptional activity and promoting its degradation (24). Therefore to determine whether ERK might play a role in increased FOXO3a levels in mutant Hdh cells, we measured the levels of total ERK1/2 and phosphorylation-activated ERK1/2 (Tyr-204) in Hdh cells by immunoblotting (Fig. 3E). Although ERK1 levels in Hdh^{7/109} cells were reduced to 42% of the levels in WT cells (Fig. 3F; $n = 3$, $p = 0.0088$), levels of ERK1 in Hdh^{109/109} cells and ERK2 levels both in Hdh^{7/109} and Hdh^{109/109} cells were not signifi-

cantly altered compared with Hdh^{7/7} cells (Fig. 3F). On the contrary, levels of phosphorylated ERK1/2 were reduced drastically in both mutant huntingtin expressing cell lines (Fig. 3E). In Hdh^{7/109} cells, pERK1 levels were 32% and pERK2 levels were 47% of the levels measured in Hdh^{7/7} cells (Fig. 3F, $n = 3$, $p = 0.0026$ and $p = 0.005$, respectively). The amount of pERK detected in Hdh^{109/109} cells was further decreased, pERK1 to 12% and pERK2 to 19% of the activated ERK levels in Hdh^{7/7} cells (Fig. 3F, $n = 3$, $p = 0.001$ and $p = 0.0022$, respectively). Next we attempted to measure the levels of FOXO3a phosphorylated by ERK kinases at Ser-294 to see whether changes in kinase activity correlate with its target protein condition. Unfortunately, we could not detect any signal of

Increased FOXO3a Activity in Huntington Disease

pFOXO3a(Ser-294) in Hdh cells, indicating that the level of phosphorylation of FOXO3a in these cells is below the detection limit of the used antibodies (data not shown). Collectively, the above data show that the levels of ERK kinases phosphorylated at Tyr-204 are significantly lower in HD model cells. Even though we were unable to measure pFOXO3a(Ser-294) levels, it remains possible that the observed increase of FOXO3a in mutant Hdh cells may partly result from inactivation of ERK kinases.

Nuclear FOXO3a Levels Are Increased in 3-NP-treated Neurons—The most vulnerable cells in HD are striatal and cortical neurons. To study the distribution of FOXO3a in the disease-relevant cell type, we determined the impact of mitochondrial toxin 3-NP on FOXO3a localization in rat primary cortical neurons. Cultured neurons were transfected with EGFP-FOXO3a fusion protein encoding vector and treated with 0.5 mM 3-NP for 2, 4, or 8 h. EGFP-FOXO3a was visualized by confocal microscopy, and the representative images of neurons left untreated and treated with 3-NP for 8 h are shown in Fig. 4A. Three independent experiments were performed, and from each indicated time point at least 35 neurons were analyzed and divided into two categories based on whether the EGFP-FOXO3a signal was mainly nuclear ($Nc \geq Cp$) or mainly cytoplasmic ($Cp > Nc$). Time-dependent gradual translocation of EGFP-FOXO3a into the nucleus was observed in accordance to the time of treatment (Fig. 4B). 75% of untreated neurons showed cytoplasmic localization of EGFP-FOXO3a. Compared with untreated cells, the number of cells with mainly nuclear EGFP-FOXO3a localization tended to increase after 3-NP treatment for 2 h, whereas in case of longer 3-NP treatments, for 4 and 8 h, mainly nuclear localization was seen in 58 and 75% of neurons, correspondingly ($n = 3$, $p = 0.32$, $p = 0.012$, and $p = 0.0098$, respectively). Subsequently, we analyzed the localization of endogenous FOXO3a protein in control and 3-NP-treated rat primary cortical neurons by immunocytochemical staining with FOXO3a antibodies. Similarly to the results obtained with the overexpressed EGFP-FOXO3a protein, 3-NP treatment induced translocation of endogenous FOXO3a protein into the nucleus (Fig. 4C). In untreated neurons, endogenous FOXO3a-like signal was mostly nuclear but was also detected in the cytoplasm, whereas in 3-NP-treated neurons, only nuclear staining was seen.

We observed increased FOXO3a protein levels concurrent with its translocation toward nucleus in mutant Hdh cells. To test whether FOXO3a translocation is accompanied by changes in FOXO3a protein levels in cortical neurons also, we analyzed FOXO3a protein levels by immunoblotting in neurons treated with 3-NP for 16 or 24 h. We found that compared with untreated neurons, FOXO3a levels showed a tendency toward increase at 16 h (1.5-fold, $n = 3$; $p = 0.17$) and were significantly increased at 24 h of treatment (Fig. 4, D and E; 1.9-fold, $n = 3$; $p = 0.02$). Taken together, these data demonstrate that 3-NP-induced mitochondrial stress leads to nuclear translocation and increased levels of FOXO3a protein in primary cortical neurons.

mRNA Levels of Foxo3a and Its Target Gene FasL Are Elevated in HD Cells—Because FOXO3a nuclear localization was accompanied by increased FOXO3a protein levels in the stud-

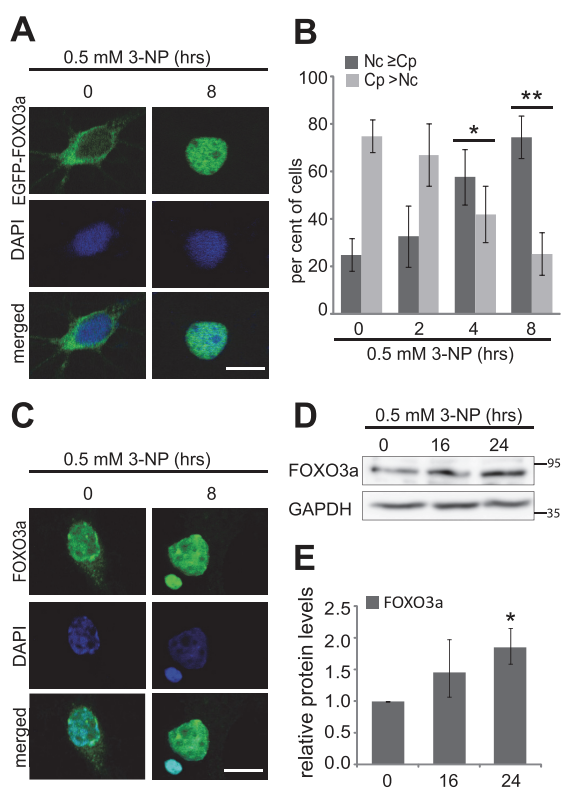


FIGURE 4. Effect of mitochondrial toxin 3-NP treatment on subcellular distribution and levels of FOXO3a in cortical neurons. A and C, representative confocal microscopy images of overexpressed EGFP-FOXO3a (A) or endogenous FOXO3a-like signal (C) in cortical neurons left untreated or treated with 3-NP for 8 h. Localization of EGFP-FOXO3a was detected by direct fluorescence, endogenous signal was detected immunocytochemically with FOXO3a antibodies, and DNA was counterstained with DAPI. Scale bar, 10 μ m. B, quantitative analysis showing percentages of primary cortical neurons with mainly nuclear ($Nc \geq Cp$) or mainly cytoplasmic ($Cp > Nc$) EGFP-FOXO3a localization when left untreated (0 h) or treated with 0.5 mM 3-NP for 2, 4, or 8 h. Shown are the mean results from three independent experiments with 35–150 neurons counted in each experiment for each time point. D, Western blot analysis of FOXO3a protein levels in cortical neurons left untreated or treated with 0.5 mM 3-NP for 16 or 24 h. GAPDH served as a loading control. E, quantification of data in D, FOXO3a signals were normalized to the levels of GAPDH. The statistical significance shown with asterisks is relative to the levels measured from untreated neurons. *, $p < 0.05$; **, $p < 0.01$; $n = 3$.

ied HD model cells, we determined *Foxo3a* mRNA levels in Hdh cells and also in 3-NP-treated primary cortical neurons by RT-qPCR. As demonstrated in Fig. 5A, expression of *Foxo3a* was increased 1.7-fold in heterozygous mutant Hdh^{7/109} cells and 1.8-fold in homozygous mutant Hdh^{109/109} cells compared with the expression levels in wild type cells ($n = 4$, $p = 0.021$ and $p = 0.0049$, respectively). Treatment of cortical neurons with 3-NP for 16 h resulted in a 1.6-fold increase in *Foxo3a* mRNA levels compared with untreated neurons (Fig. 5B; $n = 5$, $p = 0.043$). Therefore, increased levels of FOXO3a protein in HD cells might be at least partially caused by the up-regulation of *Foxo3a* mRNA expression.

To determine whether increased amounts of nuclear FOXO3a in HD cells have functional consequences, we quan-

Increased FOXO3a Activity in Huntington Disease

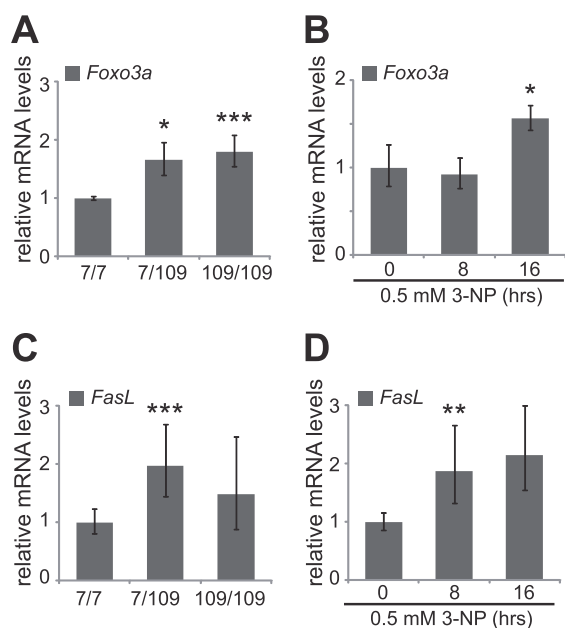


FIGURE 5. Foxo3a and FasL mRNA levels in HD model cells. RT-qPCR analysis of *Foxo3a* (A and B) and *FasL* (C and D) in Hdh cells (A and C) and in primary cortical neurons left untreated or treated with 3-NP for 8 or 16 h (B and D). *Foxo3a* or *FasL* levels were normalized to the levels of *HPRT1*. The mean values and statistical significance shown with asterisks are relative to the levels measured in Hdh^{7/7} cells or untreated neurons. *, $p < 0.05$; **, $p < 0.01$; ***, $p < 0.001$; $n = 4$ in A and C; $n = 5$ in B and D.

tified the mRNA levels of *FasL* (*Fas ligand*), one of the target genes of FOXO3a (20), in Hdh^{7/7}, Hdh^{7/109}, and Hdh^{109/109} cells, as well as in untreated and 3-NP-treated primary cortical neurons by RT-qPCR. Compared with wild type Hdh^{7/7} cells, the mRNA levels of *FasL* were elevated 2-fold in Hdh^{7/109} cells (Fig. 5C; $n = 4$, $p = 0.0032$). Compared with untreated neurons, we observed a statistically significant 1.9-fold increase in *FasL* expression after 8 h of 3-NP treatment and a 2.2-fold increase at 16 h of treatment (Fig. 5D; $n = 5$, $p = 0.0088$ and $p = 0.055$, respectively). These data suggest functional consequences of FOXO3a translocation into nucleus on its target genes.

FOXO3a mRNA Levels Are Elevated in Brain Tissue of R6/2 Mice and HD Patients—R6/2 transgenic mice carry a fragment of human *HTT* gene with 144 polyglutamine repeats and show fast progress of HD symptoms (34). We analyzed mRNA levels of *Foxo3a* in cortex of R6/2 mice and detected a tendency toward increased expression compared with wild type littermate tissue (Fig. 6A; 2.6-fold, $n = 3$, $p = 0.064$). To study FOXO3a mRNA levels in HD patients, we performed RT-qPCR of diseased and nondiseased post-mortem cerebral cortex and caudate nucleus tissue. Variable levels of FOXO3a mRNA were detected both in HD patient (one grade 2 patient, three grade 3 patients, and one grade 1 patient) and control cortex tissue (Fig. 6B; $n = 5$, $p = 0.26$). However, we observed a significant 4.6-fold increase in FOXO3a mRNA levels in patient caudate nucleus tissue (two grade 3 patients and one grade 4 patient) compared with controls (Fig. 6C; $n = 3$, $p = 0.00068$). These *in vivo* data

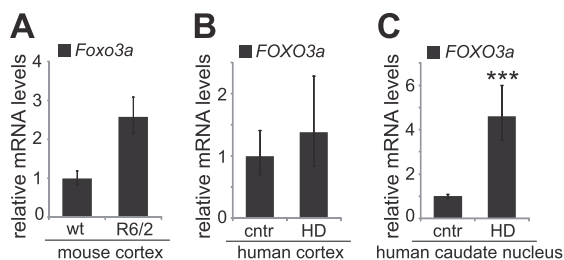


FIGURE 6. In vivo expression levels of FOXO3a mRNA. A, RT-qPCR analysis of *Foxo3a* levels in the cerebral cortex of WT and R6/2 6-week-old mice. *HPRT1* levels were determined for normalization. Shown are the mean results from three pairs of mice. B and C, FOXO3a levels in the cerebral cortex (B) and caudate nucleus (C) of HD patients and nondiseased controls (cntr). Total RNAs extracted from post-mortem human brain tissue were reverse transcribed and subjected to qPCR. FOXO3a levels were normalized to the levels of *HPRT1*, *SDHA*, and *HMBS*. Shown are the mean results from five (B) or three (C) patients and nondiseased controls. The statistical significance shown with asterisks is relative to the controls. ***, $p < 0.001$.

from R6/2 mice and HD patients further corroborate our findings in cells *in vitro* about dysregulated FOXO3a activity in HD.

Transcription Factor FOXO3a Binds to Its Own Promoter—Increased nuclear localization of FOXO3a protein and accompanying higher expression level of *Foxo3a* mRNA in HD cells led us to the hypothesis that positive autoregulation might be involved in FOXO3a signaling. By *in silico* analysis, we identified four potential Forkhead response elements (FHREs), named 1–4, in *Foxo3a* promoter less than 2 kb upstream from the transcription start site (Fig. 7A). We carried out chromatin immunoprecipitation experiments with primary neurons and Hdh^{7/7} and Hdh^{109/109} cells using FOXO3a antibodies. Acetyl histone 4 (AcH4) specific antibodies were used as positive control, and beads-only precipitated samples showed a general experimental background. To study FOXO3a binding to its own promoter, we analyzed the precipitated DNA by RT-qPCR with primers specific for the *Foxo3a* promoter region containing the potential FHREs. Amplification with primers designed against an unrelated untranscribed region (URR) on mouse or rat chromosomes (chromosome 10 and 1, respectively) served as negative control indicating random binding of the antibodies used. As shown in Fig. 7B, we detected significant enrichment of AcH4 on *Foxo3a* promoter compared with URR in rat primary cortical neurons, indicating active transcription of the gene ($n = 3$, $p = 0.00057$, $p = 0.0016$). Importantly, higher amounts of *Foxo3a* promoter DNA compared with URR were precipitated with FOXO3a antibodies in primary neurons (Fig. 7B, $n = 3$, $p = 0.032$). In WT and mutant Hdh cells, similar amounts (~0.13%) of input DNA were precipitated by AcH4 antibody, whereas 0.01 and 0.04% of input DNA was precipitated by FOXO3a antibodies in Hdh^{7/7} and Hdh^{109/109} cells, respectively (Fig. 7C; $n = 3$, $p = 0.022$ and $p = 0.0076$ compared with URR). These results demonstrate binding of endogenous FOXO3a protein to its own promoter in all studied cell types.

Regulation of FOXO3a Transcription Factor Involves Positive Feedback—To elucidate which of the potential FHREs are responsible for FOXO3a binding to its own promoter, we cloned mouse *Foxo3a* promoter regions of different lengths into a *luc2P* reporter vector (Fig. 8A) and assessed the ability of

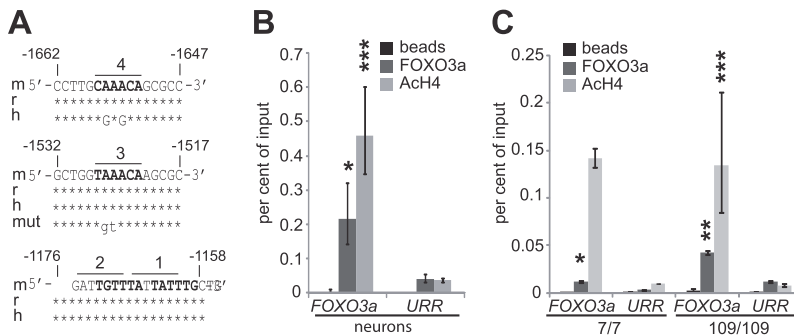


FIGURE 7. FOXO3a binds to its own promoter. *A*, *in silico* analysis of potential FHREs in mouse, rat, and human FOXO3a promoter. Shown are the conserved sequences of promoter regions containing the four identified sites that are marked in *bold*. The sequence of mutated FHRE 3 is also shown. The *numbers* indicate the positions relative to the transcription start site. *B* and *C*, chromatin immunoprecipitation analysis demonstrating FOXO3a binding to FHREs containing region in *Foxo3a* promoter in rat primary cortical neurons (*B*) and Hdh^{7/7} and Hdh^{109/109} cells (*C*). Soluble chromatin was co-immunoprecipitated with antibodies specific for FOXO3a or Ach4 or with beads alone. DNA from *Foxo3a* promoter or from an URR was amplified by qPCR. The data are presented as percentages of input DNA. The statistical significance denoted with *asterisks* is relative to values of URR obtained with the respective antibodies. *, *p* < 0.05; **, *p* < 0.01; ***, *p* < 0.001; *n* = 3 (except in case of Ach4 ChIP in Hdh^{7/7} cells, where *n* = 2).

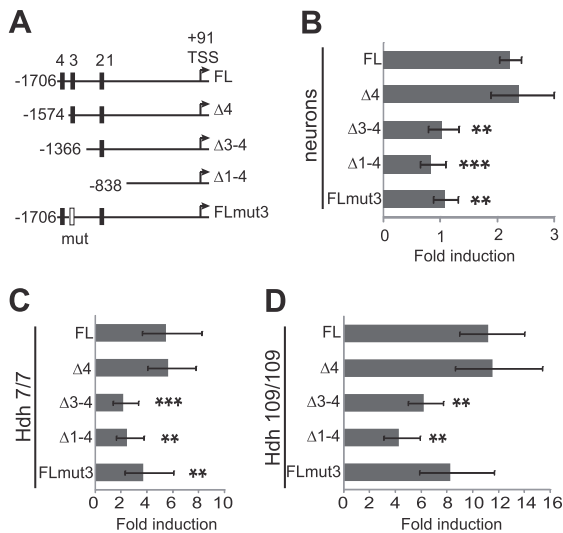


FIGURE 8. FOXO3a activates transcription from its own promoter. *A*, schematic representation of the *Foxo3a* promoter regions cloned into firefly luciferase reporter vector. The locations of potential FHREs 1–4 are indicated with *black boxes*. Mutated FHRE 3 is depicted as a *white box*. The *numbers* indicate the position relative to the transcription start site (TSS) that is shown with *arrows*. *B–D*, reporter assays with primary cortical neurons (*B*), Hdh^{7/7} (*C*), and Hdh^{109/109} cells (*D*) transfected with *Foxo3a* promoter constructs and *Renilla* luciferase construct with *EF1α* promoter (*B*) or *PGK1* promoter (*C* and *D*) for normalization. The cells were co-transfected with constructs encoding constitutively active Flag-FOXO3a-TM or empty vector. Luciferase activities were measured, and data are presented as fold induction of normalized luciferase activity in Flag-FOXO3a-TM-expressing cells compared with cells transfected with empty vector. The statistical significance denoted with *asterisks* is relative to the induction of transcription from WT full-length promoter. *, *p* < 0.05; **, *p* < 0.01; ***, *p* < 0.001; *n* > 3

Flag-tagged constitutively active triple mutant (TM) of FOXO3a (T32A,S253A,S315A-mutated AKT kinase phosphorylation sites) (20) to activate transcription from these promoters in rat primary cortical neurons and Hdh cell lines. Normalized activity of reporter transcribed from *Foxo3a* promoter encompassing potential FHRE sites 1–4 was increased more

than 2-fold in neurons, more than 5-fold in Hdh^{7/7} cells and more than 11-fold in Hdh^{109/109} cells expressing Flag-FOXO3a-TM compared with cells transfected with empty vector (*n* = 4, *p* = 0.00051, *p* = 0.0056, *p* = 0.0027, respectively; Fig. 8, *B–D*). Deletion of potential FHRE site 4 did not affect induction of promoter activation by Flag-FOXO3a-TM in any of the cell types (Fig. 8, *B–D*). However, induction of transcription from *Foxo3a* promoters containing potential FHRE sites 1–2 only or none of the FHREs was significantly decreased compared with the induction of the longest promoter in all of the cell types (Fig. 8, *B–D*). These results suggest that site 3 FHRE (TAAACA) is to a large extent responsible for the transcriptional autoregulation of FOXO3a. To verify this, we used site-directed mutagenesis to introduce two point mutations into the site 3 FHRE (Fig. 7*A*) in the context of the longest cloned *Foxo3a* promoter (Fig. 8*A*) and analyzed the effect of the mutation on the ability of Flag-FOXO3a-TM to activate reporter transcription. As shown in Fig. 8*B*, Flag-FOXO3a-TM was not able to activate transcription from *Foxo3a* promoter carrying mutations in site 3 FHRE in neurons, indicating that this site was indeed needed for autoregulation in these cells (*n* = 4, *p* = 0.0011 compared with WT promoter). Activation of transcription from the mutant *Foxo3a* promoter compared with WT full-length promoter was also reduced in Hdh^{7/7} cells (*p* = 0.0068; Fig. 8*C*), whereas the decrease seen in Hdh^{109/109} cells remained statistically nonsignificant (*p* = 0.063; Fig. 8*D*). Compared with neurons, the induction of reporter transcription from *Foxo3a* promoters without site 3 FHRE or with mutant site 3 FHRE were higher in Hdh cells, especially in Hdh^{109/109} cells, indicating that other binding sites may also play a role. Altogether, the above findings show that transcription factor FOXO3a is able to activate its own transcription by directly binding to its own promoter.

DISCUSSION

FOXO transcription factors have been implicated in neurodegenerative diseases, but their exact roles in these diseases have remained controversial (35–41). Here we report differen-

Increased FOXO3a Activity in Huntington Disease

tial immunocytochemical staining with FOXO3a antibodies in striatal Hdh cells expressing wild type and/or mutant huntingtin endogenously. We detected elevated FOXO3a protein levels in the nuclei of mutant Hdh cells and 3-NP-treated rat primary cortical neurons. Additionally, our results show that FOXO3a mRNA expression levels are increased in mutant Hdh cells, in 3-NP-treated primary neurons and in post-mortem caudate tissue of HD patients. Moreover, using chromatin immunoprecipitation and reporter assays, we demonstrate that FOXO3a directly regulates its own expression, thus forming a positive autoregulation loop.

Our subcellular fractionation experiments showed elevated FOXO3a protein levels both in the cytoplasm and nucleus in Hdh^{109/109} cells compared with Hdh^{7/7} cells. The elevated nuclear import of FOXO3a in mutant Hdh cells might be due to increased cellular stress and/or decreased growth factor signaling that are known to be caused by mutant huntingtin (42, 43). One of the kinases activated by growth factor signaling is AKT that plays a central role in promoting the survival of a wide range of cell types, partly through inactivation of FOXO factors (20, 44, 45). Controversial results describing AKT activity in HD have been reported earlier. Increased levels of activated AKT were detected in striata of Hdh^{111/111} knock-in mice and cultured mutant Hdh^{111/111} striatal cells, compared with their wild type counterparts, whereas no changes in phosphorylated FOXO1 levels were detected (46). In another study, both activated and total AKT levels were shown to be reduced in rat HD models and in lymphoblasts, lymphocytes, and post-mortem brain extracts from HD patients (47). Additionally, unchanged AKT activation in response to BDNF treatment has been reported in Hdh cells (9). Here we showed that AKT activity is not compromised in mutant Hdh cells. According to our results, total AKT levels were not reduced in Hdh^{109/109} cells compared with WT cells, and no significant differences in pAKT1/2/3(S473) or pFOXO3a(S253) levels were detected in Hdh cells with different genotypes. Therefore, increased FOXO3a nuclear levels in mutant Hdh cells seen in this study cannot be attributed to disturbed AKT activation *per se*. One explanation for increased levels of nuclear FOXO3a in HD cells could be that the amount and activity of AKT is not sufficient to maintain low levels of nuclear FOXO3a in the presence of increased amounts of the transcription factor.

Another possibility is that other signaling pathways, which modulate FOXO3a activity, are altered in mutant Hdh cells. Here we demonstrated that phosphorylated and activated ERK kinase levels are significantly lower in mutant Hdh cells. ERK has been shown to phosphorylate FOXO3a at three serine residues (Ser-294, Ser-344, and Ser-425), promoting its translocation into cytoplasm (24). Furthermore, ERK-phosphorylated FOXO3a is substrate for E3 ligase MDM2 and is directed to proteasomal degradation (24). In general, ERK1/2 is activated by oxidative stress for neuroprotection, but in Hdh^{111/111} cells, unlike in Hdh^{7/7} cells, H₂O₂ treatment does not induce ERK pathway, and these cells do not respond to protective BDNF treatment either (9). In contrast, for PC12 and ST14A cells, it has been shown that expression of mutant Htt activates ERK and inhibition of apoptotic caspases is seen (48). Although we were not able to detect pFOXO3a(S294) in Hdh cells, it remains

possible that FOXO3a phosphorylation at this or other ERK target sites might be compromised in mutant Hdh cells. Therefore, the increased level of FOXO3a and its nuclear location in Hdh^{7/109} and Hdh^{109/109} cells might partly result from decreased phosphorylation of FOXO3a by ERK kinases.

In addition, activity of JNKs, which facilitate FOXO nuclear import, has been shown to be activated by oxidative stress (37) and growth factor deprivation (49) and to be increased in a rat HD model (50). So far, phosphorylation by JNK has only been shown for FOXO4 and other FOXO family proteins lack the region targeted by JNK in FOXO4 (51). Another up-regulated kinase in HD is 5' AMP-activated protein kinase (AMPK), which is activated in response to bioenergetic failure induced by excitotoxic injury (52). AMPK acts in two ways on FOXO3a: first it blocks AKT activation and prevents FOXO3a phosphorylation by AKT, and second, AMPK phosphorylates FOXO3a in the nucleus increasing its binding to target gene *Bim* (36). Hence, it would be of interest to further study JNK and AMPK and related kinases activity in conjunction with phosphorylation of FOXO3a in HD.

A chemical model of HD utilizing mitochondrial toxin 3-NP has been widely used in rodents and also in non-human primates to mimic pathological neurodegeneration seen in HD in humans (10, 11, 33). Our results demonstrated that in Hdh^{7/7} cells, 3-NP treatment leads to similar FOXO3a localization change toward the nucleus as was seen in genetic HD models, Hdh^{7/109} and Hdh^{109/109} cells. Also, 3-NP treatment of rat primary cortical neurons led to increased nuclear translocation of endogenous FOXO3a and overexpressed EGFP-FOXO3a. Although endogenous FOXO3a-like signal showed differential initial distribution compared with EGFP-FOXO3a signal in neurons, both were located exclusively to the nuclei of primary cortical neurons after 3-NP treatment. This seeming discrepancy in subcellular localizations of endogenous and exogenous FOXO3a might arise from very different expression levels of the proteins. It is possible that the nucleus in EGFP-FOXO3a transfected neurons is saturated, and excessive protein is transported to cytoplasm; a similar phenomenon has been described for a GFP fusion protein previously (53). Additionally, in our experiments 3-NP treatment of primary neurons induced similar elevation of endogenous FOXO3a protein levels as observed in genetic HD model. Although stresses caused by mutant huntingtin protein and 3-NP induced comparable subcellular localization and protein level changes of FOXO3a, it cannot be excluded that the underlying mechanisms might be different, just as described previously for the causes of cellular energy collapse induced by mHtt or 3-NP (54).

FOXO3a translocation into the nucleus enables FOXO3a to activate its target genes. Here we show that FOXO3a target gene *FasL* is up-regulated in mutant Hdh cells and 3-NP-treated cortical neurons compared with WT Hdh cells and untreated neurons, respectively. In previous studies, controversial results considering FASL expression have been obtained with HD model cells and patient brain samples. Experiments with rat striata-derived cells expressing different N-terminal huntingtin fragments showed heightened *FasL* levels (55), whereas decreased FASL protein levels in the caudate and putamen but not in the parietal cortex of post-mortem human HD

brain have been reported (56). These differences could reflect different disease stages.

Our results reveal that in addition to *FasL*, *Foxo3a* mRNA levels are elevated in mutant *Hdh* cells and 3-NP-treated cortical neurons and most importantly in HD patient post-mortem caudate nucleus. Additionally, we show by chromatin immunoprecipitation and reporter assays that FOXO3a binds to and activates transcription from its own promoter, thus forming a positive feedback loop. Deletion and mutation analysis of *Foxo3a* promoter reporter constructs demonstrated that the principal FHRE required for FOXO3a protein to activate transcription from its own promoter is site 3, with perfect consensus sequence for FOXO3a binding. Although, comparison of our results from reporter assays with cortical neurons, WT and mutant *Hdh* cells reveals that the importance of different FHREs might vary slightly in different cell types and/or in response to mHtt expression. Previous studies have demonstrated the capacity of FOXO factors to directly activate *Foxo1* and *Foxo4* transcription (57, 58), and during the preparation of this manuscript, a paper was published by Lütznier *et al.* (59), describing the ability of FOXO3a to bind different FHREs in *Foxo3a* promoter by electrophoretic mobility shift assay and to up-regulate its own promoter in reporter assays. The latter work is in agreement with ours, suggesting positive feedback mechanism in the regulation of *Foxo3a* expression. Of the potential FHREs analyzed by Lütznier *et al. in vitro*, the highest affinity of FOXO3a was shown for site 1–2 FHREs (according to our numbering), but the functionality of these sites in cells was not demonstrated. Importantly, the site 3 FHRE, identified to be largely responsible for autoregulation in this study, was also bound by FOXO3a *in vitro* (59). We found that compared with *FasL*, the dynamics of *Foxo3a* regulation in response to 3-NP treatment in neurons differed. The levels of *FasL* mRNA increased earlier (at the 8-h time point), possibly because of nuclear translocation of already existing FOXO3a protein. The up-regulation of *Foxo3a* transcription followed later (at the 16-h time point), presumably requiring additional factors. Although the increased FOXO3a mRNA expression demonstrated in the current study could at least partially explain its higher protein levels in HD cells, it remains possible that differential regulation of FOXO3a relative half-life/degradation in the control and mutant Htt or 3-NP stressed cells is also part of the cause, especially because we demonstrated decreased levels of pERK, which has been shown to phosphorylate FOXO3a, promoting its degradation (24). Additionally, proteasomal degradation of many proteins has been shown to be interrupted by mutant HTT, although *in vivo* studies have given controversial results (60). In conclusion, the results presented here, as well as in previous studies, suggest that positive autoregulatory feedback loop helps to sustain the FOXO3a stress response and might be characteristic for FOXO family members in general.

In all of our Huntington disease models, mutant *Hdh* cells and 3-NP-treated primary neurons, we observed 1.5–2.5-fold elevated FOXO3a protein and/or mRNA levels. In R6/2 mice cortex, a tendency for increased expression was detected. Recent results, on the other hand suggested a ~60% reduction in FOXO3a levels in the striatum of 14-week-old HTT N171–83Q transgenic mice and a ~15% decrease in *Hdh*^{111/111} cells

(39). The reasons for these discrepant results remain unknown. However, we confirmed the specificity of the FOXO3a antibodies used here by RNAi-mediated knockdown of FOXO3a expression. Moreover, we found FOXO3a mRNA levels to be elevated more than 4-fold over control levels in HD patient caudate, further corroborating our results obtained in HD models.

Elevated FOXO3a activity in HD cells could lead to different outcomes: trigger cell death or promote survival by inducing stress resistance, and the result seems to depend on accompanying signals and factors (61). Previously, apoptosis has been described to be the primary cellular outcome of FOXO3a activation in neurons during growth factor deprivation or increased oxidative stress (62, 63). Given that BDNF levels were decreased and oxidative stress level was raised in HD (6, 43), it is possible that the increased FOXO3a levels observed in this study promote neuron death. Additionally, we detected up-regulated *FasL* expression along with risen FOXO3a, and previously, these changes were shown to lead to FASL-mediated apoptosis in motoneurons (64). Moreover, extrasynaptic *N*-methyl-D-aspartate receptor expression and signaling has been shown to be increased in medium spiny striatal neurons in HD, and nuclear translocation of FOXO3a has been suggested to contribute to *N*-methyl-D-aspartate receptor-dependent neuronal death (40, 65).

In contrast to the above, several lines of evidence support the protective role of FOXO factors in neurodegenerative disorders. For instance, FOXO3a and its *Caenorhabditis elegans* homologue *daf-16* have been shown to at least partially mediate the protective effect of sirtuins SIRT1 or sir-2.1 against mutant HTT toxicity in *Hdh*^{111/111} cells or in a nematode HD model, respectively (39, 66). However, the relationship might be more complex, because a recent study demonstrated that activation of SIRT1 and FOXO3a upon glucose deprivation in PC12 cells leads to differential outcomes depending on NGF availability (67). In addition, although WT FOXO3a overexpression and constantly active FOXO3a precipitate the loss of dopaminergic nigral neurons in acute oxidative stress conditions, it has been shown that FOXO3a is essential for reactive oxygen species detoxification in these neurons chronically exposed to chronic mild oxidative stress (41). Furthermore, it was demonstrated recently by Tourette *et al.* (68) that FOXO3a is an essential factor for survival of *Hdh*^{109/109} cells in stress conditions. Tourette *et al.* evaluated cell mortality in *Hdh*^{7/7} and *Hdh*^{109/109} cells in reduced serum condition along with decreased or increased FOXO3a levels. Although in *Hdh*^{7/7} cells changes in FOXO3a were not detrimental, in *Hdh*^{109/109} cells silencing FOXO3a significantly increased and overexpression of FOXO3a considerably decreased cell mortality (68). In conclusion, the results of the current study indicate that FOXO3a levels are risen in HD because of overactivated positive autoregulation loop, but further studies are needed to clarify whether FOXO3a activation is neuroprotective or detrimental in different stages of the disease.

Acknowledgments—We thank Epp Väli and Maila Rähn for technical assistance and Indrek Koppel for critical reading of the manuscript.

Increased FOXO3a Activity in Huntington Disease

REFERENCES

- Huntington's Disease Collaborative Research Group (1993) A novel gene containing a trinucleotide repeat that is expanded and unstable on Huntington's disease chromosomes. *Cell* **72**, 971–983
- Vonsattel, J. P., Myers, R. H., Stevens, T. J., Ferrante, R. J., Bird, E. D., and Richardson, E. P., Jr. (1985) Neuropathological classification of Huntington's disease. *J. Neuropathol. Exp. Neurol.* **44**, 559–577
- Gil, J. M., and Rego, A. C. (2008) Mechanisms of neurodegeneration in Huntington's disease. *Eur. J. Neurosci.* **27**, 2803–2820
- Zuccato, C., Valenza, M., and Cattaneo, E. (2010) Molecular mechanisms and potential therapeutic targets in Huntington's disease. *Physiol. Rev.* **90**, 905–981
- Sugars, K. L., and Rubinsztein, D. C. (2003) Transcriptional abnormalities in Huntington disease. *Trends Genet.* **19**, 233–238
- Zuccato, C., Ciammola, A., Rigamonti, D., Leavitt, B. R., Goffredo, D., Conti, L., MacDonald, M. E., Friedlander, R. M., Silani, V., Hayden, M. R., Timmusk, T., Sipione, S., and Cattaneo, E. (2001) Loss of huntingtin-mediated BDNF gene transcription in Huntington's disease. *Science* **293**, 493–498
- Zuccato, C., and Cattaneo, E. (2007) Role of brain-derived neurotrophic factor in Huntington's disease. *Prog. Neurobiol.* **81**, 294–330
- Gauthier, L. R., Charrin, B. C., Borrell-Pagès, M., Dompierre, J. P., Rangone, H., Cordelières, F. P., De Mey, J., MacDonald, M. E., Lessmann, V., Humbert, S., and Saudou, F. (2004) Huntingtin controls neurotrophic support and survival of neurons by enhancing BDNF vesicular transport along microtubules. *Cell* **118**, 127–138
- Ginés, S., Paoletti, P., and Alberch, J. (2010) Impaired TrkB-mediated ERK1/2 activation in Huntington's disease knock-in striatal cells involves reduced p52/p46 Shc expression. *J. Biol. Chem.* **285**, 21537–21548
- Brouillet, E., Hantraye, P., Ferrante, R. J., Dolan, R., Leroy-Willig, A., Kowall, N. W., and Beal, M. F. (1995) Chronic mitochondrial energy impairment produces selective striatal degeneration and abnormal choreiform movements in primates. *Proc. Natl. Acad. Sci. U.S.A.* **92**, 7105–7109
- Palfi, S., Ferrante, R. J., Brouillet, E., Beal, M. F., Dolan, R., Guyot, M. C., Peschanski, M., and Hantraye, P. (1996) Chronic 3-nitropropionic acid treatment in baboons replicates the cognitive and motor deficits of Huntington's disease. *J. Neurosci.* **16**, 3019–3025
- Brouillet, E., Jacquard, C., Bizat, N., and Blum, D. (2005) 3-Nitropropionic acid: a mitochondrial toxin to uncover physiopathological mechanisms underlying striatal degeneration in Huntington's disease. *J. Neurochem.* **95**, 1521–1540
- Panov, A. V., Gutekunst, C. A., Leavitt, B. R., Hayden, M. R., Burke, J. R., Strittmatter, W. J., and Greenamyre, J. T. (2002) Early mitochondrial calcium defects in Huntington's disease are a direct effect of polyglutamines. *Nat. Neurosci.* **5**, 731–736
- Puranam, K. L., Wu, G., Strittmatter, W. J., and Burke, J. R. (2006) Polyglutamine expansion inhibits respiration by increasing reactive oxygen species in isolated mitochondria. *Biochem. Biophys. Res. Commun.* **341**, 607–613
- Tang, T. S., Slow, E., Lupu, V., Stavrovskaya, I. G., Sugimori, M., Llinás, R., Kristal, B. S., Hayden, M. R., and Bezprozvanny, I. (2005) Disturbed Ca^{2+} signaling and apoptosis of medium spiny neurons in Huntington's disease. *Proc. Natl. Acad. Sci. U.S.A.* **102**, 2602–2607
- Salih, D. A., and Brunet, A. (2008) FoxO transcription factors in the maintenance of cellular homeostasis during aging. *Curr. Opin. Cell Biol.* **20**, 126–136
- van der Horst, A., and Burgering, B. M. (2007) Stressing the role of FoxO proteins in lifespan and disease. *Nat. Rev. Mol. Cell Biol.* **8**, 440–450
- Zhao, Y., Wang, Y., and Zhu, W. G. (2011) Applications of post-translational modifications of FoxO family proteins in biological functions. *J. Mol. Cell. Biol.* **3**, 276–282
- Calnan, D. R., Webb, A. E., White, J. L., Stowe, T. R., Goswami, T., Shi, X., Espejo, A., Bedford, M. T., Gozani, O., Gygi, S. P., and Brunet, A. (2012) Methylation by Set9 modulates FoxO3 stability and transcriptional activity. *Aging* **4**, 462–479
- Brunet, A., Bonni, A., Zigmond, M. J., Lin, M. Z., Juo, P., Hu, L. S., Anderson, M. J., Arden, K. C., Blenis, J., and Greenberg, M. E. (1999) Akt promotes cell survival by phosphorylating and inhibiting a Forkhead transcription factor. *Cell* **96**, 857–868
- Kops, G. J., and Burgering, B. M. (1999) Forkhead transcription factors: new insights into protein kinase B (c-akt) signaling. *J. Mol. Med.* **77**, 656–665
- Zheng, W. H., and Quirion, R. (2004) Comparative signaling pathways of insulin-like growth factor-1 and brain-derived neurotrophic factor in hippocampal neurons and the role of the PI3 kinase pathway in cell survival. *J. Neurochem.* **89**, 844–852
- Zhu, W., Bijur, G. N., Styles, N. A., and Li, X. (2004) Regulation of FOXO3a by brain-derived neurotrophic factor in differentiated human SH-SY5Y neuroblastoma cells. *Brain Res. Mol. Brain Res.* **126**, 45–56
- Yang, J. Y., Zong, C. S., Xia, W., Yamaguchi, H., Ding, Q., Xie, X., Lang, J. Y., Lai, C. C., Chang, C. J., Huang, W. C., Huang, H., Kuo, H. P., Lee, D. F., Li, L. Y., Lien, H. C., Cheng, X., Chang, K. J., Hsiao, C. D., Tsai, F. J., Tsai, C. H., Sahin, A. A., Muller, W. J., Mills, G. B., Yu, D., Hortobagyi, G. N., and Hung, M. C. (2008) ERK promotes tumorigenesis by inhibiting FOXO3a via MDM2-mediated degradation. *Nat. Cell Biol.* **10**, 138–148
- Furuyama, T., Nakazawa, T., Nakano, I., and Mori, N. (2000) Identification of the differential distribution patterns of mRNAs and consensus binding sequences for mouse DAF-16 homologues. *Biochem. J.* **349**, 629–634
- Hoekman, M. F., Jacobs, F. M., Smidt, M. P., and Burbach, J. P. (2006) Spatial and temporal expression of FoxO transcription factors in the developing and adult murine brain. *Gene Expr. Patterns* **6**, 134–140
- Brunet, A., Sweeney, L. B., Sturgill, J. F., Chua, K. F., Greer, P. L., Lin, Y., Tran, H., Ross, S. E., Mostoslavsky, R., Cohen, H. Y., Hu, L. S., Cheng, H. L., Jedrychowski, M. P., Gygi, S. P., Sinclair, D. A., Alt, F. W., and Greenberg, M. E. (2004) Stress-dependent regulation of FOXO transcription factors by the SIRT1 deacetylase. *Science* **303**, 2011–2015
- Sepp, M., Pruunsild, P., and Timmusk, T. (2012) Pitt-Hopkins syndrome-associated mutations in TCF4 lead to variable impairment of the transcription factor function ranging from hypomorphic to dominant-negative effects. *Hum. Mol. Genet.* **21**, 2873–2888
- Zuccato, C., Tartari, M., Crotti, A., Goffredo, D., Valenza, M., Conti, L., Cataudella, T., Leavitt, B. R., Hayden, M. R., Timmusk, T., Rigamonti, D., and Cattaneo, E. (2003) Huntingtin interacts with REST/NRSF to modulate the transcription of NRSE-controlled neuronal genes. *Nat. Genet.* **35**, 76–83
- Pruunsild, P., Sepp, M., Orav, E., Koppel, I., and Timmusk, T. (2011) Identification of cis-elements and transcription factors regulating neuronal activity-dependent transcription of human BDNF gene. *J. Neurosci.* **31**, 3295–3308
- Willems, E., Leys, L., and Vandesompele, J. (2008) Standardization of real-time PCR gene expression data from independent biological replicates. *Anal. Biochem.* **379**, 127–129
- Valenza, M., Rigamonti, D., Goffredo, D., Zuccato, C., Fenu, S., Jamot, L., Strand, A., Tarditi, A., Woodman, B., Racchi, M., Mariotti, C., Di Donato, S., Corsini, A., Bates, G., Pruss, R., Olson, J. M., Sipione, S., Tartari, M., and Cattaneo, E. (2005) Dysfunction of the cholesterol biosynthetic pathway in Huntington's disease. *J. Neurosci.* **25**, 9932–9939
- Beal, M. F., Brouillet, E., Jenkins, B. G., Ferrante, R. J., Kowall, N. W., Miller, J. M., Storey, E., Srivastava, R., Rosen, B. R., and Hyman, B. T. (1993) Neurochemical and histologic characterization of striatal excitotoxic lesions produced by the mitochondrial toxin 3-nitropropionic acid. *J. Neurosci.* **13**, 4181–4192
- Mangiarini, L., Sathasivam, K., Seller, M., Cozens, B., Harper, A., Hetherington, C., Lawton, M., Trotter, Y., Leach, H., Davies, S. W., and Bates, G. P. (1996) Exon 1 of the HD gene with an expanded CAG repeat is sufficient to cause a progressive neurological phenotype in transgenic mice. *Cell* **87**, 493–506
- Mojsilovic-Petrovic, J., Nedelsky, N., Boccitto, M., Mano, I., Georgiades, S. N., Zhou, W., Liu, Y., Neve, R. L., Taylor, J. P., Driscoll, M., Clardy, J., Merry, D., and Kalb, R. G. (2009) FOXO3a is broadly neuroprotective in vitro and in vivo against insults implicated in motor neuron diseases. *J. Neurosci.* **29**, 8236–8247
- Davila, D., Connolly, N. M., Bonner, H., Weisová, P., Dussmann, H., Concanon, C. G., Huber, H. J., and Prehn, J. H. (2012) Two-step activation of FOXO3 by AMPK generates a coherent feed-forward loop determining

- excitotoxic cell fate. *Cell Death Differ.* **19**, 1677–1688
37. Dávila, D., and Torres-Aleman, I. (2008) Neuronal death by oxidative stress involves activation of FOXO3 through a two-arm pathway that activates stress kinases and attenuates insulin-like growth factor I signaling. *Mol. Biol. Cell* **19**, 2014–2025
 38. Bahia, P. K., Pugh, V., Hoyland, K., Hensley, V., Rattray, M., and Williams, R. J. (2012) Neuroprotective effects of phenolic antioxidant tBHQ associate with inhibition of FoxO3a nuclear translocation and activity. *J. Neurochem.* **123**, 182–191
 39. Jiang, M., Wang, J., Fu, J., Du, L., Jeong, H., West, T., Xiang, L., Peng, Q., Hou, Z., Cai, H., Seredenina, T., Arbez, N., Zhu, S., Sommers, K., Qian, J., Zhang, J., Mori, S., Yang, X. W., Tamashiro, K. L., Aja, S., Moran, T. H., Luthi-Carter, R., Martin, B., Maudsley, S., Mattson, M. P., Cichewicz, R. H., Ross, C. A., Holtzman, D. M., Krainc, D., and Duan, W. (2012) Neuroprotective role of Sirt1 in mammalian models of Huntington's disease through activation of multiple Sirt1 targets. *Nat. Med.* **18**, 153–158
 40. Okamoto, S., Pouladi, M. A., Talantova, M., Yao, D., Xia, P., Ehrnhoefer, D. E., Zaidi, R., Clemente, A., Kaul, M., Graham, R. K., Zhang, D., Vincent Chen, H. S., Tong, G., Hayden, M. R., and Lipton, S. A. (2009) Balance between synaptic versus extrasynaptic NMDA receptor activity influences inclusions and neurotoxicity of mutant huntingtin. *Nat. Med.* **15**, 1407–1413
 41. Pino, E., Amamoto, R., Zheng, L., Cacquevel, M., Sarria, J. C., Knott, G. W., and Schneider, B. L. (2014) FOXO3 determines the accumulation of alpha-synuclein and controls the fate of dopaminergic neurons in the substantia nigra. *Hum. Mol. Genet.* **23**, 1435–1452
 42. Cattaneo, E., Zuccato, C., and Tartari, M. (2005) Normal huntingtin function: an alternative approach to Huntington's disease. *Nat Rev Neurosci.* **6**, 919–930
 43. Browne, S. E., and Beal, M. F. (2006) Oxidative damage in Huntington's disease pathogenesis. *Antioxid. Redox Signal.* **8**, 2061–2073
 44. Dudek, H., Datta, S. R., Franke, T. F., Birnbaum, M. J., Yao, R., Cooper, G. M., Segal, R. A., Kaplan, D. R., and Greenberg, M. E. (1997) Regulation of neuronal survival by the serine-threonine protein kinase Akt. *Science* **275**, 661–665
 45. Kauffmann-Zeh, A., Rodriguez-Viciana, P., Ulrich, E., Gilbert, C., Coffey, P., Downward, J., and Evan, G. (1997) Suppression of c-Myc-induced apoptosis by Ras signalling through PI(3)K and PKB. *Nature* **385**, 544–548
 46. Gines, S., Ivanova, E., Seong, I. S., Saura, C. A., and MacDonald, M. E. (2003) Enhanced Akt signaling is an early pro-survival response that reflects N-methyl-D-aspartate receptor activation in Huntington's disease knock-in striatal cells. *J. Biol. Chem.* **278**, 50514–50522
 47. Colin, E., Régulier, E., Perrin, V., Dürr, A., Brice, A., Aebischer, P., Déglon, N., Humbert, S., and Saudou, F. (2005) Akt is altered in an animal model of Huntington's disease and in patients. *Eur. J. Neurosci.* **21**, 1478–1488
 48. Apostol, B. L., Illes, K., Pallos, J., Bodai, L., Wu, J., Strand, A., Schweitzer, E. S., Olson, J. M., Kazantsev, A., Marsh, J. L., and Thompson, L. M. (2006) Mutant huntingtin alters MAPK signaling pathways in PC12 and striatal cells: ERK1/2 protects against mutant huntingtin-associated toxicity. *Hum. Mol. Genet.* **15**, 273–285
 49. Xia, Z., Dickens, M., Raingeaud, J., Davis, R. J., and Greenberg, M. E. (1995) Opposing effects of ERK and JNK-p38 MAP kinases on apoptosis. *Science* **270**, 1326–1331
 50. Perrin, V., Dufour, N., Raoul, C., Hassig, R., Brouillet, E., Aebischer, P., Luthi-Carter, R., and Déglon, N. (2009) Implication of the JNK pathway in a rat model of Huntington's disease. *Exp. Neurol.* **215**, 191–200
 51. Essers, M. A., Weijzen, S., de Vries-Smits, A. M., Saarloos, I., de Ruyter, N. D., Bos, J. L., and Burgering, B. M. (2004) FOXO transcription factor activation by oxidative stress mediated by the small GTPase Ral and JNK. *EMBO J.* **23**, 4802–4812
 52. Ju, T. C., Chen, H. M., Lin, J. T., Chang, C. P., Chang, W. C., Kang, J. J., Sun, C. P., Tao, M. H., Tu, P. H., Chang, C., Dickson, D. W., and Chern, Y. (2011) Nuclear translocation of AMPK-alpha potentiates striatal neurodegeneration in Huntington's disease. *J. Cell Biol.* **194**, 209–227
 53. Kittur, N., Darzacq, X., Roy, S., Singer, R. H., and Meier, U. T. (2006) Dynamic association and localization of human H/ACA RNP proteins. *RNA* **12**, 2057–2062
 54. Lee, J. M., Ivanova, E. V., Seong, I. S., Cashorali, T., Kohane, I., Gusella, J. F., and MacDonald, M. E. (2007) Unbiased gene expression analysis implicates the huntingtin polyglutamine tract in extra-mitochondrial energy metabolism. *PLoS Genet.* **3**, e135
 55. Sipione, S., Rigamonti, D., Valenza, M., Zuccato, C., Conti, L., Pritchard, J., Kooperberg, C., Olson, J. M., and Cattaneo, E. (2002) Early transcriptional profiles in huntingtin-inducible striatal cells by microarray analyses. *Hum. Mol. Genet.* **11**, 1953–1965
 56. Ferrer, I., Blanco, R., Cutillas, B., and Ambrosio, S. (2000) Fas and Fas-L expression in Huntington's disease and Parkinson's disease. *Neuropathol. Appl. Neurobiol.* **26**, 424–433
 57. Essaghir, A., Dif, N., Marbehant, C. Y., Coffey, P. J., and Demoulin, J. B. (2009) The transcription of FOXO genes is stimulated by FOXO3 and repressed by growth factors. *J. Biol. Chem.* **284**, 10334–10342
 58. Al-Mubarak, B., Soriano, F. X., and Hardingham, G. E. (2009) Synaptic NMDAR activity suppresses FOXO1 expression via a cis-acting FOXO binding site: FOXO1 is a FOXO target gene. *Channels* **3**, 233–238
 59. Lütznern, N., Kalbacher, H., Kronen-Herzig, A., and Rösl, F. (2012) FOXO3 is a glucocorticoid receptor target and regulates LKB1 and its own expression based on cellular AMP levels via a positive autoregulatory loop. *PLoS One* **7**, e42166
 60. Wang, J., Wang, C. E., Orr, A., Tydlacka, S., Li, S. H., and Li, X. J. (2008) Impaired ubiquitin-proteasome system activity in the synapses of Huntington's disease mice. *J. Cell Biol.* **180**, 1177–1189
 61. Neri, C. (2012) Role and therapeutic potential of the pro-longevity factor FOXO and its regulators in neurodegenerative disease. *Front. Pharmacol.* **3**, 15
 62. Gilley, J., Coffey, P. J., and Ham, J. (2003) FOXO transcription factors directly activate bim gene expression and promote apoptosis in sympathetic neurons. *J. Cell Biol.* **162**, 613–622
 63. Lehtinen, M. K., Yuan, Z., Boag, P. R., Yang, Y., Villén, J., Becker, E. B., DiBacco, S., de la Iglesia, N., Gygi, S., Blackwell, T. K., and Bonni, A. (2006) A conserved MST-FOXO signaling pathway mediates oxidative-stress responses and extends life span. *Cell* **125**, 987–1001
 64. Barthélémy, C., Henderson, C. E., and Pettmann, B. (2004) Foxo3a induces motoneuron death through the Fas pathway in cooperation with JNK. *BMC Neurosci.* **5**, 48
 65. Dick, O., and Bading, H. (2010) Synaptic activity and nuclear calcium signaling protect hippocampal neurons from death signal-associated nuclear translocation of FoxO3a induced by extrasynaptic N-methyl-D-aspartate receptors. *J. Biol. Chem.* **285**, 19354–19361
 66. Parker, J. A., Arango, M., Abderrahmane, S., Lambert, E., Tourette, C., Catoire, H., and Néri, C. (2005) Resveratrol rescues mutant polyglutamine cytotoxicity in nematode and mammalian neurons. *Nat. Genet.* **37**, 349–350
 67. Fujino, K., Ogura, Y., Sato, K., and Nedachi, T. (2013) Potential neuroprotective effects of SIRT1 induced by glucose deprivation in PC12 cells. *Neurosci. Lett.* **557**, 148–153
 68. Tourette, C., Farina, F., Vazquez-Manrique, R. P., Orfila, A. M., Voisin, J., Hernandez, S., Offner, N., Parker, J. A., Menet, S., Kim, J., Lyu, J., Choi, S. H., Cormier, K., Edgerly, C. K., Bordiuk, O. L., Smith, K., Louise, A., Halford, M., Stacker, S., Vert, J. P., Ferrante, R. J., Lu, W., and Neri, C. (2014) The Wnt receptor Ryk reduces neuronal and cell survival capacity by repressing FOXO activity during the early phases of mutant huntingtin pathogenicity. *PLoS Biol.* **12**, e1001895

Appendix 3

Publication III

Mari Sepp, Hanna Vihma*, **Kaja Nurm***, Mari Urb*, Stephanie Cerceo Page, Kaisa Roots, Anu Hark, Brady J. Maher, Priit Pruunsild and Tõnis Timmusk (2017). The Intellectual Disability and Schizophrenia Associated Transcription Factor TCF4 Is Regulated by Neuronal Activity and Protein Kinase A. *J. Neurosci.* 37: 10516–10527. doi: 10.1523/JNEUROSCI.1151-17.2017.

* Equal contribution

The Intellectual Disability and Schizophrenia Associated Transcription Factor TCF4 Is Regulated by Neuronal Activity and Protein Kinase A

Mari Sepp,¹ Hanna Vihma,^{1*} Kaja Nurm,^{1*} Mari Urb,^{1*} Stephanie Cerceo Page,² Kaisa Roots,¹ Anu Hark,¹ Brady J. Maher,^{2,3,4} Prit Pruunsild,¹ and Tõnis Timmusk¹

¹Department of Chemistry and Biotechnology, Tallinn University of Technology, 12618 Tallinn, Estonia, ²Lieber Institute for Brain Development, Johns Hopkins Medical Campus, Baltimore, Maryland 21205, and ³Department of Psychiatry and Behavioral Sciences and ⁴Department of Neuroscience, Johns Hopkins School of Medicine, Baltimore, Maryland 21205

Transcription factor 4 (TCF4 also known as ITF2 or E2-2) is a basic helix-loop-helix (bHLH) protein associated with Pitt–Hopkins syndrome, intellectual disability, and schizophrenia (SCZ). Here, we show that TCF4-dependent transcription in cortical neurons cultured from embryonic rats of both sexes is induced by neuronal activity via soluble adenylyl cyclase and protein kinase A (PKA) signaling. PKA phosphorylates TCF4 directly and a PKA phosphorylation site in TCF4 is necessary for its transcriptional activity in cultured neurons and in the developing brain *in vivo*. We also demonstrate that *Gadd45g* (growth arrest and DNA damage inducible gamma) is a direct target of neuronal-activity-induced, TCF4-dependent transcriptional regulation and that TCF4 missense variations identified in SCZ patients alter the transcriptional activity of TCF4 in neurons. This study identifies a new role for TCF4 as a neuronal-activity-regulated transcription factor, offering a novel perspective on the association of TCF4 with cognitive disorders.

Key words: bHLH; E2-2; ITF2; neuronal activity; Pitt–Hopkins syndrome; schizophrenia

Significance Statement

The importance of the basic helix-loop-helix transcription factor transcription factor 4 (TCF4) in the nervous system is underlined by its association with common and rare cognitive disorders. In the current study, we show that TCF4-controlled transcription in primary cortical neurons is induced by neuronal activity and protein kinase A. Our results support the hypotheses that dysregulation of neuronal-activity-dependent signaling plays a significant part in the etiology of neuropsychiatric and neurodevelopmental disorders.

Introduction

Transcription factor 4 (TCF4, also called ITF2, SEF2, and E2-2) is a dosage-sensitive gene with emerging functions in the nervous

system (Quednow et al., 2012; Sweatt, 2013; Forrest et al., 2014). It is one of the three mammalian genes coding for ubiquitous class A basic helix-loop-helix (bHLH) factors, also referred to as E-proteins, that regulate transcription via binding Ephrussi box (E-box) DNA elements (CANNTG) as homodimers or as heterodimers with tissue-specific bHLH factors (Massari and Murre, 2000). *TCF4* is transcribed from multiple promoters, resulting in a repertoire of functionally different protein isoforms with distinct N termini (Sepp et al., 2011).

TCF4 knock-out mice die at birth and reduction of *tcf4* expression in zebrafish leads to a general delay in embryogenesis, indicating its importance in development (Zhuang et al., 1996;

Received April 20, 2017; revised Sept. 10, 2017; accepted Sept. 16, 2017.

Author contributions: M.S., B.J.M., and T.T. designed research; M.S., H.V., K.N., M.U., S.C.P., K.R., A.H., and P.P. performed research; M.S., H.V., K.N., M.U., S.C.P., K.R., A.H., B.J.M., P.P., and T.T. analyzed data; M.S., P.P., and T.T. wrote the paper.

This work was supported by Estonian Research Council (institutional research funding IUT19-18 Grants 7257 and 8844), the National R&D program "Health" (Grant AR12098), the European Union through the European Regional Development Fund (Project No. 2014-2020.4.01.15-0012) and H2020-MSCA-RISE-2016 (EU734791), the Estonian Academy of Sciences, and the Pitt Hopkins Research Foundation and Million Dollar Bike Ride Pilot Grant Program for Rare Disease Research at UPenn Orphan Disease Center (Grants MDDR-16-122-PHP and MDDR-17-127-Pitt Hopkins). B.J.M. was supported by the Lieber Institute of the National Institutes of Health (Grant R56MH104593), the National Institutes of Health (Grant R01MH110487), a NARSAD Young Investigator Award, and a Pitt Hopkins Research Foundation Award. We thank Indrek Koppel for constructive discussions and critical reading of the manuscript; Epp Väli and Maila Rahn for technical assistance; Buket Basmanav for sharing data about TCF4 mutations in schizophrenia patients; and Hilmar Bading for pRV1, pH21, pFDelta6, and rAAV-U6-shRNA-mCherry constructs.

The authors declare no competing financial interests.

P. Pruunsild's present address: Department of Neurobiology, Interdisciplinary Center for Neurosciences, University of Heidelberg, 69120 Heidelberg, Germany.

*H.V., K.N., and M.U. contributed equally to this work.

Correspondence should be addressed to either Mari Sepp or Tõnis Timmusk, Department of Chemistry and Biotechnology, Tallinn University of Technology, Akadeemia tee 15, 12618 Tallinn, Estonia. E-mail: mari.sepp@ttu.ee or tonis.timmusk@ttu.ee.

DOI:10.1523/JNEUROSCI.1151-17.2017

Copyright © 2017 the authors 0270-6474/17/3710516-12\$15.00/0

Bergqvist et al., 2000; Brockschmidt et al., 2011). The correct E-protein dose is crucial for survival even after development has been completed, as demonstrated in fruit flies (Tamberg et al., 2015). The wide spatiotemporal expression pattern of *TCF4* in the mammalian nervous system suggests its involvement in all stages of brain development, including proliferation, differentiation, migration, and synaptogenesis, as well as in adult brain plasticity (Quednow et al., 2014). Consistently, *in vitro* studies with neural cells have provided support for its role in proliferation (Chen et al., 2014; Hill et al., 2017), cell cycle arrest (Schmidt-Edelkraut et al., 2014), survival, and epithelial-mesenchymal transition and ribosome biogenesis (Forrest et al., 2013; Slomnicki et al., 2016). *In vivo* evidence exists for the involvement of TCF4 in cell cycle exit during postnatal neurogenesis in forebrain (Fischer et al., 2014), migration of pontine nucleus and cortical neurons (Flora et al., 2007; Chen et al., 2016), formation of prefrontal cortical minicolumns (Page et al., 2017), and neurite branching restriction in olfactory neurons (D'Rozario et al., 2016). In addition, enhanced spontaneous activity of prefrontal neurons has been demonstrated recently in rats with *in utero* *TCF4* gain-of-function (Page et al., 2017), whereas decreased excitability of prefrontal neurons and enhanced long-term potentiation in the CA1 area of the hippocampus have been reported in rats with *in utero* suppression of *Tcf4* and/or *Tcf4* heterozygous knock-out mice, respectively (Kennedy et al., 2016; Rannals et al., 2016). Behavioral analyses of *Tcf4* heterozygous knock-out mice and transgenic mice with mild *Tcf4* overexpression in forebrain have revealed impaired sensorimotor gating and compromised learning and memory (Brzózka et al., 2010; Kennedy et al., 2016). Moreover, gating and cognitive functions are influenced by common *TCF4* variants in humans (Quednow et al., 2014).

Mutations in one of the *TCF4* alleles cause Pitt–Hopkins syndrome (PTHS), a rare congenital disorder characterized by severe mental and motor deficits, gastrointestinal problems, and autistic-like behavior (Sweett, 2013). PTHS-associated *TCF4* alleles vary from hypomorphic to dominant-negative (DN) and missense mutations are congregated in the C-terminal bHLH coding exon (Forrest et al., 2012; Sepp et al., 2012; Tamberg et al., 2015). Upstream *TCF4* mutations that do not affect all alternative isoforms have been linked to mild to moderate nonsyndromic intellectual disability (Kharbanda et al., 2016; Maduro et al., 2016). Single nucleotide polymorphisms in *TCF4* are among the genome-wide significant markers associated with schizophrenia (SCZ) (Schizophrenia Working Group of the Psychiatric Genomics Consortium, 2014) and rare *TCF4* coding variants outside of the bHLH exon have been identified in sporadic SCZ cases (Hu et al., 2014; Basmanav et al., 2015). Therefore, *TCF4* is a pleiotropic gene that links common and rare cognitive disorders. One of the shared causes for different cognitive disorders, including intellectual disability, autism spectrum disorder, bipolar disorder, and SCZ, may be disruption of synaptic activity-induced signaling and transcription (West and Greenberg, 2011; Ebert and Greenberg, 2013; Cross-Disorder Group of the Psychiatric Genomics Consortium, 2013; Schizophrenia Working Group of the Psychiatric Genomics Consortium, 2014). This pathway is critical for normal brain development, its responses to external stimuli, as well as for learning and memory. Here, we show that TCF4-controlled transcription in neurons is induced by neuronal activity via the cAMP pathway and is altered by *TCF4* missense variations identified in SCZ patients.

Materials and Methods

Constructs and siRNAs. The pcDNA3.1 constructs encoding TCF4 isoforms or ASCL1, pCAG-TCF4-A⁻, pCAG-GFP, reporter vectors pGL4.29 [luc2P/12μE5/Hygro], pGL4[luc2P/12μE5/TK/Hygro], pGL4[hRlucP/min/Hygro], and pGL4.83[hRlucP/EF1α/Puro] have been described previously (Sepp et al., 2011; Sepp et al., 2012; Page et al., 2017). For pcDNA-EF1α-TCF4-B⁻, pcDNA-EF1α-TCF4-A⁻, pcDNA-EF1α-TCF4-A⁻-V5/His, pcDNA-EF1α, pcDNA-SRα-ASCL1, and pcDNA-SRα the cytomegalovirus (CMV) promoter in the respective pcDNA3.1 constructs was replaced with elongation factor 1α (*EF1α*) promoter from pGL4.83 [hRlucP/EF1α/Puro] or synthetic SRα promoter (AY613994: 3403–4025). pACT (Promega) and pCMV-Tag2 (Agilent Technologies) vectors were used for the generation of constructs encoding for VP16- or Flag-fused N-terminal TCF4 deletants TCF4-M217(I⁻), TCF4-G316(NaeI), TCF4-S363(XbaI), TCF4-M430(NcoI), and TCF4-P498(PaeI), named according to the first included amino acid of TCF4-B⁻. C-terminally HA-tagged constitutively active and dominant negative forms of PKCα coding constructs pHACE-PKCαCAT (Addgene plasmid #21234) and pHACE-PKCαDN (Addgene plasmid #21235) have been described previously (Soh and Weinstein, 2003). Coding sequences of constitutively active S218D, S222D mutant of MEK (MAPK/ERK kinase) obtained from pBabe-Puro-MEK-DD (Addgene plasmid #15268) (Boehm et al., 2007), PKA catalytic subunit Cα obtained from pCaEV (Addgene plasmid #15310) (Uhler and McKnight, 1987) and a DN mutant of the PKA RI subunit (Clegg et al., 1987) were inserted into pQM-CMV-E2-N vector (Icosagen) behind the E2-tag. Sequences encoding constitutively active forms of CAMK2B (M1-C290) and CAMK4 (M1-K316) were PCR amplified from pWZL-Neu-Myr-Flag-CAMK2B (Addgene plasmid #20439) and pWZL-Neu-Myr-Flag-CAMK4 (Addgene plasmid #20441), respectively (Boehm et al., 2007), and inserted into pCMV-Tag2 (Stratagene) behind the Flag-tag. For pGL4.83[hRlucP/PGK1/Puro] mouse 3-phosphoglycerate kinase 1 (PGK1) promoter sequence (ChrX:103382066–103382573 according to NCBI37) was inserted into pGL4.83[hRlucP/Puro] (Promega). For pGL4.15[luc2P/Gadd45g/Hygro] human growth arrest, a DNA-damage-inducible protein 45 gamma (*GADD45G*) promoter sequence (chr9:92219712–92219956 according to hg19) was inserted into pGL4.15 [luc2P/Hygro] (Promega). Mutagenesis of the *GADD45G* promoter and *TCF4* was performed using complementary primers containing the respective mutation and Phusion High-Fidelity DNA polymerase (Finnzymes). pG5luc vector containing GAL4 binding sites is from Promega and pEGFP-C1 from Clontech. The shRNAs-encoding AAV *cis*-constructs were prepared by inserting annealed oligos into rAAV-U6-shRNA-mCherry (Lau and Bading, 2009). The shRNAs targeted the following sequences: rat *TCF4* exon 12 5'-CCGGAACAGACAGTATAATG-3', rat *TCF4* exon 20 5'-CGTGCGAGAAAGGAACCTGA-3', and scrambled 5'-CACTACCGTTGTTATAGGTG-3'. The scrambled siRNA Silencer Negative control #1 and *TCF4*-specific siRNAs 12 I, 12 II, 20 II (Sepp et al., 2011) and 20 I (forward: 5'-GUGCGAGAAAGGAACCGATT-3', reverse: 5'-UCAGGUUCCUUUCGCACTT-3') were from Ambion.

Cell culture and transfections. Human embryonic kidney HEK-293 (RRID:CVCL_0045) and HEK-293FT (RRID:CVCL_6911) cells were grown in MEM (PAA Laboratories) or DMEM (PAN-Biotech), respectively, supplemented with 10% fetal bovine serum, 100 U/ml penicillin, and 0.1 mg/ml streptomycin (all from PAA Laboratories). For transfection of HEK-293 cells, 0.375 μg of DNA and 0.75 μl of LipoD293 reagent (SigmaGen) were used per well of a 48-well plate or scaled up accordingly. For cotransfections, equal amounts of pGL4.29[luc2P/12μE5/Hygro], pGL4[hRlucP/min/Hygro], and effector constructs were used. For transfection of HEK-293FT cells, 10 μg of pFlag-TCF4 or empty vector, 10 μg of pQM-CMV-E2-PKA-Cα, and 40 μg of PEI (Sigma-Aldrich) were used per 10 cm plate.

Rat hippocampal and cortical mixed neuronal cultures from Sprague Dawley rat embryonic day 22.5 (E22.5) embryos were obtained and maintained as described previously (Pruunsild et al., 2011). Animal procedures were approved by the local ethics committee. For most experiments, neuronal cultures were transfected at 6–7 d *in vitro* (DIV) in Neurobasal A medium (Invitrogen); for experiments with bicuculline and 4-aminopyridine (4-AP), the transfections were performed at 10 DIV

in transfection medium (Bading et al., 1993) consisting 9:1 of salt-glucose-glycine solution containing the following (in mM): 10 HEPES, pH 7.4, 114 NaCl, 26.1 NaHCO₃, 5.3 KCl, 1 MgCl₂, 2 CaCl₂, 1 glycine, 30 glucose, and 0.5 sodium pyruvate, along with minimum Eagle's medium (with Earle's salt, without L-glutamine; Capricorn Scientific) supplemented with insulin (6.3 μg/ml), transferrin (5.7 μg/ml), and sodium selenite (7.5 ng/ml) (ITS; Sigma-Aldrich). 0.25 μg of effector protein(s) coding construct(s), 0.25 μg of firefly luciferase construct pGL4.29[luc2P/12μE5/TK/Hygro], pG5luc or pGL4.15[luc2P/GADD45G/Hygro], 10 or 20 ng of *Renilla* luciferase construct pGL4.83[hRlucP/EF1α/Puro] or pGL4.83[hRlucP/PGK1/Puro], and 1 μl of Lipofectamine 2000 reagent (Invitrogen) were used per well of a 48-well plate. For cotransfection of effectors 0.125 μg of pcDNA-EF1α-TCF4-A⁻ or pcDNA-EF1α and 0.125 μg of pcDNA-SRα-ASCL1 or pcDNA-SRα were used. In siRNA cotransfection experiments, 4.8 pmol of siRNA, 0.5 μg of DNA and 1 μl of RNAiMAX reagent (Invitrogen) were used per well of a 48-well plate. Forty hours after transfection, 25 mM KCl, 1 mM dbcAMP (dibutyl cAMP; Serva), or 1 μM phorbol 12,13-dibutyrate (PDBu; Sigma-Aldrich) was added to the culture medium for 8 h. Treatments with 50 μM bicuculline (Sigma-Aldrich) and 0.5 mM 4-AP (Tocris Bioscience) were performed 3 d after transfection for 8 h. When indicated, 5 μM nifedipine, 1 μM tetrodotoxin, 10 μM MK801, 10 μM KN-62, 10 μM H89, 10 μM Go 6983, 2 μM Go 6976, 10 μM UO126, and 10 μM TBB (all from Tocris Bioscience), 5 μM STO-609 (Sigma-Aldrich), 50 μM ddAdo (Santa Cruz Biotechnology), 50 μM APV or 30 μM KH7 (both from Cayman Chemicals) were added to the culture medium 15 min before addition of KCl or bicuculline and 4-AP.

Nucleofection and transduction of neurons. Amaxa nucleofection of neurons was performed as described previously (Pruunsild et al., 2011) using the Amaxa Rat Neuron Nucleofector Kit and O-003 program of the Nucleofector II (Lonza). The chimeric particles of adeno-associated viruses (AAV) 1 and 2 were produced as described previously (Koppel et al., 2015) using AAV1 helper pRV1, AAV2 helper pH21, adenovirus helper pFdelt6, and *Tcf4* specific or scrambled shRNAs encoding rAAV-U6-shRNA-mCherry *cis*-constructs. Primary neurons were transduced at 2 DIV. Nucleofected or AAV-transduced neurons were treated with 25 mM KCl for 6 h and harvested at 5 or 8 DIV, respectively.

In utero electroporations and histochemistry. *In utero* electroporation of pregnant Wistar rats and histochemistry were performed as described previously (Page et al., 2017). Briefly, pCAG-GFP DNA, alone or with either pCAG-TCF4-A⁻ or pCAG-TCF4-A⁻S448A, was injected into single ventricle of an E16 embryo and targeted to medial prefrontal cortex by three electrode pulses (65 V, 100 ms). P21 male and female animals were transcardially perfused with 4% paraformaldehyde in PBS and brains were dissected and postfixed for 24 h. Coronal vibratome sections were prepared and analyzed by confocal microscopy (LSM 700; Zeiss). Images were analyzed in ImageJ (RRID:SCR_003070). The distribution of cells was quantified by binning pixel intensities perpendicular to the medial surface and the coefficient of variance (CV) of these values was used as a measure of cellular distribution, with low CV indicating a uniform distribution and high CV indicating clustering of cells.

Immunocytochemistry. Immunocytochemistry was performed as described previously (Sepp et al., 2011) using the following antibodies: rabbit polyclonal anti-TCF4 (CeMines, 1:200), rabbit polyclonal anti-V5 (Sigma-Aldrich catalog #V8137; RRID:AB_261889, 1:2000), mouse monoclonal anti-tubulin III (Merck-Millipore catalog #MAB1637; RRID:AB_2210524, 1:2000), and goat anti mouse/rabbit IgG conjugated with Alexa Fluor 405, 488, 546, or 568 (Invitrogen, 1:2000). DNA was stained with DRAQ5 (1:5000; Biostatus Limited) or DAPI (Invitrogen). Samples were mounted in ProLong Gold reagent (Invitrogen) and analyzed by confocal microscopy (LSM Duo; Zeiss).

Protein electrophoresis and Western blotting. Preparation of whole-cell lysates in RIPA buffer (50 mM Tris HCl pH 8.0, 150 mM NaCl, 1% NP-40, 0.5% Na-Doc, 0.1% SDS, 1 mM DTT, 1 mM PMSF, Protease Inhibitors Cocktail Complete; Roche) and Western blotting have been described previously (Sepp et al., 2012). The following antibodies were used: rabbit polyclonal anti-TCF4 (CeMines, 1:1000), rabbit polyclonal anti-Flag (Sigma-Aldrich catalog #F7425; RRID:AB_439687, 1 μg/ml), rabbit polyclonal anti-HA (Sigma-Aldrich catalog #H6908; RRID:AB_260070,

1:1000), monoclonal anti-V5 (Thermo Fisher Scientific catalog #R960-25; RRID:AB_2556564, 1:5000), mouse monoclonal anti-E2 (5E11; Icosagen catalog #A-100-100; RRID:AB_11133493, 1:5000), mouse monoclonal anti-VP16 (2GV-4; Eurogentec, 1:5000), and HRP-conjugated goat anti mouse/rabbit IgG (Pierce, 1:5000).

Luciferase and electrophoretic mobility shift assays. Luciferase assays were performed as described previously (Sepp et al., 2011) using Passive Lysis Buffer (Promega) and the Dual-Glo Luciferase Assay (Promega). HEK-293 cell were lysed at 24 h and neurons at 48 h after transfection. Electrophoretic mobility shift assay was performed as described previously (Sepp et al., 2012) using *in vitro* translated proteins produced with TnT Quick Coupled Transcription/Translation System (Promega) and ³²P-labeled μE5 E-box oligos.

Immunoprecipitations and in vitro kinase assay. Coimmunoprecipitation was performed as described previously (Kazantseva et al., 2009). HEK-293FT cells overexpressing Flag-TCF4 and/or E2-PKA-Cα proteins were lysed 2 d after transfection and 1 mg of protein lysate was subjected to immunoprecipitation with 20 μl of anti-Flag M2 Affinity Gel (Sigma-Aldrich catalog #A2220; RRID:AB_10063035). ChIPs were performed as described previously (Kannike et al., 2014) using DIV 7 cultures of rat primary neurons, TCF4 (Cemines), or acetyl-histone H4 antibodies (Millipore catalog #06-866; RRID:AB_310270), and protein A-Sepharose slurry (GE Healthcare). PKA kinase assay was performed as described previously (Cox et al., 2000) with modifications. Briefly, HEK-293 transfected with pFlag-TCF4 constructs were lysed in RIPA buffer, diluted 1:9 in IP buffer (50 mM Tris-HCl pH 7.4, 150 mM NaCl, 1 mM EDTA, 1% Triton X-100, 1 mM DTT, Protease Inhibitor Cocktail Complete; Roche), and Flag-TCF4 proteins were immunoprecipitated using 12 μl of anti-Flag M2 Affinity Gel per 1 mg of protein lysate. HEK-293 transfected with E2-tagged PKA-Cα encoding construct were lysed in HO buffer [50 mM HEPES pH 7.5, 100 mM NaCl, 1% NP-40, 2 mM EDTA, 1 mM DTT, Protease Inhibitor Cocktail Complete (Roche), and phosphatase inhibitor cocktail PhosStop (Roche)] and E2-PKA-Cα was immunoprecipitated using 1 μg of mouse monoclonal anti-E2 (5E11; Icosagen catalog #A-100-100; RRID:AB_11133493) and 12 μl of Protein A Sepharose CL-4B (GE Healthcare) per 1 mg of protein lysate. Immune complexes were washed 4 times with IP or HO buffer, respectively, once with kinase buffer (50 mM HEPES, pH 7.5, 10 mM MgCl₂, 1 mM EGTA, 0.014% Tween 20), and resuspended in kinase buffer. Kinase reactions were performed by mixing Flag-TCF4 and E2-PKA-Cα immune complexes with 5 μM ATP and 1.67 μM [γ -³²P]ATP (6000 Ci/mmol) and incubated at 30°C for 30 min. The samples were resolved in 10% SDS-PAGE and phosphorylated proteins were visualized by autoradiography.

Reverse transcription and quantitative PCR. RNA extraction, reverse transcription, and quantitative PCR using cDNA or ChIP gDNA as template were performed as described previously (Sepp et al., 2012). The following primers were used: *Gadd45g* forward: 5'-TGTCTGACCGCTGGCGTCTA-3', reverse: 5'-AAGTCCACATTGTCAGGGTCCACA-3'; *Tcf4* exons 10–11 (Sepp et al., 2011), *Hprt1* and an unrelated rat chromosomal region (Kannike et al., 2014), and *Gadd45g* promoter F: 5'-GCTCCAGTCTGCTGGTAAACA-3', R: 5'-GCCTCAAATCTGCCGCTTTTGT-3'.

Experimental design and statistical analyses. Based on our previously published data from similar experiments and standards in the field, the sample sizes were selected as follows: three to five biological replicates for reporter assays and mRNA levels quantifications and seven biological replicates for *in utero* transfections. Biological replicates represent independent animals, primary cultures from different litters or cultures of cell lines at separate times. For each independent experiment, luciferase assays and qPCRs were performed in technical duplicates or triplicates, respectively. For most experiments, balanced design was used; however, for the analyses of TCF4 N-terminal deletion mutants and pharmacological modulators of signaling pathways, the experiments were performed in subsamples that resulted in larger sample sizes for conditions used as controls. In Figure 3d, $n = 7$ for vector and VP16-TCF4-M217 (I⁻), $n = 4$ for VP16-TCF4-G316 and VP16-TCF4-S363, and $n = 3$ for VP16-TCF4-M430 and VP16-TCF4-P498. In Figure 3e, $n = 8$ for vector, $n = 4$ for VP16-TCF4-S363 and VP16-TCF4-M430, and $n = 3$ for VP16-TCF4-G316 and VP16-TCF4-P498. In Figure 4, a and c, in case of *CMV*-

TCF4 $n = 12$ for CNTR and KCl only; $n = 7$ for vehicle + KCl; $n = 4$ for STO-609, Go 6976, ddAdo, KH7, and vehicle only; and $n = 3$ for KN-62, H89, Go 6983, U0126, TBB, dbcAMP, and PDBu; in case of *EF1 α* -TCF4 $n = 11$ for CNTR and KCl only, $n = 8$ for dbcAMP; $n = 7$ for vehicle + KCl; $n = 5$ for Go 6976; $n = 4$ for STO-609, Go 6983, and vehicle only; and $n = 3$ for KN-62, H89, U0126, TBB, ddAdo, KH7, and PDBu. The normalized data from luciferase assays and qRT-PCR analyses were subjected to log transformation, mean centering, and unit variance scaling to obtain normal and comparable distributions. ChIP-qPCR data were log-transformed; the CV values of cell distribution were not transformed. Statistical significance was tested using Prism 6 software (GraphPad, RRID:SCR_002798) by unpaired two-sided *t* tests or by one-way or two-way between-subjects ANOVA followed by Bonferroni's or Dunnett's multiple-comparisons tests as specified in the Results section and figure legends. The degrees of freedom, *p*-values and effect sizes (η_p^2 or r^2 values for ANOVA or *t* tests, respectively) are reported in the Results section for each experiment. The *post hoc* tests and the comparisons made are specified in the figure legends. If needed, the calculated means were back transformed for graphical presentation. Error bars in the figures indicate SEM.

Results

TCF4-controlled transcription is activity regulated in neurons

Previously, we have described numerous human TCF4 isoforms that differ in their N termini and internal sequences due to alternative 5' exon usage and splicing (Sepp et al., 2011). TCF4 isoforms are briefly characterized by the following: the DNA-binding bHLH domain and the transactivation domain AD2 are present in all isoforms; the transactivation domain AD1 and the nuclear localization signal (NLS) are present only in isoforms with longer N termini; the NLS is absent from TCF4 Δ isoforms; and 4 extra amino acids upstream of the bHLH domain differentiate “+” isoforms from the “-” isoforms (Fig. 1*a*). To study the functioning of TCF4 isoforms in neurons we performed μ E5 (CACCTG) E-box-dependent reporter assays with selected isoforms (TCF4-A to TCF4-I) in DIV 8–9 rat primary neurons left untreated or treated with 25 mM KCl for 8 h to model neuronal activity. As shown in Figure 1*a*, the activation of E-box-controlled transcription by all studied TCF4 isoforms in neurons was induced by KCl-mediated depolarization of neuronal membranes (two-way ANOVA, treatment \times transfection interaction $F_{(13,84)} = 8.083$, $p < 0.0001$, $\eta_p^2(\text{interaction, treatment, transfection}) = 0.556, 0.917, 0.744$; $n = 4$). In depolarized neurons strong (>20-fold), transactivation was achieved with isoforms TCF4-B⁺, TCF4-B⁻, TCF4-B Δ ⁺, and TCF4-A⁺, medium (10- to 20-fold) with isoforms TCF4-B Δ ⁻, TCF4-C⁻, TCF4-C Δ ⁻, TCF4-D⁻, TCF4-A⁻, and TCF4-F⁻, and weak (<10-fold) with isoforms TCF4-H⁻, TCF4-I⁻, and TCF4-E⁻ (Fig. 1*a*).

Next, we aimed to verify that the depolarization-induced rise in TCF4-mediated transcription requires Ca²⁺ influx to neurons and is not caused by neuronal-activity-dependent upregulation of CMV promoter (Wheeler and Cooper, 2001), which was used above for overexpression of TCF4 isoforms. In these experiments, we used TCF4-A⁻, one of the dominant isoforms expressed in the nervous system (Sepp et al., 2011). We overexpressed TCF4-A⁻ from CMV promoter or from the neuronal-activity-nonresponsive *EF1 α* promoter and included a control condition in which depolarization was performed in the presence of nifedipine, a blocker of L-type voltage-gated Ca²⁺ channels (VGCCs). As shown in Figure 1, *b* and *c*, *EF1 α* -TCF4-mediated transcription in neurons was increased by membrane depolarization similarly to CMV-TCF4-mediated transcription, although, in contrast to CMV-TCF4-A⁻, the levels of *EF1 α* promoter-controlled TCF4-A⁻ protein remained stable after KCl treat-

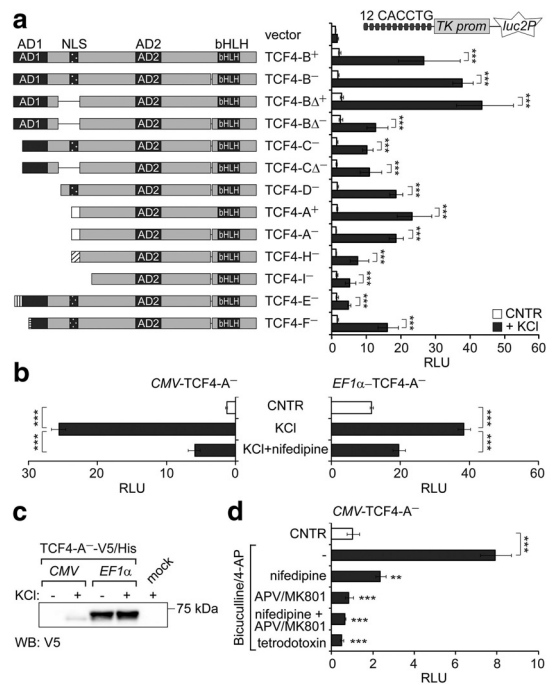


Figure 1. Identification of TCF4 as a neuronal activity-regulated transcription factor. The effects of membrane depolarization (*a*, *b*) and increased synaptic activity (*d*) on the induction of TCF4-controlled transcription in primary neurons are shown. Rat primary neurons were transfected with TCF4 isoforms encoding vectors, firefly luciferase construct carrying 12 μ E5 E-boxes in front of *TK* promoter, and *Renilla* luciferase construct with *EF1 α* promoter (*a*) or *PGK1* promoter (*b*, *d*). For overexpression of TCF4 isoforms, vectors containing *CMV* (*a*, *b*, *d*) or *EF1 α* (*c*) promoter were used. Transfected neurons were left untreated or treated with KCl (*a*, *b*) or bicuculline/4-AP (*d*) for 8 h. In *b* and *d*, tetrodotoxin, nifedipine, or APV/MK801 was used to block action potentials, VGCCs, or NMDARs, respectively. Luciferase activities were measured and data are presented as fold induced levels above the signals obtained from empty vector transfected untreated cells (*a*, *b*) or TCF4-A⁻-expressing untreated cells (*d*). Shown are the mean results from four independent experiments performed in duplicates. Error bars indicate SEM. * $p < 0.05$; ** $p < 0.01$; *** $p < 0.001$; two-way ANOVA followed by Bonferroni *post hoc* tests for comparisons across treatment (*a*) or by Dunnett's *post hoc* tests for comparisons with cells treated only with KCl (*b*) or bicuculline/4-AP (*d*). AD, Activation domain; RLU, relative luciferase units. *c*, Western blot analysis of C-terminally V5/His-tagged TCF4-A⁻ protein overexpressed from *CMV* or *EF1 α* promoter in primary neurons left untreated or treated with KCl for 8 h.

ment. The induction of TCF4-controlled transcription was effectively inhibited by nifedipine in both experimental setups (one-way ANOVA, CMV transfection $F_{(2,6)} = 168.8$, $p < 0.0001$, $\eta_p^2 = 0.983$, $n = 3$; *EF1 α* transfection $F_{(2,9)} = 83.98$, $p < 0.0001$, $\eta_p^2 = 0.949$, $n = 4$). Collectively, these data show that activation of E-box-controlled transcription by TCF4 in primary neurons is upregulated by membrane depolarization independent of isoform specificity or expression levels of TCF4.

To demonstrate that not only depolarization of neurons but also excitatory synaptic activity results in upregulation of TCF4-controlled transcription, we stimulated action potential firing in DIV 13 primary neuron cultures by application of the GABA type A receptor antagonist bicuculline together with the K⁺ channel blocker 4-AP (Hardingham et al., 2001). TCF4-A⁻-mediated transcription was increased in response to bicuculline/4-AP treatment and this induction was inhibited in the presence of the Na⁺ channel blocker tetrodotoxin (which prevents action potential generation), the L-type VGCC blocker nifedipine,

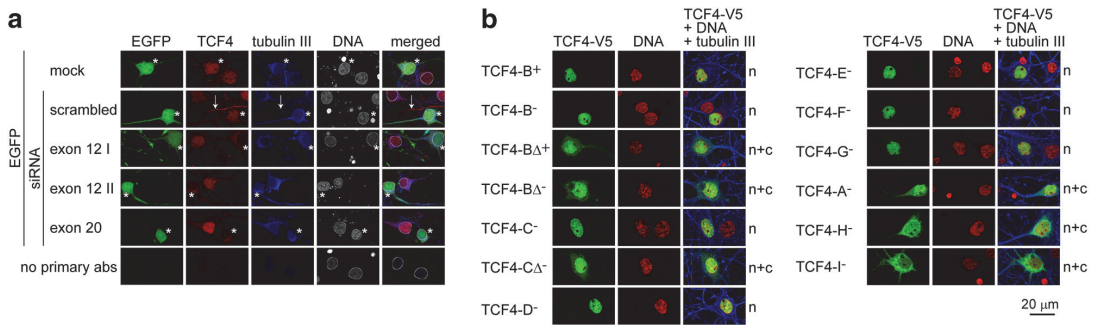


Figure 2. Intracellular distribution of endogenous and overexpressed V5-tagged TCF4 proteins in rat primary neurons. **a**, Neurons were cotransfected with *Tcf4* exon 12 or 20 specific siRNAs and an EGFP construct for identification of transfected cells (marked with asterisks); mock and scrambled siRNA transfections were performed in control. Arrows indicate nonspecific staining of glial processes with TCF4 antibodies. **b**, Neurons were transfected with TCF4–V5 constructs. Localization pattern is indicated at the right. n, Nuclear; n + c, nuclear and cytoplasmic. In **a** and **b**, tubulin III and DNA were stained to label neurons and nuclei (encircled in **a**), respectively.

and/or antagonists of *N*-methyl-D-aspartate subtype of glutamate receptors (NMDARs) 2-amino-5-phosphonoverate (APV) and MK801 (Fig. 1*d*, one-way ANOVA, $F_{(5,18)} = 24.18$, $p < 0.0001$, $\eta_p^2 = 0.870$, $n = 4$). This confirms that TCF4 is activity regulated in neurons and indicates that Ca^{2+} influx through L-type VGCCs and NMDARs is involved in triggering TCF4-controlled transcription in response to synaptic activity.

Endogenous and overexpressed TCF4 proteins are present in the nuclei of primary neurons

Next, we aimed to gain insights into the mechanisms that underlie neuronal-activity-dependent regulation of TCF4. We have shown previously that TCF4 is present in the nuclei of neurons in adult human hippocampal and cerebellar tissue sections (Sepp et al., 2011). However, in a recent study, the majority of TCF4 immunoreactivity was found in the neuronal cytoplasmic soma and dendrites of adult mouse brain (D’Rozario et al., 2016). To investigate whether the weak transactivation ability of TCF4 in primary neurons in basal conditions could be explained by the absence of TCF4 from the neuronal nuclei, we studied the distribution of TCF4 in primary neurons transfected with *Tcf4*-specific or scrambled siRNAs. In mock and scrambled siRNA-transfected neurons, we detected most of the TCF4-like signal in the nuclei, whereas in neurons transfected with three different *Tcf4*-specific siRNAs, the nuclear staining was severely reduced (Fig. 2*a*). Upon overexpression, the NLS-containing TCF4 isoforms localized to the nuclei, whereas NLS-lacking isoforms distributed to the nucleus and cytoplasm (Fig. 2*b*). These data demonstrate that, in primary neurons endogenous as well as overexpressed TCF4, proteins are present in the nuclei, corroborating our previous findings in adult human brain tissue and HEK-293 cells (Sepp et al., 2011). The differences between our results and findings by D’Rozario et al. (2016) could arise from the usage of different TCF4 antibodies. Here, we have confirmed the specificity of the endogenous nuclear signal in primary neurons, but the specificity of the endogenous cytoplasmic TCF4-like signal requires further validation, for example, by using TCF4 knock-out mice. We conclude that the regulation of TCF4 by neuronal activity cannot be attributed to its signal-dependent nuclear import.

Region between AD2 and bHLH is critical for neuronal-activity-dependent regulation of TCF4 functions

Because all assessed TCF4 isoforms were responsive to neuronal activity, we reasoned that the effect could be dictated by the common domains AD2 and/or bHLH. To elucidate the role of AD2, we compared the activities of a deletion mutant of TCF4-B⁻ that lacks AD2 but retains AD1 and the AD2-containing isoform TCF4-A⁻. In contrast to TCF4-A⁻, TCF4-B⁻ΔAD2 did not increase E-box-dependent reporter activity significantly above the vector control levels in depolarized neurons (Fig. 3*a*; two-way ANOVA, treatment × transfection interaction $F_{(2,12)} = 8.055$, $p = 0.0061$, $\eta_p^2(\text{interaction, treatment, transfection}) = 0.573, 0.811, 0.827$; $n = 3$). To study the activation domains independently of the bHLH domain, we used heterologous constructs in which AD1 or AD2 is fused with the GAL4 DNA-binding domain and the E2-tag. GAL4-AD2-E2, but not GAL4-AD1-E2, raised reporter transcription from GAL4 binding sites carrying promoter above the control levels. However, this upregulation was not activity dependent because an ~3.5-fold increase in reporter levels was recorded in GAL4-AD2-E2-expressing neurons in both basal and depolarized conditions (Fig. 3*b*; two-way ANOVA, treatment × transfection interaction $F_{(2,18)} = 3.762$, $p = 0.0431$, $\eta_p^2(\text{interaction, treatment, transfection}) = 0.295, 0.580, 0.980$; $n = 3$). These results indicate that AD2 is required for transactivation in neurons, but is not sufficient for neuronal-activity-dependent regulation of TCF4 functions.

Next, we made serial deletions of TCF4 N-terminal sequences starting with the shortest isoform TCF4-I⁻ and added SV40 LargeT NLS and the constitutively active VP16 transactivation domain to the N terminus of the deletants. VP16-TCF4-M217(I⁻), VP16-TCF4-G316, VP16-TCF4-S363, VP16-TCF4-M430, and VP16-TCF4-P498 (named according to the first included TCF4 aa using the TCF4-B sequence as a reference) were expressed at comparable levels in HEK-293 cells and bound μ E5 E-box *in vitro* (Fig. 3*c*). In HEK-293 cells, all VP16-TCF4 deletant proteins upregulated E-box-controlled transcription, even though the transactivation decreased concomitant with increased deletions in TCF4 (Fig. 3*d*; one-way ANOVA, transfection $F_{(5,22)} = 1264$, $p < 0.0001$, $\eta_p^2 = 0.997$, $n \geq 3$). Conversely, in rat primary neurons, overexpression of the shortest TCF4 deletant protein VP16-TCF4-P498 did not elicit induction of reporter activity in KCl-treated cells compared with untreated cells, whereas all other

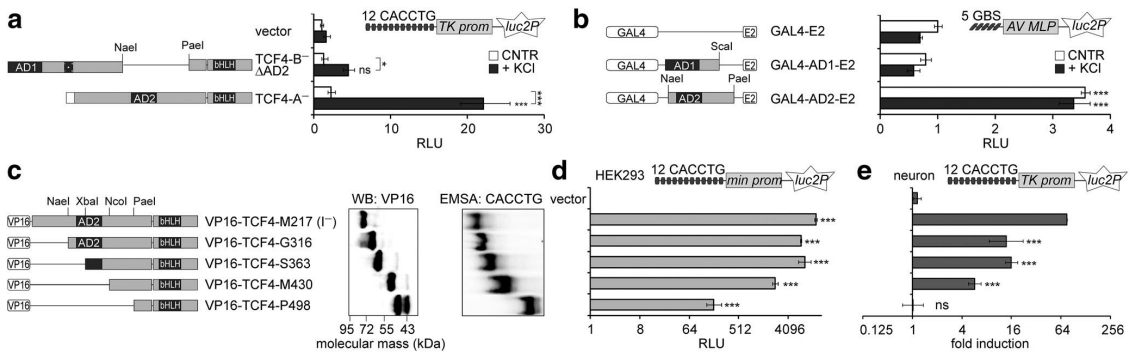


Figure 3. Mapping of the TCF4 regions required for its regulation by neuronal activity. *a, b, d, e*, Reporter assays with primary neurons (*a, b, e*) or HEK293 cells (*d*) transfected with *CMV* promoter containing constructs encoding TCF4 isoforms (*a*), E2-tagged GAL4 fusion proteins (*b*), or VP16-TCF4-I⁻ deletants (*d, e*) as indicated. Firefly luciferase constructs carrying μ E5 E-boxes (*a, d, e*) or GAL4-binding sites (*b*) and *Renilla* luciferase construct with *EF1 α* promoter were cotransfected. Neurons were left untreated or treated with KCl for 8 h. Data are presented as fold induced levels above the signals obtained from empty vector transfected untreated cells (*a, b, d*) or as fold induction of luciferase activity in KCl-treated neurons compared with untreated neurons (*e*). Shown are the means \pm SEM from at least three independent experiments (see Materials and Methods for details). Statistical significance shown with asterisks is relative to the reporter levels measured from untreated or KCl-treated cells of the first data point in each chart or between the bars connected with lines. * $p < 0.05$; ** $p < 0.01$; *** $p < 0.001$; two-way ANOVA followed by Bonferroni *post hoc* tests for comparisons across treatment and transfections (*a, b*) or one-way ANOVA followed by Dunnett's *post hoc* tests for comparisons with vector control (*d, e*). *c*, Western blot analysis of VP16-TCF4-I⁻ deletants expressed in HEK-293 cell and electrophoretic mobility shift assay (EMSA) for binding of μ E5 E-box by *in vitro* translated VP16-TCF4-I⁻ deletant proteins. AD, Activation domain; AV MLP, adenovirus major late promoter; GBS, GAL4 binding site; min, minimal promoter; RLU, relative luciferase units; TK, thymidine kinase promoter.

deletant proteins, including VP16-TCF4-M430, were able to mediate membrane depolarization-mediated induction of reporter activity (Fig. 3*e*; one-way ANOVA, transfection $F_{(4,17)} = 41.38$, $p < 0.0001$, $\eta_p^2 = 0.907$, $n \geq 3$). These results indicate that the TCF4 protein region between aa M430 and P498, in conjunction with the bHLH domain, is critical for activity-dependent regulation of TCF4.

PKA participates in the regulation of TCF4 functions by neuronal activity

In neurons, a membrane-depolarization-induced rise in intracellular Ca^{2+} levels activates many protein kinases, including Ca^{2+} -calmodulin kinases (CAMK), protein kinase A (PKA), protein kinase C (PKC), and mitogen-activated protein kinases (MAPKs) (Kotaleski and Blackwell, 2010). To elucidate which signaling pathways play a role in KCl-induced capacity of TCF4 to activate transcription in neurons, we tested whether inhibition of any of these kinases interferes with the induction. To exclude promoter-driven effects of the compounds on TCF4 levels, we performed parallel reporter experiments with TCF4-A⁻ constructs carrying the *CMV* or *EF1 α* promoter. Independent of the promoter used for TCF4-A⁻ overexpression, KCl-induced reporter levels were reduced significantly by the CAMK2 inhibitor KN-62 and the PKA inhibitor H89, but not by the CAMKK inhibitor STO-609, the Ca^{2+} -dependent PKC isoform inhibitor Go 6976, or an unrelated casein kinase inhibitor TBB (Fig. 4*a*; one-way ANOVA, *CMV* transfection $F_{(10,39)} = 54.48$, $p < 0.0001$, $\eta_p^2 = 0.933$, $n \geq 3$; *EF1 α* transfection $F_{(10,39)} = 10.44$, $p < 0.0001$, $\eta_p^2 = 0.728$, $n \geq 3$). Inconsistent results were obtained with the pan-PKC inhibitor Go 6983 and the MEK inhibitor U0126 in the two experimental settings, possibly pointing to nonspecific effects. Next, we tested whether coexpression of constitutively active (CAT) forms of CAMK2B, CAMK4 (Sun et al., 1994), PKA (Uhler and McKnight, 1987), PKC (Soh and Weinstein, 2003), or MEK (Huang and Erikson, 1994) is able to trigger TCF4-dependent transcription in neurons grown in basal conditions. The results of this assay showed that constitutively active PKA catalytic subunit α and, to lesser extent, also PKC α CAT, was able

to induce the reporter activity (Fig. 4*b*; one-way ANOVA, transfection $F_{(5,12)} = 75.66$, $p < 0.0001$, $\eta_p^2 = 0.969$, $n = 3$). We then focused on PKA and PKC and studied the effects of chemical activators and DN forms of these kinases on TCF4-dependent transcription in neurons. As demonstrated in Figure 4*c*, the reporter activity was upregulated by treatment with PKA activator dibutyryl cAMP (dbcAMP) and not with PKC activator PDBu independent of the promoter used for TCF4-A⁻ overexpression (one-way ANOVA, *CMV* transfection $F_{(3,18)} = 33.69$, $p < 0.0001$, $\eta_p^2 = 0.849$, $n \geq 3$; *EF1 α* transfection $F_{(3,22)} = 10.45$, $p = 0.0002$, $\eta_p^2 = 0.588$, $n \geq 3$). Consistently, induction of TCF4-dependent transcription by KCl-treatment was reduced by coexpression of the DN PKA-regulatory subunit R1 (Clegg et al., 1987) and not by coexpression of DN PKC α (Soh and Weinstein, 2003) in neurons (Fig. 4*d*; one-way ANOVA, transfection $F_{(2,6)} = 14.40$, $p = 0.0051$, $\eta_p^2 = 0.828$, $n = 3$). We validated all CAT and DN forms of kinases by Western blot analyses performed with the appropriate tag-specific antibodies on proteins overexpressed in HEK-293 cells (Fig. 4*e*).

cAMP is generated by nine transmembrane adenylyl cyclases (tmACs) and one soluble AC (sAC) in mammals. To discern between the contributions of different ACs to regulation of TCF4 by membrane depolarization in neurons, we selectively inhibited tmACs and sAC with ddAdo (2',3'-dideoxyadenosine) and KH7, respectively. Inhibition of sAC and not tmACs interfered with the induction of TCF4-dependent transcription in depolarized neurons independent of the promoter used for TCF4-A⁻ overexpression (Fig. 4*a*). From the above results, we concluded that signaling via sAC and PKA is needed for membrane depolarization induced TCF4-dependent transcription in primary neurons. Nevertheless, other kinases, including CAMK2 and PKC, could also play a role.

TCF4 S448 is phosphorylated by PKA and contributes to the regulation of TCF4 by neuronal activity

We next investigated whether TCF4 is a substrate for PKA. To evaluate this, we performed *in vitro* immune complex kinase assays using immunoprecipitated E2-PKA-C α from transfected

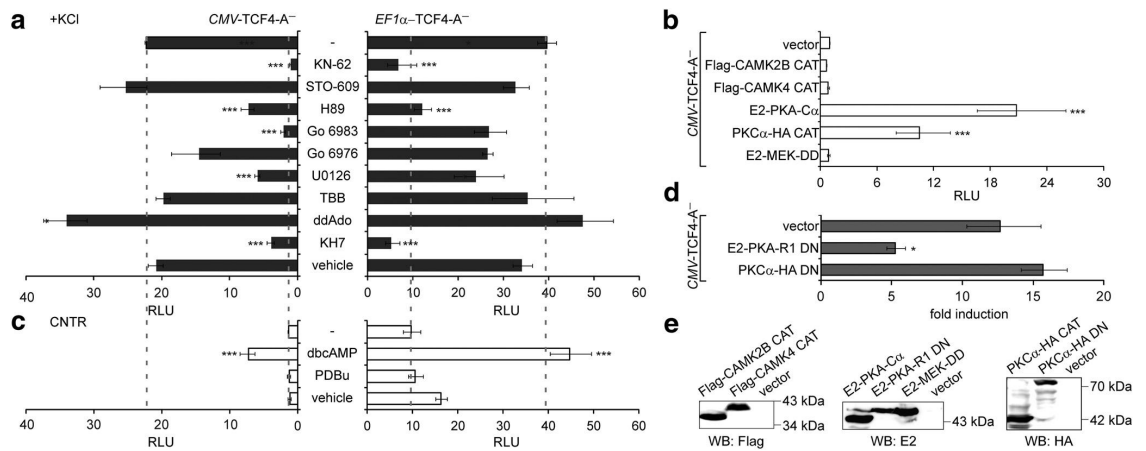


Figure 4. Identification of signaling pathways involved in the induction of TCF4-dependent transcription by neuronal activity. Shown is the effect of treatment with pharmacological inhibitors (**a**), coexpression of constitutively active kinases (**b**), treatment with kinase activators (**c**), and coexpression of DN kinase subunits (**d**) on TCF4⁻-mediated transcription. Neurons were transfected with firefly luciferase construct carrying 12 μ E5 E-boxes in front of *TK* promoter, *Renilla* luciferase construct with *EF1 α* or *PGK1* promoter, and TCF4⁻ vector with *CMV* or *EF1 α* promoter, respectively. Constructs coding for various constitutively active and DN protein kinase subunits were cotransfected in **b** and **d**, respectively. The transfected neurons were left untreated or treated with the indicated compounds for 8 h. Data are presented as fold induced levels above the signals obtained from empty vector transfected and untreated cells in **a–c** and as fold induction of luciferase activity in KCl-treated neurons compared with untreated neurons in **d**. Shown are the mean results from at least three independent experiments (see Materials and Methods for details) performed in duplicates. Error bars indicate SEM. Figures **a** and **c** are to scale and dashed lines indicate reporter levels in nontreated and KCl-treated TCF4⁻-expressing cells. Statistical significance shown with asterisks is relative to the first data point in each chart. * $p < 0.05$; ** $p < 0.01$; *** $p < 0.001$; one-way ANOVA followed by Dunnett's *post hoc* tests. RLU, Relative luciferase units. **E**, Western blot analysis of constitutively active and dominant negative protein kinase subunits overexpressed in HEK-293 cells.

HEK-293 cells as the enzyme and immunoprecipitated Flag-TCF4-M217(I⁻) or its deletion mutants Flag-TCF4-G316, Flag-TCF4-S363, Flag-TCF4-M430, or Flag-TCF4-P498 from transfected HEK-293 cells as the substrates in the presence of [γ -³²P]ATP. All Flag-TCF4 deletion proteins were immunoprecipitated at comparable levels and all except Flag-TCF4-P498 were phosphorylated in the presence of E2-PKA-C α (Fig. 5*a*). These results suggest that PKA phosphorylates TCF4 in the region between aa M430 and P498. We subsequently used NetPhos 2.0 (Blom et al., 2004) to predict phosphorylation sites in this region and identified S448 and S464 as potential PKA targets. Both of these serines are conserved in mammals, reptiles, and amphibians and S448 also in teleost fishes (Fig. 5*b*). To determine whether S448 and/or S464 are phosphorylated by PKA *in vitro*, we substituted one or both of the serines with alanines in the context of Flag-TCF4-M217(I⁻) and performed immune complex kinase assays as described above. Compared with the WT protein, phosphorylation by PKA was severely reduced when S448 was mutated, slightly reduced when S464 was mutated, and abolished in case of the double mutant (Fig. 5*c*). This indicates that, in TCF4, S448 is the major and S464 a minor site for phosphorylation by PKA. In addition, E2-PKA-C α overexpressed in HEK-293FT cells was coimmunoprecipitated with Flag-TCF4-M217(I⁻) and to lesser extent also with Flag-TCF4-P498 (Fig. 5*d*), demonstrating that TCF4 interacts with PKA, but the region containing the phosphorylation sites is not absolutely required for the association.

To elucidate whether the identified PKA phosphorylation sites in TCF4 are involved in membrane-depolarization-mediated induction of TCF4-dependent transcription in neurons, we performed reporter assays using neurons transfected with constructs encoding WT, S448A, S464A, or S448A and S464A double mutant TCF4-A⁻. Compared with WT TCF4-A⁻ overexpression, the induction of E-box-controlled luciferase activity in response to KCl treatment was reduced significantly when S448A

or the double mutant TCF4-A⁻ was expressed in neurons (Fig. 5*e*; one-way ANOVA, transfection $F_{(3,12)} = 4.836$, $p = 0.0197$, $\eta_p^2 = 0.547$, $n = 4$). This indicates that S448 is required for full induction of TCF4-dependent transcription in depolarized neurons.

In utero electroporation of TCF4 has recently been demonstrated to severely disrupt the columnar organization of pyramidal cells in layer 2/3 of the rat medial prefrontal cortex (mPFC) by inducing clustering of transfected cells in a neuronal-activity-dependent manner (Page et al., 2017). To test whether S448 is required for altering the distribution of pyramidal cells by TCF4 *in vivo*, we overexpressed WT or S448A TCF4-A⁻ in mPFC of rat embryos by *in utero* electroporation. Compared with overexpression of GFP alone, coexpression of WT TCF4-A⁻ resulted in the formation of cellular aggregates in layer 2/3 mPFC, an effect that was abolished by mutating S448 (Fig. 5*f,g*; one-way ANOVA, transfection $F_{(2,15)} = 5.567$, $p = 0.0155$, $\eta_p^2 = 0.426$, $n = 7$ except for GFP, which was $n = 4$). Altogether, the above data identify TCF4 S448 as a PKA substrate and provide evidence for the importance of S448 in the neuronal-activity-dependent regulation of TCF4 in neurons in culture as well as *in vivo*.

TCF4 participates in the neuronal-activity-induced transcription of *Gadd45g*

We next aimed to extend our studies that established TCF4 as a Ca²⁺-responsive transcription factor to a natural endogenous target gene. For this, we tested whether TCF4 participates in the regulation of *Gadd45g*, which is known to be upregulated by neuronal activity (Zhang et al., 2009). *Gadd45g* is a direct target of ASCL1 (Huang et al., 2010; Castro et al., 2011), a class II bHLH factor that requires an E-protein dimerization partner such as TCF4 for efficient DNA binding. We cloned the human *GADD45G* promoter region from -215 to +30 bp from the putative transcription start site containing two conserved ASCL1-responsive

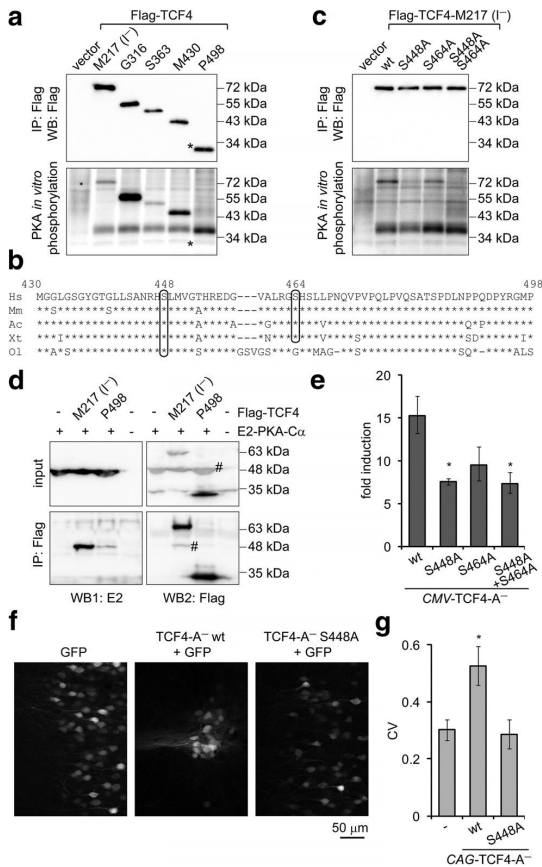


Figure 5. Identification and functional analysis of PKA phosphorylation sites in TCF4 *in vitro* and *in vivo*. **a, c.** Western blot analysis and *in vitro* phosphorylation assay with Flag-TCF4^{-/-} deletant (**a**) and point mutant (**c**) proteins overexpressed in HEK-293 cells and immunoprecipitated with Flag antibodies. Kinase E2-PKA-C α was overexpressed in HEK-293 cells and immunoprecipitated with E2 antibodies. The position of Flag-TCF4–P498 is indicated with an asterisk (*). **b.** Alignment of *Homo sapiens* (Hs) TCF4 protein region M430–P498 with the respective regions in TCF4 of *Mus musculus* (Mm), *Aroliis carolinensis* (Ac), *Xenopus tropicalis* (Xt), and *Oryzias latipes* (Ol). The predicted PKA phosphorylation sites S448 and S464 are circled. **d.** Interactions of E2-PKA-C α with Flag-TCF4. The proteins were overexpressed in HEK-293FT cells as indicated and coimmunoprecipitated with Flag antibodies. Western blots with E2 and Flag antibodies were performed sequentially, the number sign (#) marks bands from previous layer. In **a, c**, and **d**, a representative of at least two independent experiments with similar results is shown. **e.** Reporter assay with primary neurons transfected with firefly luciferase construct carrying 12 μ E5 E-boxes in front of *TK* promoter, *Renilla* luciferase construct with *EF1 α* promoter, and WT or mutant TCF4^{-/-} encoding constructs. Data are presented as fold induction of luciferase activity in 25 mM KCl-treated neurons compared with untreated neurons. **f.** Distribution of layer 2/3 pyramidal neurons expressing TCF4 and/or GFP protein in the mPFC. Rat embryos were electroporated *in utero* at E16 and coronal sections from P21 animals were subjected to confocal microscopy. **g.** Quantification of the data in **f**. Pixel intensities perpendicular to the medial surface were binned and the CV across all bins was calculated. The higher the CV value, the more clustered is the distribution of cells. Results from four (**e**) or seven (**f, g**; except for GFP, which is $n = 4$) independent experiments are shown. Error bars indicate SEM. * $p < 0.05$; one-way ANOVA followed by Dunnett's *post hoc* tests for comparisons with WT (**e**) or control GFP (**g**).

E-boxes (Huang et al., 2010), into a reporter vector (Fig. 6a) and performed luciferase assays in primary neurons. Overexpression of ASCL1 alone, but not TCF4 alone, upregulated transcription from the *GADD45G* promoter in neurons left untreated or

treated with KCl (Fig. 6b; two-way ANOVA, treatment $F_{(1,16)} = 182.6$, $p < 0.0001$; transfection $F_{(3,16)} = 36.79$, $p < 0.0001$, $\eta^2_{p(\text{interaction, treatment, transfection})} = 0.303, 0.919, 0.873$; $n = 4$). Importantly, the effect of ASCL1 on *GADD45G* promoter activity in depolarized neurons was augmented by TCF4 overexpression (Fig. 6b) and diminished by cotransfection of four different TCF4-specific siRNAs (Fig. 6c; two-way ANOVA, treatment \times transfection interaction $F_{(4,40)} = 8.151$, $p < 0.0001$, $\eta^2_{p(\text{interaction, treatment, transfection})} = 0.449, 0.877, 0.824$; $n = 5$). This demonstrates that TCF4 is involved in neuronal activity-dependent upregulation of ASCL1-mediated transcription from the *GADD45G* promoter in neurons.

To determine whether TCF4 binds and regulates the *GADD45G* promoter via the conserved E-boxes in neurons, we performed reporter assays with promoter constructs containing mutations in one or both of the E1 and E2 E-boxes (Fig. 6a) and ChIP experiments using TCF4 antibodies. In depolarized neurons, TCF4-A⁻ and ASCL1 coexpression increased transcription from WT and E1 mutant promoters compared with empty vector control. In contrast, the induction was insignificant in case of E2 mutant and lost in case of double mutants (Fig. 6d; two-way ANOVA, transfection \times treatment interaction $F_{(3,16)} = 6.667$, $p = 0.0040$, $\eta^2_{p(\text{interaction, transfection, treatment})} = 0.555, 0.729, 0.780$; $n = 4$). In ChIP experiments, we detected enrichment of TCF4 on *Gadd45g* promoter compared with an unrelated region on Chr1 that served as an indicator of unspecific background (Fig. 6e; two-way ANOVA; antibody \times genomic region interaction $F_{(1,8)} = 9.376$, $p = 0.0155$, $\eta^2_{p(\text{interaction, antibody, genomic region})} = 0.540, 0.447, 0.344$; $n = 3$). The above data demonstrate that TCF4 binds directly to the *Gadd45g* promoter in neurons, most probably by interacting with the proximal E2 E-box.

Finally, to find out whether TCF4 regulates the endogenous *Gadd45g* gene, we overexpressed VP16-fused TCF4-I⁻ or *Tcf4*-specific shRNAs in primary neurons using nucleofection or transduction of AAV vectors, respectively. Compared with EGFP control, VP16-TCF4-I⁻ increased *Gadd45g* levels both before and after 6 h depolarization (Fig. 6f; $n = 2$). Silencing of *Tcf4* to ~40% or ~10% of control levels using two different shRNAs (Fig. 6g; two-way ANOVA, transfection $F_{(2,24)} = 776.0$, $p < 0.0001$, $\eta^2_{p(\text{interaction, treatment, transfection})} = 0.066, 0.060, 0.985$; $n = 3$) decreased *Gadd45g* transcription in depolarized but not in resting neurons (Fig. 6h; two-way ANOVA, treatment \times transfection interaction $F_{(2,24)} = 10.84$, $p = 0.0004$, $\eta^2_{p(\text{interaction, treatment, transfection})} = 0.475, 0.994, 0.428$; $n = 3$). Altogether, these results demonstrate that *Gadd45g* is an endogenous target of TCF4 in neurons.

TCF4 missense variations identified in SCZ patients alter the transcriptional activity of TCF4 in neurons

The rare coding variants of TCF4 detected in sporadic SCZ cases include S102C, P156T, F211L, P299S, and G428V identified in single SCZ patients and A315V identified in 14 cases and 10 controls (Hu et al., 2014; Basmanav et al., 2015). The variations are located outside of the functional domains of TCF4, suggesting that their impact on TCF4 function might be modest and dependent on cellular context. To evaluate the potential pathogenicity of these variations in the light of the novel role of TCF4 as an activity-regulated transcription factor, we studied the impact of the substitutions on TCF4-dependent reporter transcription in primary neurons. This experiment was performed with the long TCF4 isoform B⁻ because it comprises all six sites of substitution (Fig. 7). Compared with WT TCF4-B⁻, the P299S variant increased E-box-dependent reporter levels in neurons in basal condition 1.3-fold and the G428V variant raised reporter levels 1.4- or 1.5-fold

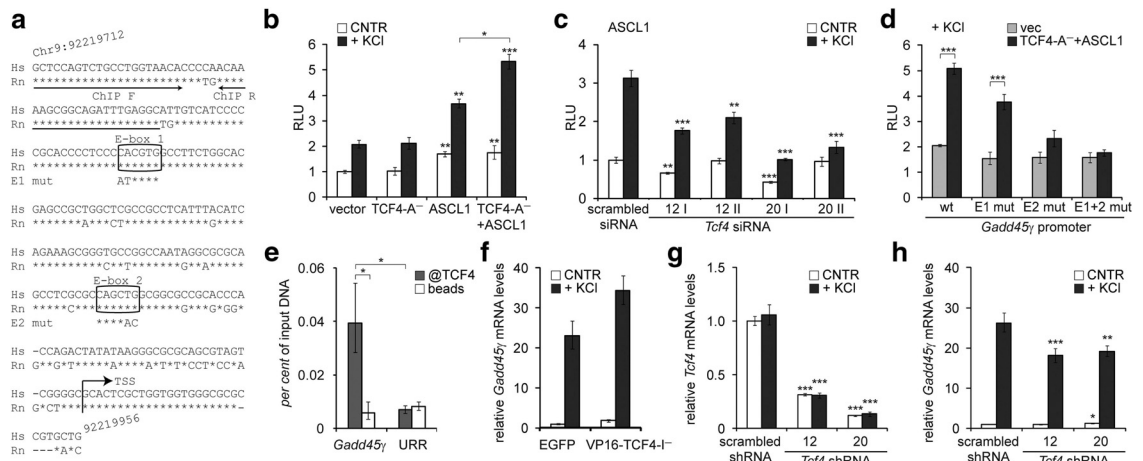


Figure 6. Regulation of *GADD45G* transcription by TCF4 in neurons. **a**, Alignment of the cloned *GADD45G* promoter region in *Homo sapiens* (Hs) with the respective region in *Rattus norvegicus* (Rn). Arrows indicate the primers used in ChIP analysis and the putative transcription start site (TSS). The two conserved E-boxes 1 and 2 are shown in boxes with the introduced mutations indicated below. **b–d**, Reporter assays with cultured primary neurons transfected with WT (**b–d**) or mutant (**d**) *GADD45G* promoter firefly luciferase constructs and *Renilla* luciferase construct with *PGK* promoter for normalization. Empty vector, *EF1 α -TCF4-A⁻* and/or SR α -ASCL1 vector (**b**, **d**) and SR α -ASCL1 vector together with TCF4-specific or scrambled siRNAs (**c**) were cotransfected as indicated. Transfected neurons were left untreated or treated with 25 mM KCl for 8 h. **e**, ChIP analysis of TCF4 binding to *Gadd45g* promoter in neurons. Chromatin was coimmunoprecipitated with TCF4 antibodies or with beads alone. The levels of bound *Gadd45g* promoter or an unrelated region (URR) on chromosome 1 were quantified by qPCR. The means of three independent experiments are presented as percentages of input DNA. **f–h**, Quantitative RT-PCR analysis of *Gadd45g* (**f**, **h**) and total *Tcf4* (**g**) mRNA expression in primary neurons nucleofected with EGFP or VP16-TCF4-1⁻ constructs (**f**) or transfected with scrambled or TCF4-specific shRNAs encoding AAV vectors (**g**, **h**). Neurons were left untreated or treated with 25 mM KCl for 6 h. **b–d**, **f–h**, Data are presented relative to the normalized reporter or mRNA levels measured in untreated control cells in each experiment. The mean results from two (**f**), three (**b**, **d**), four (**g**, **h**), or five (**c**) independent experiments are shown. Error bars indicate SEM. Statistical significance shown with asterisks is relative to the reporter or mRNA levels measured from untreated or KCl-treated neurons of the first data point of each chart or between the bars connected with lines. * $p < 0.05$; ** $p < 0.01$; *** $p < 0.001$; two-way ANOVA followed by Bonferroni *post hoc* tests for comparisons across TCF4 and ASCL1 transfections (**b**, **d**) or antibody use and genomic regions (**e**) or Dunnett’s *post hoc* tests for comparisons with untreated or KCl-treated scrambled si/shRNA samples (**c**, **g**, **h**). RLU, Relative luciferase units.

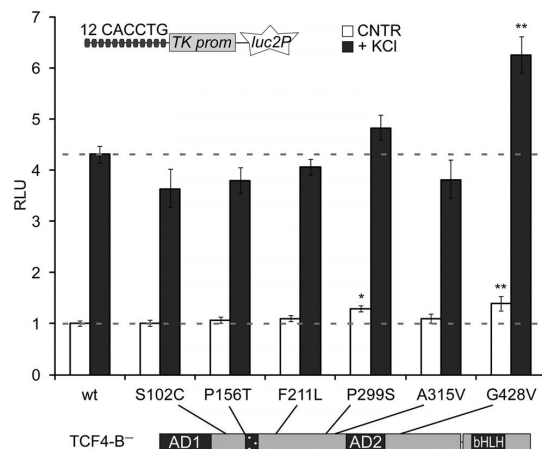


Figure 7. The effect of SCZ-linked TCF4 missense variations on the transcriptional activity of TCF4 in neurons. Reporter assay with primary neurons transfected with WT or mutant *EF1 α -TCF4-B⁻* vectors, firefly luciferase construct carrying 12 μ E5 E-boxes in front of *TK* promoter, and *Renilla* luciferase construct with *PGK1* promoter. Transfected neurons were left untreated or treated with 25 mM KCl for 8 h. Data are presented as fold induced levels above the signals obtained from untreated cells overexpressing WT TCF4-B⁻. Shown are the mean results from 5 independent experiments (except for P156T^{+KCl}, in which $n = 4$). Error bars indicate SEM. * $p < 0.05$; ** $p < 0.01$; two-way ANOVA followed by Dunnett’s *post hoc* tests for comparisons with untreated or KCl-treated WT. RLU, Relative luciferase units.

in untreated or KCl-treated neurons, respectively (Fig. 7; two-way ANOVA, treatment $F_{(1,55)} = 1339$, $p < 0.0001$, transfection $F_{(6,44)} = 9.920$, $p < 0.0001$, $\eta^2_{p(\text{interaction, treatment, transfection})} = 0.107$, 0.961, 0.520; $n = 5$ except for P156T^{+KCl}, $n = 4$). In addition, we observed a trend toward a reduction in the fold induction of E-box-dependent reporter activity in KCl-treated neurons compared with untreated neurons for four TCF4 variants: P299S (84% of WT fold induction, unpaired two-sided *t* test, $t_{(8)} = 3.081$, $p = 0.0151$, $r^2 = 0.543$, $n = 5$), P156T (85%, $t_{(7)} = 2.272$, $p = 0.0573$, $r^2 = 0.425$, $n = 4$), S102C (77%, $t_{(8)} = 2.036$, $p = 0.0762$, $r^2 = 0.341$, $n = 5$), and F211V (84%, $t_{(8)} = 1.998$, $p = 0.0808$, $r^2 = 0.333$, $n = 5$). These results raise the possibility that aberrant regulation of TCF4 transcriptional activity in neurons could play a role in SCZ.

Discussion

Here, we report that the PTHS- and SCZ-associated bHLH transcription factor TCF4 is regulated by neuronal activity. We provide evidence that this regulation requires sAC and PKA activities. Moreover, we demonstrate that TCF4 function in neurons is modified by missense variations implicated in SCZ. Our data suggest that the role of TCF4 in the etiology of SCZ and PTHS converges with the roles of many other psychiatric and neurodevelopmental disorder-associated genes on a common pathway; that is, neuronal-activity-dependent signaling (West and Greenberg, 2011; Ebert and Greenberg, 2013; Cross-Disorder Group of the Psychiatric Genomics Consortium, 2013; Schizophrenia Working Group of the Psychiatric Genomics Consortium, 2014).

Synaptic-activity-induced signaling modulates gene transcription by altering the function, localization, or expression of

transcription factors (Lyons and West, 2011). In the current study, we showed that the activity-dependent induction of E-box-controlled transcription by TCF4 in cultured cortical and hippocampal neurons is not mediated by signal-regulated nuclear import of TCF4 and is independent of its isoformal specificity. We found that only transactivation domain AD2, and not AD1 separately, functions in activating transcription in primary neurons. This is in accordance with the requirement of AD2 for TCF4 activity in the developing prefrontal cortex *in vivo* (Page et al., 2017), but different from non-neural cells, in which both AD1 and AD2 are able to mediate transcriptional activation and function synergistically (Sepp et al., 2011). Although AD2 was essential for TCF4-mediated transactivation in neurons, it was not involved in neuronal-activity-dependent regulation of TCF4. Instead, we found that, for activity responsiveness, the C-terminal ~240 aa of TCF4 are sufficient. This region contains the bHLH domain and a conserved upstream serine (S448) that was required for full depolarization-mediated TCF4 activation in primary neurons and for the ability of TCF4 to induce prefrontal layer 2/3 neuron clustering *in vivo*. Therefore, it appears that S448 phosphorylation is a central mechanism by which stimulus-dependent regulation of TCF4 is achieved.

Activity-dependent transcription in neurons is driven by several signaling pathways initiated predominantly by Ca^{2+} influx through VGCCs and/or NMDARs (Hagenston and Bading, 2011). Here, we found that Ca^{2+} signaling triggered by both of these Ca^{2+} entry routes is conveyed to TCF4. By combining pharmacological and genetic approaches, we demonstrated that the induction of TCF4-controlled transcription by membrane depolarization depends on the cAMP–PKA pathway. This result was corroborated by interaction of TCF4 with the catalytic subunit of PKA and direct phosphorylation of TCF4 at the critical S448 and S464 by PKA *in vitro*. Although the cAMP–PKA pathway has long been known to be involved in Ca^{2+} -regulated synaptic function, plasticity, and the late phase of long-term potentiation, it has generally been considered to play a modulatory role in activity-dependent gene regulation in neurons (Poser and Storm, 2001). For instance, the prototypical neuronal activity-responsive transcriptional regulator CREB (cAMP response element binding protein) is primarily stimulated by the CAMK and MAPK pathways in neurons (Hagenston and Bading, 2011), whereas PKA influences it indirectly, for example, by supporting MAPK nuclear translocation and preserving nuclear localization of CREB-regulated transcriptional coactivator 1 (Poser and Storm, 2001; Ch'ng et al., 2012). In contrast, we found here that TCF4 activity in neurons depends predominantly on the cAMP–PKA pathway, although roles for other kinases, especially for CAMK2 and PKC, cannot be ruled out. The significance of cAMP–PKA signaling in TCF4 regulation was further substantiated by our finding that of the two sources of cellular cAMP, sAC activity, but not tmAC activity, was required for depolarization-induced TCF4-dependent transcription in neurons. sAC is a free Ca^{2+} and bicarbonate-responsive enzyme that localizes to different cellular compartments, including the nucleus, and has been shown to act as a sensor of neural activity in retinal ganglion cells (Stiles et al., 2014). Together, our results reveal a novel signaling axis in cortical neurons that links Ca^{2+} influx into neurons with activation of sAC, PKA and TCF4-dependent transcription.

The mechanisms by which phosphorylation of TCF4 by PKA regulates its transactivational capacity remain undefined. Previous studies have shown that phosphorylation can affect several properties of bHLH proteins, including their stability (Hong

et al., 2011; Jo et al., 2011; Lin and Lee, 2012) and dimerization specificity (Sloan et al., 1996; Lluís et al., 2005). These regulatory mechanisms and differential modulation of DNA binding of E-protein homodimers and heterodimers by Ca^{2+} -calmodulin (Hauser et al., 2008) provide the means for signal-responsive regulation of target genes by specific bHLH dimers. Here, we demonstrate that, in primary neurons, depolarization activates TCF4:ASCL1 heterodimers, which participate in the induction of *Gadd45g* expression. *Gadd45g* codes for a member of growth arrest and DNA damage-inducible 45 protein family that are implicated in active DNA demethylation, adult cognitive function, and neuropsychiatric dysfunction (Sultan and Sweatt, 2013). Identification of a functional E-box and binding of TCF4 to its endogenous promoter establish *Gadd45g* as a direct target of TCF4. These results complement previous studies that have assigned serum response factor (SRF) and CREB as regulators of activity-dependent *Gadd45g* transcription (Zhang et al., 2009; Tan et al., 2012; Kuzniewska et al., 2016) and validate TCF4 as an activity-responsive transcription factor in the context of a natural target gene. Our findings are substantiated by recent studies that have implicated TCF4 in the regulation of synaptic stimulus-induced processes (Kennedy et al., 2016; Page et al., 2017). Kennedy et al. (2016) studied gene expression in the hippocampi of heterozygous TCF4 knock-out mice and found broad dysregulation of memory-related genes as well as differences in the induction of immediate early genes in response to experiential learning. These changes were accompanied by deficits in synaptic plasticity, learning, and memory. Page et al. (2017) demonstrated that TCF4-dependent transcription is involved in the activity-dependent formation of cortical minicolumns and in the regulation of early neuronal activity. Considering the latter data together with the results of the current study, we propose that TCF4 is involved in a positive feedback loop where it acts as sensor of neuronal activity that enhances spontaneous activity by regulating transcription.

We have shown previously that most of the PTHS-associated missense mutations impede the activation of E-box-controlled transcription by TCF4 in depolarized neurons (Sepp et al., 2012). Here, we found that two (G428V and P299S) of the six rare TCF4 missense variations identified in SCZ patients (Hu et al., 2014; Basmanav et al., 2015) increase TCF4 transcriptional activity in depolarized and/or resting neurons. In addition, several variants (P299S, P156T, S102C, and F211V) displayed a trend toward reduced signal-dependent induction of TCF4 activity. Given the polygenic nature of SCZ etiology, detecting variation-elicited functional changes is not expected to be fully correlated with a SCZ case diagnosis (Kim et al., 2017). Our results indicate that at least a subset of SCZ-linked TCF4 variants have functional consequences. The mechanisms underlying these effects remain uncharacterized, but might involve changes in TCF4 transactivation ability and/or response to neuronal activity. In contrast, most PTHS-associated missense mutations studied so far damage the ability of TCF4 to form stable dimers or bind DNA (Forrest et al., 2012; Sepp et al., 2012). Our finding that PTHS- and SCZ-linked missense substitutions have divergent effects on TCF4 functions is consistent with the accumulating evidence that both loss and gain of TCF4 expression or activity are related to cognitive diseases and even partial *TCF4* deletions and duplications may result in disturbances (Sepp et al., 2012; Talkowski et al., 2012; Ye et al., 2012; Kharbanda et al., 2016). Even so, several aspects about the role of TCF4 in SCZ remain uncertain; for example, the causality of the rare coding variants of TCF4 in SCZ has not been established and the functional implications of the SCZ-associated

common SNPs in *TCF4* are unknown. It has been suggested that SCZ might be linked to increased *TCF4* expression in the nervous system (Brzózka et al., 2010; Brennand et al., 2011; Guella et al., 2013; Quednow et al., 2014), although this is not supported by all studies (Umeda-Yano et al., 2014). We propose that the impaired cognitive functions seen in PTHS and SCZ patients could be caused in part by aberrant TCF4-dependent transcriptional response to neuronal activity that in turn could lead to incorrect neuronal connectivity and/or excitatory-inhibitory balance.

In summary, we have identified TCF4 as an activity-dependent transcriptional activator in neurons, providing a mechanistic rationale for the association of *TCF4* with disorders affecting cognitive function and development.

References

- Bading H, Ginty DD, Greenberg ME (1993) Regulation of gene expression in hippocampal neurons by distinct calcium signaling pathways. *Science* 260:181–186. [CrossRef Medline](#)
- Basmanav FB, et al. (2015) Investigation of the role of TCF4 rare sequence variants in schizophrenia. *Am J Med Genet B Neuropsychiatr Genet* 168B:354–362. [CrossRef Medline](#)
- Bergqvist I, Eriksson M, Saarikettu J, Eriksson B, Corneliussen B, Grundström T, Holmberg D (2000) The basic helix-loop-helix transcription factor E2-2 is involved in T lymphocyte development. *Eur J Immunol* 30:2857–2863. [CrossRef Medline](#)
- Blom N, Sicheritz-Pontén T, Gupta R, Gammeltoft S, Brunak S (2004) Prediction of post-translational glycosylation and phosphorylation of proteins from the amino acid sequence. *Proteomics* 4:1633–1649. [CrossRef Medline](#)
- Boehm JS et al. (2007) Integrative genomic approaches identify IKBKE as a breast cancer oncogene. *Cell* 129:1065–1079. [CrossRef Medline](#)
- Brennand KJ, Simone A, Jou J, Gelboin-Burkhardt C, Tran N, Sangar S, Li Y, Mu Y, Chen G, Yu D, McCarthy S, Sebat J, Gage FH (2011) Modelling schizophrenia using human induced pluripotent stem cells. *Nature* 473:221–225. [CrossRef Medline](#)
- Brockschmidt A, Filippi A, Charbel Issa P, Nelles M, Urbach H, Eter N, Driever W, Weber RG (2011) Neurologic and ocular phenotype in Pitt-Hopkins syndrome and a zebrafish model. *Hum Genet* 130:645–655. [CrossRef Medline](#)
- Brzózka MM, Radyushkin K, Wichert SP, Ehrenreich H, Rossner MJ (2010) Cognitive and sensorimotor gating impairments in transgenic mice overexpressing the schizophrenia susceptibility gene Tcf4 in the brain. *Biol Psychiatry* 68:33–40. [CrossRef Medline](#)
- Castro DS, Martynoga B, Parras C, Ramesh V, Pacary E, Johnston C, Drechsel D, Lebel-Potter M, Garcia LG, Hunt C, Dolle D, Bithell A, Ettwiller L, Buckley N, Guillemot F (2011) A novel function of the proneural factor Ascl1 in progenitor proliferation identified by genome-wide characterization of its targets. *Genes Dev* 25:930–945. [CrossRef Medline](#)
- Chen ES, Gigek CO, Rosenfeld JA, Diallo AB, Maussion G, Chen GG, Vailancourt K, Lopez JP, Crapper L, Poujol R, Shaffer LG, Bourque G, Ernst C (2014) Molecular convergence of neurodevelopmental disorders. *Am J Hum Genet* 95:490–508. [CrossRef Medline](#)
- Chen T, Wu Q, Zhang Y, Lu T, Yue W, Zhang D (2016) Tcf4 controls neuronal migration of the cerebral cortex through regulation of Bmp7. *Front Mol Neurosci* 9:94. [CrossRef Medline](#)
- Ch'ng TH, Uzgil B, Lin P, Avliyakov NK, O'Dell TJ, Martin KC (2012) Activity-dependent transport of the transcriptional coactivator CRTCI from synapse to nucleus. *Cell* 150:207–221. [CrossRef Medline](#)
- Clegg CH, Correll LA, Cadd GG, McKnight GS (1987) Inhibition of intracellular cAMP-dependent protein kinase using mutant genes of the regulatory type I subunit. *J Biol Chem* 262:13111–13119. [CrossRef Medline](#)
- Cox ME, Deeble PD, Bissonette EA, Parsons SJ (2000) Activated 3',5'-cyclic AMP-dependent protein kinase is sufficient to induce neuroendocrine-like differentiation of the LNCaP prostate tumor cell line. *J Biol Chem* 275:13812–13818. [CrossRef Medline](#)
- Cross-Disorder Group of the Psychiatric Genomics Consortium (2013) Identification of risk loci with shared effects on five major psychiatric disorders: a genome-wide analysis. *Lancet* 381:1371–1379. [CrossRef Medline](#)
- D'Rozario M, Zhang T, Waddell EA, Zhang Y, Sahin C, Sharoni M, Hu T, Nayal M, Kutty K, Liebl F, Hu W, Marendra DR (2016) Type I bHLH proteins daughterless and Tcf4 restrict neurite branching and synapse formation by repressing neurexin in postmitotic neurons. *Cell Rep* 15:386–397. [CrossRef Medline](#)
- Ebert DH, Greenberg ME (2013) Activity-dependent neuronal signaling and autism spectrum disorder. *Nature* 493:327–337. [CrossRef Medline](#)
- Fischer B, Azim K, Hurtado-Chong A, Ramelli S, Fernández M, Raineteau O (2014) E-proteins orchestrate the progression of neural stem cell differentiation in the postnatal forebrain. *Neural Dev* 9:23. [CrossRef Medline](#)
- Flora A, Garcia JJ, Thaller C, Zoghbi HY (2007) The E-protein Tcf4 interacts with Math1 to regulate differentiation of a specific subset of neuronal progenitors. *Proc Natl Acad Sci U S A* 104:15382–15387. [CrossRef Medline](#)
- Forrest MP, Waite AJ, Martin-Rendon E, Blake DJ (2013) Knockdown of human TCF4 affects multiple signaling pathways involved in cell survival, epithelial to mesenchymal transition and neuronal differentiation. *PLoS One* 8:e73169. [CrossRef Medline](#)
- Forrest MP, Hill MJ, Quantock AJ, Martin-Rendon E, Blake DJ (2014) The emerging roles of TCF4 in disease and development. *Trends Mol Med* 20:322–331. [CrossRef Medline](#)
- Forrest M, Chapman RM, Doyle AM, Tinsley CL, Waite A, Blake DJ (2012) Functional analysis of TCF4 missense mutations that cause Pitt-Hopkins syndrome. *Hum Mutat* 33:1676–1686. [CrossRef Medline](#)
- Guella I, Sequeira A, Rollins B, Morgan L, Torri F, van Erp TG, Myers RM, Barchas JD, Schatzberg AF, Watson SJ, Akil H, Bunney WE, Potkin SG, Macciardi F, Vawter MP (2013) Analysis of miR-137 expression and rs1625579 in dorsolateral prefrontal cortex. *J Psychiatr Res* 47:1215–1221. [CrossRef Medline](#)
- Hagenston AM, Bading H (2011) Calcium signaling in synapse-to-nucleus communication. *Cold Spring Harb Perspect Biol* 3:a004564. [CrossRef Medline](#)
- Hardingham GE, Arnold FJ, Bading H (2001) Nuclear calcium signaling controls CREB-mediated gene expression triggered by synaptic activity. *Nat Neurosci* 4:261–267. [CrossRef Medline](#)
- Hauser J, Saarikettu J, Grundström T (2008) Calcium regulation of myogenesis by differential calmodulin inhibition of basic helix-loop-helix transcription factors. *Mol Biol Cell* 19:2509–2519. [CrossRef Medline](#)
- Hill MJ, Killick R, Navarrete K, Maruszak A, McLaughlin GM, Williams BP, Bray NJ (2017) Knockdown of the schizophrenia susceptibility gene TCF4 alters gene expression and proliferation of progenitor cells from the developing human neocortex. *J Psychiatry Neurosci* 42:181–188. [CrossRef Medline](#)
- Hong J, Zhou J, Fu J, He T, Qin J, Wang L, Liao L, Xu J (2011) Phosphorylation of serine 68 of Twist1 by MAPKs stabilizes Twist1 protein and promotes breast cancer cell invasiveness. *Cancer Res* 71:3980–3990. [CrossRef Medline](#)
- Huang HS, Kubish GM, Redmond TM, Turner DL, Thompson RC, Murphy GG, Uhler MD (2010) Direct transcriptional induction of Gadd45gamma by Ascl1 during neuronal differentiation. *Mol Cell Neurosci* 44:282–296. [CrossRef Medline](#)
- Huang W, Erikson RL (1994) Constitutive activation of Mek1 by mutation of serine phosphorylation sites. *Proc Natl Acad Sci U S A* 91:8960–8963. [CrossRef Medline](#)
- Hu X, Zhang B, Liu W, Paciga S, He W, Lanz TA, Kleiman R, Dougherty B, Hall SK, McIntosh AM, Lawrie SM, Power A, John SL, Blackwood D, St Clair D, Brandon NJ (2014) A survey of rare coding variants in candidate genes in schizophrenia by deep sequencing. *Mol Psychiatry* 19:857–858. [CrossRef Medline](#)
- Jo C, Cho SJ, Jo SA (2011) Mitogen-activated protein kinase kinase 1 (MEK1) stabilizes MyoD through direct phosphorylation at tyrosine 156 during myogenic differentiation. *J Biol Chem* 286:18903–18913. [CrossRef Medline](#)
- Kannike K, Sepp M, Zuccato C, Cattaneo E, Timmusk T (2014) Forkhead transcription factor FOXO3a levels are increased in Huntington disease because of overactivated positive autoregulatory loop. *J Biol Chem* 289:32845–32857. [CrossRef Medline](#)
- Kazantseva A, Sepp M, Kazantseva J, Sadam H, Pruunsild P, Timmusk T, Neuman T, Palm K (2009) N-terminally truncated BAF57 isoforms contribute to the diversity of SWI/SNF complexes in neurons. *J Neurochem* 109:807–818. [CrossRef Medline](#)

- Kennedy AJ, Rahn EJ, Paulukaitis BS, Savell KE, Kordasiewicz HB, Wang J, Lewis JW, Posey J, Strange SK, Guzman-Karlsson MC, Phillips SE, Decker K, Motley ST, Swazey EE, Ecker DJ, Michael TP, Day JJ, Sweatt JD (2016) Tcf4 regulates synaptic plasticity, DNA methylation, and memory function. *Cell Rep* 16:2666–2685. CrossRef Medline
- Kharbanda M, Kannike K, Lampe A, Berg J, Timmusk T, Sepp M (2016) Partial deletion of TCF4 in three generation family with non-syndromic intellectual disability, without features of Pitt–Hopkins syndrome. *Eur J Med Genet* 59:310–314. CrossRef Medline
- Kim MJ, Biag J, Fass DM, Lewis MC, Zhang Q, Fleishman M, Gangwar SP, Machius M, Fromer M, Purcell SM, McCarrroll SA, Rudenko G, Premont RT, Scolnick EM, Haggarty SJ (2016) Functional analysis of rare variants found in schizophrenia implicates a critical role for GIT1-PAK3 signaling in neuroplasticity. *Mol Psychiatry* 22:417–429. CrossRef Medline
- Koppel I, Tuvikene J, Lekk I, Timmusk T (2015) Efficient use of a translation start codon in BDNF exon I. *J Neurochem* 134:1015–1025. CrossRef Medline
- Kotaleski JH, Blackwell KT (2010) Modelling the molecular mechanisms of synaptic plasticity using systems biology approaches. *Nat Rev Neurosci* 11:239–251. CrossRef Medline
- Kuzniewska B, Nader K, Dabrowski M, Kaczmarek L, Kalita K (2016) Adult deletion of SRF increases epileptogenesis and decreases activity-induced gene expression. *Mol Neurobiol* 53:1478–1493. CrossRef Medline
- Lau D, Bading H (2009) Synaptic activity-mediated suppression of p53 and induction of nuclear calcium-regulated neuroprotective genes promote survival through inhibition of mitochondrial permeability transition. *J Neurosci* 29:4420–4429. CrossRef Medline
- Lin CH, Lee EH (2012) JNK1 inhibits GluR1 expression and GluR1-mediated calcium influx through phosphorylation and stabilization of Hes-1. *J Neurosci* 32:1826–1846. CrossRef Medline
- Lluis F, Ballestar E, Suelves M, Esteller M, Muñoz-Cánoves P (2005) E47 phosphorylation by p38 MAPK promotes MyoD/E47 association and muscle-specific gene transcription. *EMBO J* 24:974–984. CrossRef Medline
- Lyons MR, West AE (2011) Mechanisms of specificity in neuronal activity-regulated gene transcription. *Prog Neurobiol* 94:259–295. CrossRef Medline
- Maduro V, Pusey BN, Cherukuri PF, Atkins P, du Souich C, Rupps R, Limbos M, Adams DR, Bhatt SS, Eydoux P, Links AE, Lehman A, Malicdan MC, Mason CE, Morimoto M, Mullikin JC, Sear A, Van Karnebeek C, Stankiewicz P, Gahl WA, Toro C, Boerkoel CF (2016) Complex translocation disrupting TCF4 and altering TCF4 isoform expression segregates as mild autosomal dominant intellectual disability. *Orphanet J Rare Dis* 11:62. CrossRef Medline
- Massari ME, Murre C (2000) Helix-loop-helix proteins: regulators of transcription in eucaryotic organisms. *Mol Cell Biol* 20:429–440. CrossRef Medline
- Page SC, Hamersky GR, Gallo RA, Rannals MD, Calcaterra NE, Campbell MN, Mayfield B, Briley A, Phan BN, Jaffe AE, Maher BJ (2017) The schizophrenia- and autism-associated gene, transcription factor 4 regulates the columnar distribution of layer 2/3 prefrontal pyramidal neurons in an activity-dependent manner. *Mol Psychiatry*. Advance online publication. Retrieved September 29, 2017. CrossRef
- Poser S, Storm DR (2001) Role of Ca²⁺-stimulated adenylyl cyclases in LTP and memory formation. *Int J Dev Neurosci* 19:387–394. CrossRef Medline
- Pruunsild P, Sepp M, Orav E, Koppel I, Timmusk T (2011) Identification of cis-elements and transcription factors regulating neuronal-activity-dependent transcription of human BDNF gene. *J Neurosci* 31:3295–3308. CrossRef Medline
- Quednow BB, et al. (2012) Schizophrenia risk polymorphisms in the TCF4 gene interact with smoking in the modulation of auditory sensory gating. *Proc Natl Acad Sci U S A* 109:6271–6276. CrossRef Medline
- Quednow BB, Brzózka MM, Rossner MJ (2014) Transcription factor 4 (TCF4) and schizophrenia: integrating the animal and the human perspective. *Cell Mol Life Sci* 71:2815–2835. CrossRef Medline
- Rannals MD, Hamersky GR, Page SC, Campbell MN, Briley A, Gallo RA, Phan BN, Hyde TM, Kleinman JE, Shin JH, Jaffe AE, Weinberger DR, Maher BJ (2016) Psychiatric risk gene transcription factor 4 regulates intrinsic excitability of prefrontal neurons via repression of SCN10a and KCNQ1. *Neuron* 90:43–55. CrossRef Medline
- Schizophrenia Working Group of the Psychiatric Genomics Consortium (2014) Biological insights from 108 schizophrenia-associated genetic loci. *Nature* 511:421–427. CrossRef Medline
- Schmidt-Edelkraut U, Daniel G, Hoffmann A, Spengler D (2014) Zac1 regulates cell cycle arrest in neuronal progenitors via Tcf4. *Mol Cell Biol* 34:1020–1030. CrossRef Medline
- Sepp M, Kannike K, Eesmaa A, Urb M, Timmusk T (2011) Functional diversity of human basic helix-loop-helix transcription factor TCF4 isoforms generated by alternative 5' exon usage and splicing. *PLoS One* 6:e22138. CrossRef Medline
- Sepp M, Pruunsild P, Timmusk T (2012) Pitt–Hopkins syndrome-associated mutations in TCF4 lead to variable impairment of the transcription factor function ranging from hypomorphic to dominant-negative effects. *Hum Mol Genet* 21:2873–2888. CrossRef Medline
- Sloan SR, Shen CP, McCarrick-Walmsley R, Kadesch T (1996) Phosphorylation of E47 as a potential determinant of B-cell-specific activity. *Mol Cell Biol* 16:6900–6908. CrossRef Medline
- Slomnicki LP, Malinowska A, Kistowski M, Palusinski A, Zheng JJ, Sepp M, Timmusk T, Dadlez L, Hetman M (2016) Nucleolar enrichment of brain proteins with critical roles in human neurodevelopment. *Mol Cell Proteomics* 15:2055–2075. CrossRef Medline
- Soh JW, Weinstein IB (2003) Roles of specific isoforms of protein kinase C in the transcriptional control of cyclin D1 and related genes. *J Biol Chem* 278:34709–34716. CrossRef Medline
- Stiles TL, Kapiloff MS, Goldberg JL (2014) The role of soluble adenylyl cyclase in neurite outgrowth. *Biochim Biophys Acta* 1842:2561–2568. CrossRef Medline
- Sultan FA, Sweatt JD (2013) The role of the Gadd45 family in the nervous system: a focus on neurodevelopment, neuronal injury, and cognitive neuroepigenetics. *Adv Exp Med Biol* 793:81–119. CrossRef Medline
- Sun P, Enslin H, Myung PS, Maurer RA (1994) Differential activation of CREB by Ca²⁺/calmodulin-dependent protein kinases type II and type IV involves phosphorylation of a site that negatively regulates activity. *Genes Dev* 8:2527–2539. CrossRef Medline
- Sweatt JD (2013) Pitt–Hopkins Syndrome: intellectual disability due to loss of TCF4-regulated gene transcription. *Exp Mol Med* 45:e21. CrossRef Medline
- Talkowski ME, et al. (2012) Sequencing chromosomal abnormalities reveals neurodevelopmental loci that confer risk across diagnostic boundaries. *Cell* 149:525–537. CrossRef Medline
- Tambergl J, Sepp M, Timmusk T, Palgi M (2015) Introducing Pitt–Hopkins syndrome-associated mutations of TCF4 to *Drosophila* daughterless. *Biol Open* 4:1762–1771. CrossRef Medline
- Tan YW, Zhang SJ, Hoffmann T, Bading H (2012) Increasing levels of wild-type CREB up-regulates several activity-regulated inhibitor of death (AID) genes and promotes neuronal survival. *BMC Neurosci* 13:48. CrossRef Medline
- Uhler MD, McKnight GS (1987) Expression of cDNAs for two isoforms of the catalytic subunit of cAMP-dependent protein kinase. *J Biol Chem* 262:15202–15207. Medline
- Umeda-Yano S, Hashimoto R, Yamamori H, Weickert CS, Yasuda Y, Ohi K, Fujimoto M, Ito A, Takeda M (2014) Expression analysis of the genes identified in GWAS of the postmortem brain tissues from patients with schizophrenia. *Neurosci Lett* 568:12–16. CrossRef Medline
- West AE, Greenberg ME (2011) Neuronal activity-regulated gene transcription in synapse development and cognitive function. *Cold Spring Harb Perspect Biol* 3:pia005744. CrossRef Medline
- Wheeler DG, Cooper E (2001) Depolarization strongly induces human cytomegalovirus major immediate-early promoter/enhancer activity in neurons. *J Biol Chem* 276:31978–31985. CrossRef Medline
- Ye T, Lipska BK, Tao R, Hyde TM, Wang L, Li C, Choi KH, Straub RE, Kleinman JE, Weinberger DR (2012) Analysis of copy number variations in brain DNA from patients with schizophrenia and other psychiatric disorders. *Biol Psychiatry* 72:651–654. CrossRef Medline
- Zhang SJ, Zou M, Lu L, Lau D, Ditzel DA, Delucinge-Vivier C, Aso Y, Descombes P, Bading H (2009) Nuclear calcium signaling controls expression of a large gene pool: identification of a gene program for acquired neuroprotection induced by synaptic activity. *PLoS Genet* 5:e1000604. CrossRef Medline
- Zhuang Y, Cheng P, Weintraub H (1996) B-lymphocyte development is regulated by the combined dosage of three basic helix-loop-helix genes, E2A, E2-2, and HEB. *Mol Cell Biol* 16:2898–2905. CrossRef Medline

Appendix 4

Publication IV

Kaja Nurm, Mari Sepp, Carla Castany-Pladevall, Jordi Creus Munchunill, Jürgen Tuvikene, Alex Sirp, Hanna Vihma, Derek J. Blake, Esther Perez Navarro, Tõnis Timmusk (2021). Isoform-Specific Reduction of the Basic Helix-Loop-Helix Transcription Factor TCF4 Levels in Huntington’s Disease. *eNeuro* 8(5): ENEURO.0197-21.2021. doi: 10.1523/ENEURO.0197-21.2021.

Disorders of the Nervous System

Isoform-Specific Reduction of the Basic Helix-Loop-Helix Transcription Factor TCF4 Levels in Huntington's Disease

Kaja Nurm,¹  Mari Sepp,¹ Carla Castany-Pladevall,^{3,4,5} Jordi Creus-Muncunill,^{3,4,5}  Jürgen Tuvikene,^{1,2} Alex Sirp,¹ Hanna Vihma,¹  Derek J. Blake,⁶ Esther Perez-Navarro,^{3,4,5} and Tõnis Timmusk^{1,2}

<https://doi.org/10.1523/ENEURO.0197-21.2021>

¹Department of Chemistry and Biotechnology, Tallinn University of Technology, Tallinn 12618, Estonia, ²Protobios LLC, Tallinn 12618, Estonia, ³Departament de Biomedicina, Facultat de Medicina i Ciències de la Salut, Institut de Neurociències, Universitat de Barcelona, Barcelona, Catalonia 08036, Spain, ⁴Institut d'Investigacions Biomèdiques August Pi i Sunyer (IDIBAPS), Barcelona, Catalonia 08036, Spain, ⁵Centro de Investigación Biomédica en Red sobre Enfermedades Neurodegenerativas (CIBERNED), Madrid, 28031, Spain, and ⁶Division of Psychological Medicine and Clinical Neurosciences, MRC Centre for Neuropsychiatric Genetics and Genomics, Cardiff University, Cardiff CF24 4HQ, United Kingdom

Abstract

Huntington's disease (HD) is an inherited neurodegenerative disorder with onset of characteristic motor symptoms at midlife, preceded by subtle cognitive and behavioral disturbances. Transcriptional dysregulation emerges early in the disease course and is considered central to HD pathogenesis. Using wild-type (wt) and HD knock-in mouse striatal cell lines we observed a HD genotype-dependent reduction in the protein levels of transcription factor 4 (TCF4), a member of the basic helix-loop-helix (bHLH) family with critical roles in brain development and function. We characterized mouse *Tcf4* gene structure and expression of alternative mRNAs and protein isoforms in cell-based models of HD, and in four different brain regions of male transgenic HD mice (R6/1) from young to mature adulthood. The largest decrease in the levels of TCF4 at mRNA and specific protein isoforms were detected in the R6/1 mouse hippocampus. Translating this finding to human disease, we found reduced expression of long TCF4 isoforms in the postmortem hippocampal CA1 area and in the cerebral cortex of HD patients. Additionally, TCF4 protein isoforms showed differential synergism with the pre-neural transcription factor ASCL1 in activating reporter gene transcription in hippocampal and cortical cultured neurons. Induction of neuronal activity increased these synergistic effects in hippocampal but not in cortical neurons, suggesting brain region-dependent differences in TCF4 functions. Collectively, this study demonstrates isoform-specific changes in TCF4 expression in HD that could contribute to the progressive impairment of transcriptional regulation and neuronal function in this disease.

Significance Statement

Historically, Huntington's disease (HD) has been considered a neurodegenerative disease. However, research of the last decade has revealed disrupted neurogenesis and cognitive dysfunction preceding pathologic neuronal cell death, suggesting that HD is also a neurodevelopmental disease. One of the major molecular mechanisms of HD is dysregulation of transcription. Studying transcription factors with functions in neurogenesis and neural plasticity is of interest for their potential participation in the cognitive impairment in HD etiology. Here, we show reduced expression of the transcription factor TCF4, previously linked with neurodevelopmental and neuropsychiatric diseases, in hippocampus and cerebral cortex of R6/1 mouse and HD patients. Our results shed light on the potential neurodevelopmental aspect of HD and could be applicable for developing alleviating therapies for HD.

Key words: basic helix-loop-helix transcription factor; Huntington's disease; neurodegenerative disease; TCF4; transcriptional regulation

Introduction

Huntington's disease (HD; OMIM #143100) is a fatal inherited neurodegenerative disorder caused by autosomal dominant mutation in the huntingtin (*HTT*) gene (The Huntington's Disease Collaborative Research Group, 1993). The mutation is a trinucleotide repeat (CAG)_n expansion in *HTT* exon 1, leading to translation of abnormal HTT protein with expanded polyglutamine tract in its N terminus. To study the disease mechanisms, different HD models have been developed, including chemically induced models using mitochondrial toxin 3-nitropropionic acid (3-NP) and genetic models in various cell-based systems and animals (for review, see Pouladi et al., 2013).

Clinically, HD is characterized by chorea and impairment of voluntary movements caused by striatal and cortical neurodegeneration that are preceded by cognitive and psychiatric disturbances (Stout et al., 2011). However, based on the critical functions of HTT in the developing nervous system a developmental basis for HD has been also proposed (Zuccato and Cattaneo, 2014; Bates et al., 2015). In fact, human and mouse embryos carrying mutant *HTT* show clear abnormalities in the developing cortex, including defects in neural progenitor differentiation and cell cycle progression (Barnat et al., 2020). Moreover, carriers of mutant *HTT* gene have changes in the striatum (van der Plas et al., 2019) and

cerebellum (Tereshchenko et al., 2020) at presymptomatic stages.

In healthy adults, cognitive functions such as learning and memory rely on neuronal plasticity and neurogenesis in the hippocampus and cerebral cortex (McClelland et al., 1995; Chambers et al., 2004; Aimone et al., 2009; Gonçalves et al., 2016; Mansvelter et al., 2019). While atrophy and neurodegeneration in striatum and cerebral cortex is a neuropathological hallmark of HD, the hippocampus remains relatively unaffected in HD patients (Ramirez-Garcia et al., 2020), although misregulated transcriptional pathway of synaptic vesicles has been observed (Neueder and Bates, 2014). On the other hand, reduced hippocampal adult neurogenesis in subgranular zone (SGZ) of the dentate gyrus (DG) has been reported in R6/2, R6/1, and YAC128 HD mouse models (Lazic et al., 2004; Gil et al., 2005; Simpson et al., 2011) and Q175FDN knock-in HD mice show deficits in hippocampal synaptic plasticity (Quirion and Parsons, 2019).

Transcriptional dysregulation is a well-characterized molecular mechanism in HD pathophysiology (for review, see Sugars and Rubinsztein, 2003; Cha, 2007; Valor, 2015). Mutant HTT has been shown to bind and disrupt the functions of general transcription factors and transcriptional regulators in HD (Dunah et al., 2002; Luthi-Carter et al., 2002; Bae et al., 2005; Zhai et al., 2005) and has impaired capacity to interact with RE1-silencing transcription factor/neuron-restrictive silencer factor (REST/NRSF), which alters the expression of many neuronal genes including brain-derived neurotrophic factor (BDNF; Zuccato et al., 2003, 2007). Furthermore, the global transcriptional dysregulation in HD has been refined in genomics, proteomics and network analysis studies (Langfelder et al., 2016; Hensman Moss et al., 2017; Ament et al., 2018).

Transcription factor 4 (TCF4) belongs to a large bHLH transcription factor family and is a dimerization partner to other bHLH proteins for binding to E-box sequences of target genes (for review, see Massari and Murre, 2000). Importantly, TCF4 should not be confused with key factor of Wnt signaling pathway TCF7L2, unofficially called TCF-4. *TCF4* is widely but not equally expressed in human brain and the use of numerous alternative 5' exons leads to generation of many different TCF4 protein isoforms (Sepp et al., 2011). TCF4 regulates many genes implicated in neurodevelopment, ion channel functions and signal transduction (Forrest et al., 2018). Furthermore, TCF4 regulates synaptic plasticity and memory, and overexpression of TCF4 results in abnormal distribution of layer 2/3 pyramidal neurons in prefrontal cortex and alters their intrinsic excitability (Kennedy et al., 2016; Page et al., 2018; Thaxton et al., 2018). A recent study by Tamberg and colleagues (Tamberg et al., 2020) showed that reduction of Daughterless (*Drosophila melanogaster* homolog of TCF4) in larvae central nervous system impairs appetitive associative learning and downregulates synaptic protein encoding genes,

Received May 3, 2021; accepted August 22, 2021; First published September 13, 2021.

The authors declare no competing financial interests.

Author contributions: K.N., M.S., J.T., and T.T. designed research; K.N., M.S., C.C.-P., J.C.-M., A.S., and H.V. performed research; K.N., M.S., C.C.-P., J.C.-M., J.T., A.S., H.V., D.J.B., E.P.-N., and T.T. analyzed data; K.N., M.S., J.T., D.J.B., E.P.-N., and T.T. wrote the paper.

This work was supported by the Estonian Research Council Institutional Research Funding IUT19-18 and Grant PRG805, the European Union through the European Regional Development Fund Project No. 2014-2020.4.01.15-0012, H2020-MSCA-RISE-2016 (Grant EU734791), and the Spanish government through the Spanish Ministry of Science, Innovation and Universities Grant PID2019-106447RB-I00 (to E.P.-N.). D.J.B. was supported by the Medical Research Council (MRC) Grant MR/L010305/1. This work has also been partially supported by "TUT Institutional Development Program for 2016-2022" Graduate School in clinical medicine receiving funding from the European Regional Development Fund under Program ASTRA 2014-2020.4.01.16-0032 in Estonia.

M. Sepp's present address: Center for Molecular Biology of Heidelberg University (ZMBH), Heidelberg D-69120, Germany.

H. Vihma's present address: Department of Cell Biology and Physiology, Neuroscience Center, University of North Carolina, Chapel Hill, NC 27599.

J. Creus-Muncunill's present address: Department of Neurology, Icahn School of Medicine at Mount Sinai, New York, NY 10029.

Acknowledgements: We thank Elena Cattaneo for support and feedback in the early stage of this study; Epp Väli, Ana López, and M. Teresa Muñoz for technical assistance; and Kaisa Roots for cloning construct pGL4.83[hRluc/P/PGK1/Puro].

Correspondence should be addressed to Tõnis Timmusk at tonis.timmusk@taltech.ee.

<https://doi.org/10.1523/ENEURO.0197-21.2021>

Copyright © 2021 Nurm et al.

This is an open-access article distributed under the terms of the Creative Commons Attribution 4.0 International license, which permits unrestricted use, distribution and reproduction in any medium provided that the original work is properly attributed.

therefore linking Daughterless, and possibly TCF4, to memory formation (Tamberg et al., 2020).

Our immunocytochemical screen of different transcription factors in a cellular model of HD revealed differential expression and/or localization of TCF4. Therefore, based on the developmental hypothesis as well as disturbed synaptic plasticity and adult neurogenesis in HD, we decided to thoroughly investigate the expression of neurodevelopmentally important TCF4 in cellular and mouse models of HD and in HD patients. We show that TCF4 levels are reduced in HD brain in an isoform-dependent and brain region-dependent manner. We further reveal differences in the ability of different TCF4 isoforms to cooperate with Class II bHLH transcription factor ASCL1 in neurons. These results implicate reduced and/or imbalanced TCF4 function as a possible factor in HD etiology.

Materials and Methods

Cell culture

The striatal progenitor Hdh^{7/7}, Hdh^{7/109}, and Hdh^{109/109} cell lines have been described previously (Zuccato et al., 2003). Briefly, Hdh^{7/7} cells are derived from wild-type (wt) mice carrying two copies of the endogenous *Htt* alleles with 7 CAG repeats; Hdh^{7/109} and Hdh^{109/109} are derived from heterozygous and homozygous *knock-in* mice with one or both *Htt* alleles containing 109 CAG repeats, respectively. Hdh cells were propagated in DMEM (Invitrogen) supplemented with 10% fetal bovine serum (PAA Laboratories), 100 U/ml penicillin and 0.1 mg/ml streptomycin (PAA Laboratories) at 33°C in 5% CO₂.

Separate rat cortical and hippocampal neuronal cultures were prepared from embryonic day (E) 21 Sprague Dawley rat embryos as described previously (Esvald et al., 2020). Where indicated, neurons were treated with 0.5 mM 3-NP (Sigma-Aldrich) for 0–16 h at 6–8 days *in vitro* (DIV).

Mice

Male R6/1 transgenic mouse (B6CBA background) expressing the N-terminal exon 1 fragment of mutant *HTT* with 115 CAG repeats (obtained originally from The Jackson Laboratory) and their wt littermate controls were used for this study. Genotyping was performed by PCR from tail biopsy samples using primers designed for the expansion of the exon 1 of the mutant *HTT* as previously described (Mangiarini et al., 1996). All mice were housed together in numerical birth order in groups of mixed genotypes with access to food and water *ad libitum* in a colony room kept at 19–22°C and 40–60% humidity, under a 12/12 h light/dark cycle. Mice were exsanguinated at 8, 12, 20, and 30 weeks of age and brain was quickly removed for cortex, hippocampi and striata dissection. All procedures were conducted in accordance with the National Institutes of Health *Guide for the Care and Use of Laboratory Animals*, and approved by the local animal care committee of the Universitat de Barcelona, following European (2010/63/UE) and Spanish (RD53/2013) regulations for the care and use of laboratory animals.

Postmortem human brain tissue

Frozen samples of hippocampus and cerebral cortex from HD patients and control individuals were obtained from the Neurologic Tissue Bank of the Biobank-Hospital Clínic-Institut d'Investigacions Biomèdiques August Pi i Sunyer (IDIBAPS) following the guidelines and approval of the local ethics committee (Hospital Clínic of Barcelona's Clinical Research Ethics Committee). Informed consent was obtained from all subjects, and experiments were performed following the guidelines and approval of the local ethics committee. Details on the sex, age, CAG repeat length, Vonsattel grade, and postmortem delay are found in Table 1.

Immunocytochemistry

Hdh cells grown on poly-L-lysine-coated coverslips were fixed and treated as previously described (Kannike et al., 2014). Rabbit polyclonal anti-TCF4 (#HLH201, CeMines) and other polyclonal antibodies (Extended Data Fig. 1-1, CeMines) were diluted 1:200 and Alexa Fluor 488-conjugated goat anti-rabbit IgG antibodies (Invitrogen) were diluted 1:2000 in 0.2% BSA and 0.1% Tween 20 in PBS. DNA was counterstained with DAPI included in the mounting medium (ProLong Gold Antifade mountant with DAPI; Thermo Fisher). The specificity of the nuclear signal of the used TCF4 antibody has been validated previously (Sepp et al., 2017).

Western blotting

Hdh cells and rat cultured cortical neurons were lysed in RIPA buffer (50 mM Tris-HCl, pH 8, 150 mM NaCl, 1% NP-40, 0.5% sodium deoxycholate, 0.1% SDS, 1 mM dithiothreitol and protease inhibitors cocktail Complete mini; Roche). Cell lysates were sonicated for 15 s with 30% amplitude on Sonics VibraCell and centrifuged at 16,100 × *g* for 15 min at 4°C. Nuclear and cytosolic fractions of Hdh cells were prepared with NE-PER Nuclear and Cytoplasmic Extraction kit (Thermo Scientific) according to the manufacturer's instructions. Protein concentrations in lysates were measured with BCA Protein Assay kit (Pierce).

Protein extraction from mouse brain and human post-mortem samples from the cerebral cortex and CA1 region of the hippocampus was performed using a lysis buffer containing 50 mM TRIS (pH 7.4), 10% glycerol, 1% Triton X-100, 150 mM NaCl, 5 μM ZnCl₂, 10 mM EGTA and protease inhibitors [2 mM phenylmethylsulfonyl fluoride (PMSF), 10 μg/μl aprotinin, and 1 μg/μl leupeptin] and phosphatase inhibitors (2 mM Na₃VO₄ and 100 mM NaF). Samples were homogenized and supernatants were collected after centrifugation at 15,000 × *g* for 15 min at 4°C. Protein concentration was measured using Dc protein assay kit (Bio-Rad Laboratories).

TCF4 isoforms A⁻, B⁻, C⁻ and D⁻ were *in vitro* translated using TnT Quick Coupled Transcription/Translation System (Promega) according to the manufacturer's instructions. The used DNA constructs have been described previously (Sepp et al., 2011). The frontal cortex lysates from E18 *Tcf4* knock-out (KO) and wt mice were a kind gift from

Table 1: Hippocampus CA1 and cerebral cortex tissue samples of HD patients

ID	Region	Pathologic diagnosis	Gender	Age (years)	CAG repeats	PMD (h:min)*
CS-497	CA1	Control	M	82		02:30
CS-1694	CA1	Control	M	58		05:00
CS-1858	CA1	Control	F	83		07:30
CS-1870	CA1	Control	F	97		07:20
CS-1888	CA1	Control	F	93		05:30
CS-1937	CA1	Control	F	83		07:33
CS-1949	CA1	Control	M	86		07:25
CS-1193	CA1	HD, Vonsattel grades 3–4	M	55	-	07:00
CS-1294	CA1	HD, Vonsattel grade 3	M	53	45 ± 2	07:00
CS-1334	CA1	HD, Vonsattel grade 1	M	73	40 ± 2	07:00
CS-1438	CA1	HD, Vonsattel grade 3	M	85	40	05:30
CS-1630	CA1	HD, Vonsattel grade 2	M	76	41	06:00
CS-1638	CA1	HD, Vonsattel grade 2	M	72	-	13:10
CS-1844	CA1	HD, Vonsattel grade 2	F	69	43	15:30
CS-1874	CA1	HD, Vonsattel grade 3	M	56	43	04:30
CS-1875	CA1	HD, Vonsattel grades 2–3	M	84	39	08:00
CS-1933	CA1	HD, Vonsattel grade 2	F	86	40	12:20
810	Cortex	Control	F	81		23:30
1679	Cortex	Control	F	90		12:20
1697	Cortex	Control	M	78		06:00
1870	Cortex	Control	F	97		07:20
1937	Cortex	Control	F	83		07:33
1949	Cortex	Control	M	86		07:25
1980	Cortex	HD, Vonsattel grade 3	F	69	-	12:30
1875	Cortex	HD, Vonsattel grades 2–3	M	84	39	08:00
1844	Cortex	HD, Vonsattel grade 2	F	69	43	15:30
1638	Cortex	HD, Vonsattel grade 2	M	72	-	13:10
1630	Cortex	HD, Vonsattel grade 2	M	76	38	06:00
909	Cortex	HD, Vonsattel grade 4	M	60	43	13:30

Details of human postmortem samples used for Western blotting to analyze protein levels of TCF4. All samples received from the Neurologic Tissue Bank-Biobanc located at the University of Barcelona School of Medicine. *PMD, postmortem delay.

Brady Maher and have been described in more detail previously (Li et al., 2019).

Equal amounts of protein were separated in 8% gel in SDS-PAGE followed by wet transfer to Hybond-C nitrocellulose membrane (GE Healthcare) or to PVDF membrane (Merck Millipore). Membranes were blocked 1 h at room temperature (RT) in PBS containing 5% skimmed milk and 0.1% Tween 20, incubated overnight at 4°C with primary antibodies and 1 h at RT with secondary antibodies in 0.1% Tween 20 (and 5% BSA for the mouse and postmortem human brain samples) and 2% skimmed milk in PBS. Antibodies were diluted as follows: 1:200 rabbit polyclonal anti-TCF4 (TCF4_02; 200 ng/ml; Forrest et al., 2018), 1:1000 mouse monoclonal anti-TCF4 (ITF-2 C-8; #sc-393407; 200 µg/ml; Santa Cruz), rabbit polyclonal anti-HDAC2 1:1000 (#sc-7899, Santa Cruz), mouse monoclonal anti-β tubulin to final concentration 30 ng/ml (E-7, DSHB), anti-α tubulin (T9026, Sigma-Aldrich) and HRP-conjugated goat anti mouse or rabbit IgG (H+L) 1:2500 (#32430 and #32460, respectively; Thermo Scientific). Chemoluminescence signal was detected using SuperSignal West Femto Chemoluminescent Substrate (Thermo Scientific) and ImageQuant 400 imaging system (GE Healthcare). Additionally, Coomassie staining was used to quantify loading in five independent Western blotting experiments with Hdh total lysates. Briefly, the membrane was stained with Coomassie solution (0.1% Coomassie Brilliant Blue R-250 dye, 25% ethanol, 7% acetic acid), followed by two washes with destaining solution

(30% ethanol, 10% acetic acid) and rinsing with tap water. Densitometric quantification was done using ImageQuant T4 v2005 software (GE Healthcare) or Gel-Pro Analyzer version 4 (Media Cybernetics).

TCF4 transcripts data mining and visualization

Mouse *Tcf4* gene structure and mRNAs were identified by analyzing genomic, mRNA and expressed sequence tag (EST) databases available at <https://genome.ucsc.edu/> and <https://www.ncbi.nlm.nih.gov/nucleotide>. Accession numbers of representative mouse mRNA or EST sequences for alternative *Tcf4* transcripts are shown in Table 2, based on Mouse Dec. 2011 GRCh38/mm10 genome assembly. Human transcript data adapted from Sepp et al. (2011) is included for reference (Human Dec. 2013, GRCh38/hg38 assembly).

RNA extraction and cDNA synthesis

Total RNA from Hdh cells and cultured cortical neurons was extracted using RNeasy Micro kit (QIAGEN) following the manufacturer's instructions. R6/1 mouse brain tissue was homogenized in QIAzol reagent (QIAGEN) and total RNA was extracted with RNeasy Lipid Tissue Mini kit (QIAGEN) according to the manufacturer's protocol including on-column DNase I treatment. First-strand cDNAs were synthesized from 1 to 5 µg of total RNA with Superscript III First-Strand synthesis system (Invitrogen) together with oligo(dT)₂₀ or a combination of oligo(dT)₂₀

Table 2: Accession numbers of representative mRNA or EST sequences for alternative *Tcf4* transcripts and protein isoforms they encode in mouse and human

Transcript	Alternative TCF4 transcripts and isoforms		
	Protein isoform	Mouse	Human
3b	B	AK133885	AK315074
3bΔ3	C	AK051958	AK299169
3c	B	AK081012	DB106801
3cΔ3	E	ENSMUST00000202354.3	FR748216
3cΔ8-9	BΔ	ENSMUST00000202772.3	FR748212
3d	B	CJ182557	M74719
4c	C	CJ115804	DC358747
7a-II	D	BY247629	AK300612
7b-I	D/G	XM_017317861	AK095041
7b-II	D	CD350230	DC350124
8a	D	BY286412	AK316165
8b*/8b-I	D	CB178848	FR748208
8b-II	D	BY252182	AK300636
8c-II	D	BB663894	CA393351
8e/8d	D	BY259217	BP230382
10a	A	U16321	AK300038
10b	I	BU058820	BP241032
10c	H	BY333068	DA664480

Reference for transcripts of human *TCF4* were obtained from Sepp et al. (2011). Data are according to Mouse Dec. 2011 (GRCm38/mm10) Assembly and Human Dec. 2013, GRCh38/hg38 assembly. *TSS differs between human and mouse. The respective human transcript is shown after slash.

and random hexamer primers (Microsynth) in case of cultured cells and R6/1 brain RNA, respectively.

Quantitative PCR (qPCR)

qPCRs were performed in triplicates using LightCycler 480 SYBR Green I Master (Roche) with cDNA from Hdh cells and 3-NP-treated cultured cortical neurons and 5× HOT FIREPol EvaGreen qPCR Mix Plus (Solis Biotdyne) with R6/1 mouse brain cDNAs on LightCycler 480 II Real Time PCR System (Roche). Levels of *Sdha* or *Hprt1* (for HD cell model experiments: Hdh and 3-NP-treated neurons, respectively) or geometric mean of *Hprt1*, *Gapdh*, and *Tbp* (for R6/1 mouse experiments) mRNA levels were used to normalize qPCR data. Primer pairs used in qPCR are shown in Table 3.

Table 3: List of oligonucleotides used in this study

Gene (transcript)	Forward primer sequence	Reverse primer sequence
<i>Tcf4 total</i>	TACGCTCCTTCAGCCAGCAC	TGGATGCAGGCTACAGTAGCTG
<i>Tcf4-B/C</i>	AGAAGACAGAAAGTAGCTCAGGGTC	GTTTGGTGGGCGAAAGGGTTCC
<i>Tcf4-A</i>	caccATGTACTGCGCATACACCATC	TGGATGCAGGCTACAGTAGCTG
<i>Tcf4-B</i>	caccATGCATCACCAACAGCGAATGG	GGACCCTGAGCTACTTCTGTCTTC
<i>Tcf4-D (8c-II)</i>	CAGCTGAAATGATTCCCCTGTG	TGGATGCAGGCTACAGTAGCTG
<i>Tcf4-D (7b-I)</i>	GTCTTGCTTGCATACATTGCCAG	GTTTGGTGGGCGAAAGGGTTCC
<i>Tcf4-I</i>	GAGAAAGCCCAAGTTAGGCTGAG	TGGATGCAGGCTACAGTAGCTG
<i>Bdnf</i>	GGCCCAACGAAGAAAACCAT	AGCATCACCCGGGAAGTGT
<i>Ascl1</i>	AACTCTATGGCGGGTCTCCGGT	CTGCCATCCTGCTTCCAAAGT
<i>Neurod1</i>	ACACGAGGCAGACAAGAAgG	TCTTGGGCTTTTGCATCaTCC
<i>Hprt1</i>	CAGTCCCAGCGCTCGTGATTA	AGCAAGTCTTTTCAGTCTCTGTC
<i>Sdha</i>	AACACTGGAGGAAGCACAC	GGAACGGATAGCAGGAGGT
<i>Gapdh</i>	TGCACCACCACTGCTTAGC	GGCATGGACTGTGGTCATGAG
<i>Tbp</i>	TGCACAGGAGCCAAGAGTGAA	CACATCACAGCTCCCCACCA

Plasmid constructs

Expression constructs pcDNA.3.1/EF1a/TCF4-B⁻ and pcDNA.3.1/EF1a/TCF4-A⁻ have been characterized previously (Sepp et al., 2017). The constructs for TCF4-C⁻, TCF4-D⁻, and TCF4-I⁻ were created similarly from the respective pcDNA3.1 constructs as described (Sepp et al., 2011) by replacing the cytomegalovirus (CMV) promoter with elongation factor 1 (EF1α) promoter from pGL4.83[hRlucP/EF1α/Puro]. pcDNA3.1/PGK/ASCL1 was cloned from pcDNA3.1/SRα/ASCL1 (Sepp et al., 2017) replacing SRα promoter with PGK promoter from pGL4.83 [hRlucP/PGK1/Puro]. Luciferase reporter system constructs pGL4.29[luc2P/12μE5/TK/Hygro] with 12 E-boxes in front of thymidine kinase promoter, and pGL4.83[hRlucP/PGK1/Puro] with phosphoglycerate kinase 1 promoter have been characterized previously (Sepp et al., 2011, 2017).

Luciferase reporter assay

Neurons plated on 48-well plates were transfected at 6 DIV using Lipofectamine 2000 (Invitrogen) with a reagent to DNA ratio 3:1. For luciferase reporter assays, 0.06 μg of TCF4 isoforms B⁻, C⁻, D⁻, A⁻, and I⁻, and 0.06 μg of ASCL1 encoding constructs were used, 0.06 μg of firefly luciferase construct pGL4.29[luc2P/12μE5/TK/Hygro], and 0.02 μg of *Renilla* luciferase pGL4.83[hRlucP/PGK1/Puro] were used. At 7 DIV, the neuronal cultures were left untreated or treated with 25 mM KCl for 8 h. Cells were lysed in Passive Lysis buffer (Promega) and Dual-Glo Luciferase assay (Promega) was used for measuring luciferase signals. Luciferase assay was performed in technical duplicates and in total three independent experiments were conducted both on cortical and hippocampal primary neurons. Normalized luciferase data were used to calculate co-operation indices between TCF4 and ASCL1 as described (Chang et al., 1996). Briefly, co-operation index shows how many times the transactivation fold is increased in neurons co-expressing different TCF4 isoforms and ASCL1 compared with the sum of transactivation folds from neurons expressing both proteins separately.

Statistical analysis

For quantification of Western blotting data TCF4 signals were normalized to the signals of β tubulin (Hdh whole

and cytoplasmic lysates; Fig. 2C,E), HDAC2 (nuclear lysates; Fig. 2E), Coomassie staining (Hdh whole lysates; Fig. 2C), or α tubulin (lysates from human CA1 region of the hippocampus and cerebral cortex; Fig. 4F,H). The data were log-transformed to ensure normal distribution, autoscaled (where indicated in the figure legend), mean and SEM were calculated, and two-tailed *t* tests were used for statistical analysis (Extended Data Figs. 2-1, 4-1). The data were back-transformed into the linear scale for graphical representation, error bars represent upper and lower limits of the back-transformed mean \pm SEM. For analysis of TCF4 protein levels in R6/1 mouse brain time series, the TCF4 signals were normalized to the signals of α tubulin, data were log-transformed, mean and mean \pm SEM were calculated for each group, and the average expression level of the respective transcript in each age group was set as 0 (1 in linear scale). Generalized linear model with Gaussian distribution using the formula genotype + age:genotype was used, followed by Wald χ^2 test (Type III test, performed with Car package in R; Fox and Weisberg, 2019) to determine *p* values of the coefficients. For graphical representation, data were back-transformed to the linear scale, with error bars showing back-transformed mean \pm SEM. qPCR data generated from Hdh cell line and 3-NP-treated rat primary cortical neurons were log-transformed and autoscaled, mean and \pm SEM values were calculated, and two-tailed paired *t* tests were performed (Extended Data Fig. 2-1). For graphical representation the data were back-transformed into the linear scale, error bars represent upper and lower limits of the back-transformed mean \pm SEM. For analysis of transcript levels in time series of R6/1 mouse brain, data were log-transformed, mean and mean \pm SEM were calculated for each group, and the average expression level of the respective transcript in eight-week-old wt animals was set as 0 (1 in linear scale). Generalized linear model with Gaussian distribution using the formula age + genotype + age:genotype was used, followed by Wald χ^2 test (Type III test, performed with Car package in R; Fox and Weisberg, 2019) to determine *p* values of the coefficients. For graphical representation, data were back-transformed to the linear scale, with error bars showing back-transformed mean \pm SEM.

For luciferase reporter assay, Firefly luciferase signals were normalized to the *Renilla* luciferase signal, data were then subjected to log transformation, mean centering, and autoscaling to obtain normal distribution. For graphical representation, the data were back-transformed to the original scale. One-way repeated-measures ANOVA with Greenhouse–Geisser correction followed by Tukey's *post hoc* test was used to determine statistical significance compared with the full-length TCF4-B⁻ in different conditions using Prism 7 software (GraphPad; Extended Data Fig. 6-1).

Numbers of independent experiments and biological samples are indicated in figure legends; R6/1 mouse samples are summarized in Table 4.

Results

Identification of TCF4 as a misregulated transcription factor in HD

Mislocalized nucleoporins and impaired nucleocytoplasmic transport have been described in several HD

models and patients (Grima et al., 2017). We used a panel of >200 antibodies (Extended Data Fig. 1-1) generated against various transcription and transcription associated factors to screen for differential immunocytochemical signals in mouse striatal progenitor cell lines Hdh^{7/7} (wt), Hdh^{7/109} (heterozygous for HD mutation), and Hdh^{109/109} (homozygous for HD mutation). Our screen revealed 8 antibodies that showed differential signals in wt and mutant Hdh cells (Fig. 1A; Extended Data Fig. 1-2), including the FOXO3 antibodies that display increased nuclear signals in the mutant cells as reported earlier (Kannike et al., 2014). It must be noted, however, that most of the used antibodies have not been validated for immunocytochemical detection of endogenous proteins, and thus the results of the screen should be interpreted with caution. Antibodies generated against the basic helix-loop-helix (bHLH) transcription factor TCF4 showed reduced nuclear signals in Hdh cell lines expressing expanded *Htt* alleles (Fig. 1A). The specificity of the nuclear signal of these TCF4 antibodies has been demonstrated, whereas the cytoplasmic signal has been shown to be unspecific (Sepp et al., 2017). Therefore, our results suggest a difference in TCF4 localization and/or expression in Hdh^{7/7}, Hdh^{7/109}, and Hdh^{109/109} cells. Considering that TCF4 is an essential transcription factor in brain development and is linked to intellectual disability (Zweier et al., 2007; Kalscheuer et al., 2008; Blake et al., 2010), we sought to further characterize the potential misregulation of TCF4 in HD.

Human *TCF4* is a complex gene with 41 exons, out of which 21 are alternative 5' exons. Human TCF4 protein isoforms with 18 different N termini and additional variance resulting from alternative splicing at the cassette exons 8–9 (full-length and δ isoforms) and exon 18 [+/- isoforms differing by four amino acids (RSRS)] have been described (Sepp et al., 2011). To elucidate the structure of the mouse *Tcf4* gene we gathered data from public databases about mouse *Tcf4* expressed sequences (Fig. 1B, C; Table 2). The general gene structure of mouse *Tcf4* is similar to human *TCF4*. Compared with the human *TCF4* gene, fewer transcripts are reported for mouse *Tcf4* and these encode protein isoforms with seven different N termini (Fig. 1B). There were two rare TCF4-B Δ and one TCF4-E isoform encoding transcripts present in the databases. Our analysis of mouse *Tcf4* data revealed seven alternative TCF4-D-coding transcripts linked to different 5' untranslated exons with translation initiation codon in exon 8 for all of them. Of note, a nucleotide addition in 5' alternative exon 7b-I prevents the expression of TCF4-G in mice and TCF4-D is coded instead (Fig. 1C). The transcript starting from exon 8d, expressed in human, has not been described in mouse. Instead, transcript 8e (with a different transcription start site) is expressed in mouse.

Collectively, we have determined that the *TCF4* gene structure is highly conserved between mouse and human and our results suggest misregulation of TCF4 in the mutant HTT-expressing mouse striatal cells.

TCF4 levels are reduced in cell-based HD models

To dissect the contribution of different TCF4 isoforms to the altered immunocytochemical signal of TCF4

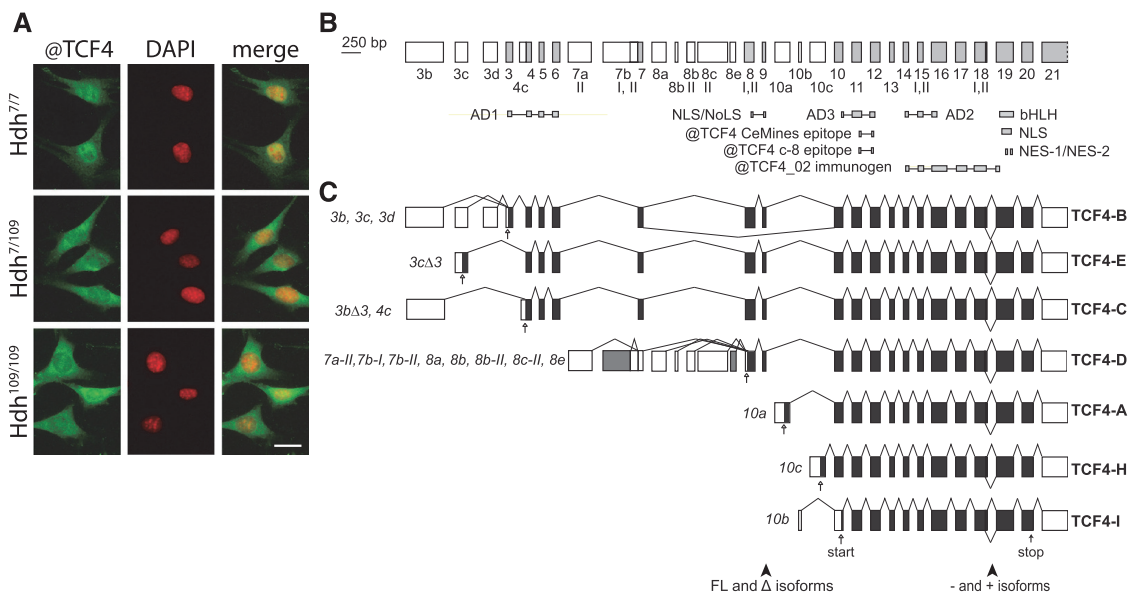


Figure 1. Differential immunocytochemical signal of endogenous TCF4 in Hdh cells and the structure and alternative splicing of mouse *Tcf4* gene. **A**, Representative micrographs showing distribution of immunocytochemical signal obtained with anti-TCF4 antibodies (#HLH210, CeMines) in Hdh^{7/7}, Hdh^{7/109}, and Hdh^{109/109} cells. Antibodies used for the immunocytochemical screen in Hdh cells are listed in Extended Data Figure 1-1. Results of the screen with additional antibodies (CeMines) that showed differential signals in wt and mutant Hdh cells are shown in Extended Data Figure 1-2. DNA was counterstained with DAPI. Scale bar: 20 μm. **B**, Mouse *Tcf4* genomic organization with exons drawn in scale. Gene structure layout and exon numbering is based on Sepp et al. (2011) for convenient comparison with human *TCF4* gene. 5' exons are marked with white boxes and internal or 3' exons are shaded in light gray. Exon names are displayed below boxes. Roman numerals designate alternative splice donor or acceptor sites, with some missing compared with the human *TCF4*. The regions encoding the respective domains of TCF4 and the epitopes of the used TCF4 antibodies [polyclonal @TCF4 (#HLH20, CeMines), polyclonal @TCF4_02 (Forrest et al., 2018), and monoclonal @TCF4 (Santa Cruz c-8)] are indicated below the gene structure. AD, activation domain; bHLH, basic helix-loop-helix; NLS, nuclear localization signal; NES, nuclear export signal; NoLS, nucleolar localization signal. **C**, Alternative transcripts of mouse *Tcf4* grouped together according to the encoded TCF4 protein isoform. Translated and untranslated regions are designated as dark gray and white boxes, respectively. Transcripts are designated with the name of the 5' exon and, where necessary, with the number of the splice site used in the 5' exon. Accession numbers of the representative mouse *Tcf4* transcripts presented here are listed in Table 2. Transcripts using the 5' exon 7b-1 (shown with gray) is translated into TCF4-D in mouse and TCF4-G in human and transcript 8e (shown with gray) is unique to mouse. The name of the protein isoform is shown on the right. The position of the first in-frame start codon for each transcript and stop codon are shown with empty and filled arrows, respectively. Arrowheads at the bottom of the panel point to the regions of alternative splicing giving rise to Δ isoform or + and - isoforms.

detected in HD cells, we next studied TCF4 protein levels in Hdh cell lines by Western blotting. First, we used cortical lysates from *Tcf4* KO mice (Li et al., 2019) to validate the specificity of two TCF4 antibodies, polyclonal antibody anti-TCF4_02 (Forrest et al., 2018) and a commercial monoclonal antibody anti-TCF4 c-8 (Santa Cruz; Fig. 2A,B) and determined the mobility pattern of different TCF4 isoforms overexpressed in HEK293 cell lysates (data not shown). We then analyzed total cell lysates of Hdh cells by Western blotting with polyclonal anti-TCF4_02 antibody (*n* = 3; Fig. 2C) and anti-TCF4 c-8 antibody (*n* = 5). Based on the predicted molecular weight (Mw) and mobility of *in vitro* translated isoforms TCF4-B⁻ and TCF4-A⁻, we divided the detected TCF4 protein bands into two groups: high Mw isoforms, similar to isoforms TCF4-B and TCF4-C and their respective +/− isoforms, and medium/low Mw isoforms, which probably correspond to TCF4-D, TCF4-A, TCF4-H, and TCF4-I and

their respective +/− isoforms. Of note, + isoforms have higher mobility than isoforms in SDS-PAGE gels as described previously (Sepp et al., 2011). We observed a significant >30% decrease of both high and low Mw TCF4 isoforms in both mutant Hdh cell lines compared with wt Hdh cells (Fig. 2C,D).

Next, to further decipher the changes in TCF4 levels we fractionated Hdh cells into cytoplasmic and nuclear lysates and analyzed the lysates by Western blotting with polyclonal TCF4_02 antibody (*n* = 3; Fig. 2E). *In vitro* translated isoforms TCF4-B⁻, TCF4-A⁻, TCF4-C⁻, and TCF4-D⁻ were used to decipher bands detected in Hdh cell lysates. TCF4 protein levels were reduced in both cytoplasmic and nuclear fractions of mutant Hdh cells (Fig. 2F). In mutant Hdh cell cytoplasm the levels of TCF4 were downregulated to ~40% of TCF4 detected in wt cells, with statistical significance only for Hdh^{109/109} (Fig. 2F). In the nuclear fraction, a visible reduction was observed in both

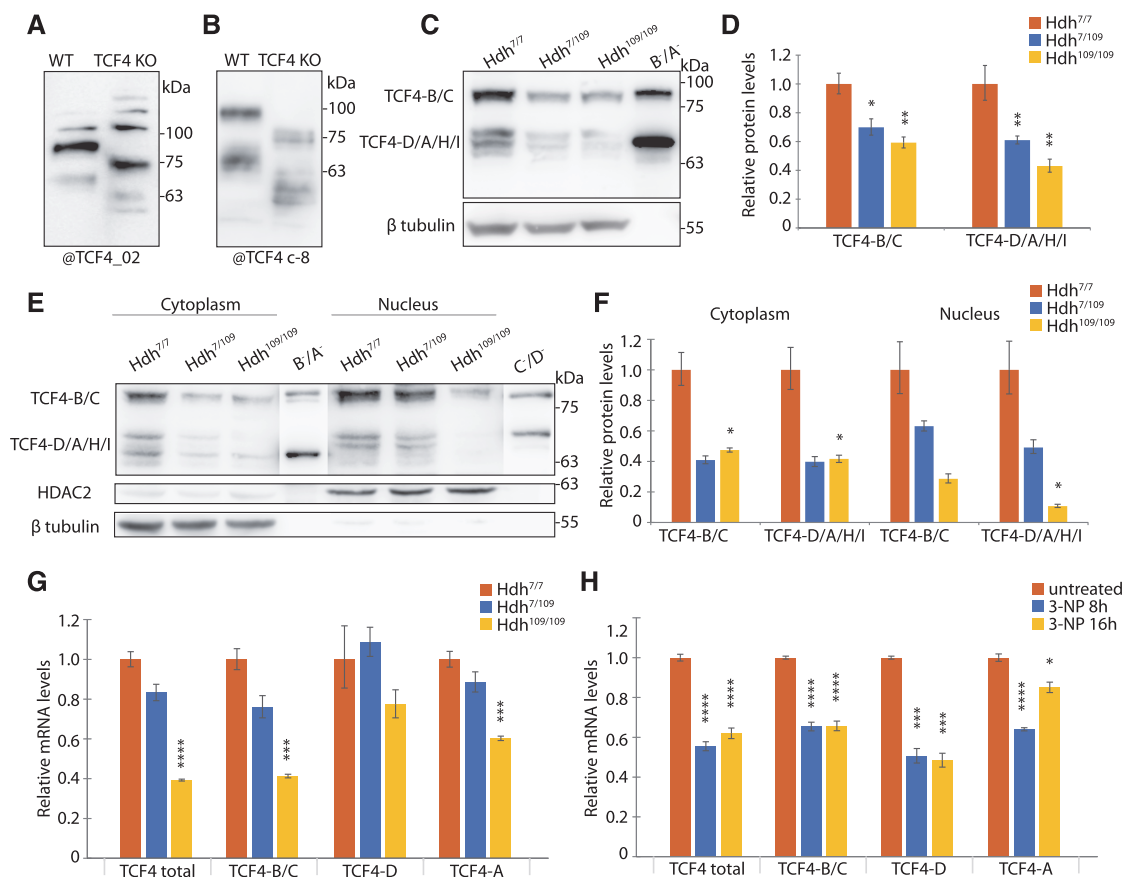


Figure 2. Protein and mRNA levels of transcription factor TCF4 in HD cell models. **A, B**, Validation of TCF4_02 polyclonal (**A**) and TCF4 c-8 monoclonal antibodies (**B**). Western blot analysis of E18 wt and *Tcf4* KO mice brain total lysates (Li et al., 2019). The KO mice express truncated TCF4 proteins that lack C terminus of the wt protein, but maintain the regions targeted by the used antibodies. **C, E**, Representative Western blot analysis of TCF4 protein levels in total lysates (**C**) and cytoplasmic and nuclear fractions (**E**; 100 and 50 µg of protein, respectively) of wt Hdh^{7/7}, heterozygous mutant Hdh^{7/109} and homozygous mutant Hdh^{109/109} cells. *In vitro* translated human TCF4-A⁻, TCF4-B⁻, TCF4-C⁻, and TCF4-D⁻ were added as controls. β tubulin served as a loading control for total and cytoplasmic lysates and HDAC2 for nuclear lysates. **D, F**, Quantification of data in **C** (*n* = 8 independent experiments) and in **E** (*n* = 3), respectively. TCF4-B and TCF4-C were quantified together as high Mw isoforms (TCF4-B/C), and TCF4-D, TCF4-A⁺, and TCF4-A⁻ together as low Mw isoforms (TCF4-D/A⁻/A⁺). In **D**, TCF4 signals were normalized to either the levels of β tubulin (for three experiments) or Coomassie Blue staining (for five experiments). In **F**, signal intensities were normalized to β tubulin signal intensities in the cytosolic fraction and to HDAC2 in nuclear fraction. The relative TCF4 levels in Hdh^{7/7} were arbitrarily set as 1. The data were log-transformed, autoscaled, means and SEMs were calculated, and statistical significance is shown relative to the levels of respective TCF4 isoforms measured in Hdh^{7/7} cells; **p* < 0.05, ***p* < 0.01, paired Student's *t* test. Precise *p* values are reported in Extended Data Figure 2-1. The data were back-transformed into the linear scale for graphical representation, error bars represent upper and lower limits of back-transformed mean ± SEM. **G, H**, RT-qPCR analysis of total *Tcf4* mRNA, transcripts encoding long (TCF4-B and TCF4-C), medium (TCF4-D), and short (TCF4-A) isoforms in mouse HD cells (**G**; *n* = 3) and in rat primary cortical neurons untreated or treated with 3-NP for 8 or 16 h (**H**; *n* = 5). *Tcf4* mRNA levels were normalized to the levels of *Sdhα* or *Hprt1* mRNA, respectively. The data were log-transformed, autoscaled, and the mean values and mean ± SEM were calculated. Statistical significance is shown relative to the expression level of the respective *Tcf4* transcripts in Hdh^{7/7} cells or untreated neurons. The data were back-transformed into linear scale for graphical depiction and error bars represent upper and lower limits of back-transformed mean ± SEM; **p* < 0.05, ****p* < 0.005, *****p* < 0.001, paired Student's *t* test (precise *p* values are reported in Extended Data Figure 2-1).

mutant cell lines with all TCF4 isoforms, albeit statistical significance was reached only for TCF4 D/A/H/I where protein levels in Hdh^{109/109} cells were reduced to 10% of the levels of these isoforms in wt cells (Fig. 2F). Taken

together, TCF4 protein levels were reduced in both fractions and especially dramatically in Hdh^{109/109} nuclear fraction. Interestingly, distinct set of medium/low Mw TCF4 isoforms were present in the nucleus compared

Table 4: R6/1 mouse samples used for quantification of TCF4 mRNA and protein levels

Age	Genotype	RT-qPCR				Western blotting		
		CX	STR	HIP	CB	CX	STR	HIP
8 weeks	wt	8	8	8	8	6	7	7
	HD	7	6	7	7	6	7	7
12 weeks	wt	8	7	8	6	6	7	6
	HD	7	7	7	7	7	5	7
20 weeks	wt	7	7	7	7	7	5	6
	HD	6	6	5	5	6	6	7
30 weeks	wt	7	6	6	6	6	4	7
	HD	6	6	6	5	6	5	6

CX, cerebral cortex; STR, striatum; HIP, hippocampus; CB, cerebellum.

with cytoplasm, although the isoform patterning did not differ between *Hdh* genotypes (Fig. 2F).

To further elucidate changes of TCF4 in HD we sought to study mRNA levels of total *Tcf4*, combination of the longer transcripts encoding TCF4-B/C and transcripts encoding the most abundant shorter protein isoforms TCF4-D and TCF4-A in mouse *Hdh* cell lines ($n=3$; Fig. 2G). Total *Tcf4* mRNA levels were pronouncedly downregulated in mutant homozygous *Hdh* cells – to 40% of total *Tcf4* levels in wt *Hdh* cells. Similarly, transcripts encoding isoforms TCF4-B and TCF4-C were reduced to 30%, and transcripts encoding TCF4-A to 40% in *Hdh*^{109/109} cells in comparison with wt cells. TCF4-D-encoding mRNAs are transcribed from seven alternative 5' exons out of which we analyzed transcripts with *8c-III* 5'exon (Fig. 1C). No significant change in TCF4-D-encoding *8c-III* transcript levels were detected (Fig. 2G).

To validate our findings from genetic HD model cell lines, we studied *Tcf4* mRNA levels in an induced chemical model, cultured neurons treated with mitochondrial toxin 3-NP. We treated rat cortical neuron cultures with 0.5 mM 3-NP at DIV6–DIV8 for 0–16 h to mimic HD ($n=5$). We determined the same *Tcf4* transcripts as in *Hdh* cells. Total *Tcf4* mRNA levels decreased in cultured cortical neurons after 8- and 16-h treatment with 3-NP to 60% of *Tcf4* levels measured in untreated neurons (Fig. 2H). We observed reduction of TCF4-B and TCF4-C encoding mRNAs in response to 3-NP treatment. After 8- or 16-h exposure to 3-NP the levels of TCF4-A encoding mRNAs were decreased to 64% or to 85% of the levels detected in untreated neurons, respectively. Again, we measured levels of *8c-III* transcript as a representative of transcripts encoding TCF4-D and observed a 50% decrease following 3-NP treatment.

Taken together, the levels of *Tcf4* transcripts are reduced in cortical neurons treated with 3-NP as well as in HD striatal cell lines. This is consistent with the reduced protein levels of TCF4 in HD striatal cells.

Differential downregulation of *Tcf4* transcripts in R6/1 mouse brain

Progressive neurodegeneration in HD is most prevalent in striatum and cerebral cortex, but other brain structures and circuits may also be affected (McColgan and Tabrizi,

2018). To extend our finding in HD cells to animal models, we decided to study *Tcf4* mRNA levels in the transgenic R6/1 mouse model of HD, where N-terminal exon 1-containing fragment of human mutant huntingtin with 115 CAG repeats is expressed. We analyzed mRNA levels in the striatum, cortex, hippocampus and cerebellum of wt and R6/1 mouse at 8, 12, 20, and 30 weeks of age.

To study in detail *Tcf4* mRNA expression in R6/1 mouse brain we quantified mRNA levels of total *Tcf4*, combination of the longer transcripts encoding TCF4-B and TCF4-C (TCF4-B/C), transcripts encoding only TCF4-B, and the most prevalent shorter transcripts encoding TCF4-D, TCF4-A, and TCF4-I by RT-qPCR (Fig. 3). There was no change in the total levels of *Tcf4* mRNAs in the cerebral cortex, striatum and cerebellum, whereas downregulation of total *Tcf4* expression was seen in the hippocampus of R6/1 mice when compared with wt mice at all the ages analyzed. More changes were detected in R6/1 mouse brain at the level of alternative transcripts with decreased longer transcripts encoding TCF4-B and TCF4-B/C in the hippocampus, transcripts encoding TCF4-A in the cerebral cortex and transcripts encoding TCF4-I in the cerebral cortex, hippocampus and striatum. Out of the studied TCF4-D encoding transcripts the expression of *8c-III* mRNA was downregulated and *7b-I* upregulated in the cerebral cortex and hippocampus of mutant versus wt mice. To sum up, we observed a reduction in total *Tcf4* mRNA levels in R6/1 mouse hippocampus, and a comprehensive study revealed an intriguing variability and specific upregulations and downregulations of certain *Tcf4* transcripts already before the onset of HD symptoms. Changes at the level of alternative *Tcf4* transcripts in the cerebral cortex and striatum, and no differences in the *Tcf4* expression in the cerebellum were observed over a time course, from 8 to 30 weeks of age, in R6/1 compared with wt mouse.

TCF4 protein levels are decreased in the hippocampus of R6/1 mouse

We next asked whether the changes detected in *Tcf4* mRNA expression were reflected in the levels of TCF4 protein isoforms in R6/1 mouse brain. We analyzed TCF4 protein levels by Western blotting with monoclonal TCF4 antibody c-8 in the striatum, cortex and hippocampus in the same mice where *Tcf4* mRNA levels were analyzed. The quality of Western blottings enabled quantification of the separate TCF4 bands that were assigned as potential B/C, D, A⁻, and A⁺ isoforms in the order of increasing mobility in PAGE based on theoretical Mw and comparisons with *in vitro* translated TCF4 isoforms (Fig. 2C,E). No band corresponding to TCF4-I was detected. The patterns of TCF4 isoforms expressed in the two pallial structures, cerebral cortex and hippocampus, were similar, whereas in the subpallial striatum the relative proportions of TCF4-D were lower (Fig. 4B,D). Comparisons of TCF4 isoform levels across wt and transgenic mice revealed decreased levels of TCF4-A⁻ in the R6/1 mouse cerebral cortex and a reduction of TCF4-B/C and TCF4-D by 30% and 40%, respectively, in R6/1 mouse hippocampus at all the ages analyzed (Fig. 4D). No statistically significant differences were detected in the striatum.

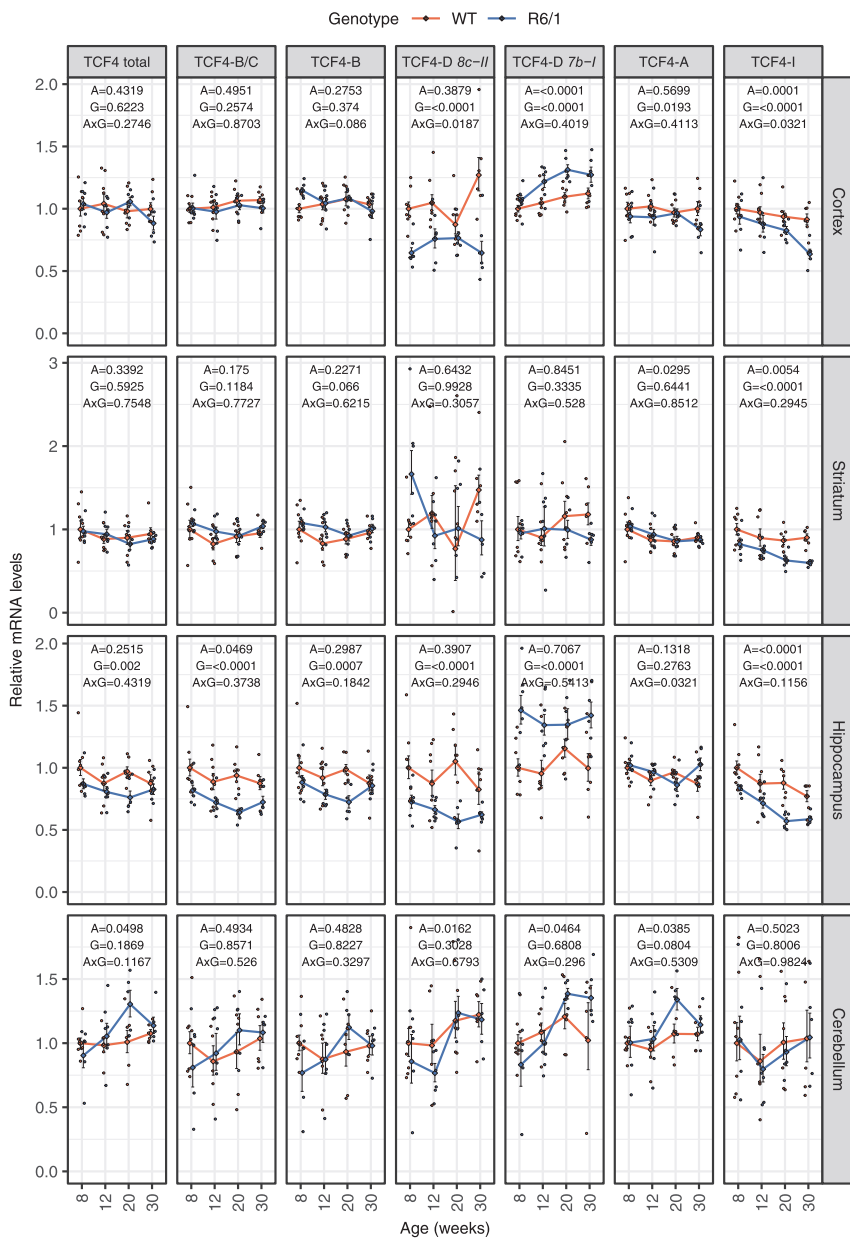


Figure 3. *Tcf4* mRNA levels in R6/1 mouse brain. RT-qPCR analysis of mRNA levels of total *Tcf4* and selected *Tcf4* transcripts encoding alternative *TCF4* isoforms. RT-qPCR analysis was conducted in cortex, striatum, hippocampus, and cerebellum from wt and R6/1 mice at four ages (8, 12, 20, and 30 weeks of age). Number of samples included in each experiment is indicated in Table 4. The transcripts encoding long isoforms TCF4-B and TCF4-C were measured together (TCF4-B/C) and separately in the case of TCF4-B; two TCF4-D encoding transcripts *8c-11*, and *7b-1* as well as transcripts encoding short isoforms TCF4-A, and TCF4-I were quantified. *Tcf4* mRNA levels were normalized to geometric mean of the levels of *Hprt1*, *Tbp*, and *Gapdh*. The average expression level of respective transcript in eight-week-old wt animals was set as 1. The average expression of the respective transcripts in respective groups is shown with lines, error bars indicate SEM, data from all individual animals are shown with dots. Generalized linear model using the formula age + genotype + age:genotype was used, followed by Wald χ^2 test to determine p values of the coefficients (shown at the top of each graph). A, age; G, genotype; A×G, interaction between age and genotype.

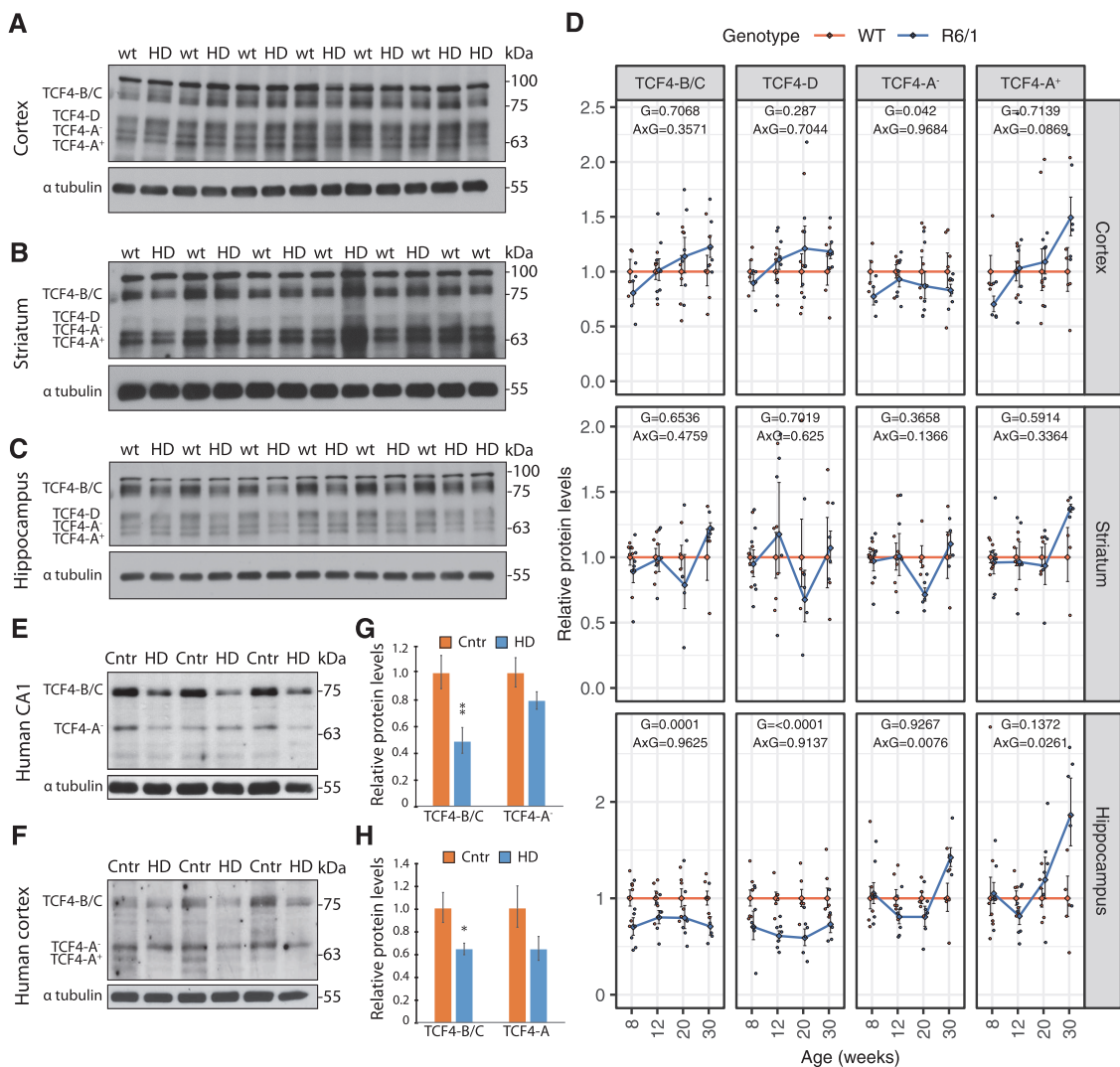


Figure 4. TCF4 protein levels in different brain regions of R6/1 mouse and HD patients. **A–C**, Western blot analysis of TCF4 protein levels in wt and R6/1 mouse cerebral cortex (**A**), striatum (**B**), and hippocampus (**C**) at 12 weeks of age (blots not shown for 8, 20, and 30 weeks of age). α tubulin served as loading control. **D**, Quantifications of Western blotting data. Number of samples included in each experiment is indicated in Table 4. The average expression level of the respective isoform in wt animals of each age group was set as 1. The average expression of the respective isoform in respective groups is shown with lines, error bars indicate SEM, data from all individual animals are shown with dots. Generalized linear model using the formula genotype + age:genotype was used, followed by Wald χ^2 test to determine p values of the coefficients (shown at the top of each graph), with G designating genotype, and A \times G designating interaction between age and genotype. **E, F**, Representative Western blot analysis of TCF4 protein levels in human hippocampal CA1 region and cerebral cortex, respectively, of healthy controls (Cntr) and HD patients (HD). α tubulin served as loading control. Human postmortem samples are described in Table 1. **G, H**, Quantification of data in **E, F**, respectively, and additional Western blottings (data not shown). For human hippocampal CA1 region a total of seven healthy controls and 10 HD patients were analyzed, and for human cortex, six healthy controls and six HD patients were analyzed. TCF4 signal intensities were normalized to α tubulin signal intensities. The relative TCF4 levels in healthy controls were arbitrarily set as 1. Data were log-transformed, means and SEMs were calculated, and two-tailed two-sample equal variance t test was used. Data were back-transformed into the linear scale for graphical representation, error bars represent upper and lower limits of back-transformed mean \pm SEM; * $p < 0.05$, ** $p < 0.01$; precise p values are stated in Extended Data Figure 4-1.

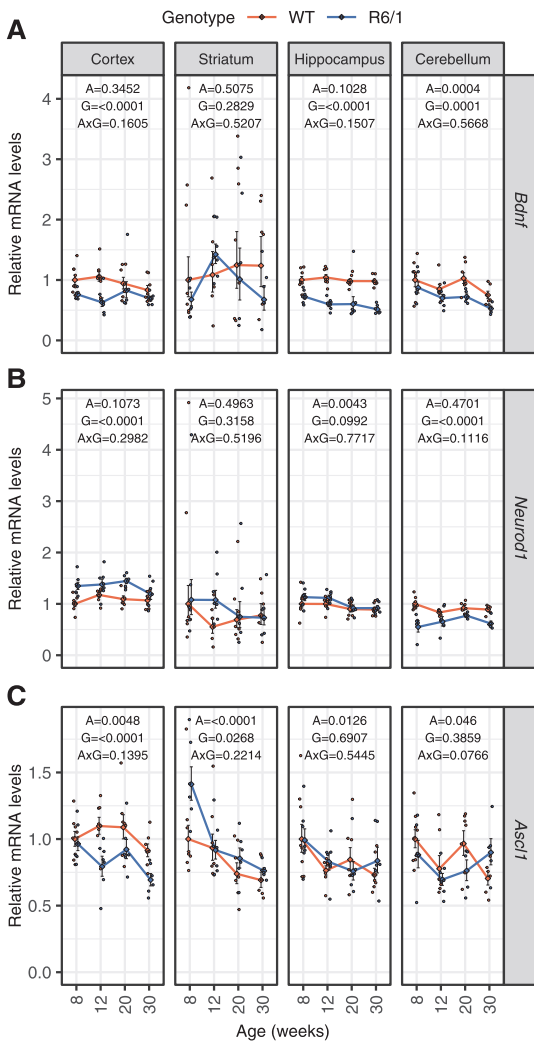


Figure 5. Expression levels of mRNAs encoding BDNF and TCF4 dimerization partners ASCL1 and NEUROD1 in R6/1 mouse brain. **A–C**, RT-qPCR analysis of *Bdnf* (**A**), *Neurod1* (**B**), and *Ascl1* (**C**) transcripts in wt and R6/1 mouse brain regions at 8, 12, 20, or 30 weeks of age from the same samples used for the analysis of *Tcf4* transcript levels. Number of samples included in each experiment is indicated in Table 4. *Bdnf*, *Neurod1*, and *Ascl1* mRNA levels were normalized to the geometric mean of the levels of *Hprt1*, *Tbp*, and *Gapdh* mRNA. The average expression level of respective transcript in eight-week-old wt animals was set as 1. The average expression of the transcripts in respective groups is shown with lines, error bars indicate SEM, data from all individual animals are shown with dots. Generalized linear model using the formula age + genotype + age:genotype was used, followed by Wald χ^2 test to determine *p* values of the coefficients (shown at the top of each graph). A, age; G, genotype; A×G, interaction between age and genotype.

Collectively, the results of Western blot analysis in R6/1 mouse brain are in good agreement with the major effects seen for *Tcf4* mRNA levels, further indicating that the changes in TCF4 are isoform and brain region specific.

High Mw isoforms of TCF4 are decreased in HD patient's hippocampus

We observed downregulation of several *Tcf4* transcripts and protein isoforms in R6/1 mouse hippocampus and cerebral cortex, therefore we next analyzed TCF4 protein levels in these regions of HD patients. Tissue lysates of hippocampal CA1 region and cerebral cortex from post-mortem HD patients and neurologically healthy controls were analyzed by Western blotting using monoclonal anti-TCF4 antibody c-8. The expression pattern of TCF4 protein isoforms in human brain tissues differed from mouse, although bands likely corresponding to TCF4-B/C and TCF4-A could be detected (Fig. 4E,F). TCF4 high Mw isoforms TCF4-B/C were significantly reduced in the hippocampus of HD patients (Fig. 4E,G), while the expression of shorter isoforms, likely TCF4-A⁻, was not significantly changed (Fig. 4G). We detected statistically significant reduction of TCF4-B/C in the cerebral cortex of HD patients and decreased levels of TCF4-A (sum of TCF4-A⁻ and TCF4-A⁺) that did not reach to statistical significance (Fig. 4F,H). Decreased TCF4 levels in human hippocampus and cerebral cortex corroborate our findings in R6/1 mouse, suggesting dysregulation of TCF4 expression in HD hippocampus and cortex in both mice and humans.

Differential expression of BDNF and TCF4 dimerization partners in R6/1 mouse brain

The reduction of wt HTT and expression of mutant HTT have been shown to decrease the levels of the neurotrophic factor BDNF (Zuccato et al., 2001), and this decrease has been observed in many HD models as well as in HD patients (Ferrer et al., 2000; Duan et al., 2003; Zhang et al., 2003). It has also been reported that TCF4 regulates BDNF expression through an enhancer region (Tuvikene et al., 2021). To this end, we quantified *Bdnf* mRNA levels in the R6/1 different brain regions (Fig. 5A). Our analysis revealed that the presence of mutant HTT significantly affects the expression of *Bdnf* gene in R6/1 mouse cerebral cortex, hippocampus and cerebellum. No change of *Bdnf* mRNA levels was detected in R6/1 mouse striatum. Moreover, the expression level of *Bdnf* mRNA was very low in the striatum compared with other brain regions studied, which is in line with the knowledge that *Bdnf* expression is very limited in the striatum and most of striatal BDNF protein is anterogradely transported there from the cortex (Altar et al., 1997). Collectively, *Bdnf* mRNA levels were reduced in the brain of R6/1 mouse used in this study, possibly partially because of decreased TCF4 levels in this model system.

Transcription factor TCF4 belongs to E-protein family of bHLH transcription factor superfamily that bind E-box DNA sequence as homodimers or heterodimers. TCF4 is one of the three E-protein partners for proneural

transcription factor ASCL1 and neuronal differentiation factor NEUROD1 (Massari and Murre, 2000; Dennis et al., 2019) that display altered gene expression in HD iPSC cells (The HD iPSC Consortium, 2017). Therefore, we determined mRNA levels of these dimerization partners in the R6/1 mouse brain regions. While the biggest decrease of many *Tcf4* mRNAs were detected in hippocampus of R6/1 mouse, mRNA levels of *Neurod1* and *Ascl1* were not affected in this brain region (Fig. 5B,C). Along with downregulation of several short *Tcf4* transcripts, the levels of *Ascl1* mRNA were reduced (Fig. 5B), whereas *Neurod1* mRNA was upregulated in R6/1 mouse cerebral cortex when compared with wt mice (Fig. 5B). Unchanged mRNA levels of *Neurod1* in the striatum and downregulated levels in the cerebellum were paralleled with almost unchanged mRNA levels of *Tcf4* in these regions (Fig. 5B). Additionally, the mRNA levels of *Ascl1* were increased in the striatum of R6/1 mouse in comparison to wt mice (Fig. 5C), whereas there was no significant change of *Ascl1* mRNA levels in the cerebellum (Fig. 5C). Collectively, the analysis of the two TCF4 dimerization partners indicate that their expression is also dysregulated in the R6/1 HD mouse model, although in a different regional pattern compared with TCF4, implying a wide-spread dysregulation of E-box-dependent transcription, even in brain regions where TCF4 was not affected.

TCF4 and ASCL1 synergistically transactivate reporter gene transcription in rat cortical and hippocampal neurons

Different transactivation capacity of specific TCF4 protein isoforms has been reported in HEK293 cells and in mixed culture of rat cortical and hippocampal neurons (Sepp et al., 2011, 2012, 2017). Additionally, TCF4-A⁻ activates *Gadd45g* promoter in co-operation with ASCL1 in unstimulated and KCl-depolarized neurons (Sepp et al., 2017). Here, we observed notable cortex and hippocampus-specific differences in the expression of different TCF4 isoforms and *Ascl1* between wt and R6/1 mouse. Therefore, we set out to comprehensively study the transactivation capability of major TCF4 protein isoforms and their synergism with dimerization partner ASCL1 separately in hippocampal and cortical neurons before and after induction of neuronal activity. For this, we transfected neurons with E-box-dependent luciferase reporter, together with different TCF4 isoform-encoding and ASCL1-encoding constructs. To mimic neuronal activity, cells were chronically depolarized using KCl. In unstimulated cells overexpressing TCF4 alone, all TCF4 protein isoforms induced reporter gene expression to relatively similar extent, except TCF4-I⁻ that induced reporter gene expression three times less compared with full-length isoform TCF4-B⁻ in both cortical and hippocampal neurons (Fig. 6A,B). KCl treatment induced TCF4-dependent transcription on average 2-fold over basal activity levels of the same TCF4 isoform, with no major differences between TCF4 isoforms. In contrast, co-expression of TCF4 and ASCL1 revealed differential upregulation of reporter activity (Fig. 6A,B). TCF4-B⁻ showed minimal increase of reporter activation in co-

operation with ASCL1, whereas ~20-fold increase over TCF4-I⁻ alone was seen when TCF4-I⁻ and ASCL1 were expressed together. We also noted that reporter activity was higher when co-expressing ASCL1 with different TCF4 isoforms in cortical neurons compared with hippocampal neurons. The reporter gene expression was further induced by KCl treatment in cells co-expressing TCF4 and ASCL1. However, the total reporter gene expression level was drastically lower in TCF4-B⁻ overexpressing neurons compared with other TCF4 isoforms under the same conditions. The highest reporter expression was seen with the shortest TCF4 isoform TCF4-I⁻ co-expressed with ASCL1 and treated with KCl, where its low initial transactivation capacity was more than fully compensated. To analyze transcriptional synergy between TCF4 and ASCL1, we calculated co-operation indices according to Chang et al. (1996). All TCF4 isoforms had a synergistic effect with ASCL1 in both cortical and hippocampal neurons (6C and 6D). The co-operation was the smallest for TCF4-B⁻, equally high for TCF4-C⁻, TCF4-D⁻, and TCF4-A⁻, and exceptionally high for TCF4-I⁻. Additionally, KCl treatment increased the synergism between TCF4 isoforms and ASCL1 in hippocampal neurons, but not in cortical neurons. To conclude, these results illustrate the TCF4 isoform-dependent differential transactivation in neurons and suggest brain region specific TCF4-dependent gene transcription. Furthermore, considering the brain region-specific dysregulation of TCF4 and its binding partners in HD, this differential synergism between TCF4 and its binding partners could also play a role in the etiology of HD.

Discussion

An increasing body of evidence suggests that HD is not only a neurodegenerative disease but also has a strong neurodevelopmental component (The HD iPSC Consortium, 2017; Siebzehrnühl et al., 2018; Barnat et al., 2020). Here, we set out to study TCF4 in the context of HD. Haploinsufficiency of TCF4 causes a rare neurodevelopmental Pitt-Hopkins syndrome, TCF4 has been linked to schizophrenia and mild to moderate intellectual disability, and has been shown to regulate neurogenesis, synaptic plasticity, memory and DNA methylation (Zweier et al., 2007; Blake et al., 2010; Kennedy et al., 2016; Jung et al., 2018; Page et al., 2018; Li et al., 2019). Here, we demonstrate that the expression of TCF4 is dysregulated in both cell-based and animal models of HD and in HD patients.

TCF4 can regulate target gene expression both as homodimers and as heterodimers with class II proneural bHLH proteins such as ASCL1 and NEUROD1. ASCL1 is considered to have several functions in neurogenesis, for example it is important in preserving the pool of nerve cell progenitors, whereas NEUROD1 plays important roles in neuronal and glial differentiation and maturation (for review, see Dennis et al., 2019). In R6/1 mouse cerebral cortex we found that *Neurod1* mRNA levels were increased, *Ascl1* mRNA levels were decreased, and total levels of *Tcf4* transcripts remained unchanged. Additionally, in the cerebral cortex we detected decreased TCF4-A⁻ protein in R6/1 mice and TCF4-B/C proteins in HD patients.

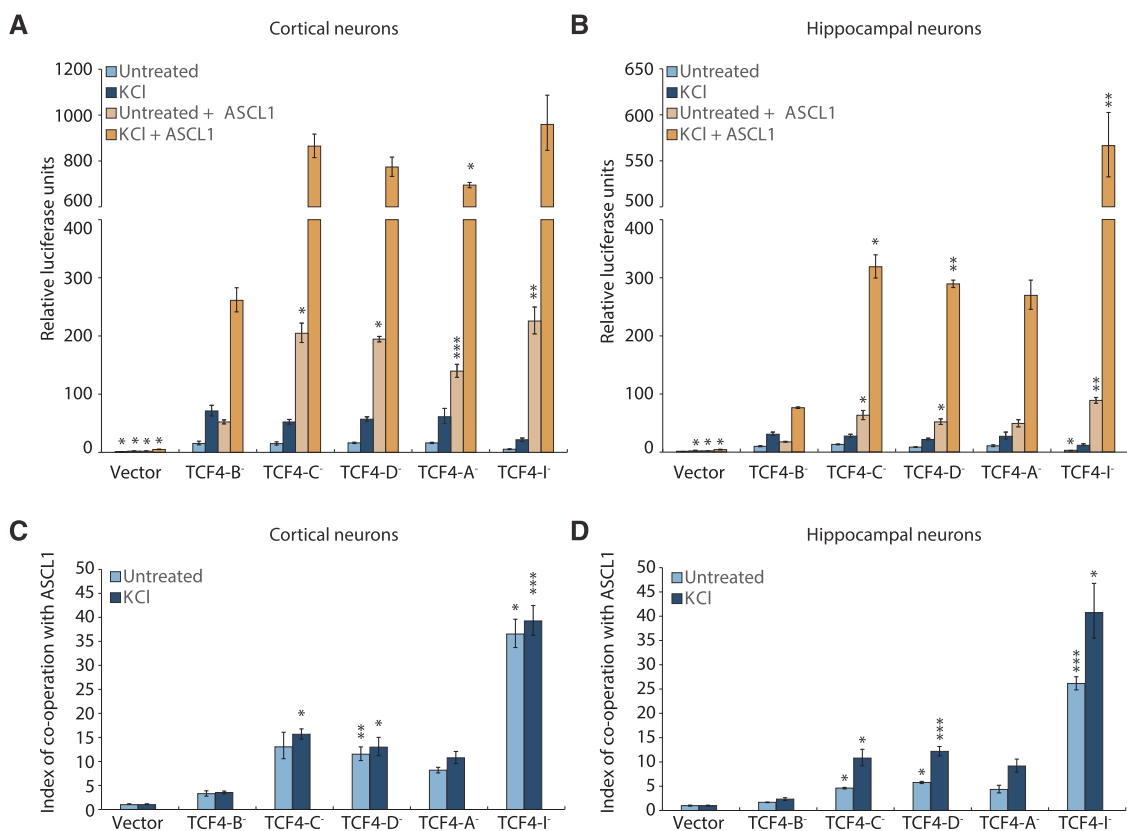


Figure 6. Differential co-operation of TCF4 isoforms with ACSL1 in cortical and hippocampal neurons. **A, B**, Specific TCF4 isoforms and ACSL1 under the control of *EF1a* and *PGK1* promoter, respectively, were overexpressed in rat primary cortical (**A**) or hippocampal (**B**) neurons at 6 DIV. For luciferase reporter assay, the cells were co-transfected with firefly luciferase reporter construct with 12 μ E5 E-boxes (CACCTG) in front of *TK* promoter, and for normalization *Renilla* luciferase construct with *PGK1* promoter was used. One day after transfection, neurons were treated with 25 mM KCl for 8 h or left untreated. Luciferase signals from three independent experiments were measured in duplicates, normalized to *Renilla* signals, log-transformed, mean-centered, and autoscaled for statistical analysis. Data were back-transformed to original scale and are presented relative to the signals measured from empty vector-transfected (Vector) untreated cells (arbitrarily set 1). **C, D**, Index of co-operation between TCF4 isoforms and ACSL1 in basal and depolarized conditions calculated from data in **A** or **B**, respectively. Normalized luciferase data were used for calculating co-operation indexes, data were log-transformed, mean-centered and autoscaled for statistical analysis and back-transformed for graphical depiction. The index value of 1 implies simple summation, while values above 1 indicate synergism and below 1 antagonism. The co-operation is expressed separately for untreated or KCl-treated cells. **A–D**, Error bars indicate SEM. One-way ANOVA followed by Tukey's *post hoc* test was used for statistical analysis (precise *p* values are reported in Extended Data Figure 6-1). Asterisks show statistical significance relative to cells overexpressing TCF4-B⁺ in basal conditions (**A, B**). For cooperation indexes, statistical significance is shown within untreated or KCl-treated cells relative to TCF4-B⁺ in the respective condition (**C, D**); precise *p* values are reported in Extended Data Figure 6-1); **p* < 0.05, ***p* < 0.01, ****p* < 0.001.

These detected changes of transcription factors might explain why the developing cerebral cortex of mutant HTT-expressing human fetuses present diminishing pool of proliferating cells and neural progenitors enter prematurely neuronal lineage specification (Barnat et al., 2020). We also found disease-dependent downregulation of *Neurod1* in the cerebellum and no significant expression change in the hippocampus of R6/1 mice, in combination with unchanged or drastically decreased *Tcf4* mRNA levels in cerebellum and hippocampus, respectively.

NEUROD1 has functions in granule cells of these two brain regions (Miyata et al., 1999; Pleasure et al., 2000; Gao et al., 2009), and co-expression of NEUROD1 and TCF4 has been demonstrated in adult mouse DG immature granule neurons (Jung et al., 2018). Moreover, decreased protein levels of NEUROD1 were reported to affect neurogenesis in the adult hippocampus of the R6/2 mice, a fast-progressing HD model (Fedele et al., 2011). The study of HD patient-derived iPSC induced into mixed neural phenotypes showed that one-third of gene

changes were in pathways regulating neuronal development and maturation, and downregulation of *NEUROD1* and *ASCL1* were also reported (The HD iPSC Consortium, 2017). Taken together, we showed HD-dependent brain region-specific altered expression levels of proneural *Ascl1* and *Neurod1* in adult mice with known relevant functions in these brain tissues. Delineating the expression of these transcription factors at earlier developmental stages of R6/1 mice could be of interest for future studies.

The human *TCF4* gene structure has been described by Sepp et al. (2011), and here we report a detailed description of mouse *Tcf4* gene structure and the numerous transcripts it encodes. The gene structure of *TCF4* is conserved between species suggesting functional relevance of potential protein isoforms. In general, the functions of alternative *TCF4* isoforms are poorly studied and the reason for multitude of 5' exons with specific promoters, isoforms with N termini of different length, and +/− isoforms of *TCF4* is still a puzzle. One of the early studies of *TCF4* (known previously as E2-2, SEF2-1, and ITF2) revealed that *TCF4-D* inhibits MYOD (Skerjanc et al., 1996), and another study showed specific inhibition of brain-specific *FGF1B* by *TCF4-B*⁺, whereas *TCF4-B*⁺ did not have any effect (Liu et al., 1998). Furthermore, differential expression was shown for *Tcf4-A* and *Tcf4-B* in immune cell types, and isoform-specific regulation was shown for normal plasmacytoid dendritic cell development (Grajkowska et al., 2017). Recently, discrepant effects of *TCF4* isoforms B and A were shown in the context of oligodendrocytes differentiation, and the authors propose that the differentiation promoting effect of *TCF4* is specific to the long isoform (Wedel et al., 2020). Additionally, alternative *TCF4* isoforms have differential transactivation potential in HEK293 cells and also in unstimulated and depolarized neurons (Sepp et al., 2011, 2017). Here, we report isoform-dependent co-operation of *TCF4* with *ASCL1* in neurons. Although functional dimerization of *TCF4* and *ASCL1* has been shown previously (Persson et al., 2000; de Pontual et al., 2009; Sepp et al., 2017), there is limited knowledge of their co-operation to activate transcription in neurons, specifically in cortical and hippocampal neurons. We found that there is a synergistic effect between all studied *TCF4* protein isoforms and *ASCL1*, although extent of the synergy varies several times depending on the *TCF4* protein isoform. For example, the low transactivation capability of *TCF4-I*[−] overexpressed alone (probably mainly homodimers) is compensated when heterodimerized with *ASCL1*, whereas full-length *TCF4-B*[−] shows limited synergism with *ASCL1*. Furthermore, we saw a depolarization-dependent increase in *TCF4-ASCL1* synergy in hippocampal but not in cortical neurons. This suggests that the neuronal activity-dependent transcriptional regulation of *TCF4* and its heterodimers could be fundamentally different in different brain regions and neuron populations. This could be relevant for developing alleviating therapies for diseases and disorders with disturbances of distinct *TCF4* isoforms in specific brain regions affected as we have reported here for HD.

Highly similar total *TCF4* expression patterns have been reported for humans, rhesus monkeys, and mice at total

TCF4 level (Jung et al., 2018). *TCF4* is involved in the early stages of neuronal development and highly expressed across the entire brain (Kim et al., 2020). In contrast, in adult brain the high expression of *TCF4* is restricted to the pallial region and cerebellum (Kim et al., 2020). Here, we observed brain region-specific differences in the proportions of *TCF4* isoforms expressed in mice, and our Western blot analysis of human *TCF4* in the hippocampus and cerebral cortex of elderly adults showed a distinctive pattern of *TCF4* isoforms divergent from that seen in adult mice. Importantly, we have validated all used *TCF4* antibodies in *Tcf4* KO mice embryonic cortical tissue lysates, therefore we believe that bands detected on human immunoblot are specific. Additionally, we validated *TCF4* antibodies with several *in vitro* translated human *TCF4* isoforms, however, we cannot completely rule out the possibility of masking *TCF4* isoform specific signals by other proteins with similar apparent Mw in Western blotting using human tissue lysates. Nevertheless, differential subcellular and brain region-specific expression of *TCF4* isoforms suggests fine-tuning of expression, likely required for precisely controlled target gene expression. In our RT-qPCR study of *Tcf4* transcripts in R6/1 mice, we observed opposite change in the levels of *TCF4-D* encoding *8c-II* and *7b-I* mRNAs. This additional layer of complexity entails potential to differentially regulate multitude of 5' alternative *TCF4* transcripts that eventually translate into the same *TCF4* isoform. Our results indicate that the possibility of specific regulation is not a mere opportunity, but these transcripts actually are expressed differentially in R6/1 mouse hippocampus and cortex.

The most notable result of our study is the decreased levels of *TCF4*, a neurodevelopmentally important transcription factor, in the hippocampus and cerebral cortex of both HD mouse model and HD patients. For a long time, the role of hippocampus in HD has been overlooked. However, recently its role in HD has been acknowledged as symptoms such as decline of cognitive functions and problems with learning new information most probably arise from dysfunctional hippocampal neurons and impaired synaptic plasticity and memory (Milnerwood et al., 2006; Puigdemívol et al., 2016; Smith-Dijak et al., 2019). Disease-dependent misregulation of BDNF and its downstream signaling pathways in HD models and patients have been well-described (Smith-Dijak et al., 2019) and BDNF is one of the master regulators of synaptic plasticity (Park and Poo, 2013). It has been shown that both loss of wt and gain of mutant HTT in HD decreases the levels of the neurotrophic factor BDNF (Zuccato et al., 2001, 2003; Gauthier et al., 2004) and increasing BDNF signaling rescues synaptic plasticity and memory in HD mice (Lynch et al., 2007; Anglada-Huguet et al., 2016). It has been recently reported that *TCF4* regulates *Bdnf* expression (Tuvikene et al., 2021), and here we report downregulation of both *TCF4* and *Bdnf* expression in the hippocampus and cerebral cortex of R6/1 mice. It is plausible that the downregulation of *TCF4* could be one of the causal mechanisms underlying the downregulation of BDNF expression in the hippocampus and cerebral cortex of HD mouse models and patients in addition to the well-

described NRSF-dependent mechanism (Zuccato et al., 2001, 2003, 2007; Conforti et al., 2013).

Spatial memory is believed to rely on adult hippocampal neurogenesis (Abrous and Wojtowicz, 2015) and impairment of spatial perception and spatial memory are reported in HD patients, correlating with their HD disease burden score (Harris et al., 2019). Additionally, R6/1 and R6/2 HD mice and the more slowly progressing YAC128 HD mice show reduced hippocampal adult neurogenesis in the SGZ of DG (Lazic et al., 2004; Gil et al., 2005; Simpson et al., 2011). Considering (1) the functions of TCF4 in neurogenesis (Schoof et al., 2020; Wang et al., 2020) and neural plasticity (Kennedy et al., 2016; Thaxton et al., 2018; Badowska et al., 2020); (2) high expression of TCF4 in hippocampal neuroepithelium and its persistence in all mature hippocampal neuron subpopulations and astrocytes and similar high expression in cortical structures (Jung et al., 2018; Kim et al., 2020); and (3) downregulation of TCF4 we show here in R6/1 mouse and HD patient hippocampus and cerebral cortex, allows to hypothesize that TCF4 might play a role in the impairment of cognitive functions in HD. In R6/1 mice, the motor and cognitive symptoms generally appear at 12–20 weeks of age (Naver et al., 2003; Bolivar et al., 2004; Giralte et al., 2013), and treatment with papaverin (inhibitor of PDE10a) or betulinic acid improve these symptoms (Giralte et al., 2013; Alcalá-Vida et al., 2021). Importantly, both of these compounds affect PKA and cAMP levels, which are known to increase TCF4 transcriptional activity (Sepp et al., 2017). It is tempting to speculate that this effect could be, at least partially, because of the increased TCF4-dependent gene expression.

To conclude, we have identified TCF4 as a dysregulated transcription factor in HD and provided evidence for the brain region-dependent regulation and functions of alternative TCF4 isoforms. Future work will elucidate the functional role of this dysregulation.

References

- Abrous DN, Wojtowicz JM (2015) Interaction between neurogenesis and hippocampal memory system: new vistas. *Cold Spring Harb Perspect Biol* 7:a018952.
- Aimone JB, Wiles J, Gage FH (2009) Computational influence of adult neurogenesis on memory encoding. *Neuron* 61:187–202.
- Alcalá-Vida R, García-Forn M, Castany-Pladevall C, Creus-Muncunill J, Ito Y, Blanco E, Golbano A, Crespi-Vázquez K, Parry A, Slater G, Samarajiva S, Peiró S, Di Croce L, Narita M, Pérez-Navarro E (2021) Neuron type-specific increase in lamin B1 contributes to nuclear dysfunction in Huntington's disease. *EMBO Mol Med* 13:e12105.
- Altar CA, Cai N, Bliven T, Juhász M, Conner JM, Acheson AL, Lindsay RM, Wiegand SJ (1997) Anterograde transport of brain-derived neurotrophic factor and its role in the brain. *Nature* 389:856–860.
- Ament SA, Pearl JR, Cattle JP, Bragg RM, Skene PJ, Coffey SR, Bergley DE, Wheeler VC, MacDonald ME, Baliga NS, Rosinski J, Hood LE, Carroll JB, Price ND (2018) Transcriptional regulatory networks underlying gene expression changes in Huntington's disease. *Mol Syst Biol* 14:e7435.
- Anglada-Huguet M, Vidal-Sancho L, Giralte A, García-Díaz Barriga G, Xifré X, Alberch J (2016) Prostaglandin E2 EP2 activation reduces memory decline in R6/1 mouse model of Huntington's disease by the induction of BDNF-dependent synaptic plasticity. *Neurobiol Dis* 95:22–34.
- Badowska DM, Brzózka MM, Kannaiyan N, Thomas C, Dibaj P, Chowdhury A, Steffens H, Turck CW, Falkai P, Schmitt A, Papiol S, Scheuss V, Willig KI, Martins-de-Souza D, Rhee JS, Malzahn D, Rossner MJ (2020) Modulation of cognition and neuronal plasticity in gain- and loss-of-function mouse models of the schizophrenia risk gene *Tcf4*. *Transl Psychiatry* 10:343.
- Bae BI, Xu H, Igarashi S, Fujimuro M, Agrawal N, Taya Y, Hayward SD, Moran TH, Montell C, Ross CA, Snyder SH, Sawa A (2005) p53 mediates cellular dysfunction and behavioral abnormalities in Huntington's disease. *Neuron* 47:29–41.
- Barnat M, Capizzi M, Aparicio E, Boluda S, Wennagel D, Kacher R, Kassem R, Lenoir S, Agasse F, Braz BY, Liu JP, Ighil J, Tessier A, Zeitlin SO, Duyckaerts C, Dommergues M, Durr A, Humbert S (2020) Huntington's disease alters human neurodevelopment. *Science* 369:787–793.
- Bates GP, Dorsey R, Gusella JF, Hayden MR, Kay C, Leavitt BR, Nance M, Ross CA, Scahill RI, Wetzel R, Wild EJ, Tabrizi SJ (2015) Huntington disease. *Nat Rev Dis Primers* 1:15005.
- Blake DJ, Forrest M, Chapman RM, Tinsley CL, O'Donovan MC, Owen MJ (2010) TCF4, schizophrenia, and Pitt-Hopkins syndrome. *Schizophr Bull* 36:443–447.
- Bolivar VJ, Manley K, Messer A (2004) Early exploratory behavior abnormalities in R6/1 Huntington's disease transgenic mice. *Brain Res* 1005:29–35.
- Cha JHJ (2007) Transcriptional signatures in Huntington's disease. *Prog Neurobiol* 83:228–248.
- Chambers RA, Potenza MN, Hoffman RE, Miranker W (2004) Simulated apoptosis/neurogenesis regulates learning and memory capabilities of adaptive neural networks. *Neuropsychopharmacology* 29:747–758.
- Chang W, Zhou W, Theill LE, Baxter JD, Schaufele F (1996) An activation function in Pit-1 required selectively for synergistic transcription. *J Biol Chem* 271:17733–17738.
- Conforti P, Mas Monteys A, Zuccato C, Buckley NJ, Davidson B, Cattaneo E (2013) In vivo delivery of DN: REST improves transcriptional changes of REST-regulated genes in HD mice. *Gene Ther* 20:678–685.
- de Pontual L, Mathieu Y, Golzio C, Rio M, Malan V, Boddaert N, Soufflet C, Picard C, Durandy A, Dobbie A, Heron D, Isidor B, Motte J, Newbury-Ecob R, Pasquier L, Tardieu M, Viot G, Jaubert F, Munnich A, Colleaux L, et al. (2009) Mutational, functional, and expression studies of the TCF4 gene in Pitt-Hopkins syndrome. *Hum Mutat* 30:669–676.
- Dennis DJ, Han S, Schuurmans C (2019) bHLH transcription factors in neural development, disease, and reprogramming. *Brain Res* 1705:48–65.
- Duan W, Guo Z, Jiang H, Ware M, Li X-J, Mattson MP (2003) Dietary restriction normalizes glucose metabolism and BDNF levels, slows disease progression, and increases survival in huntingtin mutant mice. *Proc Natl Acad Sci USA* 100:2911–2916.
- Dunah AW, Jeong H, Griffin A, Kim Y-M, Standaert DG, Hersch SM, Mouradian MM, Young AB, Tanese N, Krainc D (2002) Sp1 and TAFII130 transcriptional activity disrupted in early Huntington's disease. *Science* 296:2238–2243.
- Esvald EE, Tuvikene J, Sirp A, Patil S, Bramham CR, Timmusk T (2020) CREB family transcription factors are major mediators of BDNF transcriptional autoregulation in cortical neurons. *J Neurosci* 40:1405–1426.
- Fedelev V, Roybon L, Nordström U, Li JY, Brundin P (2011) Neurogenesis in the R6/2 mouse model of Huntington's disease is impaired at the level of NeuroD1. *Neuroscience* 173:76–81.
- Ferrer I, Goutan E, Marin C, Rey MJ, Ribalta T (2000) Brain-derived neurotrophic factor in Huntington disease. *Brain Res* 866:257–261.
- Forrest MP, Hill MJ, Kavanagh DH, Tansey KE, Waite AJ, Blake DJ (2018) The psychiatric risk gene transcription factor 4 (*TCF4*) regulates neurodevelopmental pathways associated with schizophrenia, autism, and intellectual disability. *Schizophr Bull* 44:1100–1110.

- Fox J, Weisberg S (2019) An R companion to applied regression, Ed 3. Los Angeles: SAGE.
- Gao Z, Ure K, Ables JL, Lagace DC, Nave K-A, Goebbels S, Eisch AJ, Hsieh J (2009) NeuroD1 is essential for the survival and maturation of adult-born neurons. *Nat Neurosci* 12:10.
- Gauthier LR, Charrin BC, Borrell-Pagès M, Dompierre JP, Rangone H, Cordelières FP, De Mey J, MacDonald ME, Lessmann V, Humbert S, Saudou F (2004) Huntingtin controls neurotrophic support and survival of neurons by enhancing BDNF vesicular transport along microtubules. *Cell* 118:127–138.
- Gil JMAC, Mohapel P, Araújo IM, Popovic N, Li J-Y, Brundin P, Petersén Å (2005) Reduced hippocampal neurogenesis in R6/2 transgenic Huntington's disease mice. *Neurobiol Dis* 20:744–751.
- Giralt A, Saavedra A, Carretón O, Arumi H, Tyejji S, Alberch J, Pérez-Navarro E (2013) PDE10 inhibition increases GluA1 and CREB phosphorylation and improves spatial and recognition memories in a Huntington's disease mouse model: PDE10 inhibition improves cognition in Huntington's disease. *Hippocampus* 23:684–695.
- Gonçalves JT, Schafer ST, Gage FH (2016) Adult neurogenesis in the hippocampus: from stem cells to behavior. *Cell* 167:897–914.
- Grajkowska LT, Ceribelli M, Lau CM, Warren ME, Tiniakou I, Nakandakari Higa S, Bunin A, Haecker H, Mirny LA, Staudt LM, Reizis B (2017) Isoform-specific expression and feedback regulation of E protein TCF4 control dendritic cell lineage specification. *Immunity* 46:65–77.
- Grima JC, Daigle JG, Arbez N, Cunningham KC, Zhang K, Ochaba J, Geater C, Morozko E, Stocksdale J, Glatzer JC, Pham JT, Ahmed I, Peng Q, Wadhwa H, Pletnikova O, Troncoso JC, Duan W, Snyder SH, Ranum LPW, Thompson LM, et al. (2017) Mutant huntingtin disrupts the nuclear pore complex. *Neuron* 94:93–107.e6.
- Harris KL, Armstrong M, Swain R, Erzincliglu S, Das T, Burgess N, Barker RA, Mason SL (2019) Huntington's disease patients display progressive deficits in hippocampal-dependent cognition during a task of spatial memory. *Cortex* 119:417–427.
- Hensman Moss DJ, Flower MD, Lo KK, Miller JRC, van Ommen GJB, 't Hoen PAC, Stone TC, Guinee A, Langbehn DR, Jones L, Plagnol V, van Roon-Mom WMC, Holmans P, Tabrizi SJ (2017) Huntington's disease blood and brain show a common gene expression pattern and share an immune signature with Alzheimer's disease. *Sci Rep* 7:44849.
- Jung M, Häberle BM, Tschakowsky T, Wittmann M-T, Balta E-A, Stadler V-C, Zweier C, Dörfler A, Gloeckner CJ, Lie DC (2018) Analysis of the expression pattern of the schizophrenia-risk and intellectual disability gene TCF4 in the developing and adult brain suggests a role in development and plasticity of cortical and hippocampal neurons. *Mol Autism* 9:20.
- Kalscheuer VM, Feenstra I, Van Ravenswaaij-Arts CMA, Smeets DFMC, Menzel C, Ullmann R, Musante L, Ropers H-H (2008) Disruption of the TCF4 gene in a girl with mental retardation but without the classical Pitt-Hopkins syndrome. *Am J Med Genet A* 146A:2053–2059.
- Kannike K, Sepp M, Zuccato C, Cattaneo E, Timmusk T (2014) Forkhead transcription factor FOXO3a levels are increased in Huntington disease because of overactivated positive autotfeedback loop. *J Biol Chem* 289:32845–32857.
- Kennedy AJ, Rahn EJ, Paulukaitis BS, Savell KE, Kordasiewicz HB, Wang J, Lewis JW, Posey J, Strange SK, Guzman-Karlsson MC, Phillips SE, Decker K, Motley ST, Swayze EE, Ecker DJ, Michael TP, Day JJ, Sweatt JD (2016) Tcf4 regulates synaptic plasticity, DNA methylation, and memory function. *Cell Rep* 16:2666–2685.
- Kim H, Berens NC, Ochandarena NE, Philpot BD (2020) Region and cell type distribution of TCF4 in the postnatal mouse brain. *Front Neuroanat* 14:42.
- Langfelder P, Cantle JP, Chatzopoulou D, Wang N, Gao F, Al-Ramahi I, Lu XH, Ramos EM, El-Zein K, Zhao Y, Deverasetty S, Tebbe A, Schaab C, Lavery DJ, Howland D, Kwak S, Botas J, Aaronson JS, Rosinski J, Coppola G, et al. (2016) Integrated genomics and proteomics define huntingtin CAG length-dependent networks in mice. *Nat Neurosci* 19:623–633.
- Lazic SE, Grote H, Armstrong RJE, Blakemore C, Hannan AJ, van Dellen A, Barker RA (2004) Decreased hippocampal cell proliferation in R6/1 Huntington's mice. *Neuroreport* 15:811–813.
- Li H, Zhu Y, Morozov YM, Chen X, Page SC, Rannals MD, Maher BJ, Rakic P (2019) Disruption of TCF4 regulatory networks leads to abnormal cortical development and mental disabilities. *Mol Psychiatry* 24:1235–1246.
- Liu Y, Ray SK, Yang X-Q, Luntz-Leybman V, Chiu I-M (1998) A splice variant of E2-2 basic helix-loop-helix protein represses the brain-specific fibroblast growth factor 1 promoter through the binding to an imperfect E-box. *J Biol Chem* 273:19269–19276.
- Luthi-Carter R, Hanson SA, Strand AD, Bergstrom DA, Chun Y, Peters NL, Woods AM, Chan EY, Kooperberg C, Krainc D, Young AB, Tapscott SJ, Olson JM (2002) Dysregulation of gene expression in the R6/2 model of polyglutamine disease: parallel changes in muscle and brain. *Hum Mol Genet* 11:1911–1926.
- Lynch G, Kramar EA, Rex CS, Jia Y, Chappas D, Gall CM, Simmons DA (2007) Brain-derived neurotrophic factor restores synaptic plasticity in a knock-in mouse model of Huntington's disease. *J Neurosci* 27:4424–4434.
- Mansvelter HD, Verhoog MB, Goriounova NA (2019) Synaptic plasticity in human cortical circuits: cellular mechanisms of learning and memory in the human brain? *Curr Opin Neurobiol* 54:186–193.
- Mangiarini L, Sathasivam K, Seller M, Cozens B, Harper A, Hetherington C, Lawton M, Trotter Y, Lehrach H, Davies SW, Bates GP (1996) Exon 1 of the HD gene with an expanded CAG repeat is sufficient to cause a progressive neurological phenotype in transgenic mice. *Cell* 87:493–506.
- Massari ME, Murre C (2000) Helix-loop-helix proteins: regulators of transcription in eucaryotic organisms. *Mol Cell Biol* 20:429–440.
- McClelland JL, McNaughton BL, O'Reilly RC (1995) Why there are complementary learning systems in the hippocampus and neocortex: insights from the successes and failures of connectionist models of learning and memory. *Psychol Rev* 102:419–457.
- McColgan P, Tabrizi SJ (2018) Huntington's disease: a clinical review. *Eur J Neurol* 25:24–34.
- Milnerwood AJ, Cummings DM, Dallérac GM, Brown JY, Vatsavayai SC, Hirst MC, Rezaie P, Murphy KPSJ (2006) Early development of aberrant synaptic plasticity in a mouse model of Huntington's disease. *Hum Mol Genet* 15:1690–1703.
- Miyata T, Maeda T, Lee JE (1999) NeuroD is required for differentiation of the granule cells in the cerebellum and hippocampus. *Genes Dev* 13:1647–1652.
- Naver B, Stub C, Möller M, Fenger K, Hansen AK, Hasholt L, Sørensen SA (2003) Molecular and behavioral analysis of the r6/1 Huntington's disease transgenic mouse. *Neuroscience* 122:1049–1057.
- Neueder A, Bates GP (2014) A common gene expression signature in Huntington's disease patient brain regions. *BMC Med Genomics* 7:60.
- Page SC, Hamersky GR, Gallo RA, Rannals MD, Calcaterra NE, Campbell MN, Mayfield B, Briley A, Phan BN, Jaffe AE, Maher BJ (2018) The schizophrenia- and autism-associated gene, transcription factor 4 regulates the columnar distribution of layer 2/3 prefrontal pyramidal neurons in an activity-dependent manner. *Mol Psychiatry* 23:304–315.
- Park H, Poo M (2013) Neurotrophin regulation of neural circuit development and function. *Nat Rev Neurosci* 14:7–23.
- Persson P, Jögi A, Grynfeld A, Pählman S, Axelson H (2000) HASH-1 and E2-2 are expressed in human neuroblastoma cells and form a functional complex. *Biochem Biophys Res Commun* 274:22–31.
- Pleasure SJ, Collins AE, Lowenstein DH (2000) Unique expression patterns of cell fate molecules delineate sequential stages of dentate gyrus development. *J Neurosci* 20:6095–6105.
- Pouladi MA, Morton AJ, Hayden MR (2013) Choosing an animal model for the study of Huntington's disease. *Nat Rev Neurosci* 14:708–721.
- Puigdellívol M, Saavedra A, Pérez-Navarro E (2016) Cognitive dysfunction in Huntington's disease: mechanisms and therapeutic

- strategies beyond BDNF: cognitive dysfunction in HD. *Brain Pathol* 26:752–771.
- Quiron JG, Parsons MP (2019) The onset and progression of hippocampal synaptic plasticity deficits in the Q175FDN mouse model of Huntington disease. *Front Cell Neurosci* 13:326.
- Ramirez-Garcia G, Galvez V, Diaz R, Bayliss L, Fernandez-Ruiz J, Campos-Romo A (2020) Longitudinal atrophy characterization of cortical and subcortical gray matter in Huntington's disease patients. *Eur J Neurosci* 51:1827–1843.
- Schoof M, Hellwig M, Harrison L, Holdhof D, Lauffer MC, Niesen J, Virdi S, Indenbirken D, Schüller U (2020) The basic helix-loop-helix transcription factor TCF4 impacts brain architecture as well as neuronal morphology and differentiation. *Eur J Neurosci* 51:2219–2235.
- Sepp M, Kannike K, Eesmaa A, Urb M, Timmusk T (2011) Functional diversity of human basic helix-loop-helix transcription factor TCF4 isoforms generated by alternative 5' exon usage and splicing. *PLoS One* 6:e22138.
- Sepp M, Pruunsild P, Timmusk T (2012) Pitt–Hopkins syndrome-associated mutations in TCF4 lead to variable impairment of the transcription factor function ranging from hypomorphic to dominant-negative effects. *Hum Mol Genet* 21:2873–2888.
- Sepp M, Vihma H, Nurm K, Urb M, Page SC, Roots K, Hark A, Maher BJ, Pruunsild P, Timmusk T (2017) The intellectual disability and schizophrenia associated transcription factor TCF4 is regulated by neuronal activity and protein kinase A. *J Neurosci* 37:10516–10527.
- Siebzehnrühl FA, Raber KA, Urbach YK, Schulze-Krebs A, Canneva F, Mocerri S, Habermeyer J, Achoui D, Gupta B, Steindler DA, Stephan M, Nguyen HP, Bonin M, Riess O, Bauer A, Aigner L, Couillard-Despres S, Paucar MA, Svenningsson P, Osmand A, et al. (2018) Early postnatal behavioral, cellular, and molecular changes in models of Huntington disease are reversible by HDAC inhibition. *Proc Natl Acad Sci USA* 115:E8765–E8774.
- Simpson JM, Gil-Mohapel J, Pouladi MA, Ghilan M, Xie Y, Hayden MR, Christie BR (2011) Altered adult hippocampal neurogenesis in the YAC128 transgenic mouse model of Huntington disease. *Neurobiol Dis* 41:249–260.
- Skerjanc IS, Truong J, Filion P, McBurney MW (1996) A splice variant of the ITF-2 transcript encodes a transcription factor that inhibits MyoD activity. *J Biol Chem* 271:3555–3561.
- Smith-Dijk AI, Sepers MD, Raymond LA (2019) Alterations in synaptic function and plasticity in Huntington disease. *J Neurochem* 150:346–365.
- Stout JC, Paulsen JS, Queller S, Solomon AC, Whitlock KB, Campbell JC, Carlozzi N, Duff K, Beglinger LJ, Langbehn DR, Johnson SA, Biglan KM, Aylward EH; The PREDICT-HD Investigators and Coordinators of the Huntington Study Group (2011) Neurocognitive signs in prodromal Huntington disease. *Neuropsychology* 25:1–14.
- Sugars KL, Rubinsztein DC (2003) Transcriptional abnormalities in Huntington disease. *Trends Genet* 19:233–238.
- Tamberg L, Jaago M, Säälik K, Sirp A, Tuvikene J, Shubina A, Kiir CS, Nurm K, Sepp M, Timmusk T, Palgi M (2020) Daughterless, the *Drosophila* orthologue of TCF4, is required for associative learning and maintenance of the synaptic proteome. *Dis Model Mech* 13:dmm042747.
- Tereshchenko AV, Schultz JL, Bruss JE, Magnotta VA, Epping EA, Nopoulos PC (2020) Abnormal development of cerebellar-striatal circuitry in Huntington disease. *Neurology* 94:e1908–e1915.
- Thaxton C, Kloth AD, Clark EP, Moy SS, Chitwood RA, Philpot BD (2018) Common pathophysiology in multiple mouse models of Pitt–Hopkins syndrome. *J Neurosci* 38:918–936.
- The HD iPSC Consortium (2017) Developmental alterations in Huntington's disease neural cells and pharmacological rescue in cells and mice. *Nat Neurosci* 20:648–660.
- The Huntington's Disease Collaborative Research Group (1993) A novel gene containing a trinucleotide repeat that is expanded and unstable on Huntington's disease chromosomes. *Cell* 72:971–983.
- Tuvikene J, Esvald E-E, Rähni A, Uustalu K, Zhuravskaya A, Avarlaid A, Makeyev EV, Timmusk T (2021) Intronic enhancer region governs transcript-specific Bdnf expression in rodent neurons. *Elife* 10:e65161.
- Valor LM (2015) Transcription, epigenetics and ameliorative strategies in Huntington's disease: a genome-wide perspective. *Mol Neurobiol* 51:406–423.
- van der Plas E, Langbehn DR, Conrad AL, Kosciak TR, Tereshchenko A, Epping EA, Magnotta VA, Nopoulos PC (2019) Abnormal brain development in child and adolescent carriers of mutant huntingtin. *Neurology* 93:e1021–e1030.
- Wang Y, Lu Z, Zhang Y, Cai Y, Yun D, Tang T, Cai Z, Wang C, Zhang Y, Fang F, Yang Z, Behnisch T, Xie Y (2020) Transcription factor 4 safeguards hippocampal dentate gyrus development by regulating neural progenitor migration. *Cereb Cortex* 30:3102–3115.
- Wedel M, Fröb F, Elseesser O, Wittmann M-T, Lie DC, Reis A, Wegner M (2020) Transcription factor Tcf4 is the preferred heterodimerization partner for Olig2 in oligodendrocytes and required for differentiation. *Nucleic Acids Res* 48:4839–4857.
- Zhai W, Jeong H, Cui L, Krainc D, Tjian R (2005) In vitro analysis of huntingtin-mediated transcriptional repression reveals multiple transcription factor targets. *Cell* 123:1241–1253.
- Zhang Y, Li M, Drozda M, Chen M, Ren S, Mejia Sanchez RO, Leavitt BR, Cattaneo E, Ferrante RJ, Hayden MR, Friedlander RM (2003) Depletion of wild-type huntingtin in mouse models of neurologic diseases: depletion of huntingtin in neurologic diseases. *J Neurochem* 87:101–106.
- Zuccato C, Cattaneo E (2014) Normal function of huntingtin. Oxford: Oxford University Press.
- Zuccato C, Ciammola A, Rigamonti D, Leavitt BR, Goffredo D, Conti L, MacDonald ME, Friedlander RM, Silani V, Hayden MR, Timmusk T, Sipione S, Cattaneo E (2001) Loss of huntingtin-mediated BDNF gene transcription in Huntington's disease. *Science* 293:493–498.
- Zuccato C, Tartari M, Crotti A, Goffredo D, Valenza M, Conti L, Cataudella T, Leavitt BR, Hayden MR, Timmusk T, Rigamonti D, Cattaneo E (2003) Huntingtin interacts with REST/NRSF to modulate the transcription of NRSE-controlled neuronal genes. *Nat Genet* 35:76–83.
- Zuccato C, Belyaev N, Conforti P, Ooi L, Tartari M, Papadimitou E, MacDonald M, Fossale E, Zeitlin S, Buckley N, Cattaneo E (2007) Widespread disruption of repressor element-1 silencing transcription factor/neuron-restrictive silencer factor occupancy at its target genes in Huntington's disease. *J Neurosci* 27:6972–6983.
- Zweier C, Peippo MM, Hoyer J, Sousa S, Bottani A, Clayton-Smith J, Reardon W, Saraiva J, Cabral A, Gohring I, Devriendt K, de Ravel T, Bijlsma EK, Hennekam RCM, Orrico A, Cohen M, Dreweke A, Reis A, Nurnberg P, Rauch A (2007) Haploinsufficiency of TCF4 causes syndromal mental retardation with intermittent hyperventilation (Pitt–Hopkins syndrome). *Am J Hum Genet* 80:994–1001.

Curriculum vitae

Personal data

Name: Kaja Nurm
Date of birth: 08.10.1984
Place of birth: Väike-Maarja, Estonia
Citizenship: Estonia

Contact data

E-mail: kaja.nurm@taltech.ee

Education

2010–2021 Tallinn University of Technology – doctoral studies
2013–2015 Tallinn University of Technology – Technical Teacher Master Curriculum
2007–2010 Tallinn University of Technology – MSc
2003–2007 Tallinn University of Technology – BSc
2000–2003 Paide Ühisgümnaasium

Language competence

Estonian native
English fluent
Russian beginner

Professional employment

2021–... IQVIA, Associate Statistical Programmer
2010–2021 Lab of Molecular Neurobiology, engineer
2014– ... Estonian Accreditation Centre, technical assessor
2010–2012 Nova Vita Kliinik, cytogeneticist

Scholarships and awards

2017 The best scientific publication of Tallinn University of Technology in the field of natural, exact and medical sciences in 2017
2011 First award on poster presentation at 14th annual conference of EstSHG

Courses and conferences

November 2018 Participation in 20th EstSHG annual conference, Viljandi, Estonia
April 2018 Participation in Advanced RNA-Seq Analysis course (EMBL-EBI), Cambridge, UK
March 2018 Participation in SZTest mini-symposium “Gene expression in health and disease”, Tallinn, Estonia; oral presentation
November 2017 Participation in 19th EstSHG annual conference, Rakvere, Estonia
October 2014 Participation in 14th EstSHG annual conference, Haapsalu, Estonia; oral presentation
June 2012 European Human Genetics Conference (EHGC) annual conference, Nürnberg, Germany

Supervised dissertations

Kaisa Roots, Master's Degree, 2017, (sup) Kaja Nurm; Tõnis Timmusk, Analysis of disease-related missense variations in the basic helix loop helix transcription factor TCF4, Tallinn University of Technology School of Science, Department of Chemistry and Biotechnology

Kristian Costa Dos Santos Leite, Master's Degree, 2016, (sup) Kaja Nurm; Tõnis Timmusk, Analysis of transcription and splicing in the human TCF4 exon 4 region Tallinn University of Technology School of Science, Department of Chemistry and Biotechnology

Mari Urb, Master's Degree, 2014, (sup) Kaja Nurm; Mari Sepp, Tõnis Timmusk Potential Target Genes of the Basic Helix-Loop-Helix Transcription Factor TCF4 in Rat Primary Neurons Tallinn University of Technology School of Science, Department of Chemistry and Biotechnology

Publications

Sirp, A.*; Roots, K.*; **Nurm, K.**; Tuvikene, J.; Sepp, M.; Timmusk T. (2021). Functional consequences of the basic helix-loop-helix transcription factor TCF4 missense substitutions associated with Pitt-Hopkins syndrome, mild intellectual disability, and schizophrenia. *Journal of Biological Chemistry*, in press.

Nurm, K.; Sepp, M.; Castany-Pladevall, C.; Creus-Muncunill, J.; Tuvikene, J.; Sirp, A.; Vihma, H.; Blake, D. J.; Perez-Navarro, E.; Timmusk, T. (2021). Isoform-specific reduction of the basic helix-loop-helix transcription factor TCF4 levels in Huntington's disease. *eNeuro*, 8 (5): ENEURO.0197-21.2021. DOI: 10.1523/ENEURO.0197-21.2021.

Tamberg, L.; Jaago, M.; Saalik, K.; Sirp, A.; Tuvikene, J.; Shubina, A.; Kiir, C. S.; **Nurm, K.**; Sepp, M.; Timmusk, T.; Palgi, M. (2020). Daughterless, the Drosophila orthologue of TCF4, is required for associative learning and maintenance of the synaptic proteome. *Disease Models & Mechanisms*, 13 (7), #dmm042747. DOI: 10.1242/dmm.042747.

Sirp, A.; Leite, K.; Tuvikene, J.; **Nurm, K.**; Sepp, M.; Timmusk, T. (2020). The Fuchs corneal dystrophy-associated CTG repeat expansion in the TCF4 gene affects transcription from its alternative promoters. *Scientific Reports*, 10 (1), #18424. DOI: 10.1038/s41598-020-75437-3.

Sepp, M.; Vihma, H.*; **Nurm, K.***; Urb, M.*; Page, S. C.; Roots, K.; Hark, A.; Maher, B. J.; Pruunsild, P.; Timmusk, T. (2017). The intellectual disability and schizophrenia associated transcription factor TCF4 is regulated by neuronal activity and protein kinase A. *Journal of Neuroscience*, 37, 10516–10527. DOI: 10.1523/JNEUROSCI.1151-17.2017.

Kharbanda, M.; **Kannike, K.**; Lampe, A.; Berg, J.; Timmusk, T.; Sepp, M. (2016). Partial deletion of TCF4 in three generation family with non-syndromic intellectual disability, without features of Pitt-Hopkins syndrome. *European Journal of Medical Genetics*, 59 (6-7), 310–314. DOI: 10.1016/j.ejmg.2016.04.003.

Kannike, K.; Sepp, M.; Zuccato, E.; Cattaneo, E.; Timmusk, T. (2014). FOXO3a levels are increased in Huntington Disease due to overactivated positive autofeedback loop. *Journal of Biological Chemistry*, 289 (47), 32845–32857. DOI: 10.1074/jbc.M114.612424.

Sepp, M.; **Kannike, K.**; Eesmaa, A.; Urb, M.; Timmusk, T. (2011). Functional diversity of human basic helix-loop-helix transcription factor TCF4 isoforms generated by alternative 5' exon usage and splicing. *PLoS ONE*, 6, e22138. DOI: 10.1371/journal.pone.0022138.

* Equal contribution

Elulookirjeldus

Isikuandmed

Nimi: Kaja Nurm
Sünniaeg: 08.10.1984
Sünnikoht: Väike-Maarja, Eesti
Kodakondsus: Eesti

Kontaktandmed

E-post: kaja.nurm@taltech.ee

Hariduskäik

2010–2021 Tallinna Tehnikaülikool – doktoriõpingud
2013–2015 Tallinna Tehnikaülikooli Inseneripedagoogika täiendus-õppekava (magistritase)
2007–2010 Tallinna Tehnikaülikool – MSc (geenitehnoloogia)
2003–2007 Tallinna Tehnikaülikool – BSc (geenitehnoloogia)
2000–2003 Paide Ühisgümnaasium

Keelteoskus

Eesti keel emakeel
Inglise keel kõrgtase
Vene keel algtase

Teenistuskäik

2021–... IQVIA, statistiline programmeerija
2010–2021 Molekulaarse neurobioloogia labor, insener
2014– ... Eesti Akrediteerimiskeskus, erialaassessor
2010–2012 Nova Vita Kliinik, tsütogeneetik

Stipendiumid ja tunnustused

2017 Tallinna Tehnikaülikooli 2017. aasta parim teadusartikkel loodus-, täppis- ja terviseteaduste valdkonnas
2011 Eesti Inimesegeneetika ühingu 2011.a. aastakonverentsi posterikonkursi I koht

Kursused ja konverentsid

November 2018 Osalemine Eesti Inimesegeneetika ühingu 20. aastakonverentsil, Viljandi, Eesti
Aprill 2018 Osalemine Advanced RNASeq Analysis kursusel (EMBL-EBI), Cambridge, UK
Märts 2018 Osalemine SZTest minisümposiumil “Gene expression in health and disease”, Tallinn, Eesti; suuline ettekanne
November 2017 Osalemine Eesti Inimesegeneetika ühingu 19. aastakonverentsil, Rakvere, Eesti
Oktoober 2014 Osalemine Eesti Inimesegeneetika ühingu 14. aastakonverentsil, Haapsalu, Eesti; suuline ettekanne
Juuni 2012 EHGC aastakonverents, Nürnberg, Saksamaa

Juhendatud lõputööd

Kaisa Roots, magistriskraad, 2017, (juh) Kaja Nurm; Tõnis Timmusk, Analysis of disease-related missense variations in the basic helix loop helix transcription factor TCF4 (Aluselise heeliks-ling-heeliks transkriptsioonifaktori TCF4 haigusseoseliste tähendusmuutusega variatsioonide uurimine), Tallinna Tehnikaülikool, Loodusteaduskond, Keemia ja biotehnoloogia instituut

Kristian Costa Dos Santos Leite, magistriskraad, 2016, (juh) Kaja Nurm; Tõnis Timmusk, Analysis of transcription and splicing in the human TCF4 exon 4 region (Transkriptsiooni ja splaissimise analüüs inimese TCF4 ekson 4 regioonis), Tallinna Tehnikaülikool, Loodusteaduskond, Keemia ja biotehnoloogia instituut

Mari Urb, magistriskraad, 2014, (juh) Kaja Nurm; Mari Sepp, Tõnis Timmusk Potential Target Genes of the Basic Helix-Loop-Helix Transcription Factor TCF4 in Rat Primary Neurons (Aluselise heeliks-ling-heeliks transkriptsioonifaktori TCF4 potentsiaalsed märklaudgeenid roti primaarsetes neuronites), Tallinna Tehnikaülikool, Loodusteaduskond, Keemia ja biotehnoloogia instituut

Publikatsioonid

Sirp, A.*; Roots, K*.; **Nurm, K.**; Tuvikene, J.; Sepp, M.; Timmusk T. (2021). Functional consequences of the basic helix-loop-helix transcription factor TCF4 missense substitutions associated with Pitt-Hopkins syndrome, mild intellectual disability, and schizophrenia. *Journal of Biological Chemistry*, in press.

Nurm, K.; Sepp, M.; Castany-Pladevall, C.; Creus-Muncunill, J.; Tuvikene, J.; Sirp, A.; Vihma, H.; Blake, D. J.; Perez-Navarro, E.; Timmusk, T. (2021). Isoform-specific reduction of the basic helix-loop-helix transcription factor TCF4 levels in Huntington's disease. *eNeuro*, 8 (5): ENEURO.0197-21.2021. DOI: 10.1523/ENEURO.0197-21.2021.

Tamberg, L.; Jaago, M.; Saalik, K.; Sirp, A.; Tuvikene, J.; Shubina, A.; Kiir, C. S.; **Nurm, K.**; Sepp, M.; Timmusk, T.; Palgi, M. (2020). Daughterless, the Drosophila orthologue of TCF4, is required for associative learning and maintenance of the synaptic proteome. *Disease Models & Mechanisms*, 13 (7), #dmm042747. DOI: 10.1242/dmm.042747.

Sirp, A.; Leite, K.; Tuvikene, J.; **Nurm, K.**; Sepp, M.; Timmusk, T. (2020). The Fuchs corneal dystrophy-associated CTG repeat expansion in the TCF4 gene affects transcription from its alternative promoters. *Scientific Reports*, 10 (1), #18424. DOI: 10.1038/s41598-020-75437-3.

Sepp, M.; Vihma, H.*; **Nurm, K.***; Urb, M.*; Page, S. C.; Roots, K.; Hark, A.; Maher, B. J.; Pruunsild, P.; Timmusk, T. (2017). The intellectual disability and schizophrenia associated transcription factor TCF4 is regulated by neuronal activity and protein kinase A. *Journal of Neuroscience*, 37, 10516–10527. DOI: 10.1523/JNEUROSCI.1151-17.2017.

Kharbanda, M.; **Kannike, K.**; Lampe, A.; Berg, J.; Timmusk, T.; Sepp, M. (2016). Partial deletion of TCF4 in three generation family with non-syndromic intellectual disability, without features of Pitt-Hopkins syndrome. *European Journal of Medical Genetics*, 59 (6-7), 310–314. DOI: 10.1016/j.ejmg.2016.04.003.

Kannike, K.; Sepp, M.; Zuccato, E.; Cattaneo, E.; Timmusk, T. (2014). FOXO3a levels are increased in Huntingtons disease due to overactivated positive autofeedback loop. *Journal of Biological Chemistry*, 289 (47), 32845–32857. DOI: 10.1074/jbc.M114.612424.

Sepp, M.; **Kannike, K.**; Eesmaa, A.; Urb, M.; Timmusk, T. (2011). Functional diversity of human basic helix-loop-helix transcription factor TCF4 isoforms generated by alternative 5' exon usage and splicing. *PLoS ONE*, 6, e22138. DOI: 10.1371/journal.pone.0022138.

*võrdne panus

ISSN 2585-6901 (PDF)
ISBN 978-9949-83-754-0 (PDF)